



ROLE OF IKK α IN PROSTATE CANCER BONE METASTASES

A thesis submitted in partial fulfilment for the requirements for
the degree of Doctor of Philosophy

Abdullah Aljeffery

The University of Sheffield

Faculty of Medicine, Dentistry and Health

Department of Oncology and Metabolism

August 2018

Dedication

To my family

Declaration

I hereby declare that this thesis has been composed by me and the work described within, except where specifically acknowledged, is my own and that it has not been accepted in any previous application for a degree. The information obtained from sources other than this study is acknowledged in the text or included in the references.

Abdullah Aljeffery

Contents

Dedication	II
Declaration	III
Acknowledgements	XI
Publications	XII
List of abbreviations	XIII
List of Figures	XV
List of Tables	XVIII
Summary	XIX
Graphical abstract.....	XX
CHAPTER ONE	1
General Introduction	1
1. Bone.....	2
1.1 Bone cells	2
1.1.1 Osteoblasts	2
1.1.2 Osteoclasts	3
1.2 Bone remodelling	3
1.2.1 Bone resorption.....	3
1.2.2 The reversal phase	4
1.2.3 Bone formation	4
2. Prostate Cancer	5
2.1 Epidemiology	5
2.2 Genetics	5
2.3 Pathophysiology	5
2.3.1 Tumorigenesis.....	5
2.3.2 Metastasis	8

2.3.2.1 Prostate cancer bone metastasis	10
2.3.2.2 Molecular regulation of PCa bone metastases	13
3. The NFκB signaling pathway	15
IκB kinases (IKKs)	18
3.1 Role of IKK/NFκB activity in bone remodelling	20
3.1.1 Role of IKK/NFκB in osteoclastic bone resorption.....	20
3.1.2 Role of IKK/NFκB in osteoblastic bone formation	20
3.1.3 Regulation of Wnt signalling by IKK/ NFκB in bone homeostasis	21
3.2 Role of IKK/NFκB in PCa cancer	22
3.2.1 Role of IKK/NFκB in PCa tumorigenesis	22
3.2.2. Role of IKK/NFκB in PCa metastasis	23
3.2.2.1 IKKα as a therapeutic target in PCa progression and bone metastasis .	23
Aims of this study	26
CHAPTER TWO	27
Materials & Methods	27
2.1 Preparation of compounds tested	28
2.2 Tissue culture	28
2.2.1 Tissue culture medium.....	28
2.2.2 Cell culture conditions	28
2.3 Cancer cell line cultures	29
2.3.1 Conditioned medium preparation	29
2.3.2 Cancer cell line drug treatments	30
2.4 Bone cell cultures	31
Osteoclast cultures	31
2.4.1 Isolation of bone marrow cells	31
2.4.2 Osteoclast formation cultures	31

2.4.3	Characterisation and identification of osteoclasts	32
2.4.4	Osteoblast cultures	33
2.4.5	Mouse calvarial osteoblast cultures	33
2.4.6	Saos2 cultures	34
2.4.7	MC3T3 cultures	34
2.4.8	Alkaline phosphatase assay	35
2.4.9	Bone nodule formation assay.....	35
2.4.5	Adipocyte cultures.....	36
2.4.5.1	3T3-L1 adipocyte cultures	36
2.4.5.2	3T3-L1 adipocyte Oil red staining and quantification.....	36
2.5	Molecular Biology techniques.....	37
2.5.1	Preparation of Luria-Bertani (LB) broth.....	37
2.5.2	Preparation of LB/ampicillin agar plates	37
2.5.3	Bacterial transformation	37
2.5.4	Preparation of broth culture	37
2.6	Retroviral gene delivery	38
2.6.1	IKK α overexpression constructs.....	38
2.6.2	Short Hairpin RNA (shRNA)	38
2.6.3	Kill curve and Puromycin selection.....	38
2.6.4	Retroviral transfection	38
2.7	Alamar Blue assay.....	39
2.8	Migration assays.....	39
2.9	Invasion assays	40
2.10	WESTERN BLOT.....	41
2.10.1	Preparation of cell lysates	41
2.10.2	Measuring protein concentration	42

2.10.3 Gel electrophoresis	42
2.10.4 Electrophoretic transfer.....	42
2.10.5 Immunostaining and antibody detection.....	42
2.11 Microarray of PC3 conditioned media	43
2.12 Animal work.....	44
2.12.1 <i>In vivo</i> experiments	44
2.12.2 Micro-computed tomography*	45
2.12.3 Bone histomorphometry	48
2.12.4 Tissue microarray staining	49
2.13 STATISTICAL & DATA ANALYSIS.....	51
CHAPTER THREE.....	52
Selective IKK α inhibition reduced prostate cancer cell growth and motility <i>in vitro</i>	52
3.1 Summary	53
3.2 Introduction	54
3.3 Aims	57
3.4 Results.....	58
3.4.1 IKK α is expressed in human prostate tissue samples and cell lines.....	58
3.4.2 Pharmacological inhibition of IKK α reduced prostate cancer cell growth ...	61
3.4.3 Stable IKK α knockdown reduced PC3 viability	64
3.4.4 IKK α knockdown and pharmacological inhibition reduced PC3 directional cell migration	66
3.4.5 IKK α knockdown and pharmacological inhibition reduced random PC3 migration	68
3.4.6 IKK α knockdown and pharmacological inhibition reduced PC3 invasion ...	70
3.5 Discussion	72
CHAPTER FOUR.....	75

Selective IKK α inhibition reduced.....	75
osteoclast formation <i>in vitro</i>	75
4.1 Summary	76
4.2 Introduction.....	77
4.3 Aims	78
4.4 Results.....	79
4.4.1 IKK α pharmacological inhibition reduced RANKL induced osteoclast formation <i>in vitro</i>	79
4.4.2 Cancer specific IKK α regulates PC3 induced osteoclast formation <i>in vitro</i> .	81
4.4.3 Cancer specific manipulation of IKK α regulates ability of PC3 derived factors to affect osteoclast formation <i>in vitro</i>	83
4.5 Discussion	85
CHAPTER FIVE.....	88
Selective IKK α inhibition enhanced osteoblast differentiation and bone nodule formation <i>in vitro</i>	88
5.1 Summary	89
5.2 Introduction.....	90
5.3 Aims	92
5.4 Results.....	93
5.4.1 IKK α pharmacological inhibition stimulated osteoblastic differentiation and bone nodule formation <i>in vitro</i>	93
5.4.2 IKK α inhibition stimulated osteoblastic differentiation and bone nodule formation in the presence of prostate cancer derived factors <i>in vitro</i>	95
5.4.3 IKK α knockdown in PC3 stimulated osteoblastic differentiation and bone nodule formation <i>in vitro</i>	97
5.4.4 Pharmacological IKK α inhibition and IKK α knockdown in PC3 cells suppressed 3T3L1 adipocyte differentiation <i>in vitro</i>	99

5.5 Discussion	101
CHAPTER SIX	105
Effects of SU1349 on NFκB signalling	105
in cancer and bone cells	105
6.1 Summary	106
6.2 Introduction	107
6.3 Aims	110
6.4 Results	111
6.4.1 Pharmacological inhibition of IKKα suppressed PC3 induced NFκB activation in osteoclast precursors	111
6.4.2 Pharmacological inhibition of IKKα suppressed RANKL induced NFκB activation in osteoclast precursors	113
6.4.3 Pharmacological inhibition of IKKα suppressed PC3 induced NFκB activation in osteoblast precursors	115
6.4.4 Pharmacological inhibition of IKKα suppressed Wnt signalling in osteoclast precursors	117
6.4.5 Pharmacological inhibition of IKKα enhanced Wnt signalling in osteoblast precursors	120
6.4.6 Pharmacological inhibition of IKKα reduced PC3 derived pro-inflammatory factors	124
6.5 Discussion	128
CHAPTER SEVEN	137
Effects of SU1349 on prostate cancer associated osteolysis <i>in vivo</i>	137
7.1 Summary	138
7.2 Introduction:	139
7.3 Aims	141
7.4 Results	142

7.4.1 Mice treated with the selective IKK α inhibitor SU1349 showed a trend of reduced metastatic prostate tumour growth.....	142
7.4.2 Mice treated with the selective IKK α inhibitor SU1349 exhibited increased trabecular bone volume	144
7.4.3 Mice treated with the selective IKK α inhibitor SU1349 exhibited reduced cortical bone volume	146
7.4.4 The selective IKK α inhibitor SU1349 exerts differential effects on osteoclasts and osteoblasts numbers <i>in vivo</i>	148
7.4.5 The selective IKK α inhibitor SU1349 had no significant effects on cachexia in mice	150
7.5 Discussion	152
CHAPTER EIGHT	159
General Discussion	159
APPENDIX.....	169
Appendix 1: Supplementary figures	170
Appendix 2: Solutions and Recipes	189
Appendix 3: Materials, Reagents, Apparatus and Software	194
3.1 Materials and Reagents used in this study:	194
3.2 Antibodies in this thesis:	198
3.3 Apparatus used in this thesis:	199
3.4 Software used in this thesis:	200
REFERENCES	201

Acknowledgements

Firstly, I wish to thank my supervisor Dr Aymen Idris. His enthusiasm and dedication for research is inspirational and I am grateful to have been given the opportunity to do my PhD in his group. Thank you for your time, patience and guidance. I am eternally grateful for all you have taught me about research and life in general.

I would like to extend my gratitude to Dr Silvia Marino who helped in getting me settled in the group and had taught me most of the techniques used in this research. I would also like to give special thanks to my colleagues Danielle de Ridder and Ryan Bishop who have been a constant source of support, inspiration and friendship throughout my PhD. Thank you to my colleagues in the department of oncology and metabolism, Mellanby Centre for Bone Research, University of Sheffield for the support and kindness shown to me throughout my PhD.

I would also like to acknowledge the following for their contribution to parts of the work presented in this thesis: I would like to thank Prof Simon MacKay (University of Strathclyde) for providing me with the IKK α inhibitors, giving us exclusive license to test these compounds and providing the Ki data for these compounds; I would like to thank Anne Fowles for her help in staining in the prostate cancer tissue array; I would like to thank Prof Nadia Rucci and Marco Ponzetti from the University of L'Aquila (Italy) for doing the *in vivo* experiments; I would like to thank Orla Gallagher and Mark Kinch from skelet.AL Lab for processing and embedding the mouse bone samples; and I would like to thank my colleague Danielle de Ridder for sectioning the mouse bone samples.

Finally, I would like to thank my parents and my family for their love, support and belief in me without them none of this work would have been possible.

Publications

PAPERS

Abdullah Aljeffery, Silvia Marino, Marco Ponzetti, Nadia Rucci and Aymen I. Idris. Differential effects of IKK α inhibition on trabecular and cortical bone in a prostate cancer xenograft model. (*In preparation*).

Silvia Marino, Daniëlle de Ridder, Nathalie Renema, Marco Ponzetti, Ryan T. Bishop, **Abdullah Aljeffery**, Asim Khooger, Juerg Gertsch, Mattia Capulli, Dominique Heymann, Nadia Rucci, and Aymen I. Idris. The monoacylglycerol lipase inhibitor JZL184 is osteoprotective in models of cancer associated bone disease. (*In preparation*).

ABSTRACTS for ORAL AND POSTER PRESENTATIONS

Abdullah Aljeffery, Silvia Marino and Aymen I. Idris. Regulation of prostate cancer associated bone disease by IKK α . *Medical School Annual Research Meeting*, Sheffield, UK, 2016, Poster 69. (Poster).

Abdullah Aljeffery, Silvia Marino and Aymen I. Idris. The role of IKK α in prostate cancer bone metastasis. *ECTS 2016 PhD training course*, Oxford, UK, 2016, P20. (Poster).

Abdullah Aljeffery, Silvia Marino, Marco Ponzetti, Nadia Rucci and Aymen I. Idris. Selective inhibition of IKK α decreases prostate cancer cell motility, suppresses osteoclastogenesis and stimulates osteoblast differentiation *in vitro*. *7th Annual Mellanby Centre Research Day*, Sheffield, UK, 2016, Poster 03. (SNAP oral and Poster).

Abdullah Aljeffery, Silvia Marino, Marco Ponzetti, Nadia Rucci and Aymen I. Idris. Selective inhibition of IKK α decreases prostate cancer cell motility, suppresses osteoclastogenesis and stimulates osteoblast differentiation *in vitro*. *ECTS 2017*, Salzburg, Austria, P-CANC-15. (Poster).

Abdullah Aljeffery, Silvia Marino, Marco Ponzetti, Nadia Rucci and Aymen I. Idris. Differential effects of IKK α inhibition on trabecular and cortical bone in a prostate cancer xenograft model. *ECTS 2018*, Valencia, Spain. (Oral - Poster).

List of abbreviations

ADT	Androgen deprivation therapy
Akt	Protein kinase B
ALP	Alkaline Phosphatase
AR	Androgen receptor
ATM	Ataxia-telangiectasia mutated protein kinase
c-Fms	Receptor of M-CSF
CRPC	Castration resistant prostate cancer
ECM	Extracellular matrix
EGF	Epidermal growth factor
EGFR	EGF receptor
EMT	Epithelial Mesenchymal Transition
ERα	Estrogen receptor alpha
ET-1	Endothelin-1
FGF	Fibroblast growth factors
FGFR	FGF receptor
IGF-1	Insulin growth factor 1
IκBα	Inhibitor of NF κ B alpha
IKK	I κ B kinase
IKKα	I κ B kinase subunit alpha
IKKβ	I κ B kinase subunit beta
IKKϵ	I κ B kinase subunit epsilon
IKKγ	I κ B kinase subunit gamma
IL	Interleukin
LPS	Lipopolysaccharide
MAPK	Mitogen activated protein kinases
M-CSF	Macrophage colony stimulating factor
MMP	Metalloproteinase
MSC	Mesenchymal stem cells
NEMO	NF κ B essential modulator
NFκB	Nuclear factor κ B
NIK	NF- κ B-inducing kinase
OPG	Osteoprotegerin
PCa	Prostate cancer
PDGF	Platelet-derived growth factors
PI3K	Phosphoinositide 3-kinase
PKCδ	Protein kinase C delta
PTHrP	Parathyroid hormone-related protein
RANK	Receptor activator of nuclear factor κ B
RANKL	Receptor activator of nuclear factor κ B ligand
Runx2	Runt-related transcription factor
sFRP4	Secreted frizzled-related protein 4
STAT3	Signal transducer and activator of transcription 3
TBK1	TANK-binding kinase 1
TGFβ	Transforming growth factor- β
TNF	Tumour necrosis factor

VEGF	Vascular endothelial growth factor
VCAM-1	Vascular cell adhesion molecule 1
Wnt	Wingless and Int-1 (integration site)

List of Figures

<i>Figure #</i>		<i>Page</i>
Figure 1.1	Mechanisms of metastasis	9
Figure 1.2	The ‘vicious cycle’ of bone metastasis	12
Figure 1.3	The canonical and non-canonical NFκB pathways	17
Figure 3.1	IKKα is expressed at all stages of prostate cancer progression and in cell models of prostate cancer	59
Figure 3.2	IKKα expression in prostate cancer cell lines of various metastatic potentials	60
Figure 3.3	The selective IKKα inhibitor, SU1349, reduced PC3 cell viability in a time and concentration dependent manner	63
Figure 3.4	Overexpression and knockdown of IKKα in PC3 cells affected their viability	65
Figure 3.5	IKKα regulates PC3 cell directed migration	67
Figure 3.6	IKKα regulates PC3 cell random migration	69
Figure 3.7	IKKα regulates PC3 cell invasion	71
Figure 4.1	IKKα inhibitor, SU1349, reduced RAW264.7 osteoclast formation <i>in vitro</i>	80
Figure 4.2	co-culture with PC3 cells overexpressing IKKα significantly enhanced osteoclast formation, whereas IKKα knockdown and pharmacological inhibition suppressed osteoclast formation <i>in vitro</i>	82
Figure 4.3	conditioned media from PC3 cells with IKKα overexpression significantly enhanced osteoclast formation <i>in vitro</i> , whereas pharmacological inhibition of IKKα suppressed osteoclast formation <i>in vitro</i>	84
Figure 5.1	The IKKα inhibitor, SU1349, stimulated osteoblastic differentiation and activity <i>in vitro</i>	94
Figure 5.2	The IKKα inhibitor, SU1349, stimulated osteoblastic differentiation and activity in the presence prostate cancer derived factors	96
Figure 5.3	IKKα knockdown in PC3 stimulated osteoblastic differentiation and activity <i>in vitro</i>	98
Figure 5.4	Pharmacological IKKα inhibition and IKKα knockdown in PC3 cells suppressed 3T3L1 adipocyte differentiation <i>in vitro</i>	100

<i>Figure #</i>		<i>Page</i>
Figure 6.1	SU1349 suppressed NFκB Activation by PC3 conditioned media in osteoclast precursor cells	112
Figure 6.2	SU1349 suppressed NFκB Activation by RANKL in osteoclast precursor cells	114
Figure 6.3	SU1349 suppressed NFκB Activation by PC3 conditioned media in osteoblast precursor cells	116
Figure 6.4	SU1349 suppressed GSK3β phosphorylation in osteoclast precursor cells	118
Figure 6.5	SU1349 caused a non-significant reduction in cytoplasmic β-catenin in osteoclast precursor cells.	119
Figure 6.6	SU1349 increased GSK3β phosphorylation in osteoblast precursor cells	122
Figure 6.7	SU1349 caused a significant increase in cytoplasmic β-catenin in osteoblast precursor cells	123
Figure 6.8	Pharmacological inhibition of IKKα reduced PC3 derived pro-inflammatory factors	125
Figure 7.1	The IKKα inhibitor SU1349 showed a trend in reducing prostate tumour metastatic growth <i>in vivo</i>	143
Figure 7.2	The IKKα inhibitor SU1349 increased trabecular bone volume in mice	145
Figure 7.3	The IKKα inhibitor SU1349 reduced cortical bone volume in mice	147
Figure 7.4	<i>In vivo</i> the IKKα inhibitor SU1349 reduced osteoclasts and increased osteoblast in trabecular bone, whereas in cortical bone SU1349 reduced osteoblasts and increased osteoclasts	149
Figure 7.5	Cachexia in mice was not significantly affected by the IKKα inhibitor SU1349	151

<i>Figure #</i>		<i>Page</i>
Figure S3.1.1-5	Cell viability graphs for IKKα inhibitors used in IC50 calculations (table 3.1).	170-174
Figure S3.2	SU1349 suppressed the directed migration of PC3 cells pre-treated with mitomycin-C (10μg/L) <i>in vitro</i>.	175
Figure S3.3	Concentration of SU1349 selected for invasion assay had no significant effects on PC3 viability <i>in vitro</i>	176
Figure S4.1	PC3 conditioned suppressed osteoclast formation <i>in vitro</i>	177
Figure S5.1	PC3 conditioned media stimulated osteoblastic differentiation, bone nodule formation activity and viability <i>in vitro</i>	178
Figure S5.2	PC3 conditioned media stimulated 3T3L1 adipocyte differentiation <i>in vitro</i>	179
Figure S6.1	Pharmacological IKKα inhibition reduced total β-catenin in PC3	180
Figure S7.1	Example of stained bone sections analysed for histomorphometry.	187
Figure S7.2	Combined IKKα inhibition and Docetaxel treatments showed synergistic effects on PC3 survival and favourable dose reduction potential for each drug	188

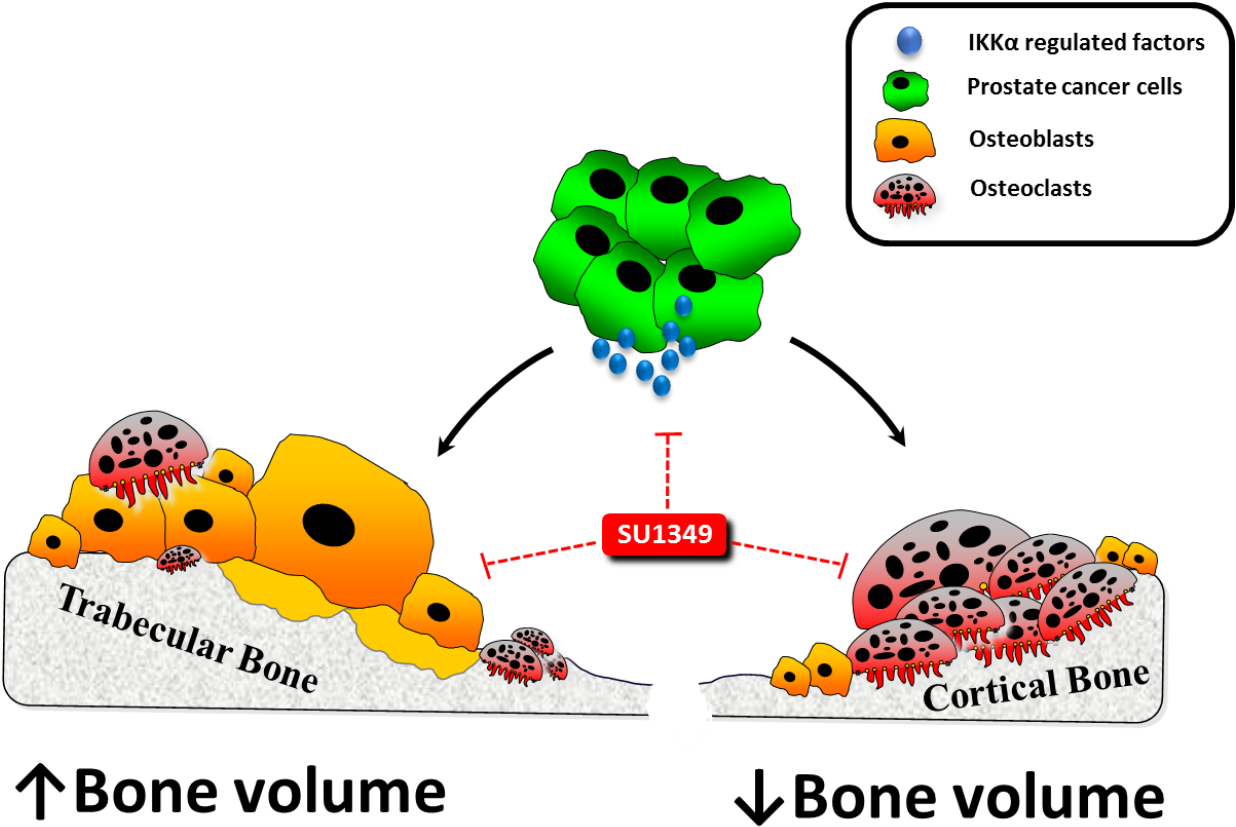
List of Tables

<i>Table #</i>		<i>Page</i>
Table 1.1	Gleason scoring and grading systems	7
Table 1.2	A summary of some of the main factors that regulate PCa bone metastasis.	14
Table 2.1	Reconstruction parameters used in NRecon software	45
Table 2.2	3D reconstruction parameters used in CTAn software	46
Table 2.3	3D bone analysis parameters calculated by μCT	47
Table 2.4	Stages and reagents for Leica tissue processor programme	49
Table 3.1	Table compares calculated IC50 values for several novel IKKα inhibitors in different prostate cancer cell lines after 48hrs of treatment in complete media	62
Table 6.1	Summary table for effects of SU1349 differentially regulated factors on prostate cancer cells, osteoclast, osteoblast and adipocytes	126- 127
Table S6.2	Raw data for human XL cytokine microarray used in section 6.4.6.	181- 186

Summary

I κ B kinase subunit alpha (IKK α), a key component of the NF κ B pathway, is implicated in prostate cancer progression and bone remodelling, but its role in the regulation of prostate cancer associated bone disease remains unknown. Here, we tested the effects of IKK α manipulation on prostate cancer cell behaviour *in vitro* and on osteolysis in a xenograft model of human prostate cancer bone metastasis. The pharmacological inhibition of IKK α using the novel and highly selective IKK α inhibitor SU1349 and stable knockdown of IKK α in PC3 cells significantly reduced cell viability, migration and invasion, whereas IKK α overexpression was stimulatory. In prostate cancer cell - osteoclast co-cultures, IKK α overexpression in PC3 enhanced RANKL-induced osteoclastogenesis, whereas SU1349 treatment and IKK α knockdown reduced these effects. Exposure of osteoblasts to SU1349 enhanced alkaline phosphatase activity and bone nodule formation. Protein microarray analysis of tumour-derived factors in PC3 conditioned medium showed that these effects were associated with significant inhibition of various NF κ B-mediated pro-inflammatory factors and reduction in PC3 conditioned medium induced NF κ B activation in osteoclast and osteoblast precursors. In osteoclast and osteoblast precursors SU1349 lead to inhibition of both canonical and non-canonical NF κ B signalling. Interestingly, NF κ B inhibition in osteoblasts was accompanied by an increase in GSK3 β phosphorylation indicative of activation of the Wnt/ β -catenin pathway, whereas the opposite occurred in osteoclast precursors. *In vivo*, administration of SU1349 (20mg/kg/3times-weekly) in immuno-deficient BALB/c mice after intra-cardiac injection with human PC3 cells enhanced trabecular bone volume and this was associated with reduced osteoclast and increased osteoblast numbers. Paradoxically, SU1349 treatment reduced cortical bone volume, and this was associated with increased osteoclast and reduced osteoblast numbers. Thus, the novel IKK α inhibitor SU1349 is of potential therapeutic value in protecting against prostate cancer-induced osteolysis. However, exacerbation of bone loss in the cortical compartment may limit its usefulness as a bone sparing agent.

Graphical abstract



Schematic representation of the effects of the IKK α inhibitor SU1349 in trabecular and cortical bone in a mouse model of prostate cancer bone metastasis.

CHAPTER ONE

General Introduction

1. Bone

Bone is a highly dynamic and specialised connective tissue that together with cartilage forms the skeleton. Bone organic component is mainly composed of type I collagen fibres that represent approximately 90% of the proteins present in the bone matrix. The remaining 10% of the organic matrix consists mainly of non-collagenous proteins. Bone mineralised inorganic component is mainly comprised of crystals of hydroxyapatite $[\text{Ca}_{10}(\text{PO}_4)_6(\text{OH})_2]$ which are insoluble salts of calcium and phosphorus (Favus, 2006).

1.1 Bone cells

The main cellular components of bone are osteoclasts, osteoblasts, lining cells and osteocytes. They play a key role in the bone remodelling cycle, a process that maintains bone structural integrity through cycles of bone resorption and bone formation (Favus, 2006).

1.1.1 Osteoblasts

Osteoblasts are cuboidal, mononuclear cells and are derived from mesenchymal stem cells (MSCs), which are pluripotent progenitor cells found in bone marrow (Favus, 2006). MSCs also differentiate into myocytes, chondrocytes and adipocytes, the latter two cell types are implicated in pathological bone remodelling (Katagiri and Takahashi, 2002). A variety of growth factors, hormones and transcription factors act together to control mesenchymal progenitor differentiation toward osteoprogenitors, pre-osteoblasts, mature osteoblasts, and finally osteocytes or bone lining cells. Runt-related transcription factor 2 (Runx2) is the main transcription factor responsible for the commitment of MSCs towards cell of the osteoblastic lineage (Karsenty and Wagner, 2002). Together with Osterix (Osx), Runx2 is also involved in osteoblast maturation (Lecka-Czernik et al., 1999).

Mature osteoblasts express high levels of the enzyme alkaline phosphatase (ALP) and their main function is to synthesize and secrete osteoid, which are proteins that make up the unmineralised bone matrix (Katagiri and Takahashi, 2002). Osteoblasts also regulate osteoclast formation and bone resorption by producing osteolytic cytokines, macrophage colony-stimulating factor (M-CSF), receptor activator of nuclear factor

κ B ligand (RANKL), and the decoy receptor for RANKL: osteoprotegerin (OPG) (Troen, 2003).

1.1.2 Osteoclasts

Osteoclasts are terminally differentiated multinucleated cells of a hematopoietic origin. Osteoclasts are formed by the fusion of multiple mononuclear precursors in response to the action of M-CSF and RANKL (Vaananen and Laitala-Leinonen, 2008).

M-CSF produced by osteoblasts binds to the c-Fms receptor, expressed by osteoclast precursors and mature osteoclasts (Weir et al., 1993). This binding commits precursors cells towards osteoclastogenesis and is important for osteoclast survival (Teitelbaum, 2000, Takayanagi, 2005). RANKL is produced by various cells including osteoblasts, osteocytes and immune cells namely T – lymphocytes and dendritic cells (Jones et al., 2002). RANKL binds to the receptor activator of nuclear factor κ B (RANK) to stimulate differentiation of precursors and fusion into mature multinucleated osteoclasts (Teitelbaum, 2000, Takayanagi, 2005). The main function of mature osteoclasts is bone resorption.

1.2 Bone remodelling

Normal bone remodelling is a highly dynamic and coordinated process that consists of two distinct phases: bone resorption and bone formation. Dysregulation of the bone remodelling cycle is the main cause of many diseases including osteoporosis, Paget's disease, rheumatoid arthritis and cancer associated bone disease.

1.2.1 Bone resorption

After a period of quiescence and in response to micro damage, bone resorption is initiated by the recruitment of osteoclasts and their precursors to sites of bone to be remodelled. It is thought that osteocytes instruct osteoblasts and bone lining cells to secrete various proteolytic enzymes to dissolve the osteoid layer in order for osteoclasts to access the underlying mineralised layer (Troen, 2003, Hadjidakis and Androulakis, 2006). Furthermore, osteocytes together with osteoblasts and other bone marrow cells, release M-CSF and RANKL, which causes osteoclasts precursors to differentiate into mature osteoclasts (Proff and Romer, 2009).

Mature osteoclasts adhere to the bone surface, polarise and release protons and chloride ions, which demineralise the bone matrix by converting hydroxyapatite into Ca^{2+} , HPO_4^{2-} and H_2O (Bar-Shavit, 2007, Hill, 1998). This uncovers the underlying organic matrix that is in turn degraded by osteoclast-derived cathepsin K and MMP9 (Teitelbaum, 2000). Both organic and inorganic degradation products are engulfed by osteoclasts and are secreted into the extracellular space (Vaananen and Laitala-Leinonen, 2008). In healthy human adults, the bone resorption phase lasts for ten days after which osteoclasts undergo apoptosis (Hill, 1998).

1.2.2 The reversal phase

The reversal phase is characterised by: osteoclasts undergoing apoptosis; migration of osteoblast precursors to the newly resorbed bone; and appearance of mononuclear macrophage-like cells. The macrophage-like cells remove the residual organic matrix to form a 'cement line' that demarcates the boundary of bone resorption and joins old bone to new (Hill, 1998, Lerner, 2006).

1.2.3 Bone formation

The recruitment of osteoblasts and their precursors to the newly resorbed site is initiated by the release of systemic and bone-derived factors such as $\text{TGF}\beta$, BMP2, IGFs, FGFs, and PDGFs (Mundy et al., 1982, Hill, 1998, Lerner, 2006). Mature osteoblasts initiate the production of new bone by producing type I collagen that together with various non-collagenous proteins form the osteoid (Katagiri and Takahashi, 2002). Osteoblasts initiate the transformation of osteoid into mineralised bone by producing ALP, which breaks down pyrophosphate an inhibitor of mineralization, and by releasing membrane bound bodies, known as matrix vesicles, throughout the collagen scaffold. These matrix vesicles contain calcium, phosphate, phospholipids and various proteins and that together induce the formation of hydroxyapatite giving rise to mature mineralised bone (Favus, 2006, Katagiri and Takahashi, 2002). The bone formation phase lasts for three months in a healthy adult human. At the end of which 65% of osteoblasts undergo apoptosis (Jilka, 1998). the remainder either differentiate into bone lining cells or transform into osteocytes (Favus, 2006).

2. Prostate Cancer

2.1 Epidemiology

Prostate cancer (PCa) is the second most common cause of cancer and the sixth leading cause of cancer death among men worldwide (Center et al., 2012). The disease usually appears in men over the age of 60 and is more common in western countries than in developing countries (Marugame and Katanoda, 2006). In the US the incidence of PCa is highest amongst African Americans and lowest amongst Asian Americans (Zeigler-Johnson et al., 2008).

Early detection and treatment of locoregional PCa has a 5 year relative survival rate that is almost 100%, while in PCa with distant metastasis the survival rate drops to 30% (Jemal et al., 2008). In a large-scale autopsy study of patients with PCa, 90% of metastases involved bone (Bubendorf et al., 2000). Although only a minority of men with PCa develop metastasis most of PCa related deaths are due to metastatic progression (Thobe et al., 2011).

2.2 Genetics

In addition to environmental and lifestyle related factors (Attard et al., 2015), 42% of the risk of developing PCa has been attributed to genetic factors (Eeles et al., 2014). Genome-wide association studies have associated 76 genetic loci of low penetrance with PCa (Eeles et al., 2014). In addition, a number of genes with rare but highly penetrant mutations have been implicated in PCa disposition, these include: *BRAC1/2*, *HOXB13*, *CHEK2*, *PALB2*, *BRIP1* and *NBS1* (Kote-Jarai et al., 2011, Leongamornlert et al., 2012, Ewing et al., 2012, Cybulski et al., 2004, Erkkö et al., 2007, Kote-Jarai et al., 2009, Hebbing et al., 2006).

2.3 Pathophysiology

2.3.1 Tumorigenesis

The cell origin of prostate cancer cells has not been fully established, however, it is thought to be primarily derived from basal or luminal epithelial cells within the

Chapter 1

General Introduction

glandular pits of the prostate, although a rarer and more aggressive form of prostate cancer is derived from neuroendocrine cells (Attard et al., 2015, Berish et al., 2018).

PCa is thought to progress from a pre-malignant condition of the prostatic gland, known as prostatic intraepithelial neoplasia (PIN) (De Marzo et al., 2007). PIN is characterised by multiple lesions that show a dysplasia of prostate epithelial cells and a reduction in basal layer cells (Schrecengost and Knudsen, 2013). PCa lesions can then develop into locally invasive adenocarcinoma and eventually into metastatic carcinoma.

Serum prostate-specific antigen (PSA) is used in patients and population screening, as a predictive, diagnostic and prognostic marker (Attard et al., 2015). PSA is used to monitor progression, response to therapy and relapse. However, since PSA is prostate specific it can also indicate damage to the prostate due to inflammatory disease (De Marzo et al., 2007). Therefore, prostate cancer diagnosis and prognosis, also requires histological grading of primary prostate cancer biopsies using the Gleason score system, which assess the level of differentiation of glandular prostatic tissue and pattern of growth into the stroma to assess the pathological stage, predict aggressiveness of prostate cancer progression and the likelihood of developing metastasis (see Table 1.1) (Sathianathan et al., 2018).

The initiation and progression of PCa is associated with mutations in a number of key genes, notably: NKX3.1, FOXA1, Myc, TMPRSS2:ERG and the AR gene (Schrecengost and Knudsen, 2013, Gil et al., 2005, Gallucci et al., 2009, Jenkins et al., 1997, Mosquera et al., 2008, Ganguly et al., 2014). Additionally, the expression of tumour suppressors such as PTEN, p53 and less frequently RB is commonly lost in PCa (Schrecengost and Knudsen, 2013, Attard et al., 2015, Sharma et al., 2010).

Chapter 1
General Introduction

Table 1.1: Gleason scoring and grading system. Traditional Gleason scoring system is made up of a total of two scores: one for the predominate histological appearance of biopsied tissue followed by a score for the second most common appearance of tissue (the two scores separated by the sum sign is shown in brackets). Gleason scores below 6 are uncommon as biopsies are usually taken after disease progression (Sathianathen et al., 2018).

Traditional Gleason score system	New Gleason grade system	Histological appearance
≤ 6 (3+3)	1	Glands are well differentiated, small and closely packed. Tumour cells are likely to grow slowly.
7 (3+4)	2	Predominately well differentiated glands and tumour cells that are likely to grow slowly. Some poorly differentiated glands (hypertrophic) with more stroma in between glands and tumour cells that are likely to grow moderately
7 (4+3)	3	Predominately poorly differentiated glands with more stroma in between glands and tumour cells that are likely to grow moderately, also some infiltration of glands at margins. Some well differentiated glands with tumour cells that are likely to grow slowly.
8 (3+5; 4+4; 5+3)	4	Few glands left. Poorly differentiated tissue. Most Tumour cells are likely to grow moderately and/or quickly.
9 (4+5; 5+4)- 10 (5+5)	5	Rare or no glands are present. Extremely poorly differentiated tissues. Tumour cells are likely to grow quickly.

Androgen and androgen receptor (AR) signalling is important in prostate development and in cancer progression (Schrecengost and Knudsen, 2013). Synthesis of androgens is primarily regulated by the hypothalamic-pituitary-testicular axis with androgen synthesis by the adrenal glands being a secondary source (Watson et al., 2015). The hypothalamus produced gonadotropin-releasing hormone (GnRH) signals to the pituitary gland to produce luteinizing hormone, which in turn stimulates testosterone production in the testis. In the prostate, androgens such as testosterone and adrenal androgens are converted to dihydrotestosterone which binds to AR to activate AR signalling (Watson et al., 2015). Patients diagnosed with early stage PCa are

Chapter 1

General Introduction

responsive to androgen deprivation therapy (ADT) through chemical or surgical castration. Most commonly agonists or antagonists of GnRH are used to downregulate testosterone production by the testis, however, as residual androgen are still produced by the adrenal glands, ADT is augmented by combining with Abiraterone which blocks androgen synthesis by the CYP17A1 (Cytochrome P450 family 17 subfamily A polypeptide 1) enzyme (Watson et al., 2015). Eventually some patients relapse and become unresponsive to ADT, and their tumours exhibit aberrant AR activation that is largely independent of circulating androgen, this is known as castration resistant PCa (CRPC) (Ganguly et al., 2014). Therefore, CRPC treatment also involves anti-androgen drugs that inhibit androgen synthesis (Abiraterone) or block androgen receptor signalling (Enzalutamide) to address aberrant activation of androgen signalling, invariably, these patients still progress to metastatic disease, where they require additionally chemotherapy treatments using docetaxel (1st line chemotherapy) or later cabazitaxel (2nd line chemotherapy) (Attard et al., 2015).

2.3.2 Metastasis

Most patients with advanced prostate cancer experience complications from lymph node and bone metastases. PCa metastasis, like other forms of metastases, follows recognised stages, these are: local invasion of surrounding tissue, intravasation into blood or lymphatic vasculature, transport through the blood or lymphatic systems to distant sites, extravasation from the vascular system and dissemination into site of metastasis, adaptation to the local environment and colonisation (Figure 1.1) (van der Pluijm, 2011, Chaffer and Weinberg, 2011).

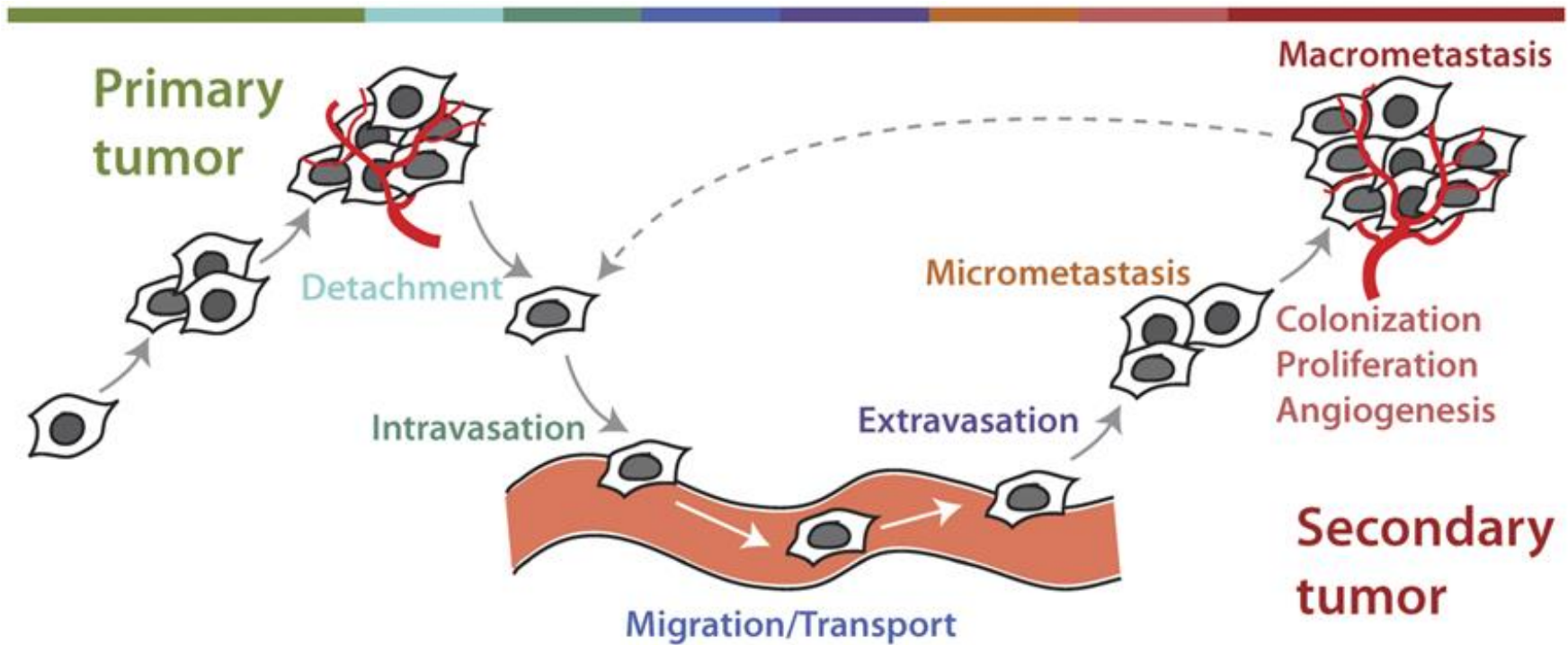


Figure 1.1 Mechanisms of metastasis. Note established (macrometastasis) can also detach and cause further metastases through the same mechanisms. See text for more details (source: ploscompbiol.org)

The PCa tumour microenvironment produces factors, such as $\text{TNF}\alpha$, $\text{TGF}\beta$ and Wnt, promotes prostate epithelial cells to undergo an epithelial-mesenchymal transition (EMT) which increases their migratory and invasive capacity. PCa cells promote production of proteases (MMPs-1/2/9) that degrade the extra-cellular matrix (ECM) to facilitates the escape of PCa cells from the stromal compartment and intravasation into the blood and lymphatic vascular system (Ganguly et al., 2014).

The homing of PCa cells to bone is mainly due to the action of various chemo-attractant factors such as $\text{TGF}\beta$, CXCL12 and VEGF (Ganguly et al., 2014). The sinusoids within the marrow of long provide a natural entry point for the circulating PCa cells (Thobe et al., 2011). The sinusoid epithelia express tethering proteins such as VCAM-1 which allow PCa cells to adhere to bone (Scott et al., 2001).

2.3.2.1 Prostate cancer bone metastasis

The development of PCa bone metastasis is a major cause of morbidity, including: bone pain, reduced mobility, pathologic fractures, spinal cord compression, hypercalcemia, anaemia and susceptibility to infection (Logothetis and Lin, 2005, Coleman, 2001). Unlike most types of cancers that metastasize to bone which typically cause osteolytic (bone-destroying) lesions, PCa in patients causes mixed lesions with more osteoblastic (bone-forming) lesions as well as the typical osteolytic lesions (Logothetis and Lin, 2005).

In bone, PCa cells interact directly with osteoblasts through cadherin-11, and release factors (BMPs-2/4/6/7, ET1, Wnt and PDGF) that promote osteoblasts proliferation to form osteoblastic lesions (Table 1) (Ganguly et al., 2014). Osteoblasts then releases factors (FGF, IGF-1, IL-6 and $\text{TGF}\beta$) that promote PCa cell growth and survival (Ganguly et al., 2014). Moreover, PCa cells and osteoblasts elevate RANKL, M-CSF and PTHrP levels which increases osteoclasts and bone resorption (Keller and Brown, 2004). Increased bone resorption further releases cytokines and factors (FGFs, IGFs and $\text{TGF}\beta$) from the bone matrix which promotes the proliferation of cancer cells and osteoblasts (Ibrahim et al., 2010). The process of tumour cells promoting growth of osteoblasts and osteoclasts, followed by osteoblasts and osteoclasts promoting growth of tumour cells is known as the vicious cycle (see Figure 1.2).

Chapter 1

General Introduction

Patients with bone metastasis are often treated with drugs that inhibits osteolytic bone resorption such as Zoledronic acid (a next generation bisphosphonate that inhibits osteoclast survival and function) and Denosumab (anti-RANKL monoclonal antibody that inhibits osteoclast differentiation and function) (Sathianathen et al., 2018). However, while these treatments are effective in reducing some of the complications associated with bone metastasis –specifically increased bone resorption- they are unsuccessful in directly reducing prostate cancer skeletal tumour growth and metastasis (Clement-Demange and Clezardin, 2015, Todenhofer et al., 2015). More recently, Radium-223, was clinically approved for the treatment of CRPC and it was shown to both alleviate bone metastatic damage and improve survival (Sathianathen et al., 2018). Radium-223 is an α -particle emitting calcium mimetic that binds to areas of newly formed bone associated with prostate cancer osteoblastic lesions and due to its short radiation penetrance and half-life, it reduces off target cytotoxic effects and is therefore well tolerated in patients.

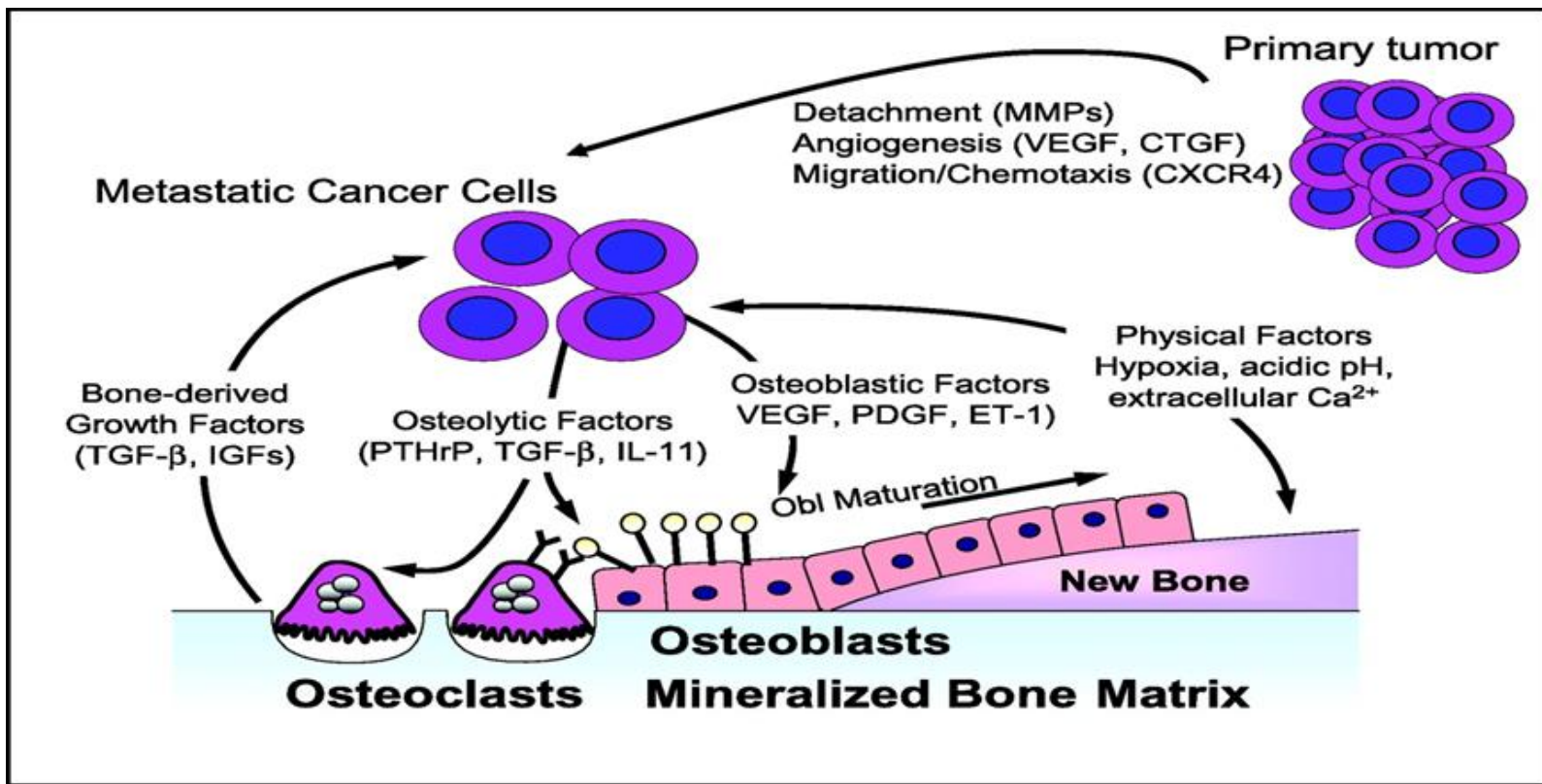


Figure 1.2: The ‘vicious cycle’ of bone metastasis. Figure depicts some of the main factors involved in the interactions between tumour cells and osteoblasts and osteoclast in the bone microenvironment (Obl = osteoblasts). See text for detail (source: (Kingsley et al., 2007))

2.3.2.2 Molecular regulation of PCa bone metastases

Many factors can regulate both PCa cell and the bone microenvironment during PCa bone metastasis. Of note is the RANK/RANKL/OPG axis, which regulates the NF κ B pathway upstream of IKK α and plays a key role in the regulation of vicious cycle associated with prostate cancer bone metastasis, is discussed below.

RANK/RANKL/OPG axis

RANKL, RANK and OPG are members of the TNF and TNF receptor superfamily (Favus, 2006). The RANK/RANKL/OPG axis regulates the NF κ B pathway which is crucial for the regulation of osteoclastogenesis and has also been implicated in bone metastasis associated with prostate cancer (Jones et al., 2006, Schramek et al., 2011). Specifically an increased RANKL/OPG ratio, which is indicative of increased NF κ B activation, has been linked to bone metastasis (Dougall and Chaisson, 2006). Invading PCa cells were shown to directly stimulate bone resorption by producing RANKL (Sabbota et al., 2010). In addition, PCa cells can release factors such as TGF β and PTHrP that stimulate bone stromal cells to increase RANKL production (Leibbrandt and Penninger, 2008). Moreover, prostate cancer cells were shown to respond to the increase in RANKL expression by promoting the expression of genes involved in osteolysis and invasion (Armstrong et al., 2008). Whilst OPG is primarily produced by bone stromal cells to inhibit NF κ B activation and therefore osteoclastogenesis, OPG has also been reported to be expressed by aggressive prostate cancer cells lines and was shown to be important for prostate cancer cell survival (Holen et al., 2002).

Other factors that regulate both PCa cell and the bone microenvironment during PCa bone metastasis are summarised in Table 1.2.

Table 1.2: A summary of some of the main factors that regulate PCa bone metastasis.

Factor	Source	Effects			References
		PCa & Bone metastasis	OB	OC	
BMPs-2/4/6/7	PCa	↑	↑		(Canalis, 2009, Ganguly et al., 2014)
ET-1	PCa	↑	↑		(Ganguly et al., 2014, Russo et al., 2010, Yin et al., 2003).
Wnt-1	PCa	↑	↑		(Anastas and Moon, 2013, Gaur et al., 2005, Hall et al., 2005)
PDGFs	PCa/BMx	↑	↑		(Sanchez-Fernandez et al., 2008, Ustach et al., 2010).
TGFβ	PCa/BMx	↑	↑↓	↑	(Janssens et al., 2003, Maeda et al., 2004, Quinn et al., 2001).
IGF-1	PCa/OB/OC / BMx	↑	↑	↑	(Ganguly et al., 2014, Ryan et al., 2007).
FGFs-1/8/9	PCa/ BMx	↑	↑		(Valta et al., 2008, Ganguly et al., 2014).
M-CSF	PCa/OB	↑		↑	(Ide et al., 2008)
PTHrP	PCa	↑	↑	↑	(Liao et al., 2008, Roodman, 2004)
ILs-6	PCa/OB	↑	↑	↑	(Ara and Declerck, 2010, Nguyen et al., 2014a).
TNFα	PCa	↑	↓	↑↓	(Abu-Amer et al., 2000, Nanes, 2003, Kim et al., 2011)
VEGF	PCa/OB	↑	↑	↑	(Schipani et al., 2009, Yang et al., 2008, Yang et al., 2012).
MMPs-1/2/9	PCa/BMx	↑		↑	(Ganguly et al., 2014, Krane and Inada, 2008)
EGFs	PCa/BMx	↑	↑↓	↑	(Schneider et al., 2009, Chang et al., 2015).

BMXs, bone matrix; OB, osteoblasts; OC, osteoclasts; Arrows indicate stimulation or inhibition of proliferation or activity.

3. The NF κ B signaling pathway

I κ B kinase (IKK), a key member of the NF κ B family, is implicated in the regulation of inflammation, cell death, immunity, bone remodelling and oncogenesis (Clement et al., 2008, Hayden and Ghosh, 2004, Gilmore, 2006, Basseres and Baldwin, 2006). IKK family members consist of IKK α , IKK β , IKK γ , IKK ϵ and TBK1. IKKs are important in regulating The classic IKK complex which consists of IKK α , IKK β and IKK γ and are involved in the regulation of the canonical NF κ B pathway (Oeckinghaus et al., 2011). An IKK α dimer regulates the non-canonical NF κ B pathway (Clement et al., 2008) (Figure 1.3).

The canonical IKK/NF κ B pathway is activated by various inflammatory factors including RANKL, TNF α , IL-1, bacterial and viral antigens. Upon activation, the IKK α /IKK β /IKK γ complex is formed and phosphorylates inhibitory I κ B proteins that bind to NF κ B proteins normally found in the cytoplasm. This leads to the dissociation of I κ B α protein and the translocation of NF κ B p65/p50 dimers to the nucleus and activation of target genes (Karin and Ben-Neriah, 2000). Several studies have shown that IKK α does not play an essential role in the activation of the canonical pathway while IKK β and IKK γ are essential (Hacker and Karin, 2006, Lee and Hung, 2008).

The non-canonical IKK/NF κ B pathway is activated by a restricted number of stimuli that are members of the TNF superfamily, which include RANKL, lymphotoxin β , CD40L, BAFF and LPS. This leads to the stabilization of NIK kinase which phosphorylates IKK α dimers that in turn phosphorylate the inhibitory p100 subunit bound to cytoplasmic RelB (Oeckinghaus et al., 2011). Phosphorylation of the p100 subunit and allows for its partial degradation and processing to p52. The RelB-p52 complex then translocates to the nucleus where it binds and activates the expression of target genes. Activated IKK α translocates to the nucleus and activate the expression of NF κ B-dependent genes directly by phosphorylating histones H3 (Yamamoto et al., 2003).

Chapter 1

General Introduction

Canonical NF κ B signalling is understood to be primarily responsible for regulating innate immunity and inflammation whilst non-canonical NF κ B signalling is more important for adaptive immunity and secondary lymphoid organogenesis (Baud and Karin, 2009, Polley et al., 2016). It is important to note that the NF κ B pathway is also activated by IKK kinases independent mechanisms, that phosphorylate I κ B and cause the nuclear translocation of NF κ B (Perkins, 2006, Perkins and Gilmore, 2006).

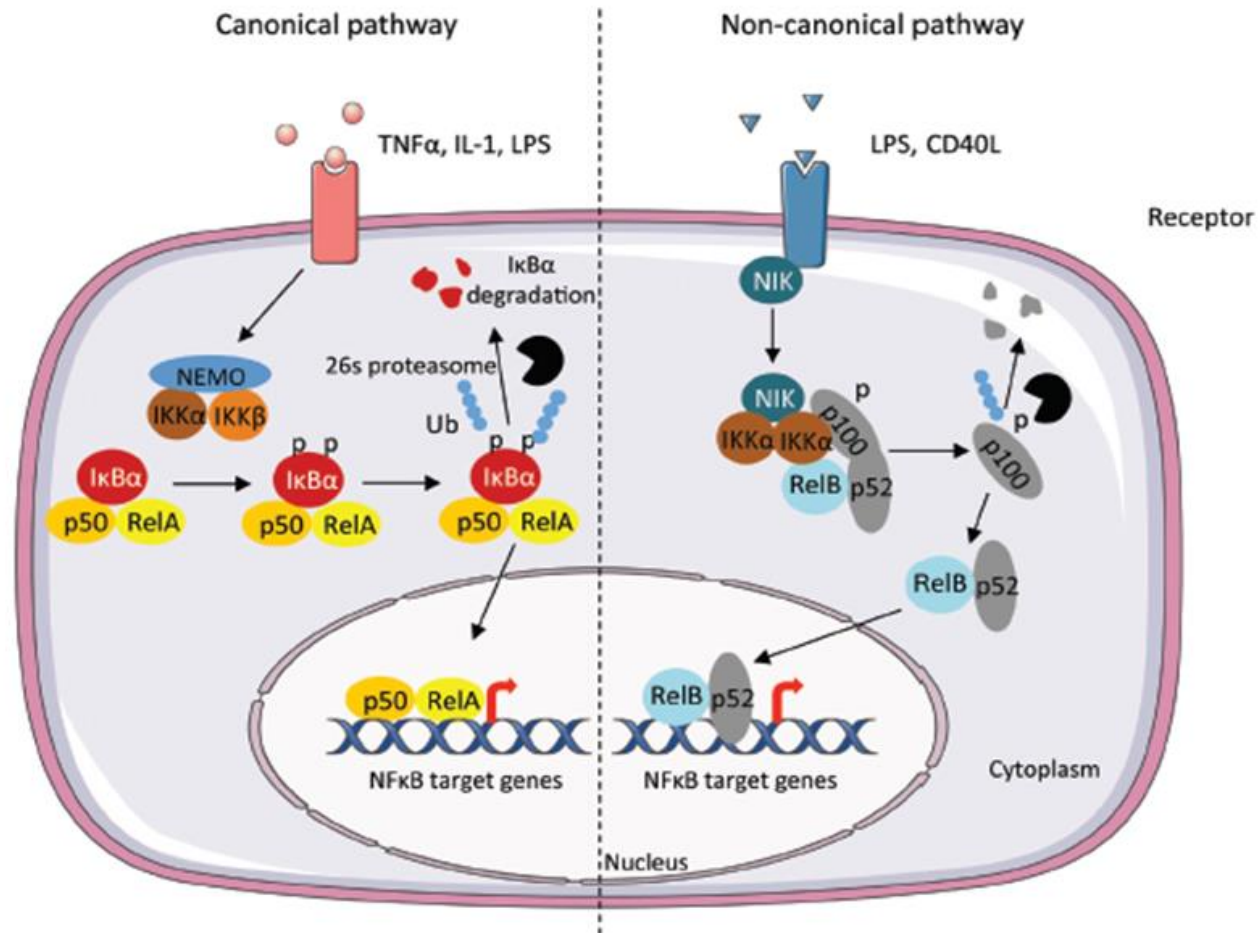


Figure 1.3: The canonical and non-canonical NFκB pathways. Activation of the respective pathways results in the phosphorylation (p) of inhibitory proteins followed by ubiquitylation (Ub) and subsequent proteasomal degradation. See text for more detail. (source: (Viennois et al., 2013))

I κ B kinases (IKKs)

IKK α shares a high degree of homology with IKK β with around 50% sequence identity and 70% structure similarity, both kinases contain a N-terminal kinase domain, a leucine-zipper domain for protein dimerization and a C-terminal helix-loop-helix (Hacker and Karin, 2006). Unlike IKK β that has primarily cytoplasmic functions, activated IKK α has additional important nuclear functions that can also be NF κ B- and kinase-independent.

IKK α nuclear and NF κ B independent roles

IKK α has been shown to have a role in regulating NF κ B independent gene expression in response to diverse signalling pathways and transcription factors including: PI3K/Akt, TGF β /Smad, ATM, PKC δ , Notch, Fox2/Numb, STAT3, p53, p73, ER α , AP-1 and E2F (Ozes et al., 1999, Yoshida et al., 2008, Yamaguchi et al., 2007, Fernandez-Majada et al., 2007, Marinari et al., 2008, Liu et al., 2012, Ammirante et al., 2010, Furuya et al., 2007, Park et al., 2005, Tu et al., 2006, Huang et al., 2012).

In the nucleus IKK α promotes gene expression by directly phosphorylating transcription factors such as p65 to enhance its DNA binding and transactivation (Jiang et al., 2003, Gloire et al., 2007), also by phosphorylating key epigenetic chromatin modifiers at the promoters of these genes to enhance expression, this includes: phosphorylation of histone H3 which opens-up chromatin structure (Yamamoto et al., 2003), phosphorylation of transcriptional coactivators such as CBP (CREB-binding protein) to enhance their activity (Huang et al., 2007) and phosphorylation of transcriptional repressors like SMART/HDAC3 complexes to suppress their activity (Gloire et al., 2007). It is important to note that activated nuclear IKK α has also been shown to have kinase independent functions in the regulation of epidermal keratinocyte differentiation and chondrocyte differentiation (Hu et al., 2001, Sil et al., 2004, Olivotto et al., 2015).

IKK α role in development

Knockout of IKK α in mice results in perinatal lethality (i.e. Immediately before birth or soon after birth), with the foetuses displaying thickened skin, stunted limbs, as well as skeletal and craniofacial deformities (Hu et al., 1999, Takeda et al., 1999). These morphological defects were subsequently revealed to be due to a disruption of proper epidermal–mesodermal interaction and to be independent of IKK α kinase activity and NF κ B activation (Sil et al., 2004). IKK α knockout mice were also described to show defective development of Peyer’s patch (lymphatic tissue in lowest part of small intestine) (Cildir et al., 2016). In comparison knockout of IKK β in mice are more severe, resulting in embryonal lethality (around day 14) and severe liver degeneration and apoptosis (Tanaka et al., 1999).

In humans, two cases of a lethal autosomal recessive syndrome characterised by severe fetal encasement malformations- similar to those occurring in IKK α knockout mice- were described in a consanguineous Finnish family (Lahtela et al., 2010). The fetal abnormalities included defective craniofacial development and seemingly absent limbs which were bound to the trunk and encased under the skin, as a result this syndrome is also known as “cocoon syndrome”. Genetic analysis revealed that it was caused by a homozygous missense mutation, in *CHUCK* that encodes for IKK α , which resulted in reduced expression levels of a truncated IKK α with a missing kinase domain. More recently a *de novo*- heterozygous- mutation in the *CHUK* gene, resulting in IKK α with an inactive kinase, was identified in patients with EEC/AEC like syndrome (Ectodermal dysplasia, Cleft lip/palate & Ankyloblepharon-Ectodermal defects-Cleft lip/palate) (Khandelwal et al., 2017). These patients display orofacial clefting, limb abnormalities, defects in the skin, hair and nails as well as immunodeficiency.

IKK α dysregulation in disease

A dysregulated role for IKK α has been reported in a variety of cancers including: prostate cancer, breast cancer, pancreatic cancer, colorectal cancer, gastric cancer, liver cancer and osteosarcoma (Fernandez-Majada et al., 2007, Park et al., 2005, Shiah et al., 2006, Hirata et al., 2006, Furuya et al., 2007, Huang et al., 2012). IKK α has also been identified to have a role in osteoarthritis (Olivotto et al., 2015), diabetes (Starkey et al., 2006) and fear memory (Lubin and Sweatt, 2007).

3.1 Role of IKK/NFκB activity in bone remodelling

3.1.1 Role of IKK/NFκB in osteoclastic bone resorption

The IKK/NFκB pathway plays an important role in osteoclast differentiation, activity and survival (Soysa and Alles, 2009). Early studies in mice show that deletions of *NFκB1* (encodes p105 precursor of p50) and *NFκB2* (encodes p100 precursor of p52) had increased bone volume due to lack of osteoclasts (Iotsova et al., 1997). Later studies showed that mice with IKKα deletion exhibited impaired osteoclast differentiation (Chaisson et al., 2004). Similarly, mice with deletion of RelB, a component of the NFκB non-canonical pathway, also showed impaired osteoclast differentiation (Vaira et al., 2008). Deletion of IKKβ in mice, were more pronounced, with mice displaying reduced osteoclast formation, which resulted in increased bone volume (Otero et al., 2010).

Pharmacological studies by our group have shown that combined inhibition of IKKα and IKKβ reduces osteoclastic bone resorption and prevents bone loss in mouse models of postmenopausal osteoporosis (Idris et al., 2009, Idris et al., 2010). Conversely, constitutive activation of the canonical NF-κB pathway resulted in RANKL independent osteoclastogenesis and severe bone loss in mice through a mechanism involving RelB and p52 (Otero et al., 2012, Otero et al., 2010)

3.1.2 Role of IKK/NFκB in osteoblastic bone formation

A number of studies have shown that the IKK/NFκB pathway negatively regulates osteoblast bone formation. Inhibition of the NFκB pathway using mutants deficient in IKKγ or with super IκBα repressor promoted osteoblast differentiation *in vitro* and promoted bone formation in mice (Chang et al., 2009). Selective inhibition of IKKβ increased osteoblast differentiation *in vitro* and bone formation *in vivo* (Alles et al., 2010).

3.1.3 Regulation of Wnt signalling by IKK/ NF κ B in bone homeostasis

Historically, the IKK/NF κ B pathway was not thought to be very important for osteoblast biology, this is in contrast to the crucial role of the IKK/NF κ B pathway in osteoclast differentiation and bone resorption function that was recognised early on (Novack, 2011). Indeed later work demonstrated that activation of IKK/NF κ B pathway inhibits osteoblast differentiation and bone formation function (Chang et al., 2009). The IKK/NF κ B pathway was shown to negatively regulate the Wnt signalling pathway in osteoblasts, which is important for osteoblast differentiation and function, (Chang et al., 2013, Marino et al., 2018). Wnt signalling, particularly canonical Wnt signalling which is dependent on β -catenin, promotes osteoblast differentiation and bone formation function whilst inhibiting osteoclast differentiation and osteoclast bone resorption (Krishnan et al., 2006). NF κ B pathway inhibition was established to enhance osteoblastic differentiation and function via its effects on enhancing Wnt/ β -catenin signalling (Chang et al., 2013, Marino et al., 2018).

In canonical Wnt signalling, in the absence of activation or in the presence of Wnt signalling antagonists (such as Dkks, sFRPs or SOST), β -catenin is constitutively phosphorylated in the cytoplasm by GSK3 β (glycogen synthase kinase 3 beta) which marks it for proteosomal degradation. Canonical Wnt activation occurs when activating Wnts (such as Wnt1, Wnt3a, Wnt10b) bind the frizzled receptor (a 7-transmembrane domain) and the lipoprotein receptor-related protein 5 and 6 (LRP5/6) coreceptors. The signal is then transduced through proteins including Disheveled, Axin, and Frat-1 that inhibit GSK3 β activity by its phosphorylation, this leads to the accumulation of β -catenin in the cytoplasm and eventually β -catenin is shuttled to the nucleus where it associates with the TCF/LEF transcription factors to activate the expression of Wnt regulated genes (Krishnan et al., 2006). Non-canonical Wnt signalling is independent of β -catenin and is not as well characterised as canonical Wnt signalling, nonetheless, non-canonical Wnt signalling activation by Wnt5a has been shown to enhance canonical Wnt signalling to promote osteoblast differentiation (Okamoto et al., 2014).

3.2 Role of IKK/NFκB in PCa cancer

3.2.1 Role of IKK/NFκB in PCa tumorigenesis

NFκB is a major effector in PCa pathogenesis, involved in tumour growth, survival, invasion and metastasis (Nguyen et al., 2014b). NFκB was shown to be constitutively activated in the advanced PCa cell line model, PC3, compared to the early stage PCa cell line model, LNCaP, and normal prostate epithelia (Gasparian et al., 2002). Increased nuclear localisation of NFκB-p65/p50 and phosphorylated IκBα was observed during PCa progression in transgenic adenocarcinoma of the mouse prostate (TRAMP) mouse model (Shukla et al., 2005). Nuclear NFκB localisation and IκBα phosphorylation was also associated with human PCa progression (Shukla et al., 2004). Moreover, an elevated expression of NFκB is observed in patients with CRPC (McCall et al., 2012).

Inhibition of the NFκB pathway, decreased PC3 invasiveness *in vitro*, this was associated with a reduction in pro-invasive factors such as VEGF and MMP-9 (Huang et al., 2001). Similarly, NFκB inhibition was shown to suppress epithelial to mesenchymal transition in PCa cells and suppress snail-dependent migration and invasion (Baritaki et al., 2009). Overexpression of NFκB enhanced the activation of CXCL12/CXCR4 pathway- known to be associated with PCa bone metastasis (Taichman et al., 2002)- and increased PCa cell adhesion and migration through endothelial cells which is one of the earliest steps in metastasis (Kukreja et al., 2005).

Blocking the NFκB pathway in PC3 increased susceptibility to apoptosis *in vitro* (Shukla and Gupta, 2004). Interestingly, the NFκB pathway is activated in PCa cells by exposure to radiation and chemotherapy (Chendil et al., 2002, Huang et al., 2001), this could be a survival mechanism that contributes to PCa resistance to these therapies (Nguyen et al., 2014b). Moreover, inhibition of NFκB has been demonstrated to sensitize PCa cells to radiotherapy and chemotherapy (Codony-Servat et al., 2013). Collectively, the NFκB pathway is an attractive anti-cancer target that can be used in conjunction with conventional therapeutic strategies.

3.2.2. Role of IKK/NFκB in PCa metastasis

Microarray analysis showed the NFκB pathway to be dysregulated in metastatic prostate cancer patients (Setlur et al., 2007). Activated nuclear NFκB was found to be significantly upregulated in PCa lymph node metastasis (Ismail et al., 2004). Furthermore, nuclear NFκB p65 subunit in primary tumours was found to be highly predictive of PCa lymph node metastasis (Lessard et al., 2006). NFκB pathway upregulation, evident by increased phosphorylation of IκBα, was associated with metastasis in CRPC patients (McCall et al., 2012). Moreover, NFκB was shown to increase AR expression, and both positively correlated with metastatic CRPC (Zhang et al., 2009).

Inhibition of NFκB in PC3 delayed occurrence of lymph node metastasis in orthotopic mouse models (Huang et al., 2001). Activation of NFκB through EZH2 silencing of the BAB2IP tumour suppressor was shown to be an important driver in PCa (lymphatic and bone) metastasis in mice (Min et al., 2010).

The NFκB pathway is significantly more active in the PCa cell lines known to cause bone metastasis, PC3 and C4-2B, than in the LNCaP cell line which does not normally cause bone metastasis. However, activating the NFκB pathway in LNCaP did induce bone metastasis when injected in mice, while inactivating the NFκB pathway in PC3 and C4-2B inhibited their ability to cause bone metastasis (Jin et al., 2013). PC3 cells lacking NFκB function could no longer promote osteolytic bone resorption when co-cultured with rat marrow cells on bone (Andela et al., 2003); bone resorption is thought to be necessary for PCa induced bone metastasis (Kavitha et al., 2014).

3.2.2.1 IKKα as a therapeutic target in PCa progression and bone metastasis

IKKα was shown to be more important in the development of PCa than IKKβ (Shukla et al., 2005, Nguyen et al., 2014b). A number of publications from Karin and colleagues investigated the role of IKKα in PCa. They showed that using an inactive IKKα mutant in TRAMP mice reduced PCa tumour growth, inhibited metastasis and increased expression of the tumour suppressor maspin (Luo et al., 2007). The ablation of maspin restored metastasis. IKKα, activated by RANKL, translocates to the nucleus

Chapter 1

General Introduction

to directly interact with the maspin promoter and inhibit its expression. Furthermore, in mouse and human PCa samples activated nuclear $IKK\alpha$ levels associated with metastatic progression, lower maspin expression and greater infiltration of inflammatory cells expressing RANKL. In another study, inactivating $IKK\beta$ in TRAMP mice prostate epithelia had no effect on PCa initiation and progression (Ammirante et al., 2010). A follow up study showed that $IKK\alpha$ activation of the transcription factor E2F1 and its downstream target Bmi1 enhanced survival and proliferation of prostate progenitor stem cells thought to be important in the emergence of a castration resistant subpopulation and development of CRPC (Ammirante et al., 2013). It is important to note that the mouse model used by Luo *et al.* does not generate bone metastasis, the metastases reported were in lymph nodes and internal organs.

Bortezomib was the first clinically approved 26S proteasome inhibitor developed to block the $NF\kappa B$ pathway as an anti-cancer agent (Richardson et al., 2005). In PCa, bortezomib had little or no reduction in the expression of most $NF\kappa B$ regulated genes, however, there was an increased $NF\kappa B$ p65 recruitment to the IL-8 promoter, increased IL-8 expression and increased $IKK\alpha$ nuclear localization (Manna et al., 2013). Increased IL-8 expression has been associated with PCa progression and metastasis (Singh and Lokeshwar, 2011). Inhibiting $IKK\alpha$ significantly reduced p65 recruitment to the IL-8 promoter and IL-8 expression (Manna et al., 2013). This indicates that inhibiting both $IKK\alpha$ and the proteasome may increase efficacy of using bortezomib in treating PCa.

Most of the drugs developed by the pharmaceutical industry to inhibit the $NF\kappa B$ pathway have targeted $IKK\beta$, however, these drugs have not proved successful in clinical trials (Verstrepen and Beyaert, 2014). Developing therapeutic inhibitors of the $NF\kappa B$ pathway by targeting $IKK\beta$ is limited by the fact that it can have detrimental systemic effects on innate immunity (Baud and Karin, 2009). Targeting $IKK\alpha$ is thought to be a safer therapeutic option as it is not essential for the canonical $NF\kappa B$ pathway and may therefore result in less serious side effects (Huang and Hung, 2013). However, $IKK\alpha$ might be a more effective anti-cancer target than $IKK\beta$ exactly because it is involved in both the canonical and non-canonical $NF\kappa B$ pathways, and it

Chapter 1

General Introduction

may in fact result in more adverse effects, which in a cancer setting may still be acceptable and warrants further investigation.

Aims of this study

The aim of this thesis is to establish if selective pharmacological inhibition of IKK α might be of value in the treatment of bone metastasis associated with prostate cancer.

I hypothesise that inhibition of IKK α in highly metastatic prostate cancer cells suppresses bone metastasis, reduces skeletal tumour growth and inhibits osteolytic bone damage in preclinical mouse models of advanced prostate cancer.

The specific aims of the work reported in this thesis are:

- To establish whether selective inhibition of IKK α kinase activity affects:
 - prostate cancer cell growth, migration and invasion *in vitro and in vivo*
 - prostate cancer cell ability to influence
 - osteoclast signalling and differentiation *in vitro and in vivo*
 - osteoblast signalling, differentiation and activity *in vitro in vivo*
 - osteoclast differentiation *in vitro*
 - osteoblast differentiation and activity *in vitro*

- To test the effects of a selective pharmacological inhibitor of IKK α kinase activity on cancer bone metastasis, skeletal tumour growth and osteolysis *in vivo*

CHAPTER TWO

Materials & Methods

2.1 Preparation of compounds tested

The structurally related IKK α kinase inhibitors: SU1257 (non-active control), SU1261, SU1349, SU1361, SU1411, SU1266 and SU1087; were kindly gifted to us by Prof Simon MacKay (University of Strathclyde; patented by the university of Strathclyde and CRUK). The IKK α inhibitors were dissolved in dimethyl sulfoxide (DMSO) at a concentration of 30 mM for all drugs except drugs SU1349 and SU1361 which were dissolved at 10mM. Serial dilutions of the IKK α inhibitors were made and stored at -20°C. Chemotherapy drugs: 5-fluorouracil, cyclophosphamide, doxorubicin, docetaxel, paclitaxel, tamoxifen and rapamycin were all purchased from Sigma-Aldrich (Dorset, UK) and dissolved in DMSO at 10mM according to manufacturer's instructions and stored at 4°C or -20°C, with the exception of cyclophosphamide which was prepared fresh by dissolving in DMEM at 100mM.

2.2 Tissue culture

2.2.1 Tissue culture medium

Human PC3 and LNCaP prostate cancer cells, human Saos2 osteosarcoma cells, mouse RAW264.7 osteoclast precursors and mouse 3T3L1 preadipocytes were cultured in DMEM + GlutaMAX supplemented with 10% FCS, 100 U/ml penicillin and 100 μ g/ml streptomycin (standard DMEM). Mouse calvarial osteoblasts, mouse osteoclasts, mouse bone-marrow cells, and mouse MC3T3 osteoblast precursors cells were cultured in α MEM + GlutaMAX supplemented with 10% fetal calf serum (FCS), 100 U/ml penicillin and 100 μ g/ml streptomycin (standard α MEM).

2.2.2 Cell culture conditions

Cell culture work was carried out in a laminar flow hood sprayed with 70% (v/v) ethanol before use. All solutions were pre-warmed to 37°C before use in cell culture work. Plastic ware was bought pre-sterilised or autoclaved prior to use. Standard conditions of 5% CO₂: 95% air at 37°C in a humidified atmosphere was used to maintain cell cultures. Phase-contrast microscopy was used to examine confluence of cell cultures.

2.3 Cancer cell line cultures

Human cancer cell lines used include: LNCaP (androgen sensitive adenocarcinoma cell line derived from prostate cancer lymph node metastasis in a male patient; AR+ and PSA+); C4-2 (androgen insensitive cell line derived from LNCaP lymph node metastasis after injection in castrated nude mice; AR+ and PSA+); C4-2B4 (androgen insensitive cell line derived from LNCaP bone metastasis after injection in castrated nude mice; AR+ and PSA+); PC3 (androgen independent neuroendocrine cell line derived from prostate cancer bone metastasis in male patient; AR- and PSA-) and PC3 clones (PC3-GFP, PC3-BT and PC3-NW1) that were kindly provided by Dr Ning Wang and Prof Colby Eaton (University of Sheffield) (Berish et al., 2018). The PC3 cell clones were harvested after intracardiac injection in mice and metastasis to bone, specifically: PC3-GFP is GFP labelled and harvested after metastasis to bone, the related PC3-BT has the same origin as PC3-GFP, however, it was harvested after three cycles of injection in mice and metastasis to bone, and PC3-NW1 is Luciferase labelled and harvested after metastasis to bone. Cancer cells were cultured in 75 cm² flasks and passaged every 48-72 hours at a ratio of 1:3 – 1:6 for all PCa cells used, culture medium was removed, the cells washed in PBS and were detached by addition of trypsin. The trypsin was inactivated by adding twice the volume of standard medium to the cells, which were then transferred to a fresh sterile 15 ml tube that was then centrifuged at 1200 rpm for 3 minutes. The supernatant was discarded, and 1 ml standard medium was added to suspend cells, before a fraction of the suspension was placed into a new 75 cm² flask containing 15 ml standard medium.

2.3.1 Conditioned medium preparation

PC3 cells were cultured in 6-well plates in standard medium and allowed to reach 80% confluence, before replacing medium with serum free medium. After 16 hours under standard culture conditions, the medium was then removed and filtered through a 0.2 µm filter to obtain conditioned medium. Serum free medium was also added to empty wells with no cancer cells to obtain a conditioned medium control.

2.3.2 Cancer cell line drug treatments

Human PC3 cells were seeded at density of 3000 cell/well of 96 well plates. After 24 hours under standard culture conditions, the media was replaced with either fresh standard or serum free DMEM with drug or vehicle control at desired concentration and a final total volume of 100-150 μ l. At the end of the experiment cell viability was assessed using the Alamar Blue assay.

2.3.2.1 Combinational treatments with chemotherapeutic agents

PC3 cells were seeded at density of 3000 cell/well of 96 well plates in 100 μ l standard media. After 24 hours the media was replaced with serum free media and treated with 1 μ M SU1349 and/or specific concentrations of chemotherapeutic agents in serum free media for 48-72hrs. At the end of the experiment cell viability was assessed using the Alamar Blue assay.

For synergy and dose reduction analysis. PC3 cells were treated with different concentrations of docetaxel for 24 hours in serum free media before additional treatments 0.45 μ M or 1.5 μ M SU1349 or vehicle and left 48 hours. At the end of the experiment cell viability was assessed using the Alamar Blue assay. The Alamar Blue values were used to calculate the combination index (CI) and dose reduction index (DRI) using ComboSyn software (www.combosyn.com).

2.4 Bone cell cultures

Osteoclast cultures

2.4.1 Isolation of bone marrow cells

Bone marrow cells (BM) were harvested from the tibia and femur of C57BL/6 female mice sacrificed aged 8-12 weeks. The hind limbs were dismembered using sterile scalpel and placed in tubes containing ice-cold PBS. In a hood, as much of the soft tissue was removed using a scalpel before the ends of the bone were cut off. The bone marrow cells were flushed out of the bone marrow cavity into a petri dish using a 5 ml syringe containing standard α MEM with a 25 gauge (G) needle attached. The BM cells in α MEM were passed through syringes with needles of decreasing size (19G-25G) to reach a single cell suspension. The suspension was centrifuged in a 15ml tube at 1200rpm for 3 minutes. The pellet was resuspended in 10mls of standard α MEM, it was then transferred to a fresh 100 mm petri-dish and cultured under standard conditions for 24 hours to allow attachment of stromal cells. The non-adherent cells were seeded in new plates for osteoclast formation experiments.

2.4.2 Osteoclast formation cultures

2.4.2.1 RANKL and M-CSF generated osteoclast cultures from mouse bone marrow cells

For osteoclast PC3 co-cultures, non-adherent total bone marrow cells were seeded in 96-well plate at 8×10^5 cells/well in 150 μ l of standard α MEM. After 24 hours PC3 cells at 200 cells/well were added. Cancer cells were allowed to settle for 6 hours before addition of 100 ng/ml RANKL, 10 ng/ml of M-CSF and drug treatments (SU1349 or vehicle) to avoid affecting cancer cell adherence. Cultures were maintained under standard conditions, while replacing 50% of the medium supplemented with fresh drug treatments, M-CSF and RANKL every 48 hours. The cultures were maintained for up to 7 days.

For osteoclast – conditioned medium co-culture, non-adherent cells from total bone marrow culture were plated in 96-well plates at 12×10^3 cells/well in standard α MEM. After 24 hours conditioned medium from PC3 cells (10% v/v), 100 ng/ml RANKL, 10

ng/ml of M-CSF and drug treatments (SU1349 or vehicle) were added to the bone marrow osteoclast precursors and were cultured under standard conditions, while replacing 50% of the medium supplemented with fresh conditioned medium, drug treatments, M-CSF and RANKL every 48 hours. The cultures were maintained for up to 7 days.

2.4.2.2 RANKL generated osteoclast cultures from RAW264.7 cells

RAW264.7 cells were plated at 2000 cells/well of a 96-well plate in 100 µl of standard DMEM. After 24 hours the cultures were supplemented with RANKL (50ng/ml) and drug treatments (SU1349 or vehicle). Treatments were refreshed after 48hrs by replacing 50% of culture medium and the experiment was terminated 72hrs after the first addition of RANKL. Osteoclasts were fixed and identified using Tartrate-resistant Acid Phosphatase (TRAcP) staining.

2.4.3 Characterisation and identification of osteoclasts

2.4.3.1 Culture fixation

Osteoclast culture media was removed, and the wells were washed twice with PBS to terminate cultures. Cells were fixed by incubating with 150 µl of 4% (v/v) paraformaldehyde in PBS for 10 minutes at room temperature. The paraformaldehyde was removed, and the cells were washed twice with PBS and stored at 4°C in 200 µl of 70% ethanol (v/v).

2.4.3.2 Tartrate-resistant Acid Phosphatase (TRAcP) staining

Osteoclasts were identified using Tartrate-resistant Acid Phosphatase (TRAcP) staining as described in (van't Hof et al., 1995, Marino et al., 2014). In brief, the fixed cells were incubated with 100 µl of TRAcP staining solution at 37°C for 45 minutes. The solution was then removed, and the cells were washed twice with PBS and stored at 4°C in 200 µl of 70% ethanol (v/v). A Leica DMIL light microscope using a 10x and 20x objective lens was used to count TRAcP positive cells (TRAcP+) with 3 or more nuclei as osteoclasts.

2.4.4 Osteoblast cultures

2.4.4.1 Isolation of primary osteoblasts

Primary osteoblasts were harvested from calvarial bones of 2-day-old mice by sequential collagenase digestion. The calvaria were first washed in Hank's balanced salt solution (HBSS) before incubating in a tube containing 2 ml of collagenase type 1 (1 mg/ml) in HBSS for 10 minutes at 37°C with frequent agitation. The supernatant was discarded and 4ml of fresh collagenase type 1 (1mg/ml in HBSS) was added to the calvariae and it was further incubated for 30 minutes. 6 ml of standard α MEM was mixed with the resultant cell suspension (fraction 1). The remaining calvarial tissue was washed in PBS and incubated with 4 ml of 4 mM ethylenediaminetetraacetic acid (EDTA) in PBS at 37°C for 10 min in a water bath with constant agitation. Another 6 ml of standard α MEM was mixed with the resultant cell suspension (fraction 2). Fraction 3 was obtained by adding 4 ml of collagenase type 1 (1 mg/ml) in HBSS to the remaining calvarial tissue and incubated for 20 min at 37°C with constant agitation. The three fractions were combined together and centrifuged at 1200 rpm for 3 minutes. After discarding the supernatant, the pellet was resuspended in standard α MEM and cultured in a 75cm² flask under standard conditions at a density of 3 calvariae per flask. After 24 hours the medium was changed to leave behind only adherent cells and the media was refreshed every 48 hours thereafter until confluence was reached.

2.4.4.2 Passage of primary osteoblasts

Primary osteoblasts were detached from 75cm² culture flasks by incubating with 4 ml of trypsin for 3 minutes at 37°C and this was confirmed microscopically. The trypsin was then inactivated by adding 8 ml of standard α MEM to the flask. The cell suspension was then transferred to a 15 ml tube and centrifuged at 12000 rpm for 3 minutes. The pellet was resuspended in standard α MEM before plating in 96-well plate at 8×10^3 cells/well in 150 μ l or in 12-well plate 3×10^5 cells/well in 1 ml of standard α MEM.

2.4.5 Mouse calvarial osteoblast cultures

For assessment of differentiation, mouse calvarial osteoblasts were seeded in 96-well plate at 8×10^3 cells/well in 150 μ l of standard α MEM. After 24 hours the culture wells

Chapter 2

Materials & Methods

were treated with SU1349 or vehicle and left for 48 hours before cell viability was assessed by the Alamar Blue assay and the wells were lysed in preparation for the alkaline phosphatase assay.

For assessment of bone nodule formation, mouse calvarial osteoblasts were seeded in 12-well plate at 3×10^5 cells/well in 1 ml of standard α MEM. Upon reaching confluence the media was changed to osteogenic α MEM media supplemented with 1% foetal bovine serum, 50 ng/ml ascorbic acid, 2mM β -glycerophosphate and drug treatment (SU1349 or vehicle). Cultures were maintained under standard conditions, while refreshing culture medium every 48-72 hours. The cultures were maintained for up to 21 days.

2.4.6 Saos2 cultures

Saos2 cells were seeded in 24-well plates at 1.5×10^5 cells/well in 1 ml of standard DMEM media. Upon reaching confluence the media was changed to osteogenic DMEM media containing 1% foetal bovine serum and where indicated media was supplemented with 50 ng/ml ascorbic acid and 2mM β -glycerophosphate. Additionally, the Saos2 cultures were treated with PC3 conditioned media 20% (v/v) or serum free control DMEM and/or drug treatments (SU1349 or DMSO vehicle). Treatments were refreshed every 48-72hr for 10-21 days. At the end of experiments cell viability of culture wells were assessed by the AlamarBlue assay before proceeding with lysis of wells for alkaline phosphatase assay or fixing of wells for Alizarin red staining.

2.4.7 MC3T3 cultures

MC3T3 cells were seeded in a 24-well plate at 1.5×10^5 cells/well in 1 ml of standard α MEM media. Upon reaching confluence the media was changed to osteogenic α MEM media supplemented with 1% foetal bovine serum, 50 ng/ml ascorbic acid and 2mM β -glycerophosphate. Additionally, The MC3T3 cultures were treated with PC3 conditioned media 20% (v/v) or serum free control α MEM and/or drug treatments (SU1349 or DMSO vehicle). Treatments were refreshed every 48-72hr for up to 21 days. At the end of experiments cell viability of culture wells were assessed by the

AlamarBlue assay before proceeding with lysis of wells for alkaline phosphatase assay or fixing of wells for Alizarin red staining.

2.4.8 Alkaline phosphatase assay

Osteoblast differentiation was determined using the Alkaline phosphatase (ALP) assay. The assay measures the rate of conversion of colourless p-nitrophenol phosphate into yellow coloured p-nitrophenol by spectrophotometry. The measured absorbance values are proportional to alkaline phosphatase enzyme levels that are expressed at higher levels by osteoblast during differentiation.

At the end of osteoblast differentiation experiments, cell culture wells were rinsed with PBS before being incubated with lysis buffer (Appendix table 2.2) at 150 μ l for 96-well plate cultures or 500 μ l for 24-well plate cultures for 20 minutes. Serial dilutions of p-nitrophenol (0 – 30 nM) were used to create a standard curve. 50 μ l of the standard solutions and lysates samples were plated in duplicates in a fresh 96-well plate and an equal amount of substrate solution was added. A Biotek Synergy HT plate reader was used to measure the absorbance and the readings were made at 414 nm at 37°C every 5 minute for 30 minutes. The slope of the linear part of the kinetic curve generated was used to quantify ALP activity and this was expressed as fold change over control. Where appropriate, cell numbers as determined by Alamar Blue assay was used to normalise Alkaline Phosphatase activity (section 2.9).

2.4.9 Bone nodule formation assay

Osteoblastic bone nodule formation function was assessed by Alizarin Red S staining and quantification. Alizarin Red S binds to calcium deposits found in the mineralized extracellular matrix produced by osteogenic cells, which precipitates and forms brick-red deposits (Chang et al., 2000, Coelho et al., 2000).

At the end of experiments osteogenic cultures were fixed in 70% ethanol (v/v). Alizarin Red S staining solution was made fresh to a final concentration of 40mM in distilled water and the pH was adjusted to 4.1-4.3 using ammonium hydroxide. Fixed osteogenic cultures were washed with PBS and incubated at room temperature with 1 ml of Alizarin Red S staining solution for 20 minutes with gentle agitation on a rocker. The staining solution was removed, and culture wells were washed with distilled water

until water runs clear before removing water and allowing plates to dry overnight. The culture wells were scanned, and staining was quantified by ImageJ as described in Shah *et al.*, (Shah et al., 2016).

2.4.5 Adipocyte cultures

2.4.5.1 3T3-L1 adipocyte cultures

3T3-L1 preadipocytes cells were seeded at 2×10^5 cells/well of 24 well plate in 1ml of standard DMEM. 48hrs post confluence the media was changed to differentiation media containing standard DMEM supplemented with 0.5mM IBMX, 1 μ M dexamethasone and 1 μ g/ml insulin, plus/minus PC3 conditioned media 20% (v/v) or drug treatments (SU1349 or DMSO vehicle). After 48hrs the differentiation media was replaced with maintenance media containing standard DMEM, insulin (1 μ g/ml) and PC3 conditioned media or drug treatments. 50% of the media was replaced with fresh maintenance media plus experimental treatments every 48-72hrs for 14 days. The viability of cultures wells was assessed by the AlamarBlue assay before fixing wells in preparation of oil red staining.

2.4.5.2 3T3-L1 adipocyte Oil red staining and quantification

0.3 % Oil Red O stock solution was prepared in isopropanol in advance. Cell cultures were fixed in 10% formalin for at least 30 minutes. The cells were then washed twice in PBS and incubated in 60% isopropanol for 5 minutes. In the mean while Oil Red O staining solution was freshly prepared by diluting 3 parts Oil Red O stock solution to 2 parts of distilled water. The 60% isopropanol solution was removed before incubating culture wells in Oil Red O staining solution for 30 minutes. The solution was removed, and the culture wells were washed in water several times until water runs clear. The culture wells were allowed to completely dry before destaining with 250 μ l with 100% isopropanol for at least 10 minutes. Absorbance of destained sample was measured at 490-520nm.

2.5 Molecular Biology techniques

2.5.1 Preparation of Luria-Bertani (LB) broth

20 g of LB broth was dissolved in 1 litre of distilled water, autoclaved and ampicillin (for IKK α overexpression construct) added to the cooled media at a final concentration of 100 μ g/ml.

2.5.2 Preparation of LB/ampicillin agar plates

40g of agar powder was dissolved in 1 litre of distilled water, which was then autoclaved and then cooled at room temperature to approximately 50°C before adding ampicillin at 100 μ g/ml, and then about 20 ml of LB agar media was poured into 150mm petri dishes and left to set and was stored at 4°C.

2.5.3 Bacterial transformation

5 μ l of IKK α overexpression or GFP vector DNA was used to transform bacteria using the One Shot TOP10® Chemically competent E.coli system (Invitrogen) as per manufacturer's instructions. The resultant bacterial cultures were grown overnight at 37°C on selective agar plates, single colonies were picked the next day for expansion in LB broth culture.

2.5.4 Preparation of broth culture

LB bacterial growth medium was prepared using 10 μ l of 100mg/ml of ampicillin (for IKK α overexpression construct) or carbenicillin (for IKK α ShRNA knockdown constructs) in 1 L of broth culture. A freshly picked bacterial colony from an agar plate or ~5 μ l of bacterial glycerol stock was used to inoculate 100 ml of LB broth in a 500 ml conical flask. The flasks were covered with foil and left overnight at 37°C in a shaking incubator at 300rpm for the bacteria to grow. The next day, a High Speed QIAGEN Midi prep kit was used to recover DNA from the bacterial cultures according to manufacturer's instructions. The recovered DNA was quantified using NanoDrop™ and stored at -20°C until further use. Also, some of the LB culture was set aside to prepare glycerol stocks by adding 150 μ l of glycerol to 850 μ l of bacterial suspension in a 2 ml cryogenic vial and stored at -80°C.

2.6 Retroviral gene delivery

2.6.1 IKK α overexpression constructs

The IKK α gene was overexpressed in human PC3 prostate cancer using a lentiviral delivery system. The IKK α overexpression construct and a GFP control construct were kindly provided by Dr Yousef Abu-Amer (Washington University School of Medicine). The constructs used a pMXs vector with a puromycin selection cassette. Construct DNA was adsorbed onto paper and recovered by incubating with 100 μ l of MilliQ water at 37°C for 30 min, it was then quantified using NanoDrop™ and stored at -20°C.

2.6.2 Short Hairpin RNA (shRNA)

A vector-based short hairpin RNA (shRNA) method was used to generate knockdowns of IKK α expression in human parental PC3 prostate cancer cells. Three TRC human individual clones (TRCN-504, -505 and -506) and one empty vector control were supplied in glycerol (Thermo Scientific, Germany) ready for expansion in LB broth culture before use in transfection of PC3 cells.

2.6.3 Kill curve and Puromycin selection

Cells were plated 3000 cells per well in 96 well plate. Puromycin (ThermoFisher) was prepared in standard medium at 0, 0.25, 0.5, 0.75, 1, 1.5 and 2 μ g/ml. The growth media was replaced with media containing serial dilutions of puromycin and incubated at 37°C for 48 hours. The viability of cells was measured using the AlamarBlue assay and the percentage of cell survival was calculated. The minimum antibiotic concentration that kills 100% of the cells was found to be 1 μ g/ml and was subsequently used to select for successfully transfected cells.

2.6.4 Retroviral transfection

On day 1, HEK293ET cells were seeded (25 x 10⁵ cells per T25 flask) in 5 ml of medium and allowed to grow overnight. By day 2 cells should have reached ~80% confluence and the media was changed at least 5 minutes before transfection reagents were added. Transfection mixture was prepared with 5 μ g of vector DNA, 5 μ g of gag and pol DNA, 5 μ g of pMD2.G vector, 40 μ l of polyethylenimine (PEI) transfection reagent and 450 μ l of standard DMEM medium. After gently aspirating 5 ml of the

culture media, 5 ml of the transfection mixture was added to the flask and cultured under standard conditions. On Day 3, HEK293ET cells media was again changed and the recipient PC3 cells were seeded at a density of 7.5×10^5 PC3 cells per T75 flask. On day 4, the viral supernatant was collected and briefly centrifuged, before taking 1 ml (containing the virus; back up 1 ml aliquots were also stored at -80°C) and adding it to 10 μl of 5 $\mu\text{g/ml}$ polyberene (Sigma-Aldrich) and 9 ml of standard DMEM, the mixture was then filtered through a 0.45 μm low protein binding filter before adding it to the recipient PC3 cells. On day 5, the medium for the recipient PC3 cells was replaced with selection medium of standard DMEM plus 1 $\mu\text{g/ml}$ puromycin. The transfected PC3 cells were maintained in selection for at least two passages. The efficiency of the IKK α knockdown or overexpression was determined by western blot analysis.

2.7 Alamar Blue assay

Alamar Blue assay exploits a nontoxic dye containing resazurin which is blue in colour and non-fluorescent when in an oxidized state, that is taken up and reduced by metabolically active cells to resorufin which is red in colour and fluorescent. The degree of change in colour/fluorescence is proportional to the number of metabolically active viable cells. Cell viability is measured by adding the AlamarBlue reagent (10% v/v) in a hood at the end of the culture period to each well. Cell cultures were left for 3 hours in standard culture conditions, after which fluorescence was measured (excitation, 530 nm, emission 590 nm) using a SpectraMax® M5 microplate reader. To correct for background fluorescence, AlamarBlue was also added to wells containing standard media and no cells or treatments.

2.8 Migration assays

The wound healing assay was used to measure 2D directional migration of PC3 cells transfected with mock or IKK α knockdown constructs. PC3 cells were plated at 200×10^3 cells/well of 24-well plate in standard DMEM. After 24 hours, the confluent monolayer was scratched using a P10 pipette tip, the wells were washed at least 3 times to remove any cell debris and replaced with serum free DMEM. The IKK α inhibitor solubilised in serum free DMEM was added to some of the wells and the plate was

Chapter 2

Materials & Methods

placed in humidified microscope maintained at 37°C and 5% CO₂. Migration was monitored for up to 12 hours with a Leica AF6000 Time Lapse imaging system. Images were captured sequentially at 15-minute intervals. The T scratch software was used to calculate percentage wound closure.

For random migration assay, PC3 cells were plated in 24 well plates (1x10³ cells/well). Cells were pre-treated with vehicle or SU1349 (1µM) for 3 hours. Migration of 30-50 individual cells per well was monitored for 8 hours with a Leica AF6000 Time Lapse microscope with images captured sequentially at 15-minute intervals. Cell velocity and accumulated distance travelled by cells (total track length) were measured using the Chemotaxis and Migration tool in ImageJ.

2.9 Invasion assays

Growth factor reduced matrigel was defrosted on ice and diluted to a concentration of 1.5mg/ml using ice-cold serum free DMEM and pre-cooled (in -20°C freezer) pipette tips. 20 µl of diluted matrigel was used to coat Corning™ transwell inserts which was inserted over a 24-well tissue culture plate. The matrigel coated inserts were allowed to dry in the incubator at 37 °C for at least 3 hours. 500 µl of DMEM containing 10% foetal bovine serum was added to the bottom of the tissue culture wells, while PC3 cells at 50 x 10³ in 200 µl in serum free DMEM plus drug treatment was carefully added to the top of the insert. The culture plates containing the insert were placed in the tissue incubator under standard culture conditions for 72hrs. At the end of the experiments the matrigel on top of insert mesh containing non-invading cells was carefully removed using a cotton swab. The cells were quickly fixed in 100% ethanol for 5 minutes, followed by staining by incubating in eosin for 1 minute and haematoxylin for 5 minutes (briefly washed in water after each stain). The inserts mesh was removed using a scalpel and mounted using DPX on glass slides. At least five non-overlapping colour images of each insert at 20x magnification were taken on a Leica AF4000 microscope and the average count was analysed using ImageJ.

2.10 WESTERN BLOT

Western blot was used to measure protein expression in cells as previously described in (Idris, 2012).

2.10.1 Preparation of cell lysates

For prostate cancer cells, cells were plated in 6-well plate at $3-6 \times 10^5$ cells/well in standard medium until 80% confluence was reached. Before harvesting cells were incubated in medium with or without serum for 16 hours.

For RAW264.7 and MC3T3 signalling experiments cells seeded at 1.5×10^5 cells/well in 12-well plates. After 48hrs, cells were pre-treated with vehicle or SU1349 for 1 hour in serum free media before stimulation with PC3 conditioned media 20% (v/v) for 10-15 min or before stimulation with 150 ng RANKL for 5-10min.

After cells were exposed to their conditions for the desired period of time the medium was then discarded, and ice-cold PBS was used to wash the cell monolayer before cells being gently scraped in 80-100 μ l of RIPA lysis buffer (appendix table 2.3) with 2% (v/v) protease inhibitor cocktail and 0.4% (v/v) phosphatase inhibitor cocktail and left on ice for 5 minutes. The cell lysate was transferred to a new eppendorf tube and centrifuged at 14000g for 10 minutes at 4°C. The supernatant fraction of proteins was collected and stored at -20°C until further use.

For studies involving cytoplasmic/nuclear fractionation, RAW264.7 and MC3T3 cells were seeded at 3×10^5 cells/well in 6-well plates. After 48hrs, cells were pre-treated with vehicle or SU1349 for 1 hour in serum free media before stimulation with PC3 conditioned media 20% (v/v) for 45 minutes. The monolayer was washed in ice cold PBS before scrapping in 100 μ l of Cytoplasmic lysis buffer (Appendix table 2.3) supplemented with protease and phosphatase inhibitor for up to 10 minutes until the cytoplasmic wall is lysed as observed on a microscope. The lysates were then centrifuged at 800 x g for 5 minutes at 4°C and the supernatant containing the cytoplasmic fraction was stored at -20°C for later use. The pellet was washed three time in ice-cold cytoplasmic lysis buffer and centrifuged at 800 x g for 5 minutes at 4°C after every wash. The pellet was then resuspended in 50 μ l of complete RIPA

buffer and centrifuged at 14000g for 10 minutes at 4°C. The supernatant corresponding to the nuclear fraction was collected and stored at -20°C for later use

2.10.2 Measuring protein concentration

Protein concentration was measured by the bicinchoninic acid (BCA) Pierce protein assay (Pierce, USA). Serial dilutions of bovine serum albumin (BSA) standards (0-2000 µg/µl) were used to generate the standard curve. 10 µl of standard BCA dilution standards and protein samples (1:5 diluted in H₂O) were plated in duplicates in a 96-well plate, and to each well 200 µl of BCA solution (made of copper sulphate diluted in bicinchoninic acid at 1:50) was added. The plate was incubated for 15-30 minutes at 37°C. The absorbance was then measured at 562 nm on a DYNEX MRX II microplate reader and the BSA standard curve was used to calculate the protein concentration in each sample.

2.10.3 Gel electrophoresis

Criterion™ XT BioRad (12% Bis-Tris) pre-cast gels were positioned into a vertical electrophoresis tank filled with TGS running buffer. A 5X sample loading protein buffer was mixed with cell lysates (50-100 µg) then heated at 95°C for 5 minutes, before loading into the pre-cast gel wells. Magic Marker XP western standard and Kaleidoscope pre-stained standard were used to identify molecular weights. Gels were run at constant voltage of 150-180V for 45 minutes to 1 hr and 45 minutes.

2.10.4 Electrophoretic transfer

The proteins resolved on the polyacrylamide gel were transferred to a polyvinylidene difluoride (PVDF) membrane (Hybond™-P membrane, Amersham). The PVDF membrane was first activated in 100% methanol and then allowed to equilibrate in transfer buffer for 5 minutes. The gel and PVDF membrane were sandwiched between two thick blotting paper pads pre-soaked in transfer buffer and placed in the transfer apparatus at a constant current of 90 mA for 2.5 hours.

2.10.5 Immunostaining and antibody detection

The PVDF membrane was incubated at room temperature on a rocker for 1 hour in 5% milk solution (w/v dried non-fat milk in TBST) to block non-specific antibody binding sites. The membrane was then washed in Tris buffer saline solution with 0.1% (v/v)

Chapter 2

Materials & Methods

Tween 20 (TBST) for 10 minutes 3 times and incubated overnight at 4°C on a rocker with the primary antibody (at 1:1000 in 5% BSA in TBST). The following day, TBST was used to wash the membrane 3 times for 10 minutes and the membrane was then incubated with the HRP-conjugated secondary antibody (at 1:10000 in 5% milk in TBST) for 1 hour at room temperature. The membrane was washed again with TBST for 10 minutes and this was repeated 3 times, before visualising on a Chemidoc Imaging system (BioRAD) using Clarity™ western ECL substrate (Bio-Rad) chemiluminescent detection system. Native and phosphorylated proteins were detected using rabbit antibodies IKK α , phospho-p100, p100, p52, phospho-I κ B, I κ B, β -catenin, GSK3 β and phospho-GSK3 β , (1:1000 dilution, Cell Signalling Technology, USA). Bands were quantified using Image Lab Software (BioRAD) and levels of Actin or GAPDH (Sigma-Aldrich, UK) were used for normalization.

2.11 Microarray of PC3 conditioned media

PC3 cells were seeded at 3×10^5 cells/well in 6 well plate. After 24 hours the cells were incubated for 16 hours with vehicle or 1 μ M SU1349 in serum free medium. Conditioned medium was collected and protein expression in the conditioned medium was measured with the Proteome Profiler Human XL Cytokine Array Kit by R&D systems as per manufacturer's instructions. The arrays were analyzed following chemiluminescent detection on a Chemidoc Imaging system (BioRAD).

2.12 Animal work

All procedures involving mice and their care were approved by and performed in compliance with the guidelines of Institutional Animal Care and Use Committee of Universities of Sheffield (England, UK) and L'Aquila (L'Aquila, Italy), and received institutional approval and conducted in conformity with laws and policies (UK Home Office and Italian authorities). *In vivo* experiments were performed by our collaborators: Marco Ponzetti and Prof Nadia Rucci in L'Aquila (Italy). MicroCT and bone histomorphometry was done in Sheffield.

2.12.1 *In vivo* experiments

BALB/c nu/nu mice were obtained from Charles River (Milan, Italy). 4-week-old male BALB/c nu/nu athymic mice were anesthetized with intraperitoneal injections of pentobarbital (60 mg/kg). 1×10^5 of luciferase expressing PC3 cells in 0.1 ml of PBS were intra-cardiacaly injected -into the left ventricle- using a tuberculin syringe with a 271/2G needle. Dosage and treatment regimen was based on previous data from Prof Simon MacKay (University of Strathclyde, UK; personnel communication). Animals were divided into two groups (8 animals per group) and received intraperitoneal injection of 150 μ l solution of SU1349 dissolved in mannitol at 20mg/kg 3x-weekly or vehicle control (see appendix 2.7). Animals were monitored daily for cachexia (evaluated by body weight waste), behaviour and survival. The development of metastasis was monitored by Bioluminescence imaging and X-ray analysis (36 KPV for 10 seconds) using a Cabinet X-ray system (Faxitron model n.43855A; Faxitron X-Ray Corp., Buffalo Grove, IL, USA) and IVIS SpectrumCT In Vivo Imaging System (PerkinElmer, UK). Radiographs were scanned using the Bio-Rad scanning densitometer (Hercules, CA, USA), model GS800, and quantification of the area of interest was done using the Bio-Rad Quantity One image analysis software to quantify tumour size. Animals were sacrificed by carbon dioxide inhalation 40 days after intra-cardiac injection, or earlier if they displayed signs of serious distress. At the end of the experiment animals were subjected to anatomical dissection to remove the hind legs and were fixed in 4% paraformaldehyde (v/v) in PBS.

2.12.2 Micro-computed tomography*

Bone volume and architecture of mouse tibia was assessed by microcomputer tomography (μ CT). The bone samples were wrapped in parafilm (to prevent desiccation) and placed in a 2 ml syringe (with both ends cut). This was then placed *ex vivo* into the μ CT scanner (SkyScan), then scanned after being fixed in an upright position on a platform within the scanner. The x-ray radiation source was set to 60kV and 150 μ A using the SkyScan. A 180° scan with a rotation step of 0.6 degrees was used using a 0.5 mm aluminium filter. The pixel size was set at 9 μ m for scanning mouse tibia. 3D image stacks were produced by reconstructing the data from the rotation image projections using the NRecon software (SkyScan). For trabecular bone measurements were taken near the proximal tibial metaphysis, 500 frames distal to the growth plate at baseline were chosen for reconstruction. For cortical bone, measurements of 100 frames situated 700 frames distal to the reference line, of the proximal diaphysis were selected for reconstruction. The parameters for reconstruction are shown in Table 2.1.

Table 2.1: Reconstruction parameters used in NRecon software

Parameter	Description	Setting
Smoothing	Removes noise and smoothes images	Width of 1 pixel
Beam Hardening factor correction	Corrects for the absorption of lower energy x-ray on the outside of specimen	9 %
Ring correction level	Corrects for the non-linear behaviour of pixels causing ring artifacts	3

Analysis of the reconstructed images were done using the CTAn software by SkyScan. A free-hand drawing tool was used to select the region of interest (ROI) at 3-7 different levels, and the software used auto-interpolation between these levels produced the total ROI.

For trabecular bone, the point where the calcified cartilage ridges of growth plate fuse together was set as the reference line. At 200 frames distal to the reference point,

measurements were performed, 5 μ m apart, in trabecular bone specified by ROI. For cortical bone analysis, ROI was selected by an 8-figure drawing, which comprised only the cortex as a hollow tube. Measurements for 3D-reconstruction were performed on all 100 frames selected previously. A total bone analysis at the cortical level was also performed on these reconstructed frames. The analysis parameters for 3D-reconstruction are shown in Table 2.2.

Table 2.2: 3D reconstruction parameters used in CTAn software

Parameter	Description	Setting
Smoothing	Smooths images and removes noise	Median filter; 2D space, radius 1
Threshold	Segments the foreground from background to binary images	Global; low level 100, high level 255
Despeckle	Removes speckles from binary images	Image; remove white speckles <150 voxels
3D-Model	Creates a 3D surface from binary images	Adaptive rendering; file saved as .p3g
3D-Analysis	Calculates 3D parameters of binary images	Requested for basic values, trabecular thickness, number and separation

Analysis was performed on trabecular bone volume, trabecular thickness, trabecular separation, trabecular number, trabecular porosity and trabecular pattern factor as shown in Table 2.3. Cortical bone analysis was performed on cortical bone volume, cortical thickness, cortical diameter, and cortical porosity. All calculations were saved as .csv files. 3D models of tibia were visualised using the CTVol software by SkyScan.

Table 2.3: 3D bone analysis parameters calculated by μ CT

Parameter	Abbreviation (unit)
Trabecular bone volume fraction	BV/TV (%)
Trabecular bone volume	Tb. BV (mm ³)
Trabecular Thickness	Tb.Th (μ m)
Trabecular Separation	Tb.Sp (μ m)
Trabecular Number	Tb.N (1/mm)
Trabecular Porosity	Tb.Po (%)
Trabecular Pattern factor	Tb.Pf (1/mm)
Cortical bone volume fraction	BV/TV (%)
Cortical bone volume	Ct.BV (mm ³)
Cortical Porosity	Ct.Po (%)

** microCT methods sections were based on the theses of previous students in our group: Silvia Marino and Antonia Sophocleous*

2.12.3 Bone histomorphometry

Fixed mouse tibia were washed in PBS then decalcified with EDTA (pH 7.2) on a gentle rocker at 4°C for 1 month, the decalcification solution refreshed three time weekly. Bone samples underwent different stages of dehydration with ethanol dilutions and defatting with xylene as shown in Table 2.4.

Table 2.4: Stages and reagents for Leica tissue processor programme

Stage	Reagent	Time (hours)
1	70% Ethanol	02.00
2	95% Ethanol	02.00
3	100% Ethanol	02.00
4	100% Ethanol	02.00
5	100% Ethanol	02.00
6	Xylene	04.00
7	Xylene	04.00
8	Paraffin Wax	02.00
9	Paraffin Wax	02.00

Fixed mouse tibia were washed in PBS then decalcified with EDTA (pH 7.2) on a gentle rocker at 4°C for 1 month, the decalcification solution refreshed three time weekly. Bone samples underwent various stages of dehydration following the procedure summarize in Table 2.4, the samples were placed in freshly prepared paraffin-based infiltration solution for 4 hours at 60°C then embedded in moulds with paraffin wax. Sections of 4 µm were cut using a Leica microtome, at least 3 non-consecutive sections were collected every interval of 20 µm and mounted on glass slides. Randomly selected cross sections from each sample were stained with tartrate-resistant acid phosphatase (TRAcP) and counter staining with haematoxylin. TRAcP staining was performed using standard methods as follows:

Chapter 2

Materials & Methods

1. De-wax the sections in xylene twice for 5 minutes each
2. Rinse in 100% ethanol twice for 5 minutes each
3. Rinse in 95% IMS (industrial methylated spirit) for 5 minutes
4. Rinse in 70% IMS for 5 minutes then deionized water for 1 minute
5. Stain sections with TRAcP staining solution (see details in Appendix 2.5) for 20 minutes at 37°C
6. Rinse sections in water stain in haematoxylin solution for 20 seconds
7. Rinse in deionized water for 2 minutes
8. Rinse in 70% IMS for 10 seconds
9. Rinse in 95% IMS for 10 seconds
10. Rinse in 100% ethanol twice for 30 seconds each
11. Immerse in Xylene for 3 minutes
12. Mount in DPX

The Osteomeasure software was used for histomorphometry analysis of bone sections which was performed on trabecular and cortical bone 200µM distal from the growth plate at 20x magnification.

2.12.4 Tissue microarray staining

Prostate cancer tissue microarray (PR242b, US Biomaz Inc.) was stained using the following protocol (done by Anne Fowles):

1. The pre-treatment module was pre-heated to 85°C and PBST was warmed to 35°C.
2. Dewax sections and hydrated in 95% ethanol
3. Block endogenous peroxidase with 3% H₂O₂ for 15 minutes.
4. Quench sections in water then place in pre-warmed pre-treatment module in warm PBST.
5. Retrieve antigen in citrate buffer (see appendix 2.6) for 10 minutes at 80°C and collect in warm PBST.
6. Block with 5% normal goat serum for 1 hour for rabbit antibodies or 2.5% horse serum for 30 minutes for mouse antibodies.
7. Incubate in primary antibody (mouse anti-IKKα monoclonal-antibody at 5mg/ml (Novus Biologicals)) overnight in the cold room. Wash three times in PBST.
8. Incubate with secondary SS Boost (Cell Signalling) kit for rabbit antibodies or IMPRESS reagent (Vector) for mouse antibodies for 30 minutes. Wash three times in PBST.

Chapter 2

Materials & Methods

19. Apply DAB (from kit) 1 drop in 1 ml. wait for ~ 3 minutes. Wash in water and counterstain in Haematoxilin.

2.13 STATISTICAL & DATA ANALYSIS

All statistical analysis was done using GraphPad Prism version 6.0. Student's T test was performed to determine the significance level of differences between two sets of results. For multiple comparison between groups analysis of variance (ANOVA) followed by a post-hoc test. A p- value of 0.05 or below was considered statistically significant. The half maximal inhibitory concentration (IC50) was calculated by non-linear regression analysis using the 4 parameter slope fit equation for dose-inhibition response in GraphPad.

Chapter 3

Selective IKK α inhibition reduced prostate cancer cell growth and motility *in vitro*

CHAPTER THREE

Selective IKK α inhibition reduced prostate cancer
cell growth and motility *in vitro*

Chapter 3

Selective IKK α inhibition reduced prostate cancer cell growth and motility *in vitro*

3.1 Summary

Previous work by Karen and colleagues demonstrated that IKK α activation is correlated with prostate cancer progression in mouse models and in human patients. I hypothesized that IKK α expression will correlate with prostate cancer progression and prostate cancer cell metastatic ability. Additionally, I hypothesized using a verified selective inhibitor of IKK α will suppress the growth, migration and invasion of prostate cancer cells *in vitro*. I show that there is no association between total IKK α expression and prostate cancer progression or the metastatic ability of various prostate cancer cell lines. This is in broad agreement previous work that showed activation of IKK α and not its expression is correlated with prostate cancer progression. I also show for the first time that the verified selective IKK α inhibitor, SU1349, significantly inhibited prostate cancer cell growth, migration and invasion *in vitro*. Consistently, IKK α knockdown in PC3 cells reduced their viability, migration and invasion *in vitro*, whereas, IKK α overexpression in PC3 was stimulatory. Overall, the results of this chapter show that selective IKK α inhibition reduces both the growth and motility of prostate cancer cell tested, highlighting its therapeutic potential.

3.2 Introduction

The NF κ B pathway plays an important role in primary prostate cancer tumour growth and progression to metastatic disease (Nguyen et al., 2014b). Microarray analysis showed the NF κ B pathway to be highly dysregulated in prostate cancer patients (Setlur et al., 2007). Increased activation of the NF κ B pathway, as evident by the increased nuclear localisation of NF κ B-p65/p50 and I κ B- α phosphorylation, was observed during prostate cancer progression in humans and in the TRAMP mouse model of prostate cancer disease (Shukla et al., 2004, Shukla et al., 2005). Activated nuclear NF κ B-p65 was found to be both highly predictive of- and significantly upregulated in- prostate cancer lymph node metastases (Ismail et al., 2004, Lessard et al., 2006). Moreover, evidence of increased NF κ B pathway activation –indicated by elevated phospho-p65 and phospho-I κ B α expression- was observed in patients with the advanced castration resistant prostate cancer (McCall et al., 2012). Whereas inhibition of NF κ B has been demonstrated to sensitize prostate cancer cells to chemotherapy and radiotherapy (Codony-Servat et al., 2013).

In prostate cancer cells, the NF κ B pathway has been shown to regulate cell growth, survival, migration and invasion (Nguyen et al., 2014b, Huang et al., 2001, Baritaki et al., 2009, Taichman et al., 2002, Kukreja et al., 2005). In cell line models of human prostate cancer, the NF κ B pathway was shown to be constitutively activated in the highly metastatic PC3 cell line model of advanced prostate cancer as compared to the weakly metastatic LNCaP cell line model of early stage prostate cancer or to normal prostate epithelia (Gasparian et al., 2002). Inhibition of the NF κ B pathway in PC3 increased its susceptibility to apoptosis and reduced its invasiveness *in vitro* (Shukla and Gupta, 2004, Huang et al., 2001). Furthermore, while LNCaP cells are weakly metastatic and typically never metastasize to bone (Simmons et al., 2014), activation of the NF κ B pathway in LNCaP did induce bone metastasis when injected in mice, whereas inactivation of the NF κ B pathway in highly metastatic PC3 cells inhibited its ability to causes bone metastasis in mice (Jin et al., 2013).

Chapter 3

Selective IKK α inhibition reduced prostate cancer cell growth and motility *in vitro*

The I κ B kinases, IKK β and IKK α , are important in the regulation of the NF κ B pathway (Clement et al., 2008). Although some studies have shown that IKK β plays a more essential role in the regulation of the canonical NF κ B pathway than IKK α (Hacker and Karin, 2006, Lee and Hung, 2008, Ammirante et al., 2010), IKK α - which is involved in the regulation of both the canonical and non-canonical NF κ B pathway, was shown to play a more important role in the development of prostate cancer than the IKK β (Shukla et al., 2005, Nguyen et al., 2014b).

Work by Karin and colleagues show that genetic inactivation IKK α in TRAMP mouse model of prostate cancer, reduced prostate tumour growth and metastasis (Luo et al., 2007). Furthermore, they also show that phosphorylated and nuclear IKK α in mouse and human sections correlated with tumour progression and metastasis. The TRAMP mice used in this study generated soft tissue metastasis and was not suitable for studying the characteristic bone metastasis associated with prostate cancer, therefore, the role of IKK α in prostate cancer bone metastasis remains unknown.

Currently, there are no commercially available selective IKK α inhibitors. Most of the drugs developed by the pharmaceutical industry to inhibit the NF κ B pathway have either been non-specific IKK α/β inhibitors or have targeted IKK β , however, these drugs have not proved successful in clinical trials (Verstrepen and Beyaert, 2014). It is thought that as IKK β is essential in the regulation of the canonical NF κ B pathway and therefore innate immunity, targeting IKK β could have detrimental effects in a clinical setting (Baud and Karin, 2009). IKK β inhibitors that have been tested were shown to cause significant toxicity including liver and intestinal toxicity with side effects including the development of skin, liver and intestinal inflammatory disease (Pasparakis, 2009, Anthony et al., 2017). It is for this reason that some have argued that because IKK α is understood not be essential for canonical NF κ B pathway signalling, selective targeting of IKK α might be a better therapeutic option and is less likely to result in serious side effects (Huang and Hung, 2013).

IKK α inhibitors that have been described in literature either do not report enough details about their specificity and activity or they report pharmacodynamics readouts

Chapter 3

Selective IKK α inhibition reduced prostate cancer cell growth and motility *in vitro*

that are not specific to IKK α , for example, phosphorylation of I κ B α might be reported, which involves both IKK β and IKK α activity, rather than p100 phosphorylation and processing to p52 which is IKK α specific (Llona-Minguez et al., 2013, Asamitsu et al., 2008, Liou et al., 2013, Doppler et al., 2013, Storz, 2013). We were provided exclusive license by Prof Simon McKay (University of Strathclyde) to test a panel of novel and selective small molecular inhibitors of IKK α in prostate cancer. Although these compounds are patented and details about them have not been published, McKay's group have recently published details on an earlier generation of inhibitors (Anthony et al., 2017). Anthony *et al.* utilised recent high-resolution crystal structures of IKK α and IKK β to identify key differences around the ATP binding site within the IKK kinase domain -where IKK α appeared more flexible than IKK β - to design structure-based compounds. These compounds are 4-substituted 2-amino-5-cyanopyrrolo[2,3-d]pyrimidines that selectively bind IKK α and inhibit IKK α -specific pharmacodynamics markers (p100 phosphorylation) without affecting markers that are also common to IKK β (I κ B α degradation and p65 phosphorylation).

In the light of above, the study of selective IKK α inhibition in prostate cancer and prostate cancer bone metastasis, using these novel IKK α inhibitors, may shed more light on its therapeutic potential -alone or in combination with existing therapies- for a more effective treatment of patients with advanced prostate cancer.

Chapter 3

Selective IKK α inhibition reduced prostate cancer cell growth and motility *in vitro*

3.3 Aims

The aim of this chapter is to investigate if IKK α expression is correlated with prostate cancer progression and prostate cancer cell metastatic ability in human prostate tissue sections and in commonly used prostate cancer cell lines. Additionally, to investigate the efficacy of a verified -‘first in class’- selective IKK α inhibitor on the growth, migration and invasion of prostate cancer cells *in vitro*. Furthermore, to validate the effects of pharmacological inhibition of IKK α in prostate cancer cells through the generation and use of prostate cancer cells with IKK α overexpression and knockdown.

3.4 Results

3.4.1 IKK α is expressed in human prostate tissue samples and cell lines

To explore if total IKK α expression is correlated with prostate cancer cell metastatic ability and prostate cancer progression, IKK α expression in various prostate cancer tissues and cell line models was examined by immunohistochemistry and western blots. First, with help from Anne Fowles (University of Sheffield), we examined IKK α expression, in a commercially available microarray panel (PR242b, US Biomaz Inc.) which contains human paraffin embedded prostate adenocarcinoma tissue from cases of various stages of prostate cancer progression and adjacent normal tissue. Prostate cancer progression is based on the Gleason score which is a grading system of how likely the prostate cancer will grow and spread based on the microscopic appearance of prostate tissue. The tissue microarray was probed with a monoclonal anti-IKK α antibody or a control anti-IgG antibody followed by assessment of DAB immunohistochemical staining intensity. As shown in Figure 3.1, There were no significant differences in overall IKK α expression with prostate cancer progression, as evident by the progressive loss of tissue differentiation, from normal prostatic tissue to cancerous prostatic tissue with increasing Gleason scores. Overall IKK α expression was similar in all stages of prostate cancer progression. IKK α was also expressed in the aggressive human prostate cancer cell line model PC3 and in PC3 cells that have successfully metastasized to mouse bone after intra-cardiac injection in BALB/c mice (section provided by Anne Fowles) (Figure 3.1).

Furthermore, I examined total IKK α expression in human cell line models of prostate cancer with variable metastatic abilities, including: weakly metastatic LNCaP cells; moderately metastatic but non bone-tropic LNCaP derived C4-2 cells; moderately metastatic and bone-tropic LNCaP derived C4-2B4 cells; and the highly metastatic and bone tropic PC3 cells. As shown in Figure 3.2, there was also no significant difference in overall IKK α expression between total lysates of these cells as assessed by western blot analysis (Figure 3.2).

Chapter 3

Selective IKK α inhibition reduced prostate cancer cell growth and motility *in vitro*

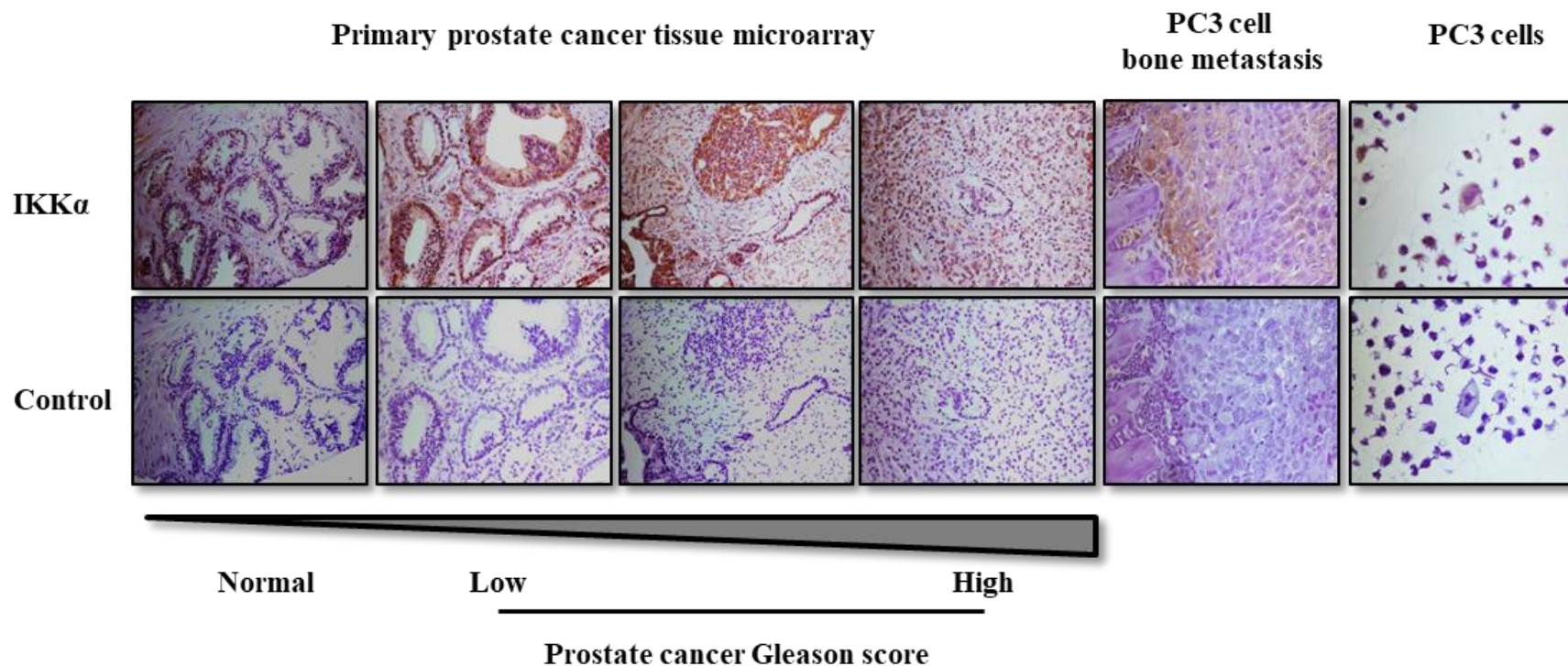


Figure 3.1: IKK α is expressed at all stages of prostate cancer progression and in cell models of prostate cancer. Immunohistochemistry (DAB) staining of monoclonal anti-IKK α and control anti-IgG antibodies: human prostate tissue microarray representing a range from normal to primary prostate cancer tissue with increasing Gleason scores (higher Gleason scores indicate increased likelihood of cancer growth and metastasis); human PC3 cell metastasis in mouse bone after intra-cardiac injection in BALB/c mice (section courtesy of Anne Fowles from Dr Colby Eaton's group); and PC3 cells suspended in agar. Immunohistochemistry work was done by Anne Fowles.

Chapter 3

Selective IKK α inhibition reduced prostate cancer cell growth and motility *in vitro*

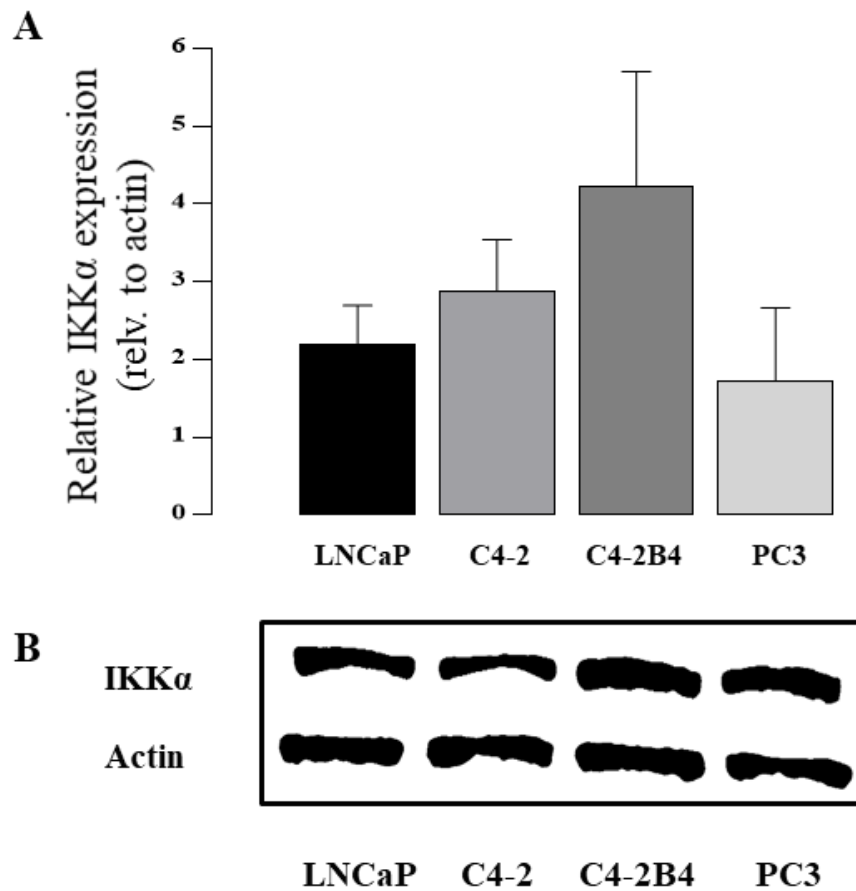


Figure 3.2: IKK α expression in prostate cancer cell lines of various metastatic potentials. **A:** Western blot analysis of total IKK α expression relative to actin in: LNCaP (cell line model of early PCa), C4-2 (androgen insensitive cell line of LNCaP lineage), C4-2B4 (bone metastatic cell line of LNCaP lineage) and PC3 (aggressive cell line model of advanced PCa). Cells were grown in standard media before being serum starved overnight and lysed. Total cellular protein (70 μ g/lane) were probed using rabbit anti-IKK α and anti-actin antibodies. All values in the graphs are mean \pm s.d. and are obtained from 3 independent experiments. **B:** Shows representative western blot images.

Chapter 3

Selective IKK α inhibition reduced prostate cancer cell growth and motility *in vitro*

3.4.2 Pharmacological inhibition of IKK α reduced prostate cancer cell growth

To investigate the role of IKK α kinase activity on human prostate cancer cell viability, I blind tested a panel of seven drugs that included six novel structurally-related IKK α kinase inhibitors and a non-specific control on the viability of human prostate cancer cell lines of various metastatic abilities, these include: LNCaP, C4-2, C4-2B4, PC3 and PC3-BT (PC3 clones harvested from bone marrow of mice after 3 cycles of PC3 intra-cardiac injection and metastasis to bone; personnel communication: Anne Fowles). We were given exclusive license to test these novel IKK α inhibitors in prostate cancer by Prof Simon MacKay (University of Strathclyde). The Alamar Blue assay was used to assess prostate cancer cell viability in complete media after 48hrs and calculate the IC₅₀ values. All drugs tested, except for SU1257 (the control; personnel communication: MacKay), showed efficacy in reducing prostate cancer cell viability, however, SU1349 showed the most potent reduction in cell viability across the different cell lines tested as shown by the IC₅₀ values (Table 3.1). Subsequently provided Ki data (MacKay, unpublished data), which compares the selectivity of each drug for the related IKK α vs. IKK β kinases, revealed SU1349 to also be the most selective drug against IKK α kinase activity (Table 3.1).

Chapter 3

Selective IKK α inhibition reduced prostate cancer cell growth and motility *in vitro*

Drug	IC ₅₀ (μ M)					K _i (nM)*		
	Cell	LNCaP	C4-2	C4-2B4	PC3	PC3-BT	IKK α	IKK β
SU1257		> 30	> 30	> 30	> 30	> 30	10,000	5,000
SU1261		0.69 (\pm 0.01)	0.39 (\pm 0.02)	0.48 (\pm 0.02)	1.46 (\pm 0.28)	0.95 (\pm 0.11)	10	680
SU1349		0.25 (\pm0.05)	0.16 (\pm0.01)	0.24 (\pm0.03)	1.35 (\pm0.36)	0.24 (\pm0.01)	16	3,352
SU1361		0.85 (\pm 0.09)	0.43 (\pm 0.03)	0.61 (\pm 0.10)	1.94 (\pm 0.7)	0.75 (\pm 0.04)	8	960
SU1411		1.04 (\pm 0.14)	1.33 (\pm 0.78)	1.21 (\pm 0.63)	1.24 (\pm 0.09)	1.37 (\pm 0.13)	54	840
SU1266		2.81 (\pm 0.19)	3.28 (\pm 0.87)	2.72 (\pm 0.37)	2.21 (\pm 0.12)	1.88 (\pm 0.1)	NT	NT
SU1087		~11	14.22 (\pm 3.92)	10.12 (\pm 2.36)	~10.4	19.07 (\pm 6.82)	3	5

Table 3.1: Table compares calculated IC₅₀ values for several novel IKK α inhibitors in different prostate cancer cell lines after 48hrs of treatment in complete media. Cell lines tested include: LNCaP, C4-2, C4-2B4, PC3 and PC3-BT (PC3 clones harvested from bone marrow of mice after 3 cycles of PC3 intra-cardiac injection and metastasis to bone); * K_i values for IKK α and IKK β for each drug courtesy of Prof Simon MacKay, University of Strathclyde (NT = not tested). Alamar blue assay was used to calculate mean IC₅₀ \pm s.d. from 3 independent experiments. Lower IC₅₀ values indicate potency, while lower K_i values indicate selectivity. Highlighted in bold are the IC₅₀ and K_i values for SU1349 which was selected for use in all follow up experiments. (See figures S3.1.1-5 for original dose response graphs in appendix 1).

Chapter 3

Selective IKK α inhibition reduced prostate cancer cell growth and motility *in vitro*

Also, SU1349, showed a time and concentration dependent reduction on prostate cancer cell viability, as shown by the dose response in PC3 over 24hr and 48hr period (figure 3.3).

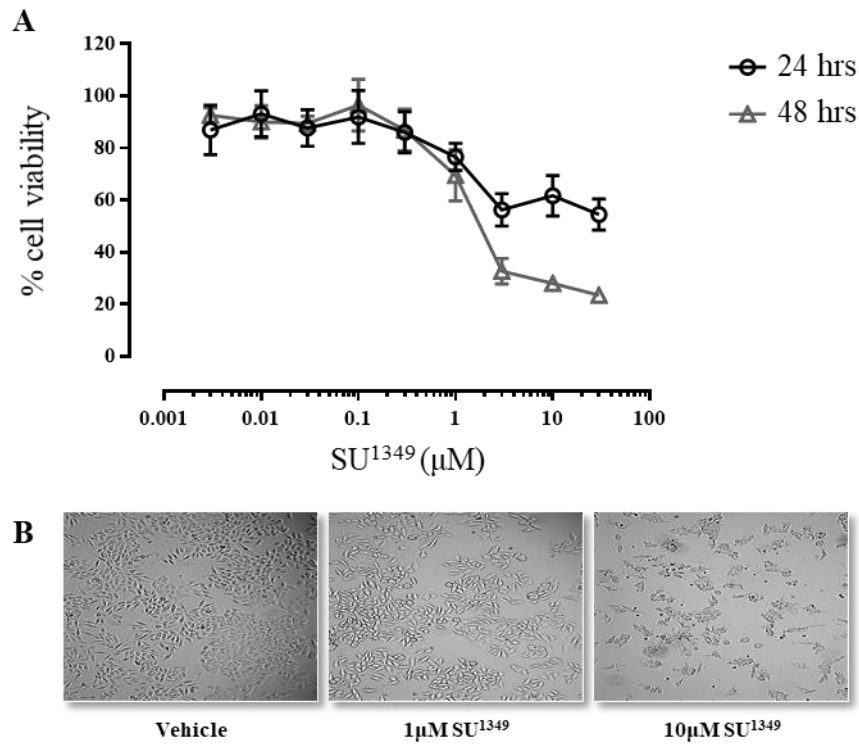


Figure 3.3. The selective IKK α inhibitor, SU1349, reduced PC3 cell viability in a time and concentration dependent manner. A: Shows Alamar blue cell viability results for PC3 after treatment with SU1349 after 24 and 48hrs in complete media, as a percentage of the vehicle control (0.3% DMSO). Values in the graphs are mean \pm s.d. and are obtained from 3 independent experiments. **B:** Representative microscopy images of PC3 after 48hrs treatment with IKK α kinase inhibitor, SU1349, or vehicle control (0.3% DMSO).

Chapter 3

Selective IKK α inhibition reduced prostate cancer cell growth and motility *in vitro*

3.4.3 Stable IKK α knockdown reduced PC3 viability

To validate the effects of pharmacological inhibition of IKK α and to investigate the role of cancer specific expression of IKK α expression levels in human PC3 viability, I generated PC3 clones with stable IKK α overexpression and knockdown vectors using a lentviral transfection system and puromycin selection. I used an IKK α overexpressing pMXs vector and a GFP expressing control vector - kindly gifted to us by Prof Yousef Abu-Amer (Washington university, USA)- to successfully generate PC3 clone that overexpress IKK α (IKK α ^{OE}) by ~20 fold (p<0.001) compared to its mock GFP-transfected control (see Figure 3.4: A and B). I used shRNA vectors from two human TRC clones (-504 and -505; Thermo Fisher), to successfully generate two PC3 clones with stable IKK α knockdown (IKK α ^{KD1} and IKK α ^{KD2}) corresponding to reductions in IKK α expression by 77% (p<0.01) and 59% (p<0.01) respectively, compared to PC3 cells transfected with a pLKO.1 empty (mock) control vector (see Figure 3.4: A and B).

Next, I examined the effects of genetic manipulation of IKK α on PC3 cell viability. PC3 cells were seeded at 3000/well of a 96-well plate and allowed to grow in complete media for 24 hours before using the Almar Blue assay to measure cell viability. I show that in PC3-IKK α ^{OE} cells viability was enhanced by 42% (p<0.05), while in PC3-IKK α ^{KD1} and PC3-IKK α ^{KD2}, viability was reduced by 33% (p<0.001) and 23% (p<0.01) respectively (see Figure 3.4: C).

Chapter 3

Selective IKK α inhibition reduced prostate cancer cell growth and motility *in vitro*

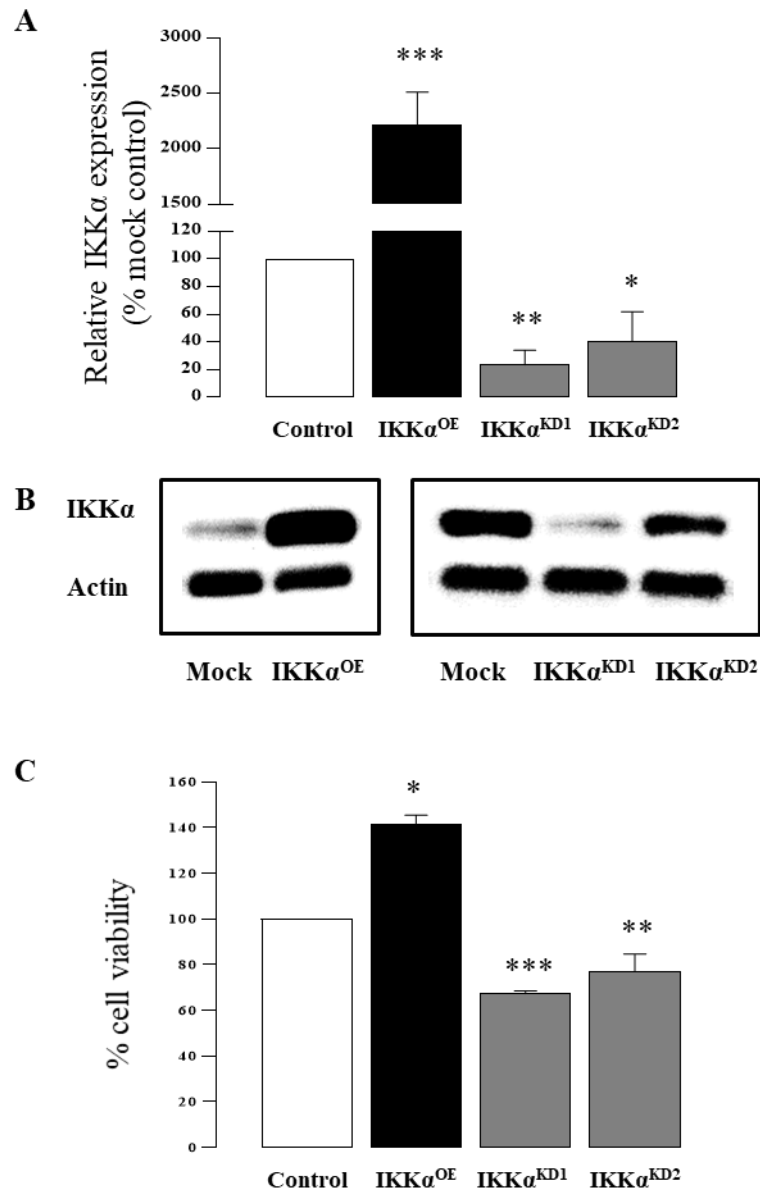


Figure 3.4. Overexpression and knockdown of IKK α in PC3 cells affected their viability. **A:** Western blot analysis of relative IKK α expression in PC3 cells transfected with an IKK α overexpression vector (OE) or one of two shRNA IKK α knockdown vectors (KD1 and KD2) compared to mock vector controls. Total cellular protein (50 μ g/lane) were probed using rabbit anti-IKK α and anti-actin antibodies. Expression results are expressed as percentage of actin loading control. **B:** Representative western blot images shown below. **C:** Alamar Blue assay comparing viability of PC3 cells overexpressing or downregulating IKK α to their mock controls after 24hrs in standard media. All values in the graphs are mean \pm s.d. and are obtained from 3 independent experiments. (Statistics: t-test; * = $P \leq 0.05$; ** = $P \leq 0.01$; *** = $P \leq 0.001$).

Chapter 3

Selective IKK α inhibition reduced prostate cancer cell growth and motility *in vitro*

3.4.4 IKK α knockdown and pharmacological inhibition reduced PC3 directional cell migration

To investigate the role of IKK α in PC3 cell migration, I tested the effects of IKK α overexpression, knockdown and pharmacological inhibition on PC3 migration using the wound healing assay (as detailed in section 2.8). Briefly, for each experimental condition the PC3 cell monolayer was scratched and the media was replaced with serum free media containing 1 μ M SU1349 or a vehicle control before assessing percentage wound closure after 12 hours using a Leica time lapse imaging system. As shown in Figure 3.5 (panel A and B): PC3-IKK α ^{OE} showed significantly increased migration by 61% (p<0.01) compared to its mock transfected control; PC3-IKK α ^{KD1} and PC3-IKK α ^{KD2} showed reduced migration by 27% (p<0.01) and 23% (p<0.05) respectively compared to their mock transfected controls; while PC3 treated with 1 μ M SU1349 showed reduced migration by 26% (p<0.01) compared to the vehicle treated control. These effects were not associated with significant changes in PC3 cell viability as measured by the Alamar Blue assay in these wells at the end of the experiment, see Figure 3.5: C. As these migration experiments were carried out in serum free media and over a period of 12hrs, which is less than the PC3 doubling times of 36 hours, the confounding effects of proliferation can be considered negligible. Nonetheless, as a proof of principle, I repeated the experiment for SU1349 only using a pre-treatment with Mitomycin C -to block cell proliferation- and saw an almost identical reduction in PC3 migration (see appendix Figure S3.2).

Chapter 3

Selective IKK α inhibition reduced prostate cancer cell growth and motility *in vitro*

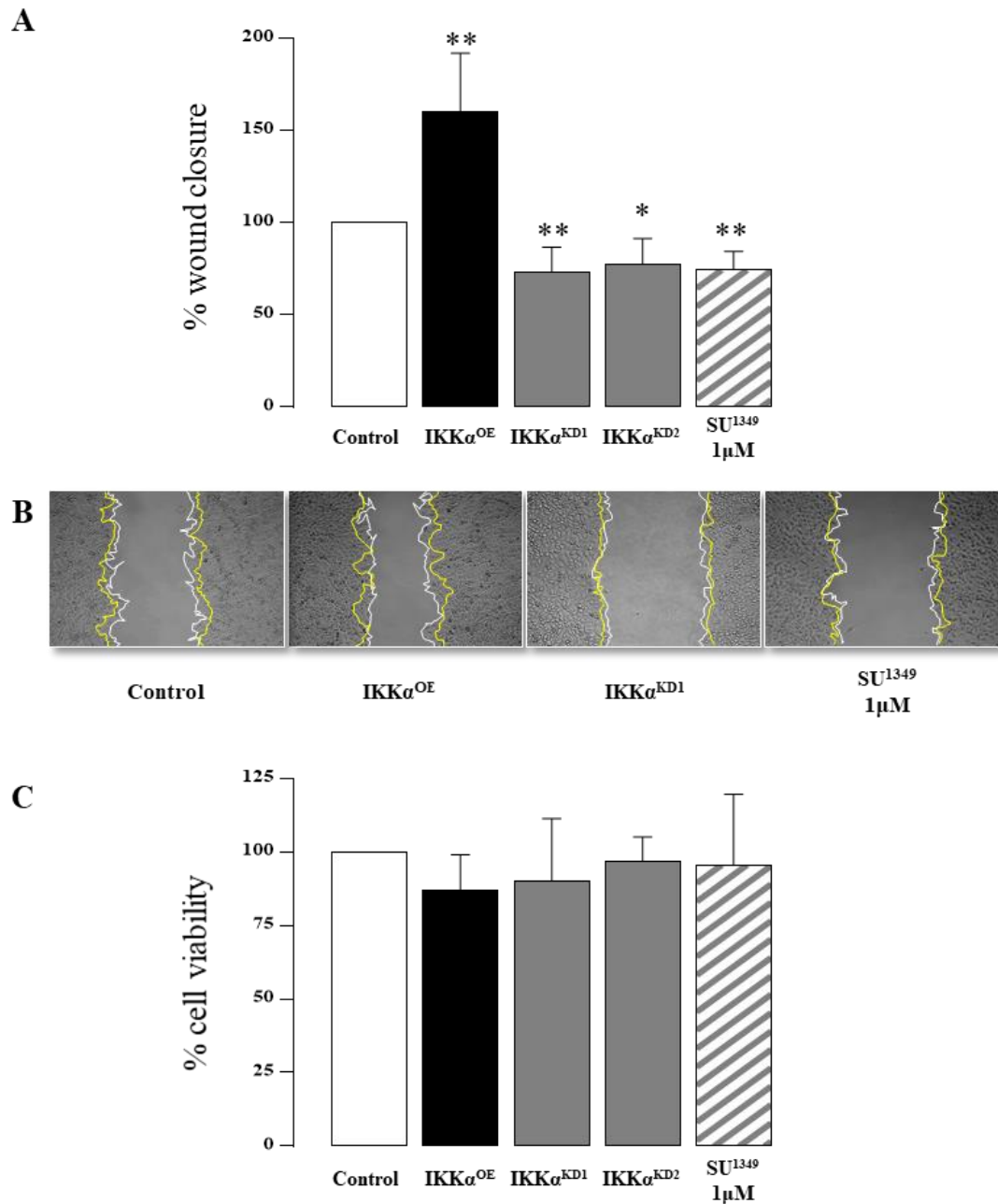


Figure 3.5. IKK α regulates PC3 cell directed migration. **A:** compares the migration of PC3 cells with IKK α overexpression (OE), IKK α knockdowns (KD1 and KD2) or PC3 cells treated with 1 μ M SU1349 after 12 hours compared to their respective mock transfected and/or vehicle treated (0.1% DMSO) controls. **B:** Representative microscopy images of PC3 migration edge at start of experiment (yellow line) and after 12 hours (white line). **C:** Viability of PC3 cells at the end of the migration experiment assessed using the Alamar blue assay. Values in the graphs are mean \pm s.d. and are obtained from 3 independent experiments (* = $P \leq 0.05$; ** = $P \leq 0.01$).

Chapter 3

Selective IKK α inhibition reduced prostate cancer cell growth and motility *in vitro*

3.4.5 IKK α knockdown and pharmacological inhibition reduced random PC3 migration

Next, I studied the effects of IKK α knockdown, overexpression and pharmacological inhibition on PC3 random migration (detailed in section 2.8). The migration of single PC3 cells was monitored in serum free media over a 6-hour period using a Leica time lapse imaging system. The path, directionality, distance and velocity of individual PC3 cells were tracked and analysed using a manual tracker utility on ImageJ. Results in Figure 3.6 (panel A and B) show that compared to their respective controls: PC3-IKK α^{OE} showed significantly increased cell velocity by 53% and distance travelled by 55% ($p < 0.05$), PC3-IKK α^{KD1} and PC3-IKK α^{KD2} showed reduced cell velocity and distance travelled by 48% ($p < 0.05$), while treatment of PC3 with 1 μ M SU1349 reduced both cell velocity and distance travelled by 50% ($p < 0.001$). Figure 3.6 (panel C), show representative summary windrose plots of the directionality and distance of PC3 cell paths as they are tracked relative to their starting points.

Chapter 3

Selective IKK α inhibition reduced prostate cancer cell growth and motility *in vitro*

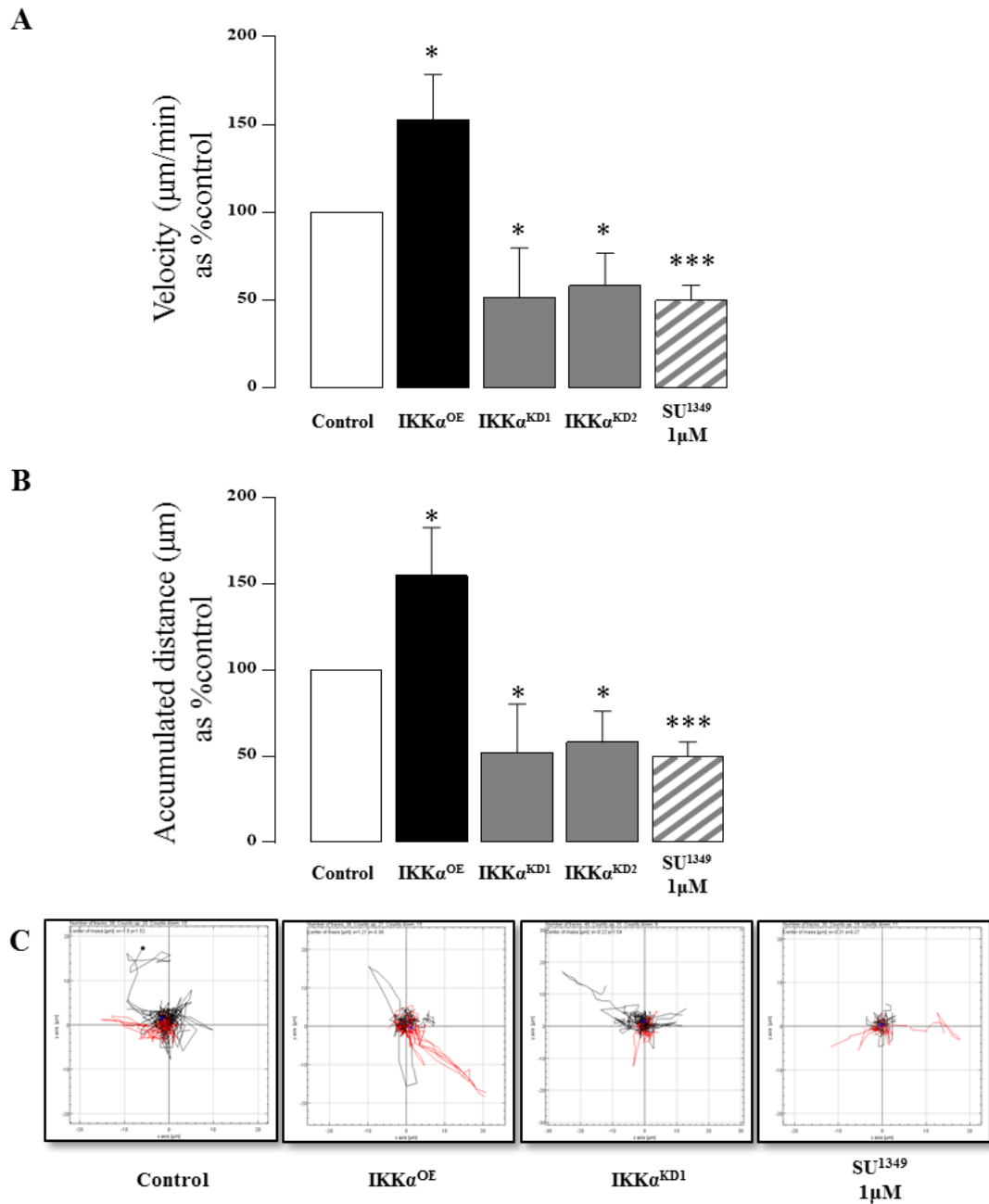


Figure 3.6. IKK α regulates PC3 cell random migration. The movements of PC3 cells with IKK α overexpression (OE), IKK α knockdowns (KD1 and KD2) or PC3 cells treated with 1µM SU1349 were tracked over 6 hours using a time lapse microscope and compared to their respective mock transfected and/or vehicle treated (0.1% DMSO) controls. Cells were treated with SU1349 or vehicle (0.1% DMSO) before the start of the experiment, At least 50 cells per experimental well were tracked. **A:** compares the velocity (µm/min) of tracked cells. **B:** compares the accumulated distance travelled (µm) of tracked cells. **C:** Summary plots of tracked PC3 cell random migration directionality and distance in a representative experimental well (red or black line represents up or down end points for tracked cells). Values in the graphs are mean \pm s.d. and are obtained from 3 independent experiments (* = $P \leq 0.05$).

Chapter 3

Selective IKK α inhibition reduced prostate cancer cell growth and motility *in vitro*

3.4.6 IKK α knockdown and pharmacological inhibition reduced PC3 invasion

To investigate the role of IKK α in PC3 invasion, I looked at the effects of IKK α overexpression, knockdown and pharmacological inhibition on PC3 cell invasion using the matrigel invasion assay (as detailed in section 2.9). In brief, PC3 cells in serum free media were added to a matrigel coated transwell mesh that sits on top of a well containing with media with 10% serum. Due to the chemoattractant effects of serum, the number of cells that have successfully invaded the matrigel and which are trapped by the transwell mesh are stained and quantified. Figure 3.6 shows that compared to their respective controls PC3 cell invasion was: increased in PC3-IKK α ^{OE} by 51% (p<0.01), reduced in PC3-IKK α ^{KD1} and PC3-IKK α ^{KD2} by 43% (p<0.01) and 44% (p<0.01) respectively, while PC3 cell treatment with 0.3uM SU1349 reduced PC3 cell invasion by 38% (p<0.01). Of note, 0.3uM SU1349 had no significant effects on PC3 viability over 72hrs (see appendix figure S3.3).

Chapter 3

Selective IKK α inhibition reduced prostate cancer cell growth and motility *in vitro*

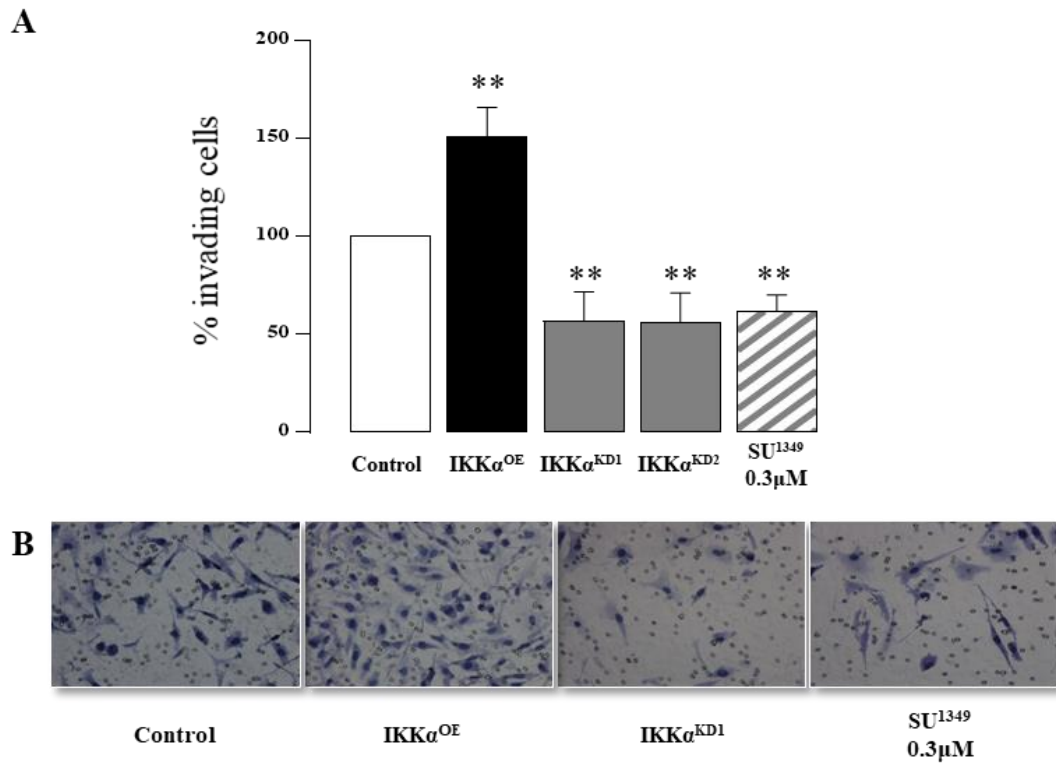


Figure 3.7. IKK α regulates PC3 cell invasion. **A:** Transwell matrigel invasion assay comparing the invasion of PC3 cells overexpressing IKK α (OE), downregulating IKK α (KD1 and KD2) or PC3 cells treated with 0.3 μ M SU1349 after 72hrs compared to their respective controls. 5×10^4 of PC3 cells in 200 μ l of serum free media plus 0.3 μ M SU1349 or vehicle (0.03% DMSO) were added to a transwell coated with a matrigel (20 μ l at 1.5mg/ml). 500 μ l of media containing 10% serum were added to well of a 24-well plate below the transwell insert to act as a chemoattractant. After 72hrs the number of invading cells, trapped by the transwell mesh, were stained and quantified from 5 representative microscopy fields at 20x. **B:** Representative microscopy images of invading PC3 cells (eosin and hematoxylin stained). Values in the graphs are mean \pm s.d. and are obtained from 3 independent experiments (** = $P \leq 0.01$).

Chapter 3

Selective IKK α inhibition reduced prostate cancer cell growth and motility *in vitro*

3.5 Discussion

The aim of this chapter is, first, to characterize if total IKK α expression is correlated with prostate cancer progression and prostate cancer cell line metastatic ability; and second, to establish for the first time the effects of selective IKK α pharmacological inhibition on prostate cancer growth, migration and invasion *in vitro* and to validate these effects through the use of IKK α overexpression and knockdowns in prostate cancer cells.

Increased expression of IKK α in tissues has been associated with certain cancers including hepatocellular carcinoma, skin squamous cell carcinoma, head and neck squamous cell carcinomas (Jiang et al., 2010, Alameda et al., 2011, Nottingham et al., 2014); in prostate cancer evidence of increased IKK α activation and not increased total IKK α expression has been associated with prostate cancer. Previous work by Luo *et al.*, show that activated IKK α - i.e. nuclear and phosphorylated IKK α - is correlated with prostate cancer stage and progression in mouse and human tissue sections (Luo et al., 2007). Our analysis of a prostate cancer tissue samples indicates that total IKK α is not correlated with prostate cancer progression. Furthermore, my analysis of total IKK α expression in various human prostate cancer cell lines, did not find a significant correlation between metastatic ability and total IKK α expression. Based on these results, combined with previous studies, one can speculate that physiologically and in the context of prostate cancer, IKK α dysregulation occurs mainly at the level of its activity and not its expression level. IKK α is ubiquitously expressed and IKK α knockout in mice is perinatally lethal, and results in severe skin and skeletal abnormalities (Takeda et al., 1999, Hu et al., 1999). Subsequent work showed that introduction of a catalytically inactive form of IKK α rescued IKK α knockout mice from these morphological abnormalities, highlighting the importance of IKK α kinase independent function in normal development (Sil et al., 2004). A kinase independent role for nuclear IKK α have been demonstrated to be important for the regulation of differentiation of epidermal keratinocytes and chondrocytes (Hu et al., 2001, Sil et al., 2004, Olivotto et al., 2015). Therefore, targeting IKK α kinase activity without

Chapter 3

Selective IKK α inhibition reduced prostate cancer cell growth and motility *in vitro*

affecting its expression and its important kinase independent functions may lower unwanted side effects.

With this in mind, I went on to test a first in class family of verified- selective- IKK α inhibitors on the viability of human prostate cancer lines of varying metastatic abilities (courtesy of Prof Simon McKay, University of Strathclyde, UK). The lead compound, SU1349, was selected as it had the highest selectivity for IKK α over the related IKK β , in addition, to showing the most potent effects on cell viability across the different prostate cancer cell line I tested. Previously, the plant derived compound, apigenin- which was described as an IKK kinase inhibitor that binds with greater affinity to IKK α than IKK β in qualitative *ex vivo* pulldown assays- was shown to sensitises PC3 cells to apoptosis and reduce PC3 proliferation (Shukla and Gupta, 2004, Shukla et al., 2015). These findings highlight the importance of IKK α activity in prostate cancer cell proliferation.

To investigate this further and to validate the effects of SU1349 on prostate cancer cells in subsequent experiments I successfully generated clones of the prostate cancer cell lines, PC3, with IKK α overexpression and IKK α knockdowns. Genetic manipulation of IKK α expression in PC3 also affected its viability: whereas, IKK α overexpression significantly increased PC3 viability, IKK α knockdowns significantly reduced PC3 viability. These results are in agreement with previous work by Shukla *et al.* that reported shRNA knockdown of IKK α in PC3 decreased their proliferation due to cell cycle arrest (Shukla et al., 2015).

Next I examined the effects of the selective IKK α inhibitor, SU1349, as well as IKK α overexpression and knockdown on PC3 migration. The directed migration was significantly enhanced in PC3 cell with IKK α overexpression, whereas IKK α knockdown and SU1349 treatment significantly reduced PC3 directed migration. Similarly, in random migration experiments, both the total distanced travelled and the velocity of tracked PC3 was significantly enhanced with IKK α overexpression, where IKK α knockdown and SU1349 treatment significantly inhibited the distance travelled and velocity of PC3 cells. Previously, Shukla *et al.* show that apigenin reduced PC3

Chapter 3

Selective IKK α inhibition reduced prostate cancer cell growth and motility *in vitro*

migration in wound healing assays (Shukla and Gupta, 2004, Shukla et al., 2015). While overexpression of the NF κ B p65 subunit and downstream target of IKK α was shown to increase prostate cancer cell migration (Kukreja et al., 2005).

Encouraged by these results, I examined the effects of IKK α modulation on PC3 matrigel invasion. I show that whereas overexpression of IKK α in PC3 significantly enhanced invasion, both IKK α knockdown and pharmacological inhibition reduced PC3 invasion. Previously, siRNA inhibition of IKK α in PC3 was shown to reduce invasion (Mahato et al., 2011). Also, the inhibition of the NF κ B pathway in PC3 was associated with a reduction in pro-invasive factors such as VEGF and MMP-9 (Huang et al., 2001). I found similar effects by SU1349 in suppressing PC3 derived factors important for its growth, migration and invasion in chapter 6.

In this chapter, I show that in the context of prostate cancer, overall IKK α expression is not associated with prostate cancer progression in human sections or the metastatic ability of commonly used human prostate cancer cell lines. This is in broad agreement with previous work that correlated IKK α activity and not expression with prostate cancer. I also show for the first time, that targeting the kinase activity of IKK α , using the verified selective IKK α kinase inhibitor SU1349, significantly reduced prostate cancer cell growth, migration and invasion *in vitro*. Moreover, I was able to validate the effects of SU1349 on prostate cancer cells through the successful generation of PC3 clones with IKK α overexpression and knockdowns. Altogether, my results confirm the importance of IKK α in the regulation of prostate cancer growth and metastatic behaviour, it indicates that targeting IKK α kinase activity might be a valuable therapeutic option in the treatment of prostate cancer.

CHAPTER FOUR

Selective IKK α inhibition reduced osteoclast formation *in vitro*

Chapter 4

Selective IKK α inhibition reduced osteoclast formation *in vitro*

4.1 Summary

The NF κ B pathway is known to play an important role in osteoclast differentiation, activity and survival. Previously, cells derived from mice with IKK α deletion were shown to exhibit impaired osteoclast formation *in vitro*. I hypothesize that selective pharmacological inhibition of IKK α will suppress osteoclast formation *in vitro*. In this chapter, I show that pharmacological IKK α inhibition- using the verified IKK α inhibitor SU1349- significantly suppressed osteoclast formation in RAW264.7 pre-osteoclast cultures and in mouse total bone marrow cultures *in vitro*. To validate this, I also show that prostate cancer specific IKK α manipulation regulated the ability of PC3 cells to influence osteoclast formation in prostate cancer-bone marrow cell co-cultures, with IKK α overexpression enhancing osteoclast formation and IKK α knockdown inhibiting osteoclast formation *in vitro*. This indicates that pharmacological IKK α inhibition may be useful in the treatment of osteolytic bone damage associated with prostate cancer bone metastasis.

4.2 Introduction

The IKK/NF κ B pathway is known to play an important role in osteoclast differentiation, activity and survival (Soysa and Alles, 2009). Mice with deletions of *NF κ B1* (encodes p105 precursor of p50) and *NF κ B2* (encodes p100 precursor of p52) had increased bone volume due to lack of osteoclasts (Iotsova et al., 1997). Also, mice with IKK β deletions showed increased bone growth as a result of reduced osteoclast formation (Otero et al., 2010). Hematopoietic cells derived from mice with IKK α deletions also exhibited impaired osteoclast differentiation *in vitro* (Chaisson et al., 2004), *in vivo* these mice had a reduced number of multinucleated osteoclasts when compared to wild type littermates. Similarly, mice with deletions of RelB, a component of the non-canonical NF κ B pathway, also showed impaired osteoclast differentiation (Vaira et al., 2008).

The NF κ B pathway was also shown to regulate the ability of prostate cancer cells to promote osteoclastogenesis. Genetic constitutive activation of the NF κ B pathway in LNCaP was shown to induce osteoclastogenesis in bone marrow cultures *in vitro*, whereas parental control cells failed to induce osteoclastogenesis (Jin et al., 2013). Also, the NF κ B pathway was shown to regulate PC3 induced osteoclast formation in RAW264.7 cultures (Akech et al., 2010, Kavitha et al., 2014).

Previous pharmacological studies by our group have shown that combined inhibition of IKK α and IKK β reduces osteoclasts numbers and associated osteolytic damage in a breast cancer bone metastasis model in rats and in a mouse model of postmenopausal osteoporosis (Idris et al., 2009, Idris et al., 2010). Conversely, constitutive activation of the canonical NF- κ B pathway in mice was shown to result in RANKL independent osteoclastogenesis and severe bone loss in mice (Otero et al., 2012, Otero et al., 2010). Collectively, these studies suggest that inhibition of IKK α will disrupt prostate cancer cell ability to enhance osteoclastogenesis and may be useful in the treatment prostate cancer associated osteolysis.

Chapter 4

Selective IKK α inhibition reduced osteoclast formation *in vitro*

4.3 Aims

In this chapter I aim to investigate the effects of pharmacological IKK α inhibition on RANKL induced osteoclastogenesis *in vitro*, in the presence and absence of prostate cancer cells or their derived factors. Also investigate the prostate cancer specific effects of IKK α inhibition on their ability to influence osteoclastogenesis *in vitro*.

Chapter 4

Selective IKK α inhibition reduced osteoclast formation *in vitro*

4.4 Results

4.4.1 IKK α pharmacological inhibition reduced RANKL induced osteoclast formation *in vitro*

A previously study reports that cells derived from mice with IKK α deletion exhibited impaired osteoclast formation *in vitro* (Chaisson et al., 2004). Here, I investigated the effects of selective pharmacological inhibition of IKK α , using the verified IKK α inhibitor SU1349, on osteoclast formation in cultures with the macrophage-like osteoclast precursor cells, RAW264.7. RAW264.7 cells were co-treated with RANKL (50ng/ml) and different concentrations of SU1349 (0.1-1 μ M) or a vehicle control for 72hrs. As shown in Figure 4.1, SU1349 reduced RANKL induced osteoclast formation in a concentration dependent manner (by 43% at 0.3 μ M to 86% at 1 μ M, $p < 0.0001$). Similarly, in the absence of RANKL over the same period, RAW264.7 cell viability also showed a concentration dependent reduction ($IC_{50} = 0.32 \pm 0.06 \mu$ M).

Chapter 4

Selective IKK α inhibition reduced osteoclast formation *in vitro*

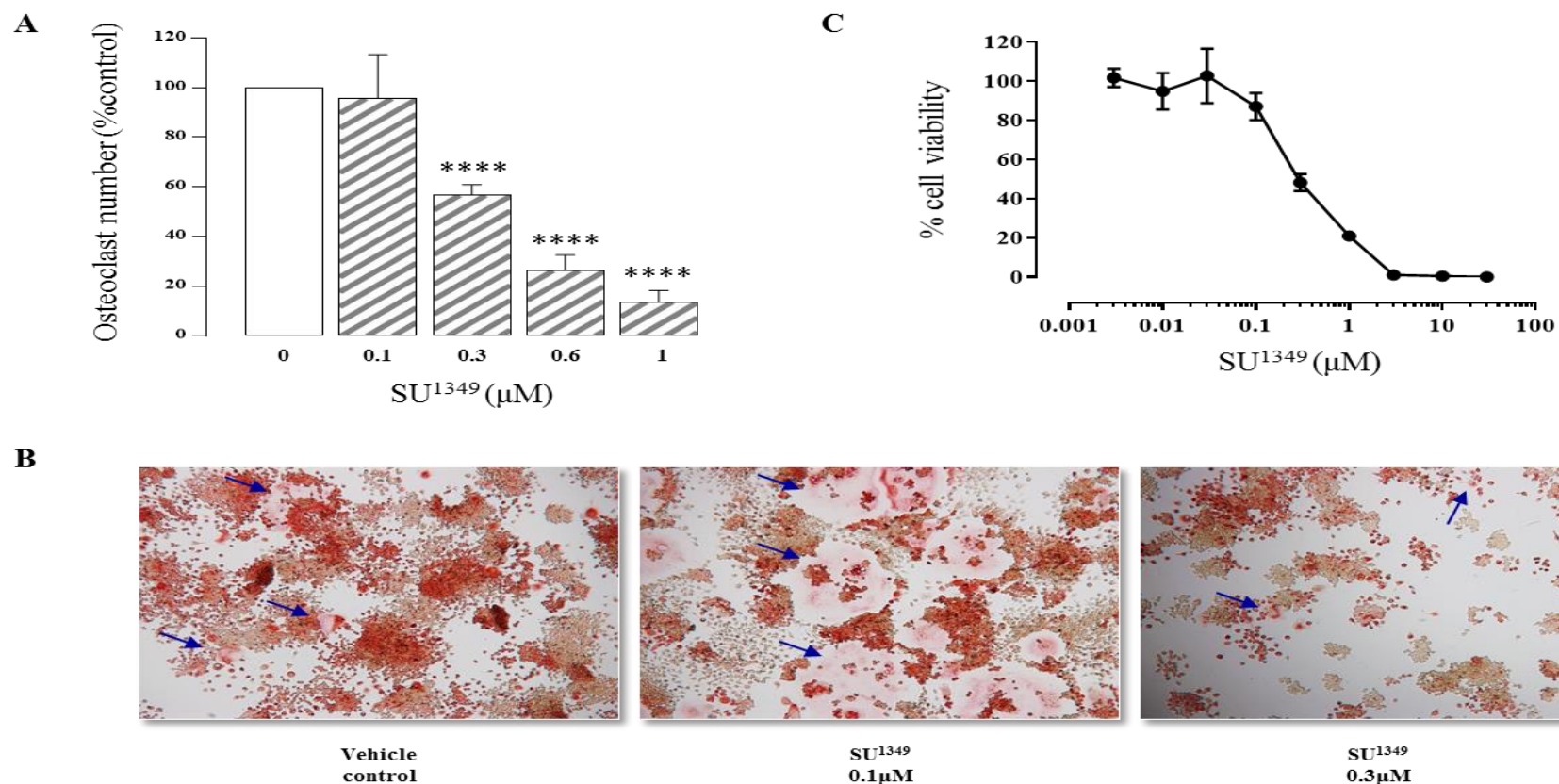


Figure 4.1: IKK α inhibitor, SU1349, reduced RAW264.7 osteoclast formation *in vitro*. **A:** Shows the number of RANKL (50 ng/ml) generated osteoclasts in RAW264.7 cultures after treatment for 72hrs with different concentrations of the IKK α inhibitor SU1349. RANKL and SU1349 or vehicle treatments were refreshed after 48hrs. Osteoclast numbers was assessed by counting multinucleated TRAcP positive cells. **B:** representative microscopy images of TRAcP stained osteoclast cultures (at 10x magnification); arrows indicate osteoclasts. **C:** viability of RAW264.7 cells, measured by alamar Blue, after 72hrs treatment with different concentrations of SU1349. Values in the graphs are mean \pm s.d. and are obtained from 3 independent experiments (**** = $P \leq 0.0001$).

Chapter 4

Selective IKK α inhibition reduced osteoclast formation *in vitro*

4.4.2 Cancer specific IKK α regulates PC3 induced osteoclast formation *in vitro*

Next, I used a co-culture system with human prostate cancer cells and mouse bone marrow cells in the presence of M-CSF and RANKL, in order to study the effects of both prostate cancer-specific and systemic IKK α inhibition on osteoclastogenesis *in vitro*. As shown in figure 4.2, co-cultures with PC3-IKK α^{OE} enhanced osteoclastogenesis by 55% ($p < 0.05$), whereas PC3-IKK α^{KD1} and PC3-IKK α^{KD2} suppressed osteoclastogenesis by 91% ($p < 0.0001$) and 93% ($p < 0.0001$) respectively. Finally, treatment of co-cultures with 0.1 μ M SU1349 suppressed osteoclastogenesis by 93% ($p < 0.0001$).

Chapter 4

Selective IKK α inhibition reduced osteoclast formation *in vitro*

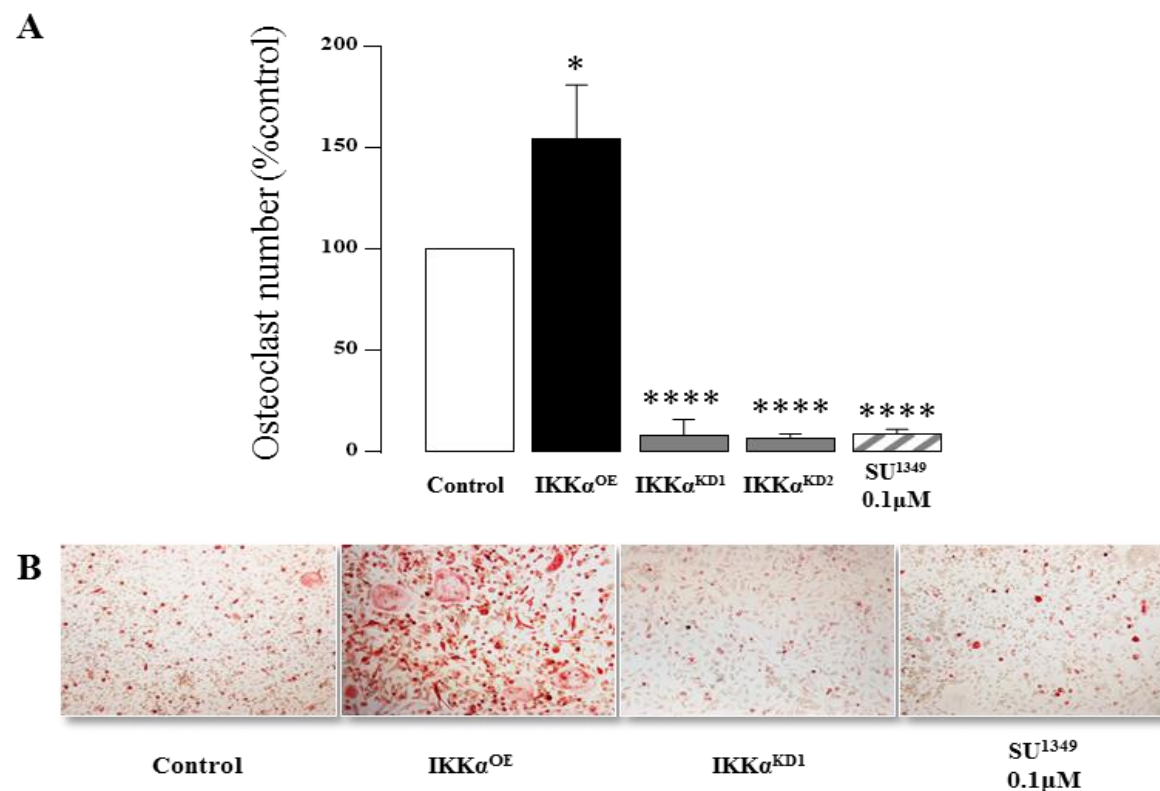


Figure 4.2: Overexpressing of IKK α in PC3 significantly enhanced osteoclast formation, whereas IKK α knockdown and pharmacological inhibition in PC3 suppressed osteoclast formation *in vitro*. **A:** Shows the number of M-CSF (10 ng/ml) and RANKL (100 ng/ml) generated osteoclasts in mouse bone marrow cultures co-plated with PC3 cells (200 cells/well). Wells were seeded with PC3 cells: with IKK α overexpression (IKK α ^{OE}), IKK α knockdowns (IKK α ^{KD1} and IKK α ^{KD2}), PC3 mock controls plus 0.1 μ M SU1349 or vehicle control. Media was refreshed every 48hrs plus/minus drug treatments and cultures were maintained for up to 7 days. Osteoclasts number was assessed by counting multinucleated TRAcP positive cells. Values in the graphs are mean \pm s.d. and are obtained from 3 independent experiments (**** = $P \leq 0.0001$). **B:** representative microscopy images of TRAcP stained osteoclast cultures.

Chapter 4

Selective IKK α inhibition reduced osteoclast formation *in vitro*

4.4.3 Cancer specific manipulation of IKK α regulates ability of PC3 derived factors to affect osteoclast formation *in vitro*

Next, I studied the effects of IKK α overexpression and IKK α knockdowns in PC3 cells on the ability of their tumour derived factors -using conditioned media- to affect osteoclast formation in mouse bone marrow cultures *in vitro*. Additionally, I studied the effects of IKK α pharmacological inhibition on osteoclast formation in the presence and absence of PC3 derived factors. As shown in figure 4.3, conditioned media from PC3 cells overexpressing IKK α , significantly enhanced osteoclast formation in M-CSF and RANKL stimulated mouse bone marrow cultures by 144% ($p < 0.01$) compared to its mock control, whereas conditioned media from PC3 with IKK α knockdowns had no significant effects on osteoclast formation- in the M-CSF and RANKL treated cultures- compared to their mock controls. 0.1 μ M SU1349 significantly suppressed osteoclast formation in the presence and absence of PC3 conditioned media by 66% ($p < 0.01$) and by 84% ($p < 0.001$) respectively (figure 4.3).

Chapter 4

Selective IKK α inhibition reduced osteoclast formation *in vitro*

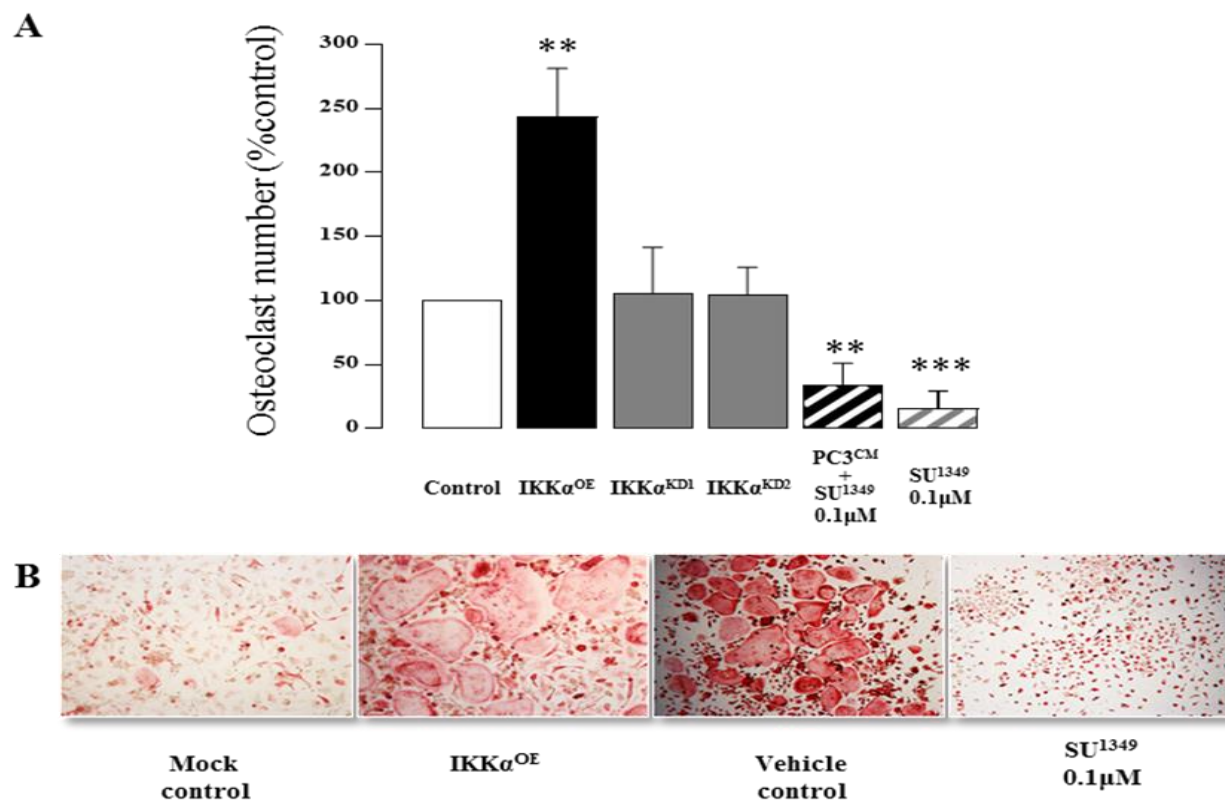


Figure 4.3: conditioned media from PC3 cells over-expressing IKK α significantly enhanced osteoclast formation *in vitro*, whereas pharmacological inhibition of IKK α suppressed osteoclast formation *in vitro*. **A:** Shows the number of M-CSF (10 ng/ml) and RANKL (100 ng/ml) generated osteoclasts from mouse bone marrow cultures treated with 10% (v/v) conditioned media from PC3 cells with IKK α overexpression (IKK α ^{OE}) or IKK α knockdowns (IKK α ^{KD1} and IKK α ^{KD2}), or treated with 0.1 μ M SU1349 in the presence and absence of PC3 conditioned media (PC3^{CM}). Treatments were refreshed every 48hrs and cultures were maintained for up to 7 days. Osteoclasts number was assessed by counting multinucleated TRAcP positive cells and expressed as percentage of its mock and/or vehicle treated control. Values in the graphs are mean \pm s.d. and are obtained from 3 independent experiments (** = $P \leq 0.01$). **B:** representative microscopy images of TRAcP stained osteoclast cultures.

4.5 Discussion

The NF κ B pathway plays an important role in osteoclast differentiation, activity and survival (Soysa and Alles, 2009). Previous findings in our group show that osteoclast formation is inhibited by parthenolide- a non-selective IKK α/β inhibitor-(Idris et al., 2010), and by selective IKK β inhibition (Idris et al., 2010, Marino et al., 2018). Also, previous work has revealed that genetic inactivation of IKK α in mouse hematopoietic cells impaired osteoclastogenesis *in vitro* and reduced the number of multinucleated osteoclasts in mouse bones (Chaisson et al., 2004). My results show that in cultures with the macrophage-like osteoclast precursor RAW264.7 cells, selective IKK α inhibition -using SU1349- reduced RANKL induced osteoclastogenesis and the viability of RAW264.7 cells in a concentration dependent manner. Moreover, in cultures with total mouse bone marrow cells, 0.1 μ M of SU1349, significantly suppressed M-CSF and RANKL induced osteoclastogenesis in the presence and absence of prostate cancer cell derived factors. Furthermore, the same concentration of 0.1 μ M of SU1349, did not affect the viability of the osteoclast precursor cells as indicated by the number of TRAPc positive cells present at the end of the experiment. My results are in agreement with previous findings and confirm that targeting IKK α in osteoclast precursors reduces RANKL osteoclast formation *in vitro*. It is possible that SU1349 may also be affecting osteoclast survival and this should be explored in future experiments.

Previously, Jin *et al.* showed that conditioned media from LNCaP cells with genetic NF κ B activation (constitutively active IKK β) promotes osteoclastogenesis in mouse bone marrow cultures and increased the expression of the osteoclastic RANKL and PTHrP genes in prostate cancer cells (Jin et al., 2013). In agreement with this, my results show that IKK α regulates the ability of prostate cancer cells to influence osteoclastogenesis *in vitro*. IKK α overexpression in PC3 significantly enhanced osteoclastogenesis in mouse bone marrow cultures whether in direct co-culture experiments or in experiments with conditioned media treatments.

However, IKK α knockdown in PC3 significantly suppressed osteoclast formation in mouse bone marrow cultures in direct co-culture experiments but not in experiments

Chapter 4

Selective IKK α inhibition reduced osteoclast formation *in vitro*

with conditioned media treatments. Conditioned media from PC3 with IKK α knockdown did not have a significant effect on osteoclastogenesis, this might be due to the concentration of RANKL in these cultures masking the subtle effects of IKK α knockdown in PC3. Additionally, in conditioned media experiments mouse bone marrow cells were treated with conditioned media once every 48hrs, whereas, in a co-culture system the PC3 cells are constantly releasing factors that can influence bone marrow culture for the duration of the experiment. Moreover, the RANKL in these cultures can itself directly promote the production of NF κ B regulated osteoclastic factors by PC3 cells. It is also possible that IKK α knockdown in PC3 may result in the production of factors that inhibit osteoclastogenesis and this might be more pronounced in a co-culture experiments as opposed to experiments with conditioned media for the reason explained above. Results from chapter 6, show that IKK α inhibition in PC3 cells using SU1349 was associated with an overall downregulation of pro-osteoclastic PC3 derived factors. This would suggest that IKK α knockdown in PC3 would similarly result in a downregulation of PC3 derived pro-osteoclastic factors and thus reduced ability to support osteoclast formation.

Interestingly I noted that conditioned media from parental PC3 cells suppressed RANKL induced osteoclastogenesis in mouse bone marrow cultures (figure S4.1). In contrast to my findings, previous studies in mouse primary bone marrow cells reported no significant effects for PC3 conditioned media on osteoclastogenesis (Fradet et al., 2013), while another study reported a significant stimulation of osteoclast differentiation even in the absence of RANKL (Alsulaiman et al., 2016). However, a study on human peripheral blood mononuclear precursors report a significant inhibition of osteoclastogenesis by PC3 conditioned media (Borghese et al., 2013). This indicates that at least in the PC3 cells I used, there are factors present in PC3 conditioned media that can inhibit osteoclastogenesis, nonetheless, experiments with IKK α overexpression and knockdown in PC3, indicate that IKK α does regulate pro-osteoclastic PC3 derived factors.

In conclusion, my results in this chapter show that verified IKK α inhibitor, SU1349, directly suppress osteoclastogenesis *in vitro* as well as suppressing the ability of prostate cancer cells to promote osteoclastogenesis *in vitro*. Future experiments should also

Chapter 4

Selective IKK α inhibition reduced osteoclast formation *in vitro*

explore the effects of SU1349 on mature osteoclast survival and activity such as in bone resorption assays. Overall, my results shows promise for the use of the selective IKK α inhibitor SU1349 in alleviating osteolytic bone damage associated with prostate cancer bone metastasis in preclinical mouse models.

CHAPTER FIVE

Selective IKK α inhibition enhanced osteoblast differentiation and bone nodule formation *in vitro*

5.1 Summary

The NF κ B pathway is known to negatively regulate osteoblast differentiation and function. Previous studies have shown that both genetic and pharmacological inhibition of the NF κ B pathway enhances osteoblast differentiation and function *in vitro* and *in vivo*. I hypothesize that pharmacological inhibition of IKK α , using the verified selective IKK α inhibitor SU1349, will enhance osteoblast differentiation and bone nodule formation *in vitro*. I show that pharmacological IKK α inhibition significantly enhanced osteoblastic differentiation and bone nodule formation *in vitro*. Moreover, prostate cancer specific inhibition of IKK α enhanced the ability of prostate cancer cells and their derived factors to stimulate osteoblast differentiation and bone nodule formation *in vitro*. Furthermore, since the differentiation of osteoblasts and adipocytes from common mesenchymal progenitors is largely mutually exclusive: I hypothesized and successfully demonstrate that pharmacological IKK α inhibition and prostate cancer-specific inhibition of IKK α suppresses adipocytes differentiation in pre-adipocyte 3T3L1 cultures *in vitro*. My results reveal an inhibitory role for IKK α in the regulation of osteoblastic differentiation and function *in vitro*.

5.2 Introduction

Historically, the NF κ B pathway was not thought to be important for osteoblast differentiation in contrast to the crucial role of the NF κ B pathway in osteoclast differentiation that was recognised much earlier (Novack, 2011). Early studies in mice with *NF κ B1* (p105/p50) and *NF κ B2* (p100/p52) double knockout showed increased bone volume due to osteoclast inhibition, however, osteoblast function and bone formation in these mice was shown not to be impaired (Iotsova et al., 1997, Boyce et al., 2010).

Later studies demonstrated that the NF κ B pathway negatively regulates osteoblast differentiation and function. The inflammatory cytokine TNF α and activator of the NF κ B pathway reduced bone formation *in vitro* and *in vivo* (Gilbert et al., 2005, Li et al., 2007b). Gilbert and colleagues, demonstrated that TNF α downregulates the expression of Runx2 and osterix transcription factor that are essential for osteoblast differentiation (Lu et al., 2006a, Gilbert et al., 2005). Furthermore, TNF α inhibited the production of type I collagen and osteocalcin- important for bone formation- by osteoblasts (Ding et al., 2009a). High levels of TNF α was shown to induce apoptosis in the MC3T3 osteoblastic cell line via activation of the NF κ B pathway (Kitajima et al., 1996) .

Initially, studies highlighted the inhibitory role of the canonical NF κ B pathway in osteoblasts. Inhibition of the NF κ B p65 in mice deficient in IKK γ or with super I κ B α repressor promoted osteoblast differentiation *in vitro* and promoted osteoblast bone formation *in vivo* (Chang et al., 2009). Similarly, selective inhibition of IKK β increased osteoblast differentiation and function *in vitro*, as well as and bone formation *in vivo* (Alles et al., 2010, Marino et al., 2018).

Later work demonstrated the importance of the non-canonical NF κ B pathway for osteoblasts differentiation and function. RelB, a member of the non-canonical NF κ B pathway, was shown to negatively regulate osteoblast differentiation and bone formation. Osteoblastic precursor cells from RelB knockout mice, showed increased proliferation and differentiation *in vitro*, moreover, they displayed increased bone

Chapter 5

Selective IKK α inhibition enhanced osteoblast differentiation and bone nodule formation *in vitro*

volume due to increased osteoblast bone formation *in vivo* (Soysa et al., 2010, Yao et al., 2014). Whereas, overexpression of non-canonical NF κ B p52 and RelB proteins were linked to the inhibition of osteoblast differentiation from mesenchymal stem cells (Zhang et al., 2014).

The general inhibitor of IKK α/β , parthenolide, was shown to promote osteoblast differentiation and bone nodule formation function *in vitro* through a mechanism that involves the activation of the Wnt/ β -catenin pathway (Zhang et al., 2017b). However, the specific role of IKK α inhibition in the regulation of osteoblast differentiation and function *in vitro* remains unknown. Since prostate cancer bone metastatic lesions in patients are known to produced mixed osteoblastic as well as osteolytic lesions, it is important to characterise the effects of selective IKK α inhibition on osteoblast differentiation and function *in vitro* and *in vivo*.

Chapter 5

Selective IKK α inhibition enhanced osteoblast differentiation and bone nodule formation *in vitro*

5.3 Aims

In this chapter I aim to investigate the effects of pharmacological IKK α inhibition using the verified selective IKK α inhibitor, SU1349, on osteoblast differentiation and bone nodule formation *in vitro* as well as investigating the prostate cancer specific effects of IKK α inhibition on their ability to influence osteoblast differentiation and bone nodule formation *in vitro*.

5.4 Results

5.4.1 IKK α pharmacological inhibition stimulated osteoblastic differentiation and bone nodule formation *in vitro*

Previous work has shown that pharmacological NF κ B inhibition, using parthenolide a general inhibitor of IKK α/β , stimulates osteoblast differentiation and function *in vitro* (Zhang et al., 2017b). Here, I investigated the effects of selective pharmacological inhibition of IKK α , using the verified IKK α inhibitor SU1349, on osteoblastic differentiation as quantified by alkaline phosphatase (ALP) activity and osteoblastic bone nodule formation function as assessed by Alizarin red staining, in different osteoblastic cell models. In the human osteoblast-like Saos2 cell line, SU1349 had a biphasic effect on Saos2 differentiation and bone nodule formation after 3 weeks of treatments depending on concentration tested. As shown in figure 5.1, 0.01 μ M SU1349 increased ALP activity in Saos2 cells and bone nodule formation in Saos2 cells, by 34% ($p<0.05$) and 61% ($p<0.01$) respectively, without affecting their cell viability. However, 0.1 μ M SU1349 reduced ALP activity in Saos2 cells and bone nodule formation in Saos2 cells by 42% ($p<0.01$) and 59% ($p<0.05$) respectively, in the same cultures 0.1 μ M SU1349 reduced Saos2 cell viability by 38% ($p<0.01$). In mouse calvarial osteoblasts, 0.1 μ M SU1349 increased their ALP activity after 48hrs by 35% ($p<0.05$) (figure 5.1: E). In longer experiments in mouse calvarial osteoblasts, 0.01 μ M SU1349 increased bone nodule formation by 38% ($n=1$) after 3 weeks of treatment without affecting their cell viability, whereas, 0.1 μ M SU1349 had no significant effects on bone nodule formation or cell viability (figure 5.1: F-H).

Chapter 5

Selective IKK α inhibition enhanced osteoblast differentiation and bone nodule formation *in vitro*

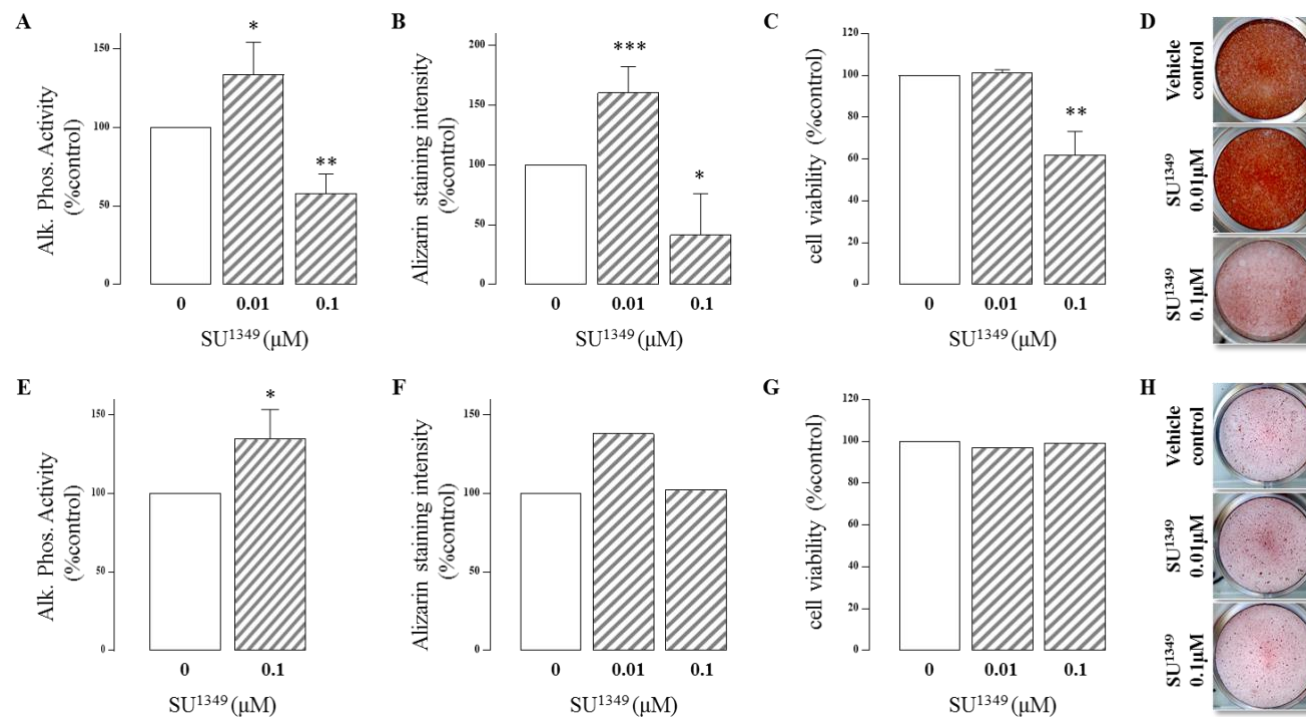


Figure 5.1: The IKK α inhibitor, SU1349, stimulated osteoblastic differentiation and activity *in vitro*. Saos2 cells (in 1% FBS media) and mouse calvarial osteoblast (in 1% FBS media plus ascorbic acid and β - glycerophosphate) were treated with different concentrations of SU1349 or vehicle control for up to 3 weeks. Treatments were refreshed every 48hrs. At the end of the experiments culture wells were assessed for: osteoblastic differentiation by measuring alkaline phosphatase activity; osteoblastic bone nodule formation by quantifying Alizarin red staining intensity; and cell culture viability using the Alamar Blue assay. **A-D:** Shows differentiation, bone nodule formation, viability and representative images for Saos2 cultures treated with 0.01 μ M or 0.1 μ M SU1349 for 3 weeks. **E:** Shows differentiation for mouse calvarial osteoblasts after 48hrs in treatment with 0.1 μ M SU1349. **F-H:** Shows bone nodule formation and cell viability for mouse calvarial osteoblast cultures ($n=1$) treated with 0.01 μ M or 0.1 μ M SU1349 for 3 weeks; including representative images. Values in the graphs are mean (expressed as % of vehicle control) \pm s.d. and are obtained from 3 independent experiments.

5.4.2 IKK α inhibition stimulated osteoblastic differentiation and bone nodule formation in the presence of prostate cancer derived factors in vitro

Next, I investigated the effects of IKK α pharmacological inhibition on osteoblastic differentiation and bone nodule formation function in the presence of PC3 conditioned media. In the human osteoblast-like Saos2 cultures in the presence of PC3 conditioned media, SU1349 had a biphasic effect after 10 days of treatments depending on the concentration of SU1349. As shown in figure 5.2, 0.01 μ M SU1349 increased Saos2 bone nodule formation, by 23% ($p < 0.05$) without significantly affecting their ALP activity or viability. However, 0.1 μ M SU1349 reduced bone nodule formation in Saos2 by 56% ($p < 0.0001$) and ALP activity in Saos2 by 40% ($p < 0.001$), whilst Saos2 cell viability was increased by 12% ($p < 0.001$). In contrast, after 3 weeks of treatment, in cultures with mouse MC3T3 osteoblastic cell line (used instead of mouse calvarial osteoblasts, due to lack of access to mouse calvarial osteoblasts) in the presence of PC3 conditioned media, only 0.1 μ M SU1349 increased the ALP activity of MC3T3 cells by 40% ($p < 0.05$) without significantly affecting their viability, and this was associated with a non-significant trend of increased Alizarin staining (figure 5.2: E-H). 0.01 μ M SU1349 had no significant effects on MC3T3 differentiation, Alizarin staining or viability after 3 weeks of treatment. It is important to state here that although MC3T3 did stain with Alizarin red, microscopic examination revealed that this was not associated with obvious bone nodule formation unlike in Saos2 and mouse calvarial osteoblasts cultures.

Chapter 5

Selective IKK α inhibition enhanced osteoblast differentiation and bone nodule formation *in vitro*

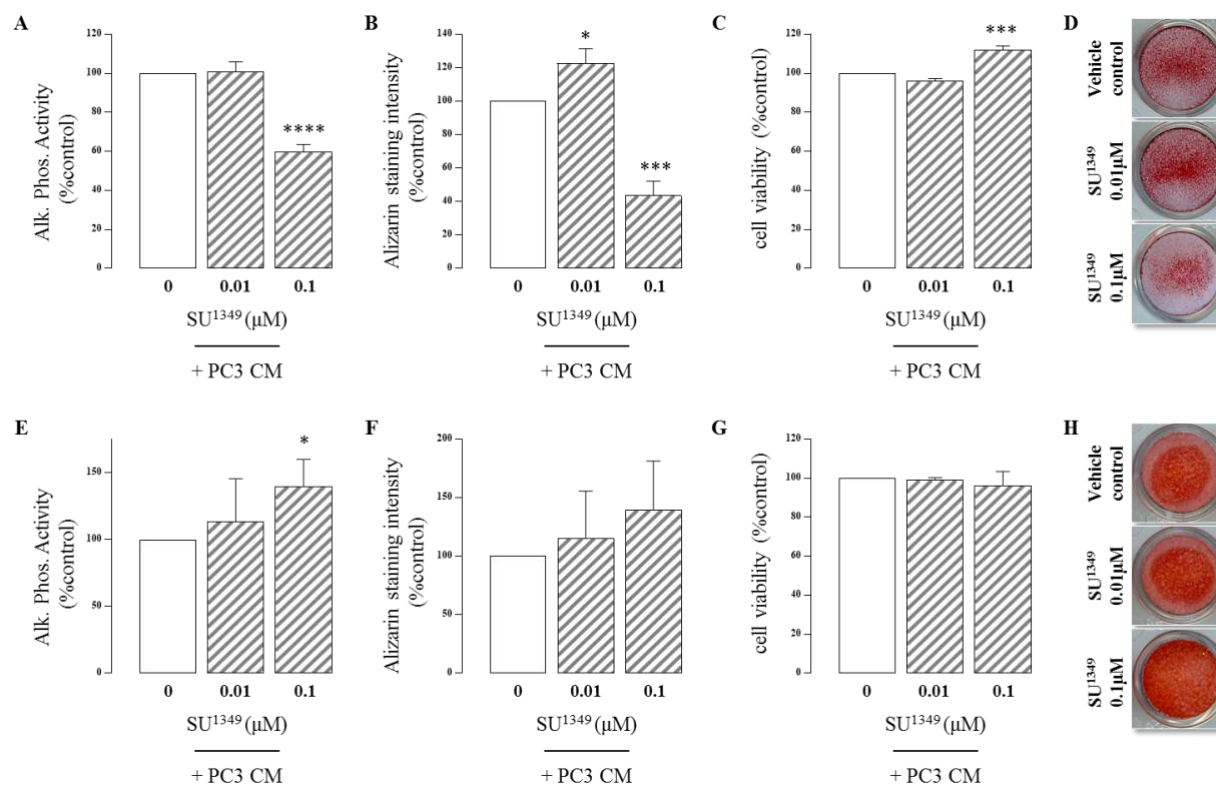


Figure 5.2: The IKK α inhibitor, SU1349, stimulated osteoblastic differentiation and activity in the presence prostate cancer derived factors *in vitro*. Saos2 and MC3T3 cells (in 1% FBS media plus ascorbic acid and β - glycerophosphate) were treated with 0.01 μM or 0.1 μM SU1349 in the presence of PC3 conditioned media (20% v/v) for up to 3 weeks. Treatments were refreshed every 48hrs. At the end of the experiments culture well were assessed for: osteoblastic differentiation by measuring alkaline phosphatase activity; osteoblastic bone nodule formation by quantifying Alizarin red staining intensity; and cell culture viability using the Alamar Blue assay. **A-D:** Shows results for experiments in Saos2 after 10 days. **E-H:** Shows results for experiments in MC3T3 after 3 weeks. Values in the graphs are mean (expressed as % of vehicle control) \pm s.d. and are obtained from 3 independent experiments.

5.4.3 IKK α knockdown in PC3 stimulated osteoblastic differentiation and bone nodule formation *in vitro*

Next, I investigated the prostate cancer specific effects of IKK α inhibition on osteoblastic differentiation and osteoblastic bone nodule formation activity in the human osteoblast-like Saos2 cells. As shown in figure 5.3 (A-D): conditioned media from PC3 with IKK α knockdown IKK α ^{KD1} but not IKK α ^{KD2} increased Saos2 bone nodule formation by 25% ($p < 0.001$) and showed a non-significant increase in ALP activity by $29\% \pm 13$ ($p > 0.05$) without significantly affecting cell viability. Also shown in figure 5.3 (E-H), PC3 cells with IKK α knockdown, IKK α ^{KD1} but not IKK α ^{KD2}, in direct co-culture experiments increased ALP activity in Saos2 cultures by 33% ($p < 0.05$) and bone nodule formation in Saos2 cultures by 15% ($p < 0.05$) and this was associated with a modest reduction in Saos2 cell viability by 9% ($p < 0.001$).

Chapter 5

Selective IKK α inhibition enhanced osteoblast differentiation and bone nodule formation *in vitro*

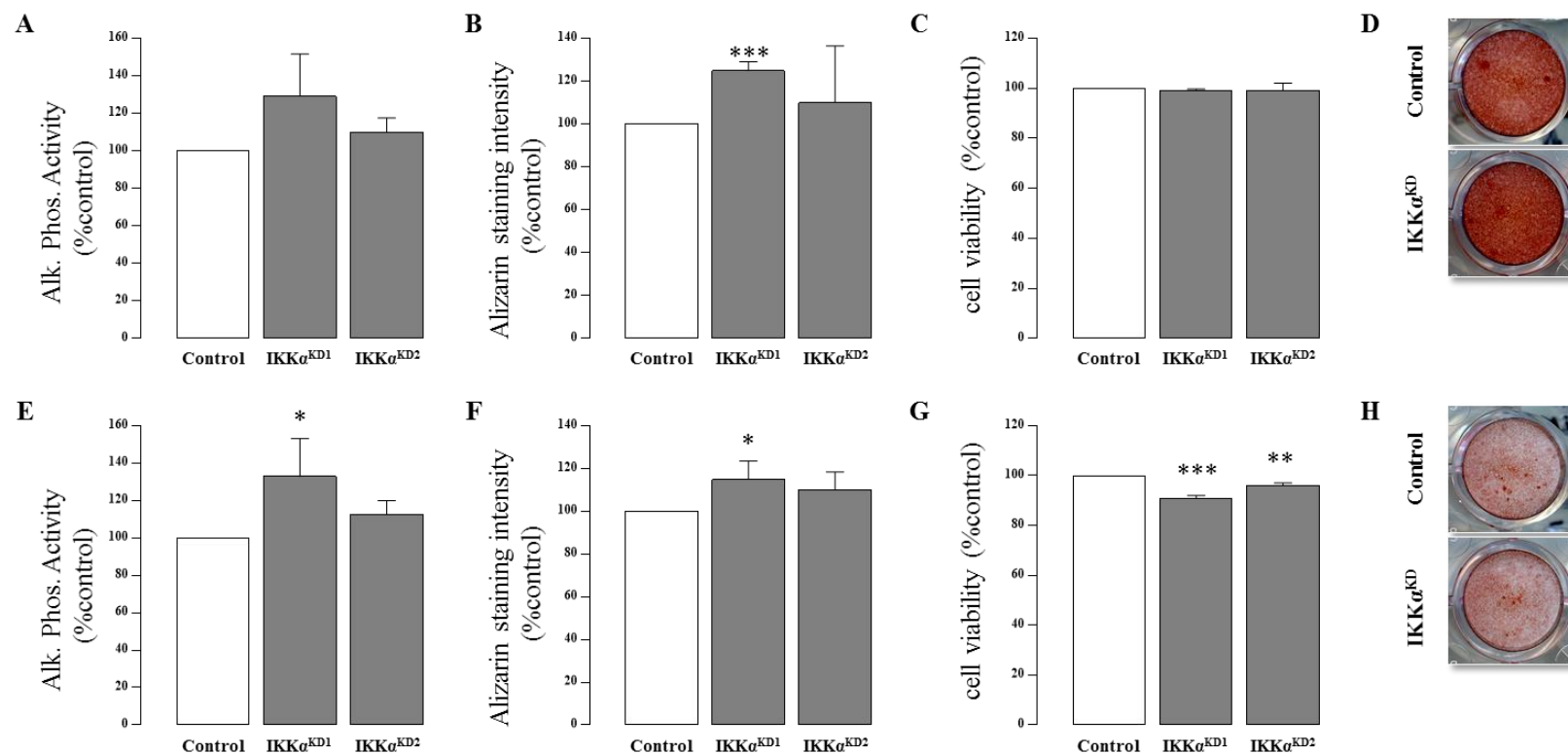


Figure 5.3: IKK α knockdown in PC3 stimulated osteoblastic differentiation and activity *in vitro*. Saos2 cells were treated with conditioned media (20% v/v) from PC3 cells with IKK α knockdown or mock transfected PC3 control. In separate experiments, Saos2 cells were directly co-cultured with PC3 cells (1000 cells/well) with IKK α knockdown or mock transfected PC3 controls. At the end of the experiments (after ~3 weeks) culture wells were assessed for: osteoblastic differentiation by measuring alkaline phosphatase activity; osteoblastic bone nodule formation by quantifying Alizarin red staining intensity; and cell culture viability using the Alamar Blue assay. **A-D**: Shows results for differentiation, bone nodule formation and viability in Saos2 cultures treated with conditioned media (20% v/v) from PC3 cells with IKK α knockdown or mock transfected PC3 control. **E-H**: Shows results for differentiation, bone nodule formation and viability in Saos2 cultures directly co-cultured with PC3 cells with IKK α knockdown or mock transfected control. Values in the graphs are mean (expressed as % of mock control) \pm s.d. and are obtained from 3 independent experiments.

5.4.4 Pharmacological IKK α inhibition and IKK α knockdown in PC3 cells suppressed 3T3L1 adipocyte differentiation *in vitro*.

Bone marrow adiposity has been linked to prostate cancer bone metastasis (Laurent et al., 2016, Morris and Edwards, 2016). The differentiation of osteoblasts and adipocytes from mesenchymal stem cells in the bone marrow microenvironment is understood to be largely mutually exclusive (Muruganandan and Sinal, 2014). Because I found that both pharmacological IKK α inhibition and IKK α knockdown in PC3 stimulated osteoblastic differentiation *in vitro*, I investigated the effects of both pharmacological IKK α inhibition and PC3 specific IKK α knockdown on the differentiation in 3T3L1 pre-adipocyte cells. Adipocyte differentiation was assessed by quantifying oil red staining. As shown in figure 5.4 (A-C), 1 μ M SU1349 significantly suppressed adipocyte differentiation by 78% ($p < 0.0001$) without significantly affecting cell viability in these cultures. Also shown in figure 5.4 (D-F), treatment of 3T3L1 cells with conditioned media from PC3 cells with IKK α knockdown, IKK α ^{KD1} and IKK α ^{KD2}, suppressed adipocyte differentiation by 16% ($p < 0.05$) and 19% ($p < 0.01$) respectively (figure 5.4 (D-F)).

Chapter 5

Selective IKK α inhibition enhanced osteoblast differentiation and bone nodule formation *in vitro*

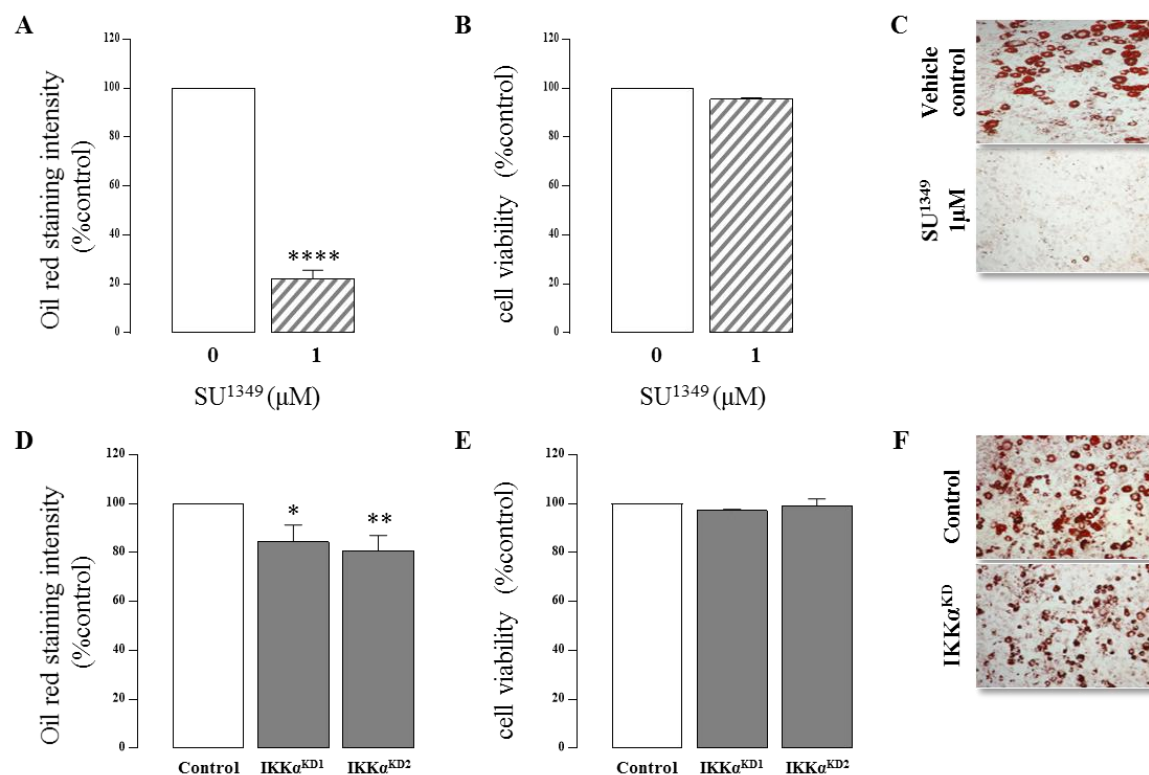


Figure 5.4: Pharmacological IKK α inhibition and IKK α knockdown in PC3 cells suppressed 3T3L1 adipocyte differentiation *in vitro*. 3T3L1 cells were differentiated (as described in section 2.4.5) in the presence and absence of 1 μ M SU1349 or conditioned media (20% v/v) from PC3 cells - PC3 with IKK α knockdown or mock transfected PC3 controls- for 15 days. At the end of the experiments the differentiation of 3T3L1 cultures was assessed by quantifying eluted oil red staining measured by spectrophotometry and the viability was measured using the Alamar Blue assay. **A-C:** Shows the differentiation and viability of 3T3L1 cells after treatment with 1 μ M SU1349 or vehicle control; representative images are shown (5x magnification). **D-F:** Shows the differentiation and viability of 3T3L1 cells after treatment with conditioned media from PC3 with IKK α knockdown or mock transfected PC3 controls; representative images are shown (5x magnification). Values in the graphs show means (expressed as % of control) \pm s.d. obtained from 3 independent experiments.

5.5 Discussion

Most types of cancers that metastasize to bone typically cause osteolytic lesions, however, prostate cancer patients characteristically display mixed lesions with more osteoblastic lesions as well as the typical osteolytic lesions (Logothetis and Lin, 2005). In view of this I investigated the effects of pharmacological IKK α inhibition on osteoblast differentiation and function *in vitro*, as well the prostate cancer specific effects of IKK α knockdown on its ability to influence osteoblast differentiation and function *in vitro*. I used different complementary models of osteoblast cells. Primarily, I used human Saos2 osteosarcoma cell line which is a model of mature osteoblasts that highly expresses ALP and has an enhanced ability to form bone nodules *in vitro*. Also, where possible this was complemented with using non-cancer derived osteoblast cell models such as primary mouse calvarial osteoblasts (which I had limited access to) or mouse MC3T3 cells. MC3T3 cells are a pre-osteoblast model and although certain sub-clones of this cell line are able to form bone nodules *in vitro*, the MC3T3 cells I used did not appear to produce obvious bone nodules unlike Saos2 and mouse calvarial osteoblasts cultures.

Previous studies report that the NF κ B pathway negatively regulates osteoblast differentiation and function (Iotsova et al., 1997, Boyce et al., 2010). Pharmacological inhibition of NF κ B, using a peptide inhibitor of NEMO, was shown to stimulate osteoblastic differentiation and bone nodule formation in mouse bone marrow cells and in osteoblastic MC3T3 cells (Li et al., 2007b). While, genetic inactivation of NF κ B, using a constitutively activated I κ B α , was also shown to inhibit differentiation in the osteoblastic Saos2 cell line *in vitro* by inhibiting BMP/Smad signalling (Eliseev et al., 2006). In agreement with these findings I show that selective IKK α inhibition, using SU1349, promoted osteoblastic differentiation and bone nodule formation in mouse calvarial osteoblasts and in the osteoblastic Saos2 cell line. However, SU1349 also appeared to have a biphasic effect on osteoblast differentiation and function, where higher concentration of SU1349 suppressed Saos2 differentiation, bone nodule formation and cell viability. In support of this, NF κ B was previously reported to have

Chapter 5

Selective IKK α inhibition enhanced osteoblast differentiation and bone nodule formation *in vitro*

a pro-survival role in osteoblasts and NF κ B inhibition was shown to induce apoptosis in a human foetal osteoblast cell lines (Xiao et al., 2009).

The IKK α inhibitor, SU1349, stimulated osteoblastic differentiation and bone nodule formation in the presence of PC3 conditioned media: it increased bone nodule formation in experiments with Saos2 without affecting Saos2 differentiation in these experiments, however, SU1349 did increase MC3T3 differentiation. It is possible that stimulatory effects of SU1349 on Saos2 differentiation in the presence of PC3 conditioned media were masked: first, because I had established that PC3 conditioned media in itself stimulated osteoblastic differentiation (as well as osteoblastic function and viability; see figure S5.1); second, unlike my previous experiment (that were performed in the absence of PC3 conditioned media) these cultures were co-treated with ascorbic acid and β -glycerophosphate both of which are known to promote osteoblast differentiation (Langenbach and Handschel, 2013); third, the addition of ascorbic acid and β -glycerophosphate, accelerated bone nodule formation and therefore resulted in an earlier termination of experiments by day 10 compared to day 21 in previous experiments in the absence of ascorbic acid and β -glycerophosphate, it is possible that longer treatments are needed to detect the effects on ALP-activity. Nonetheless, in agreement with experiment in the absence of PC3 conditioned media, higher concentrations of SU1349, significantly inhibited Saos2 differentiation and bone nodule formation, while surprisingly, it also resulted in a modest but significant increase in Saos2 viability. Cellular differentiation is generally understood occur at the expense of proliferation and vice versa (Ruijtenberg and van den Heuvel, 2016)

My results also show that knockdown of IKK α in PC3 stimulated Saos2 differentiation and bone nodule formation *in vitro*. These results suggest that knockdown of IKK α in PC3 cells promotes the production of pro-osteoblastic factors or supresses the production of osteoblastic inhibitors. PC3 cells are known to release factors such as Wnts and BMPs that promote osteoblast differentiation and function, as well as expressing the DKK-1 or SOST which strongly inhibits Wnt signalling (Ganguly et al., 2014, Hall et al., 2005, Heiland et al., 2010). The NF κ B pathway was demonstrated to have a direct inhibitory role on Wnt and BMP protein expression (Tarapore et al.,

Chapter 5

Selective IKK α inhibition enhanced osteoblast differentiation and bone nodule formation *in vitro*

2016). Furthermore, NF κ B activation through TNF α was shown to activate the expression of the Wnt inhibitors, DKK1 and SOST (Heiland et al., 2010). While, genetic inhibition of DKK1 in PC3 was shown to promote osteoblast differentiation and bone nodule formation in mouse bone marrow cultures (Hall et al., 2005). Interestingly, in chapter 6, I show that SU1349 suppressed the expression of PC3 cell derived factors that are known to negatively regulate osteoblast differentiation and function, which supports the possibility that knockdown of IKK α in PC3 might be stimulating osteoblastic differentiation and bone nodule formation through a similar mechanism.

Bone marrow adiposity has been linked to prostate cancer bone metastasis (Laurent et al., 2016, Morris and Edwards, 2016). Conditioned media from adipocytes has been demonstrated to promote PC3 proliferation and migration (Onuma et al., 2003, Laurent et al., 2016). Interestingly, I have observed a previously unreported role for PC3 conditioned media in the promotion of adipocyte differentiation (figure S5.2). Since, the differentiation of osteoblasts and adipocytes from mesenchymal stem cells in the bone marrow microenvironment is understood to be largely mutually exclusive (Muruganandan and Sinal, 2014) and because I observed that both pharmacological IKK α inhibition and knockdown of IKK α in PC3 promoted osteoblast differentiation and function: I hypothesized that the opposite effects would be observed in adipocyte differentiation experiments using the mouse pre-adipocyte 3T3L1 cell line. My results clearly confirm my hypothesis, showing a significant inhibition on adipocyte differentiation with SU1349 treatment and a more modest but significant inhibition in adipocyte differentiation with conditioned media treatments from PC3 with IKK α knockdowns. Interestingly, in support of my findings, a previous study reports that inhibiting the IKK α related IKK β , using an antisense oligonucleotide inhibitor, also resulted in the inhibition of 3T3L1 adipocyte differentiation and this was associated with increasing Wnt/ β -catenin in these cells (Helsley et al., 2016). My present results suggest a previously unknown role for IKK α in prostate cancer-adipocyte interactions. However, further studies on bone marrow derived osteoblasts and adipocytes precursors *in vitro* and *in vivo* are needed to confirm these results

Chapter 5

Selective IKK α inhibition enhanced osteoblast differentiation and bone nodule formation *in vitro*

In conclusion, my results show that both pharmacological IKK α inhibition and IKK α knockdown in PC3 promotes osteoblast differentiation and function *in vitro* while inhibiting adipocyte differentiation *in vitro*. Indicating that a shared mechanism, involving IKK α , that promotes the differentiation of osteoblasts over adipocytes from early precursor cells. Further experiments are needed to elucidate whether IKK α inhibition might mediate some of its effects on osteoblast differentiation and function through the Wnt/ β -catenin pathway.

CHAPTER SIX

Effects of SU1349 on NF κ B signalling in cancer and bone cells

6.1 Summary

In previous chapters I show that verified IKK α inhibitor, SU1349, reduced prostate cancer cell growth and motility, suppressed osteoclast formation, and stimulated osteoblast differentiation and function, *in vitro*. These results are consistent with inhibition of the NF κ B pathway. In this chapter, I investigate if SU1349 inhibits NF κ B signalling in osteoclasts, osteoblasts and prostate cancer cells. I show that SU1349 suppressed PC3-induced activation of both canonical and non-canonical NF κ B pathway in osteoblast and osteoclast precursors⁷. Therefore, I also investigated the effects of SU1349 on the Wnt/ β -catenin pathway. Significant cross-regulation is known to exist between the NF κ B and Wnt/ β -catenin pathways, with Wnt/ β -catenin activation being important for enhancing osteoblast differentiation and function whereas it has an inhibitory role in osteoclasts. I show that SU1349 had differential effects on Wnt/ β -catenin signalling, where it activated Wnt/ β -catenin signalling in osteoblast precursors, as shown by the increased phosphorylation of GSK3 β and increased levels of cytoplasmic β -catenin, whereas the opposite effect was observed in osteoclast precursors. Collectively, these results confirm that the differential effects of SU1349 on osteoclast and osteoblast differentiation can be explained both by its effects on the NF κ B pathway and by its differential effects on Wnt signalling in these cell types. The NF κ B pathway regulates expression of pro-inflammatory factors that are important in prostate cancer growth and metastasis to bone. Investigate if treatment of PC3 cells with SU1349 will downregulate PC3 production of pro-inflammatory factors. I show that SU1349, downregulates the production of various pro-inflammatory factors by PC3 prostate cancer cells. The downregulation of these pro-inflammatory factors explains- at least in part- the observed inhibitory effects of SU1349 on PC3 cell growth and motility, also the ability of PC3 cells to promote osteoclastogenesis *in vitro* described in previous chapters. Moreover, a majority of the downregulated factors are also involved in the negative regulation of osteoblast differentiation and thus may explain why PC3 cell specific IKK α inhibition enhanced osteoblast differentiation and function in co-cultures and conditioned media experiments.

6.2 Introduction

Activation of NF κ B pathway signalling occurs through the canonical NF κ B pathway, which is characterised by a rapid and reversible activation, and the non-canonical NF κ B pathway which is characterised by a delayed and persistent activation (Shih et al., 2011). The canonical NF κ B pathway is activated by a wide range of ligands binding to receptors, including: tumour necrosis factor receptor 1 (TNFR1), Toll-like receptors (TLRs), interleukin-1 receptor (IL1R), and T-cell receptors (TCR). While a more restricted set of ligands acting through specific receptors that include RANK, CD40, lymphotoxin β receptor (LT β R) and B-cell activating factor receptor (BAFFR) activate the non-canonical NF κ B pathway in addition to activating the canonical pathway (Verstrepen and Beyaert, 2014, Sun, 2017). Canonical NF κ B pathway activation is characterised by phosphorylation of cytoplasmic I κ B α by IKK α in a complex with IKK β and IKK γ , this allows for the rapid degradation of I κ B α and the release and translocation of p65-p50 heterodimer into the nucleus. Whereas, in non-canonical NF κ B activation: activated IKK α homodimers phosphorylate p100 which allow for its partial processing to p52, followed by the translocation of the p52-RelB heterodimer into the nucleus. (Oeckinghaus et al., 2011). Although, the canonical and non-canonical NF κ B pathway have distinct characteristics, significant cross-regulation exists between the two pathways (Shih et al., 2011).

Activation of the NF κ B pathway plays a central role in inducing the expression of pro-inflammatory factors (Tak and Firestein, 2001). Prostate tumour derived inflammatory factors (such as IL-6 and IL-1 β) have been shown to promote prostate cancer cell growth and survival, while other prostate tumour derived inflammatory factors (such as IL-8, CXCL12, MMP-9 and VEGF) have been shown to promote prostate cancer cell metastasis and invasion (Nguyen et al., 2014b, Pu et al., 2009, Stark et al., 2015). In the bone metastatic niche, prostate tumour derived inflammatory cytokines play an important role in regulating the differentiation and function of osteoclasts and osteoblasts; in turn osteoclasts and osteoblasts release inflammatory factors that promote the growth and establishment of prostate tumour metastasis in bone (Roca and McCauley, 2015).

Chapter 6

Effects of IKK α on the NF κ B pathway

Prostate cancer cells promote osteoclast differentiation and function, by producing pro-inflammatory factors such as: RANKL, PTHrP, M-CSF, IL-6, and TNF α ; most of these factors promote NF κ B activation and are themselves regulated by the NF κ B pathway (Gupta et al., 2012, Jin et al., 2013, Kavitha et al., 2014, Nguyen et al., 2014a). Jin *et al.*, have previously reported that activation of NF κ B in prostate cancer cells leads to increased expression of PTHrP and RANKL which are known to promote osteoclastogenesis (Jin et al., 2013). PC3 conditioned media was shown to increase the expression of osteoclastic genes in RAW264.7 osteoclast precursor cells and to regulate RAW264.7 osteoclastogenesis through the production of a variety of pro-inflammatory cytokines including IGF-1, TGF β , TNF α , and M-CSF (Akech et al., 2010, Kavitha et al., 2014). A study by Armstrong *et al.*, highlighted the importance of the NF κ B in the cross-talk between prostate cancer cells and osteoclasts *in vivo*, where they showed that injection of PC3 cells into mice induced stromal and systematic RANKL expression, moreover, injected PC3 cells were shown to respond to the increase in RANKL expression by promoting the expression of genes involved in osteolysis and invasion (Armstrong et al., 2008). Recently, work by Marino and colleagues, from our group, demonstrate that disrupting NF κ B activation is effective in reducing breast cancer induced osteolysis *in vivo* (Marino et al., 2018). Marino *et al.*, used a selective pharmacological inhibitor of IKK β to suppress breast cancer- and RANKL- induced NF κ B activation in osteoclasts, as shown by reduced phosphorylation of I κ B α (Marino et al., 2018).

Prostate cancer cells also produce a variety factors that regulate osteoblast differentiation and function, including pro-inflammatory: TGF β , TNF α and IL-1 β (Barrack, 1997, Tang and Alliston, 2013, Ganguly et al., 2014, Graham et al., 2010, Ritchie et al., 1997, Ide et al., 1997, Thomas and Hamdy, 2000, Schulze et al., 2012). Prostate tumour derived cytokines such as IL-1, IL-6 and TNF α where shown to promote RANKL expression by osteoblasts in bone and thereby promote osteoclastogenesis (Gupta et al., 2012, Kavitha et al., 2014, Roca and McCauley, 2015). Additionally, PC3 conditioned media was shown to induce the expression of NF κ B-regulated chemokines in osteoblasts, these include: IL-8, CXCL5 (ENA-78),

Chapter 6

Effects of IKK α on the NF κ B pathway

CCL5 and CXCL1 (Schulze et al., 2012). These effects were mediated by IL-1 β present in PC3 conditioned media activating the NF κ B pathway in osteoblasts. IL-1 β increased p65 phosphorylation, which in turn increased IL-1 β expression in osteoblasts and in PC3 cells. The study by Schulze *et al.*, highlights the importance of NF κ B in the cross-talk between prostate cancer cells and osteoblasts (Schulze et al., 2012). Increased NF κ B activation is known to inhibit osteoblastic differentiation and function, by promoting β -catenin degradation and thereby suppressing Wnt signalling, whereas, blocking NF κ B activation was shown to enhance osteoblastic differentiation and function (Le Henaff et al., 2015, Chang et al., 2009, Chang et al., 2013, Ma and Hottiger, 2016). Prostate cancer cell produced TNF α (an activator of NF κ B signalling) has been shown to inhibit osteoblast differentiation by disrupting Wnt signalling (Heiland et al., 2010, Tse et al., 2012). Chang *et al.*, showed that a small molecular inhibitor of IKK β was effective in blocking TNF α induced NF κ B activation in mouse MSCs, as shown by the suppression of I κ B α -phosphorylation/degradation and p65-phosphorylation, and that this reversed the inhibitory effects of TNF α on the osteoblastic differentiation of MSCs (Chang et al., 2013). Marino *et al.*, showed that inhibition of the NF κ B pathway, using the general inhibitor of IKK α / β parthenolide, enhanced osteoblast differentiation and this was associated with increased β -catenin activation (Marino et al., 2017).

The evidence presented above highlights the importance of the NF κ B pathway in regulating the behaviour and interaction of prostate cancer cells, osteoclasts and osteoblasts. Therefore, it is important to establish the effects of the verified IKK α inhibitor, SU1349, on NF κ B signalling in prostate cancer cells, osteoclasts and osteoblasts, in order to better understand the effects of SU1349 on these cells and their ability interact *in vitro* and *in vivo*.

Chapter 6

Effects of IKK α on the NF κ B pathway

6.3 Aims

In this chapter I aim to investigate the role of IKK α /NF κ B signalling pathway in the interactions between prostate cancer cells and bone cells, in particular osteoclasts and osteoblasts. Additionally, to investigate the effects of pharmacological inhibition by verified IKK α inhibitor, SU1349, on both canonical and non-canonical NF κ B signalling in osteoclasts and osteoblasts. Also, in this chapter I aim to investigate the effects of IKK α pharmacological inhibition, by SU1349, on PC3 prostate cancer cell derived pro-inflammatory soluble factors that are involved in the regulation of prostate cancer cells, osteoclasts and osteoblasts.

6.4 Results

6.4.1 Pharmacological inhibition of IKK α suppressed PC3 induced NF κ B activation in osteoclast precursors

Previous work has shown that PC3 conditioned media induced the expression of osteoclastic genes in RAW264.7 osteoclast precursor cells (Akech et al., 2010). Here, I first investigate if PC3 conditioned media activated the NF κ B pathway in the osteoclast precursor cells RAW264.7 using western blots. RAW264.7 cells cultured in serum free media were treated with PC3 conditioned media (20% v/v) for 10-15mins or left untreated. As shown in figure 6.1, there was a significant increase in phospho-I κ B by 430% ($p < 0.05$) and this was associated with a significant degradation of total I κ B by 94% ($n=2$; $p < 0.0001$), indicating activation of canonical NF κ B signalling. There was also a non-significant increase in phospho-p100 by 61% ($\pm 24\%$, $p = 0.069$) and this was associated with a non-significant increase in total p52 levels by 51% ($\pm 21\%$, $p = 0.051$), indicating activation of non-canonical NF κ B signalling. The effects on total p100 were not significant ($p = 0.19$).

In chapter 4, I show that SU1349 suppressed osteoclastogenesis in the presence of PC3 derived factors. Next, I investigated the effects of the IKK α inhibitor, SU1349, on PC3 induced NF κ B activation in RAW264.7 cells. RAW264.7 cells were pre-treated with 10 μ M SU1349 for 1 hour before stimulation with PC3 conditioned media (20% v/v). As shown in figure 6.1, there was a significant suppression of both canonical and non-canonical NF κ B activation. SU1349 suppressed phospho-p100 by 34% ($p < 0.0001$), which was associated with total p100 increase by 253% ($\pm 92\%$; $p = 0.052$) and total p52 reduction by 48% ($p < 0.05$), indicating an inhibition of p100 processing to p52. Also, phospho-I κ B was reduced by 60% ($p < 0.01$), which was associated with an increase in total I κ B by 146% ($n=2$; $p < 0.01$), indicating a suppression of I κ B degradation.

Chapter 6

Effects of IKK α on the NF κ B pathway

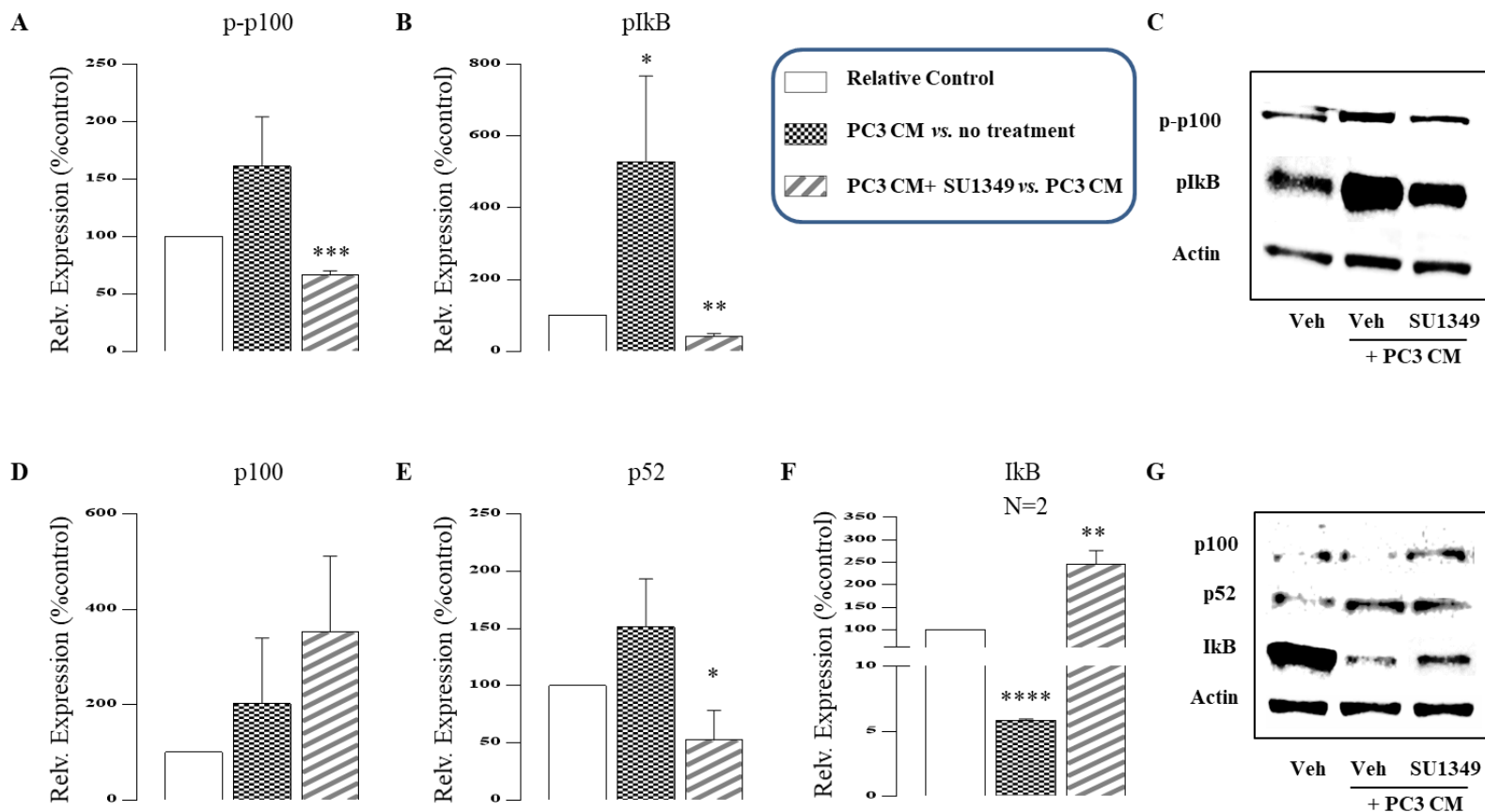


Figure 6.1: SU1349 suppressed NF κ B Activation by PC3 conditioned media in osteoclast precursor cells. RAW264.7 cells were pre-treated with 10 μ M SU1349 or vehicle control (1% DMSO) for 1hour in serum free media before stimulation with PC3 conditioned media (20% v/v) for 10-15mins. Total cellular lysates (50 μ g/lane) were subjected to western blot analysis. **A-C:** western blot analysis of phospho-proteins: phospho-p100 (p-p100) and phospho-I κ B (pIkB); representative blot image shown. **D-G:** western blot analysis of total proteins: NF κ B p100; p52; and I κ B; representative blot image shown. Values in the graphs are mean (expressed as % of control) \pm s.d. and are obtained from 3 independent experiments.

6.4.2 Pharmacological inhibition of IKK α suppressed RANKL induced NF κ B activation in osteoclast precursors

In chapter 4, I show that SU1349 suppressed RANKL-induced osteoclastogenesis including in RAW264.7 cells. Here, I first show that RANKL activated the canonical-NF κ B pathway in the osteoclast precursor cells RAW264.7 using western blots. RAW264.7 cells in serum free media were treated with RANKL (150ng/ml) for 5mins or were left untreated. As shown in figure 6.2, there was an increase in phospho-I κ B by 371% (\pm 275%; $p=0.12$), however, although phospho-I κ B levels were increased consistently in 3 independent experiments, it did not reach statistical significant due to considerable variability in the magnitude of this increase between experiments. Nonetheless, there was a significant reduction in total I κ B by 63% ($p<0.001$), further indicating canonical-NF κ B activation by RANKL that is promoting I κ B degradation. RANKL effects on the non-canonical NF κ B, at this time point (5min), did not appear to be significant on the whole, as shown by the non-significant effects on phospho-I κ B and total p52 by RANKL, however, there was an associated increase in total p100 by 27% ($p<0.001$).

Next, I show that the IKK α inhibitor, SU1349, suppressed RANKL induced canonical-NF κ B activation in RAW264.7 cells. RAW264.7 cells were pre-treated with 10 μ M SU1349 for 1 hour before stimulation with RANKL (150ng/ml). As shown figure 6.2, SU1349 suppressed phospho-I κ B by 71% ($p<0.05$), however, this was associated with an unanticipated reduction in total I κ B by 45% ($p<0.05$). The effects of SU1349 had non-significant effects on the non-canonical NF κ B pathway after 5min of RANKL stimulation.

Chapter 6

Effects of IKK α on the NF κ B pathway

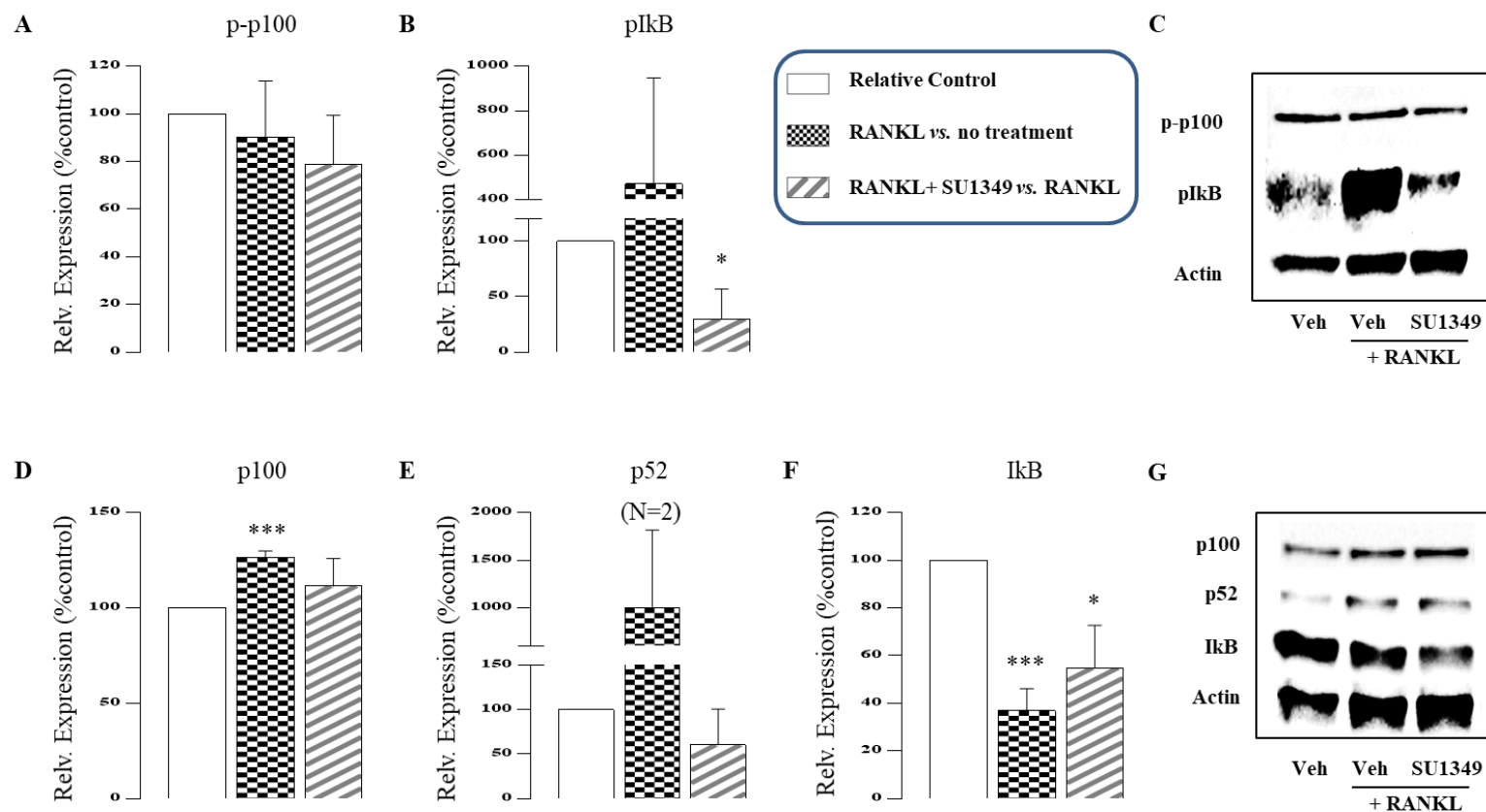


Figure 6.2: SU1349 suppressed NF κ B Activation by RANKL in osteoclast precursor cells. RAW264.7 cells were pre-treated with 10 μ M SU1349 or vehicle control (1% DMSO) for 1hour in serum free media before stimulation with RANKL(150ng/ml) for 5mins. Total cellular lysates (50 μ g/lane) were subjected to western blot analysis. **A-C**: western blot analysis of phospho-proteins: phospho-p100 (p-p100) and phospho-I κ B (pIkB); representative blot image shown. **D-G**: western blot analysis of total proteins: NF κ B p100; p52; and I κ B; representative blot image shown. Values in the graphs are mean (expressed as % of control) \pm s.d. and are obtained from 3 independent experiments.

6.4.3 Pharmacological inhibition of IKK α suppressed PC3 induced NF κ B activation in osteoblast precursors

Schulze *et al.*, previously report that PC3 conditioned media induced the expression of NF κ B-regulated chemokines in osteoblasts (Schulze et al., 2012). However, they did not directly explore the effects of PC3 conditioned media on the NF κ B in osteoblasts. Here, I established that PC3 conditioned media activated the NF κ B pathway in the osteoblast precursor cells MC3T3s using western blots. MC3T3s cells in serum free media were treated with PC3 conditioned media (20% v/v) for 10-15mins or left untreated. Figure 6.3 shows, that there was a significant activation of the canonical NF κ B pathway by PC3 conditioned media, as shown by the increase in phospho-I κ B by 85% ($p < 0.05$) and this was associated an increase in degradation as shown by the decrease of total I κ B by 23% ($p < 0.001$). Although PC3 conditioned did not have a significant effect on phospho-p100, there was an associated a decrease in total p100 by 50% ($p < 0.01$) and an increase in total p52 levels 221% ($p < 0.05$), indicating an activation of non-canonical NF κ B signalling.

Previous work has shown that inhibition of NF κ B activation enhances osteoblastic differentiation and function (Chang et al., 2013). Consistently, I show in chapter 5, that SU1349 - in the presence of PC3 derived factors - stimulated osteoblastic differentiation and bone nodule formation *in vitro*. Therefore, here I first established the effects of the IKK α inhibitor, SU1349, on PC3 mediated NF κ B activation in MC3T3 cells. MC3T3s cells were pre-treated with 10 μ M SU1349 for 1 hour before stimulation with PC3 conditioned media (20% v/v). As in shown figure 6.3, there was a significant suppression of both canonical and non-canonical NF κ B activation. SU1349 suppressed phospho-p100 by 52% ($p < 0.01$), this was associated with an increase in total p100 by 175% ($n=2$; $p < 0.0001$) and total p52 reduction by 44% ($p < 0.01$), indicating an inhibition of p100 processing to p52. Also, phospho-I κ B was reduced by 56% ($p < 0.05$) and this was associated with a non-significant increase in total I κ B by 24% ($\pm 19\%$; $p = 0.29$).

Chapter 6

Effects of IKK α on the NF κ B pathway

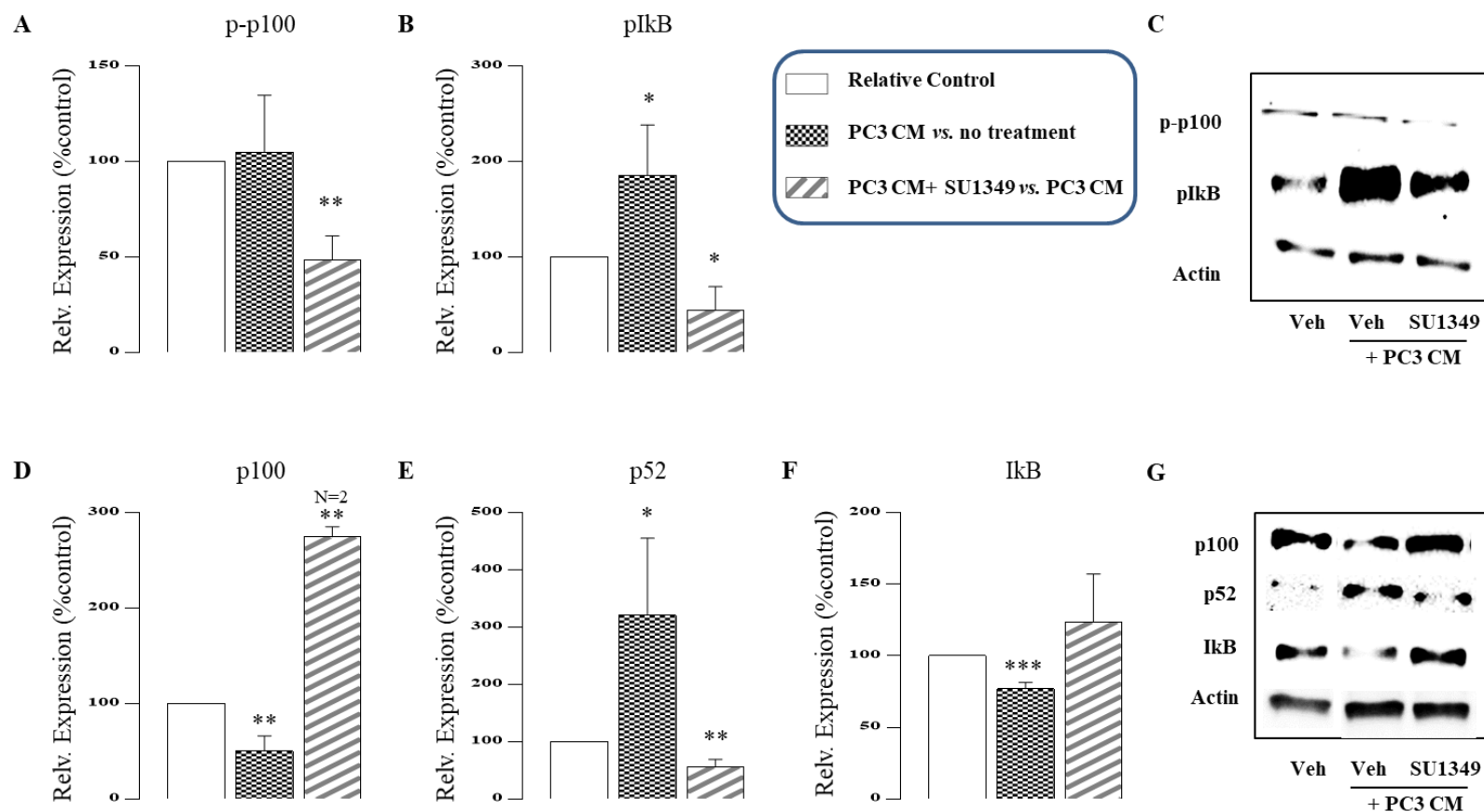


Figure 6.3: SU1349 suppressed NF κ B Activation by PC3 conditioned media in osteoblast precursor cells. MC3T3 cells were pre-treated with 10 μ M SU1349 or vehicle control (1% DMSO) for 1 hour in serum free media before stimulation with PC3 conditioned media (20% v/v) for 10-15mins. Total cellular lysates (50 μ g/lane) were subjected to western blot analysis. **A-C**: western blot analysis of phospho-proteins: phospho-p100 (p-p100) and phospho-I κ B (pI κ B); representative blot image shown. **D-G**: western blot analysis of total proteins: NF κ B p100; p52; and I κ B; representative blot image shown. Values in the graphs are mean (expressed as % of control) \pm s.d. and are obtained from 3 independent experiments.

6.4.4 Pharmacological inhibition of IKK α suppressed Wnt signalling in osteoclast precursors

Activation of Wnt signalling is known to inhibit osteoclast differentiation (Albers et al., 2013). In the same western blots where I show SU1349 suppressed PC3 induced NF κ B activation, I found that SU1349 also suppressed activation of Wnt signalling in RAW264.7 cells. As shown in figure 6.4, PC3 conditioned appeared to activate the Wnt pathway, as shown by the non-significant increase in phospho-GSK3 β by 146% (\pm 61%; $p=0.054$). However, SU1349 suppressed Wnt activation, as shown by the significant reduction in phospho-GSK3 β by 40% ($p<0.01$).

Wnt activation is characterized by increased GSK3 β phosphorylation, which protects cytoplasmic β -catenin from degradation, and thus allows for increased nuclear translocation of β -catenin (Carayol and Wang, 2006). Therefore, in order to further validate the effects of SU1349 on Wnt signalling, I next investigated the effects of SU1349 on β -catenin subcellular levels. First, I established the effects of PC3 conditioned media on p65 (nuclear p65 is indicator of NF κ B activation) and β -catenin subcellular shuttling in the osteoclast precursor cells RAW264.7. RAW264.7 cultures in serum free media were treated with PC3 conditioned media (20% v/v) for 45mins or left untreated. As shown in figure 6.5, PC3 conditioned media significantly reduced levels of the canonical NF κ B transcription factor p65 in the nucleus by 32% ($p<0.05$) and this was associated with a non-significant increase in cytoplasmic p65 levels. PC3 conditioned media did not appear to significantly affect levels of cytoplasmic β -catenin. Pre-treatment of RAW264.7 cells with 10 μ M SU1349 for 1 hour before additional treatment with PC3 conditioned media, appeared to increase nuclear p65 levels by 167% (\pm 72%; $p=0.082$) and cause a modest but non-significant reduction in cytoplasmic β -catenin by 16% (\pm 10%; $p=0.2$). Nuclear β -catenin in RAW264.7 cells was not detected.

Chapter 6

Effects of IKK α on the NF κ B pathway

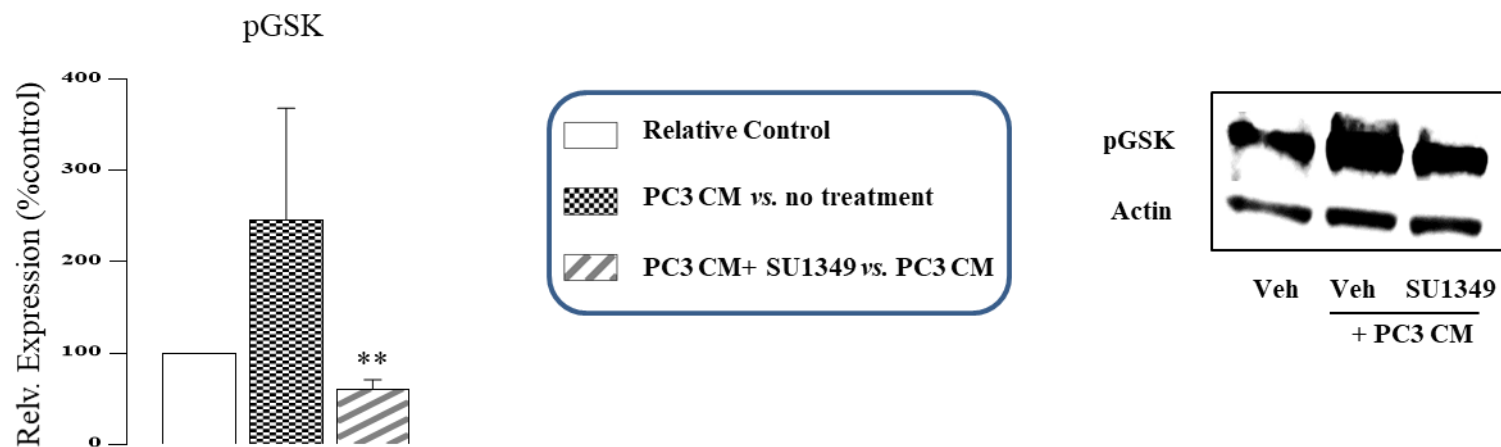


Figure 6.4: SU1349 suppressed GSK3 β phosphorylation in osteoclast precursor cells. RAW264.7 cells were pre-treated with 10 μ M SU1349 or vehicle control (1% DMSO) for 1 hour in serum free media before stimulation with PC3 conditioned media (20% v/v) for 10-15mins. Total cellular lysates (50 μ g/lane) were subjected to western blot analysis. Western blot analysis of PC3 conditioned media effect on phospho-GSK3 β (pGSK) levels and SU1349 effect on phospho-GSK3 β (pGSK) levels in the presence of PC3 conditioned media; representative blot image shown. Values in the graphs are mean (expressed as % of control) \pm s.d. and are obtained from 3 independent experiments.

Chapter 6

Effects of IKK α on the NF κ B pathway

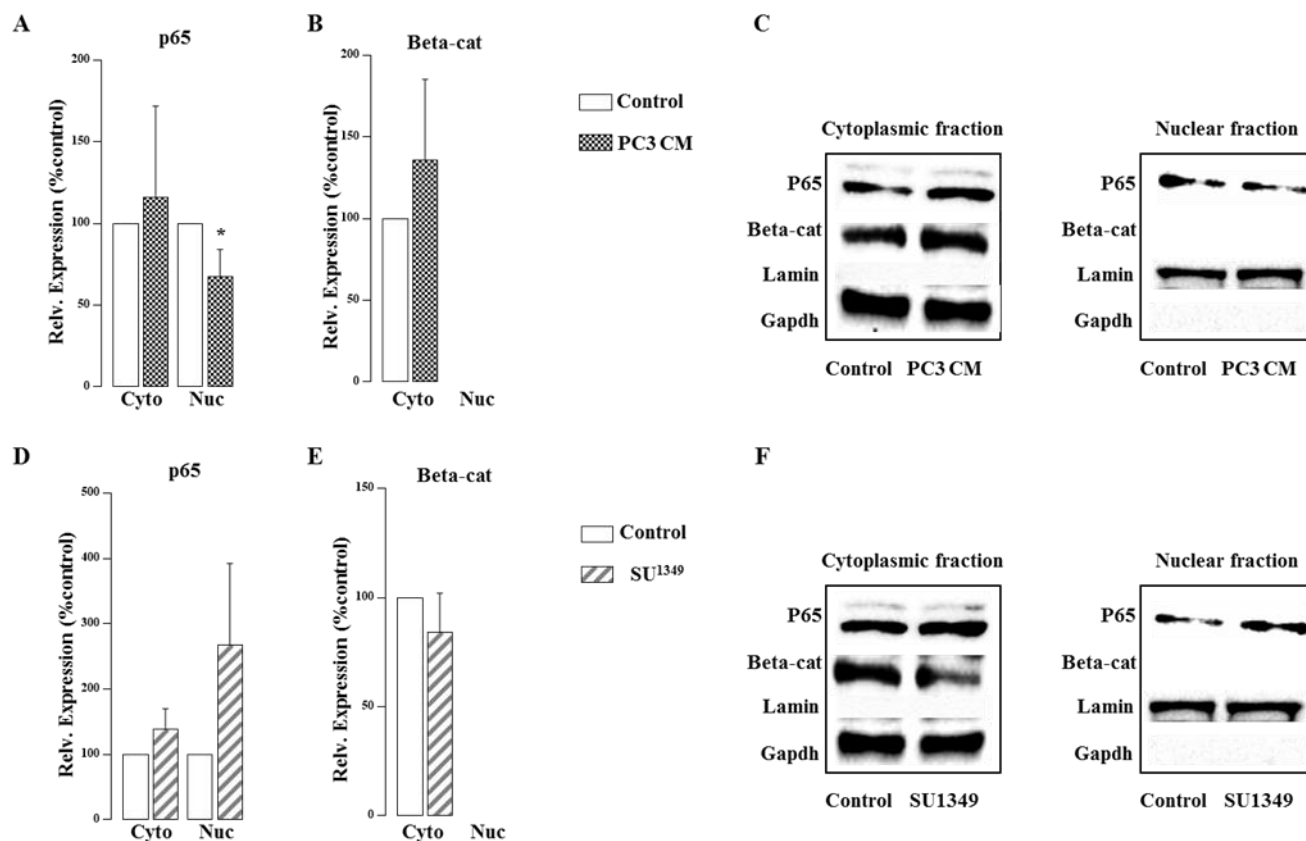


Figure 6.5: SU1349 caused a non-significant reduction in cytoplasmic β -catenin in osteoclast precursor cells. RAW264.7 cells were pre-treated with 10 μ M SU1349 or vehicle control (1% DMSO) for 1 hour in serum free media before stimulation with PC3 conditioned media (20% v/v) for 45mins. Cytoplasmic fraction (80 μ g/lane) and all of the nuclear fraction were subjected to western blot analysis. **A-C:** western blot analysis of PC3 conditioned media effect on nuclear and cytoplasmic p65 and β -catenin levels; representative blot image shown. **D-F:** western blot analysis of SU1349 effect on nuclear and cytoplasmic p65 and β -catenin levels in the presence of PC3 conditioned media; representative blot image shown. Values in the graphs are mean (expressed as % of control) \pm s.d. and are obtained from 3 independent experiments

6.4.5 Pharmacological inhibition of IKK α enhanced Wnt signalling in osteoblast precursors

Previous work has shown that NF κ B inhibition enhances osteoblastic differentiation and function and this is associated with increased Wnt/ β -catenin signalling (Chang et al., 2013, Marino et al., 2018). In the same western blots where I show SU1349 suppressed PC3 induced NF κ B activation, I found that SU1349 also increased activation of Wnt signalling in MC3T3 cells. In figure 6.6, I show that PC3 conditioned media appeared to activate the Wnt pathway, as shown by the non-significant increase in phospho-GSK3 β levels. However, SU1349 treatment increased Wnt activation, as shown by the increase in phospho-GSK3 β by 46% ($p < 0.05$). Wnt activation is characterized by increased GSK3 β phosphorylation, which protects cytoplasmic β -catenin from degradation, and thus it allows for increased nuclear translocation of β -catenin (Carayol and Wang, 2006). Therefore, in order to further validate the effects of SU1349 on Wnt signalling, I next investigated the effects of SU1349 on β -catenin subcellular levels.

First, I established that PC3 conditioned media on p65 (nuclear p65 is indicator of NF κ B activation) and β -catenin subcellular shuttling in the osteoclast precursor cells MC3T3. MC3T3 cells in serum free media were treated with PC3 conditioned media (20% v/v) for 45mins or left untreated. As shown in figure 6.7, PC3 conditioned media appeared to promote p65 shuttling from the cytoplasm to the nucleus, as shown by the significant reduction in cytoplasmic p65 by 38% ($p < 0.05$) and appeared to cause a non-significant increase in nuclear p65 by 124% ($\pm 80\%$; $p = 0.2$). MC3T3 showed high expression of β -catenin that was predominately localised to the nucleus. PC3 conditioned media did not have any significant effects on nuclear or cytoplasmic levels of β -catenin.

Pre-treatment of MC3T3 cells with 10 μ M SU1349 for 1 hour before additional treatment with PC3 conditioned media, appeared to reduce p65 shuttling to the nucleus and protect cytoplasmic β -catenin from GSK3 β mediated proteasomal degradation. As shown in figure 6.7, SU1349 increased cytoplasmic p65 levels by 40% ($p < 0.01$) and reduced nuclear p65 by 24% ($p < 0.0001$), indicating an inhibition of NF κ B mediated

Chapter 6

Effects of IKK α on the NF κ B pathway

shuttling of p65 to the nucleus. SU1349 treatment was associated with a significant increase in cytoplasmic β -catenin levels by 16% ($p < 0.01$), indicating protection from proteasomal degradation. However, SU1349 did not have significant effects on nuclear β -catenin levels which showed a non-significant reduction by 10% ($\pm 11\%$; $p = 0.44$).

Chapter 6

Effects of IKK α on the NF κ B pathway

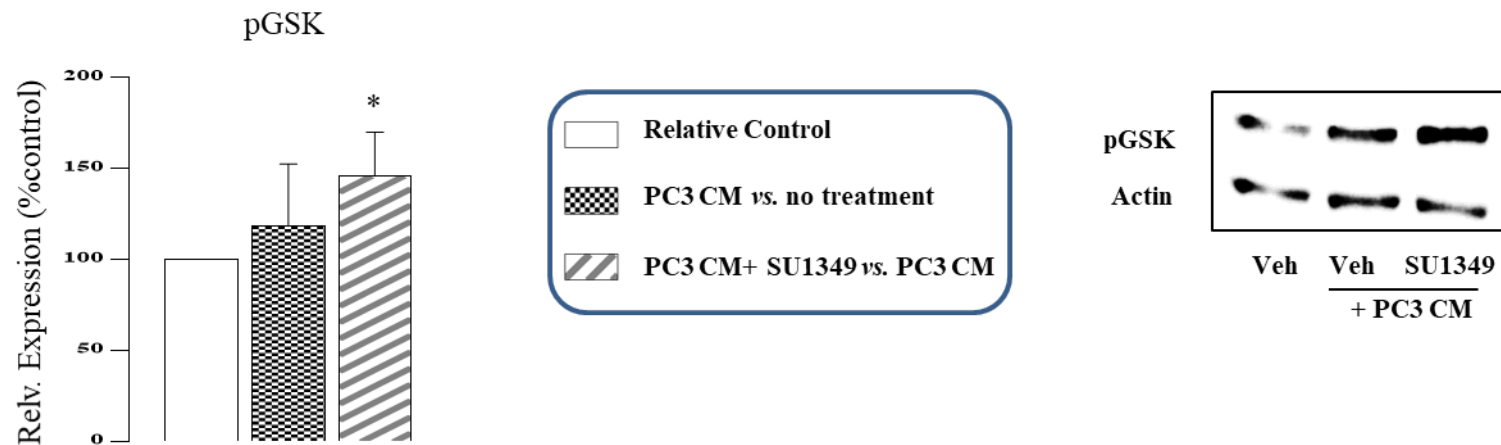


Figure 6.6: SU1349 increased GSK3 β phosphorylation in osteoblast precursor cells. MC3T3 cells were pre-treated with 10 μ M SU1349 or vehicle control (1% DMSO) for 1 hour in serum free media before stimulation with PC3 conditioned media (20% v/v) for 10-15mins. Total cellular lysates (50 μ g/lane) were subjected to western blot analysis. Western blot analysis of PC3 conditioned media effect on phospho-GSK3 β (pGSK) levels and SU1349 effect on phospho-GSK3 β (pGSK) levels in the presence of PC3 conditioned media; representative blot image shown. Values in the graphs are mean (expressed as % of control) \pm s.d. and are obtained from 3 independent experiments.

Chapter 6

Effects of IKK α on the NF κ B pathway

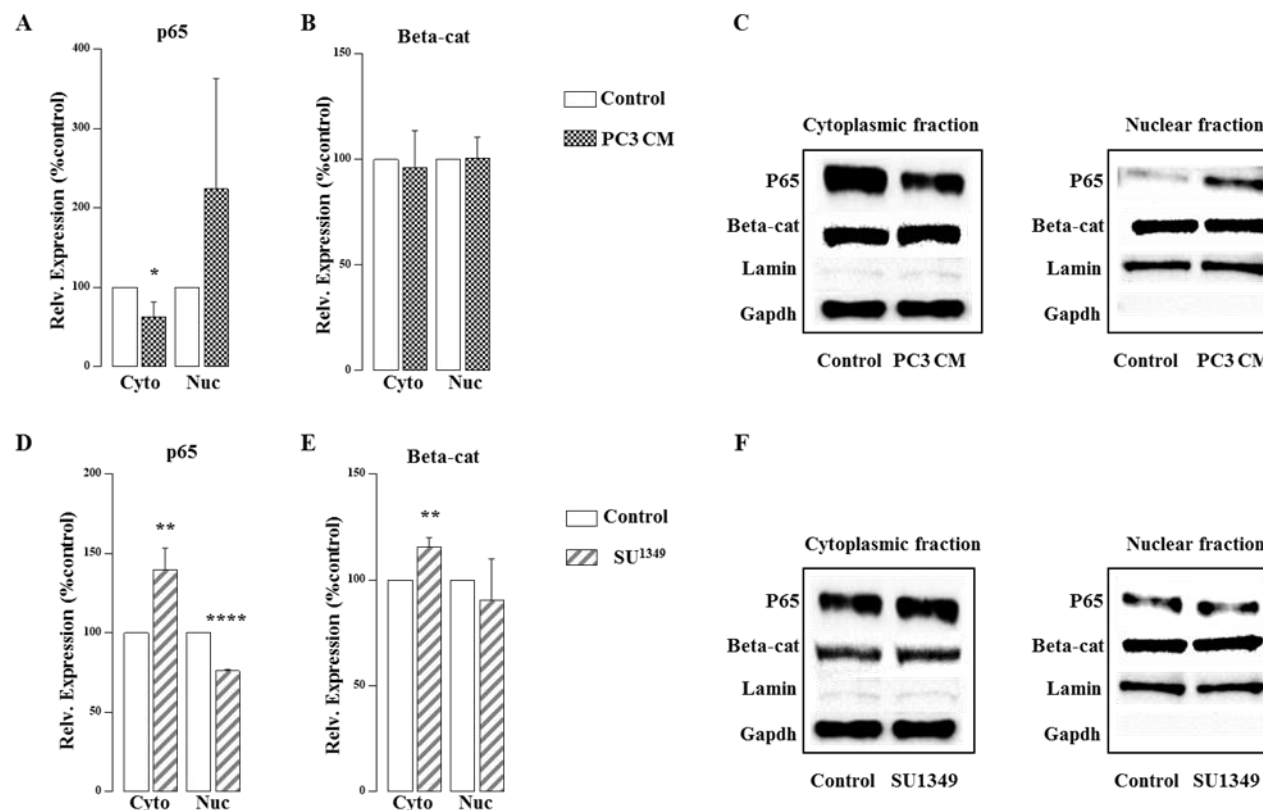


Figure 6.7: SU1349 caused a significant increase in cytoplasmic β -catenin in osteoblast precursor cells. MC3T3 cells were pre-treated with 10 μ M SU1349 or vehicle control (1% DMSO) for 1 hour in serum free media before stimulation with PC3 conditioned media (20% v/v) for 45mins. Cytoplasmic fraction (80 μ g/lane) and all of the nuclear fraction were subjected to western blot analysis. **A-C:** western blot analysis of PC3 conditioned media effect on nuclear and cytoplasmic p53 and β -catenin levels; representative blot image shown. **D-F:** western blot analysis of SU1349 effect on nuclear and cytoplasmic p53 and β -catenin levels in the presence of PC3 conditioned media; representative blot image shown. Values in the graphs are mean (expressed as % of control) \pm s.d. and are obtained from 3 independent experiments.

6.4.6 Pharmacological inhibition of IKK α reduced PC3 derived pro-inflammatory factors

Activation of the NF κ B pathway plays a central role in inducing the expression of pro-inflammatory factors (Tak and Firestein, 2001). In this chapter I showed that PC3 conditioned media activated NF κ B signalling in osteoclast and osteoblast precursors. Moreover, in chapter 3, I show SU1349 suppressed PC3 growth and motility. Here I investigated the effects of the verified IKK α inhibitor, SU1349, on the levels of PC3 derived pro-inflammatory factors, which could inhibit PC3 cells ability to influence osteoclasts and osteoblast, also inhibit the ability of PC3 cells to promote their own growth and motility. Two membrane-based microarrays, with capture antibodies for 102 human cytokines that are spotted in duplicate on the membrane, were incubated with conditioned media from PC3 cells treated with 1 μ M SU1349 or vehicle control for 24 hrs in serum free media, before undergoing chemiluminescence detection and analysis. The effect of SU1349 treatment on the production of soluble factors by PC3 was expressed as percentage of vehicle treatment. As shown in figure 6.8 (panel A), 22 soluble factors were considered to be significantly differentially regulated with SU1349 treatment (this was based on whether the standard deviation in means from spotted duplicates for each factor were small enough within the array and were adequately different between the arrays- i.e. that percent changes were going in the same directions; furthermore, differences were confirmed by visual inspection of probes on each array blot to limit false positives). Also shown in figure 6.8 (panel B), a Venn diagram of the overlapping role for these pro-inflammatory factors in the regulation of prostate cancer cell growth and metastasis, as well as the regulation of cells found within the bone metastatic niche notably osteoclasts, osteoblasts and adipocytes. Table 6.1, shows a summary of effects based on the literature for each of the 22 factors in prostate cancer cells, osteoclasts, osteoblasts and adipocytes.

Chapter 6

Effects of IKK α on the NF κ B pathway

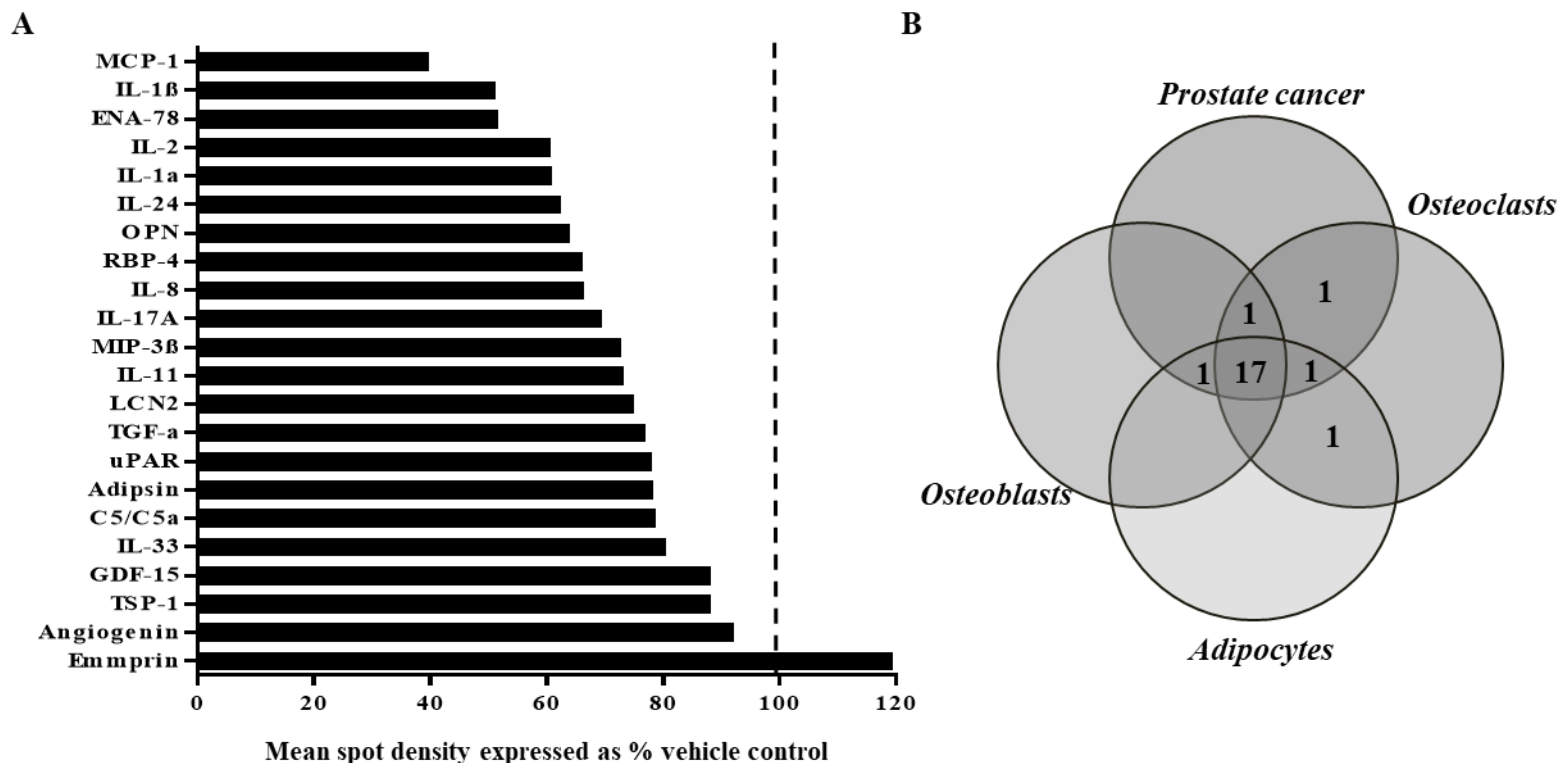


Figure 6.8: Pharmacological inhibition of IKK α reduced PC3 derived pro-inflammatory factors. **A:** Microarray analysis of soluble factors in PC3 conditioned media treated with 1 μ M SU1349 or vehicle control (0.1% DMSO) for 24hrs, using Proteome ProfilerTM Human XL Cytokine Array Kit (R&D systems). **B:** Venn diagram of microarray results shows differentially expressed factors have overlapping roles in the regulation of prostate cancer cells & cells found in the bone microenvironment.

Chapter 6

Effects of IKK α on the NF κ B pathway

Table 6.1: Summary table for effects of SU1349 differentially regulated factors on prostate cancer cells, osteoclasts, osteoblasts and adipocytes. Effects on cells (reported in the literature) are indicated by: \uparrow = positive; \downarrow = negative; $\uparrow\downarrow$ = positive and/or negative; \leftrightarrow = an ambiguous association; -- = no association found. References for effects are also included.

Protein	Prostate cancer	Osteoclast	Osteoblast	Adipocytes	Refs
MCP-1	\uparrow	\uparrow	\leftrightarrow	\downarrow	(Lu et al., 2009, Li et al., 2007a, Lu et al., 2007, Kanda et al., 2006)
IL-1β	\uparrow	\uparrow	\downarrow	\downarrow	(Voronov et al., 2003, Lee et al., 2010, Taichman and Hauschka, 1992, Bing, 2015, Trebec-Reynolds et al., 2010)
ENA-78	\uparrow	\uparrow	\leftrightarrow	\downarrow	(Begley et al., 2008, Sundaram et al., 2013, Roca et al., 2018, Hsu et al., 2013, Chavey and Fajas, 2009, Kabir et al., 2014)
IL-2	\uparrow	\uparrow	—	\uparrow	(Belldegrun et al., 2001, Ries et al., 1989, Vielma et al., 2013, Huh et al., 2014)
IL-1α	\uparrow	\uparrow	\downarrow	\downarrow	(Ricote et al., 2004, Tani-Ishii et al., 1999, Tanabe et al., 2004, Um et al., 2011, Sauane et al., 2008)
IL-24	\downarrow	—	$\uparrow\downarrow$	\leftrightarrow	(Sauane et al., 2008, Lee et al., 2012, Kragstrup et al., 2017, Kragstrup et al., 2016, Strong et al., 2017)
OPN	\leftrightarrow	\uparrow	\downarrow	\downarrow	(Thoms et al., 2012, Yamate et al., 1997, Huang et al., 2004, Tardelli et al., 2016, Zeyda et al., 2011)
RBP-4	\uparrow	\leftrightarrow	$\uparrow\downarrow$	\downarrow	(Uehara et al., 2013) (Ghanem et al., 2017, Hogstrom et al., 2008, Norseen et al., 2012, Leitch et al., 2013)
IL-8	\uparrow	\uparrow	\leftrightarrow	\downarrow	(Neveu et al., 2014, Bendre et al., 2003, Bussard et al., 2010, Kobashi et al., 2009)
IL-17A	\uparrow	\downarrow	$\uparrow\downarrow$	\downarrow	(Zhang et al., 2017a, Kitami et al., 2010, Croes et al., 2016, Qu et al., 2016, Wang et al., 2017, Ahmed and Gaffen, 2013)

Chapter 6

Effects of IKK α on the NF κ B pathway

MIP-3β	↑*	↑	↑	↔	(Peng et al., 2015, Lee et al., 2017, Qin et al., 2014, Tourniaire et al., 2013) *retracted
IL-11	↑	↑	↑↓	↓	(Furuya et al., 2005, Kudo et al., 2003, Matsumoto et al., 2012, Keller et al., 1993)
LCN2	↑	↓	↓	↑	(Tung et al., 2013, Kim et al., 2015, Rucci et al., 2015, Zhang et al., 2008)
TGF-α	↑	↑	↑	↑↓	(Liu et al., 1993, Takahashi et al., 1986, Panagakos, 1994, Butterwith et al., 1992)
uPAR	↑	↑	↓	↑	(Margheri et al., 2005, Furlan et al., 2007, Kanno et al., 2010)
Adipsin	↔	—	—	↔	(Ribeiro et al., 2012)
C5/C5a	↑	↑	↔	↓	(Nitta et al., 2013, Ignatius et al., 2011, Phielers et al., 2013)
IL-33	↓	↓	↑	↑	(Saranchova et al., 2016, Saleh et al., 2011, Han et al., 2015)
GDF-15	↑↓	↑	↓	↓	(Husaini et al., 2015, Westhrin et al., 2015, Yanagitai et al., 2012, Ding et al., 2009b)
TSP-1	↑	↑	↓	↑↓	(Firlej et al., 2011, Amend et al., 2015, DuBose et al., 2012, Varma et al., 2008)
Angiogenin	↑	↓	—	—	(Li et al., 2011, Morita et al., 2008)
Emmprin	↑	↑	↑	—	(Hao et al., 2010b, Rucci et al., 2010, Lu et al., 2013, Hao et al., 2010a)

Abbreviations: **MCP-1** (Monocyte chemotactic protein-1 aka. CCL2); **ENA-78** (Epithelial-neutrophil activating peptide; aka. CXCL5); **OPN** (Osteopontin); **RBP-4** (Retinol binding protein 4); **MIP-3 β** (Macrophage inflammatory protein 3 beta aka. CCL19); **LCN2** (Lipocalin-2); **TGF- α** (Transforming growth factor- α); **uPAR** (Urokinase plasminogen activator receptor); **C5/C5a** (Complement component C5/C5a); **GDF-15** (Growth Differentiation Factor 15); **TSP-1** (Thrombospondin-1); **Emmprin** (Extracellular matrix metalloproteinase inducer aka. CD147).

6.5 Discussion

The NF κ B pathway is known to be important in the regulation of prostate cancer cells, osteoclasts and osteoblasts and their interactions *in vitro* and *in vivo* (Tak and Firestein, 2001, Nguyen et al., 2014b, Pu et al., 2009, Stark et al., 2015, Roca and McCauley, 2015). In previous chapters I presented effects for the novel IKK α inhibitor, SU1349, in prostate cancer cells, osteoclasts and osteoblasts that are consistent with inhibition of the NF κ B pathway. In this chapter I verify that the IKK α inhibitor, SU1349, exerts its effects on prostate cancer cells, osteoclasts and osteoblasts—at least in part- through the inhibition of the NF κ B signalling and shed light on SU1349 mechanism of action.

Effects of SU1349 on NF κ B signalling in osteoclasts and osteoblasts

I show, in RAW264.7 osteoclast precursor cells, that PC3 conditioned media significantly activated the canonical NF κ B pathway, as shown by the increase in phospho-I κ B α and I κ B α degradation, in addition, PC3 conditioned media activated the non-canonical NF κ B pathway as shown by the increase in phospho-p100 and the increased processing of p100 to p52. This is in agreement with previous studies that show PC3 conditioned media activates RAW264.7 osteoclastogenesis (Kavitha et al., 2014) and that PC3 cells produce a variety of factors that can activate both the canonical and/or the non-canonical NF κ B pathways including classic NF κ B activators such as RANKL and TNF α (Gupta et al., 2012, Kavitha et al., 2014). I show that the selective IKK α inhibitor, SU1349, significantly suppressed PC3 induced canonical and non-canonical NF κ B activation. This is evidenced by reduced I κ B α phosphorylation and total I κ B α protection from degradation, in addition to reduced p100 phosphorylation and inhibition of p100 to p52 processing.

Furthermore, I show that SU1349 suppressed RANKL induced activation of canonical NF κ B signalling, as shown by the significant suppression of I κ B α phosphorylation, however, unexpectedly this was not associated with I κ B α protection from degradation, rather total I κ B α levels were further reduced. This can be explained by a study which reports that certain forms of I κ B α can exist free of association with p65 and this free I κ B α can be degraded independently of phosphorylation by IKKs (Mathes et al.,

Chapter 6

Effects of IKK α on the NF κ B pathway

2008), therefore, it is possible that reduced I κ B α that I observed in this experiment might be due to IKK independent degradation. Moreover, no significant effects were observed in non-canonical NF κ B signalling after RAW264.7 treatment with RANKL, this can be explained by the fact that these experiments were stopped after 5min of RANKL stimulation in contrast to experiments with PC3 conditioned media which were stopped 10-15min after stimulation, this agrees with the literature which reports that canonical NF κ B activation is known to be more rapid in comparison to non-canonical NF κ B activation that is known to be slower (Shih et al., 2011).

In MC3T3 osteoblast precursor cells, PC3 conditioned significantly activated the canonical NF κ B pathway as shown by the increase in phospho-I κ B α and I κ B α degradation, in addition, PC3 conditioned media activated the non-canonical NF κ B pathway as evident by the increase in p100 processing to p52. Previous studies report that conditioned media from PC3 cells regulate osteoblast differentiation through factors that include TGF β , TNF α and IL-1 β which also are known to activate the NF κ B pathway in osteoblasts (Graham et al., 2010, Ganguly et al., 2014). Schulze *et al.*, demonstrated that PC3 derived IL-1 β caused a rapid expression of NF κ B-regulated chemokines in osteoblasts (Schulze et al., 2012). I demonstrate that pre-treatment of MC3T3 cells with the selective IKK α inhibitor, SU1349, significantly suppressed PC3 induced NF κ B activation of canonical and non-canonical signalling. This is evident by the reduction in I κ B α and p100 phosphorylation as well as the inhibition of p100 processing to p52. These results are further supported by subsequent sub-cellular fraction analysis which show PC3 conditioned media increased p65 nuclear shuttling and this was suppressed by SU1349 pre-treatment.

Effects of SU1349 on Wnt/ β -catenin signalling in osteoclasts and osteoblasts

Activation of Wnt signalling has also been demonstrated to inhibit osteoclast differentiation (Albers et al., 2013) and promote osteoblast differentiation (Gaur et al., 2005). In the absence of Wnt activation GSK3 β constitutively phosphorylates cytosolic β -catenin which targets it for proteasomal degradation, however, activation of Wnt signalling blocks GSK3 β inhibitory role by phosphorylating GSK3 β , this protects cytoplasmic β -catenin from degradation, as a result it increases cytoplasmic

Chapter 6

Effects of IKK α on the NF κ B pathway

levels of β -catenin which ultimately allows for the nuclear translocation of β -catenin and the activation of Wnt-regulated gene expression (Carayol and Wang, 2006). Significant crosstalk exists between the NF κ B and Wnt/ β -catenin pathways, previously, NF κ B activation has been shown to inhibit osteoblast differentiation by promoting β -catenin degradation and thereby inhibiting Wnt signalling (Le Henaff et al., 2015, Chang et al., 2009, Chang et al., 2013, Ma and Hottiger, 2016). Since I had previously observed that the IKK α inhibitor, SU1349, suppressed osteoclast differentiation and stimulated osteoblast differentiation, I hypothesised that SU1349 might inhibit Wnt signalling in osteoclast precursors and activate Wnt signalling in osteoblast precursor cells, this might further explain- at least in part- the differential effects of SU1349 on osteoclast and osteoblast differentiation. Although not statistically significant, PC3 conditioned media appeared to activate Wnt signalling in osteoblast precursors (MC3T3 cells) and more so in osteoclast precursors (RAW264.7 cells), as evident by the increase in phosphorylation of GSK3 β . PC3 conditioned media contain factors that activate both the NF κ B pathway (such as RANKL and TNF α) and Wnt pathway (such as ET-1 and Wnts) simultaneously (Armstrong et al., 2008, Chang et al., 2013, Ganguly et al., 2014). Pre-treatment of cells with SU1349 prior to exposure to PC3 conditioned media stimulation significantly suppressed phosphorylation of GSK3 β in RAW264.7 cells, in contrast, SU1349 significantly increased phosphorylation of GSK3 β in MC3T3 cells. The differential effects of SU1349 on phosphorylation of GSK3 β , were further supported in subsequent sub-cellular fractionation analysis, as shown by the significant increase in cytoplasmic β -catenin in MC3T3 cells and an apparent decrease in cytoplasmic β -catenin in RAW264.7 cells (statistically non-significant). Collectively my results indicate that IKK α inhibitor, SU1349, inhibits Wnt activation in osteoclast precursors whilst stimulating Wnt activation in osteoblast precursors. Interestingly, SU1349 also reduced total β -catenin levels in PC3 (figure S6.1); reduced β -catenin expression was previously associated with suppressing prostate cancer progression in mice (Shukla et al., 2007).

Differential effects of SU1349 on canonical vs non- canonical NF κ B pathway?

In subcellular fractionation experiments, the response of p65 in MC3T3 cells confirmed NF κ B activation by PC3 conditioned media and inhibition of NF κ B by SU1349 in total cellular extracts. Surprisingly, results from sub-cellular fractionation experiments showed that PC3 conditioned media significantly reduced nuclear p65 in RAW264.7 cells, whereas SU1349 significantly increased nuclear p65. This seemingly, contradicts the RAW264.7 cells results in total cellular extracts. I would have expected an increase in nuclear p65 as PC3 conditioned media contains a variety of factors - described previously- that activate the NF κ B pathway. However, previous studies report that PC3 cells when compared to less aggressive prostate cancer cells such as LNCaP, produce relatively high amount of the potent NF κ B inhibitor, Osteoprotegerin (OPG), which was reported to be important for prostate cancer cell survival (Holen et al., 2002). Factors such as OPG present in PC3 conditioned media might explain the inhibitory effect of PC3 conditioned media on nuclear p65 seen in RAW264.7 cells. Similarly, it might in part explain my observation that PC3 conditioned media suppressed RANKL induced osteoclast formation in mouse total bone marrow cultures (figure S3.1), in addition to completely preventing RANKL induced osteoclastogenesis in RAW264.7 cells (results not shown). Furthermore, I would have anticipated a reduction in nuclear p65 due to NF κ B inhibition by SU1349 in osteoclast precursors similar to my results in osteoblast precursors. However, the unexpected increase in nuclear p65 in RAW264.7 seen with SU1349 treatment is supported by a previous study which report that genetic inactivation of IKK α in mouse macrophages leads to an increase in p65 nuclear accumulation, due to delayed p65 turnover, in response to activation of the NF κ B pathway (Lawrence et al., 2005). Lawrence *et al.*, demonstrate that normal IKK α function attenuates NF κ B activation in macrophages by directly phosphorylating p65 which accelerates p65 promoter clearance and therefore leads to the resolution of inflammation. Since RAW264.7 cells are considered macrophage-like cells, this might partially explain the increase in nuclear p65 I observed with SU1349 treatment. Moreover, the increase in nuclear p65 in RAW264.7 with SU1349 treatment might partially explain why I had observed that osteoclasts generated from RAW264.7 cultures in the presence of 0.1 μ M SU1349 appeared to

Chapter 6

Effects of IKK α on the NF κ B pathway

be considerably larger in size (however not in number) when compared to control cultures (figure 4.1 (B)), this indicates SU1349 at this concentration might have prolonged the NF κ B activation signal in these RAW264.7 cells.

It is possible to speculate that the differential effects of SU1349 on nuclear p65 and Wnt activation in RAW264.7 and MC3T3 cells might be explained by different effects on canonical and non-canonical NF κ B signalling that are cell type specific. First, considering the fact that although the accumulation of nuclear p65 in osteoclast precursors has been demonstrated to be dependent on IKK α inhibition, classically, nuclear p65 is an indicator of canonical NF κ B activation for which the activity of IKK β is important. Second, previous studies report that IKK β decreases β -catenin dependent transcriptional activation, whereas IKK α increases β -catenin dependent transcriptional activity, and this was shown to be due to IKK β promoting β -catenin degradation while IKK α was shown to stabilize cytoplasmic β -catenin (Lamberti et al., 2001, Carayol and Wang, 2006). Taken altogether, this indicates that observed effects of SU1349 on signalling in RAW264.7 cells might be primarily due to inhibition of non-canonical NF κ B activation which is dependent on IKK α activity, whereas the effects of SU1349 in MC3T3 cells might be primarily due to inhibition of canonical NF κ B activation which is more dependent on IKK β activity. To understand the relative contribution of canonical and non-canonical NF κ B pathway future signalling experiments should explore a more comprehensive analysis of other members of the NF κ B pathway such as p50 and RelB, in addition to exploring nuclear and cytoplasmic localisation over an extended range of time points. The signalling time points I investigated are relatively short and are more optimised for detecting effects on canonical NF κ B signalling, which is more rapid transit in nature occurring within minutes' after stimulation, compared to non-canonical signalling which is slower and may need hours to fully affect the levels of its target proteins (Shih et al., 2011, Yilmaz et al., 2014).

Simon McKay's group - that designed SU1349- recently published their results on an earlier generation of SU1349 related inhibitors (Anthony et al., 2017). They show, using the U2OS osteosarcoma cell model, that their two lead IKK α -selective inhibitors successfully inhibited p100 phosphorylation, a marker of the non-canonical NF κ B

Chapter 6

Effects of IKK α on the NF κ B pathway

pathway, without affecting markers of canonical NF κ B signalling, namely, I κ B α degradation and p65 phosphorylation (only at relatively high concentrations (100 μ M) of one of their lead inhibitors that there was detectable inhibition of I κ B α degradation). Although the K_i values for SU1349 indicate a far greater selectivity for IKK α over IKK β compared to the K_i values reported for the first-generation IKK α inhibitors published by Anthony *et al.*, my results clearly show that SU1349 significantly suppressed canonical NF κ B signalling in both osteoclast and osteoblast precursors. Other than accepting the possibility that SU1349 at the concentrations used in my experiments is affecting IKK β activity (at 10 μ M which is nearly threefold higher than the IKK β K_i value of 3.4 μ M), my results could also indicate that IKK α is more important in canonical NF κ B signalling than previously understood.

A number of early influential studies on mouse embryonic fibroblasts (MEFs) have reported that IKK α - unlike IKK β - is dispensable for canonical NF κ B signalling (Li *et al.*, 1999b, Li *et al.*, 1999c, Tanaka *et al.*, 1999), specifically, early studies show that lack of IKK α did not prevent cytokine induced I κ B α degradation (Li *et al.*, 1999a, Hu *et al.*, 1999, Takeda *et al.*, 1999). However, more recent studies in mice and humans highlight a far more important role for IKK α in canonical NF κ B signalling than previously appreciated (Adli *et al.*, 2010, Khandelwal *et al.*, 2017). Adli *et al.*, show in MEFs that IKK α is important in canonical NF κ B signalling in reporter assays, and even though it did not induce I κ B α degradation, it was still able to release p65 from I κ B α and induce p65 phosphorylation and NF κ B DNA binding. Furthermore, Adli *et al.*, demonstrated that IKK α was essential in inducing I κ B α degradation in HeLa cells where it was not essential for I κ B α degradation in MEFs, indicating that the relative importance of IKK α vs. IKK β in I κ B α degradation maybe cell type or species specific (Adli *et al.*, 2010). Therefore, the results reported by Anthony *et al.*, that their lead IKK α inhibitors did not affect canonical NF κ B pharmacodynamics markers, might be specific to the osteosarcoma U2OS cell line. Furthermore, IKK α was shown to be constitutively active in the U2OS cells which might exaggerate the reported effects on non-canonical vs canonical NF κ B signalling (Leopizzi *et al.*, 2017, Anthony *et al.*, 2017). More recently, Khandelwal *et al.*, showed that patients with rare ectodermal dysplasia syndromes who also displayed immunodeficiency, possessed a *de novo*,

Chapter 6

Effects of IKK α on the NF κ B pathway

heterozygous, mutation in the gene encoding IKK α . The mutation results in IKK α proteins lacking kinase activity and are predicted to act in a dominant negative fashion to inhibit the IKK complex –with IKK β and IKK γ - and block canonical NF κ B signalling (Khandelwal et al., 2017). Collectively these results demonstrate an important role for IKK α in canonical NF κ B signalling.

Effects of SU1349 on NF κ B regulated pro-inflammatory factors in prostate cancer cells

Microarray data presented in this chapter show that SU1349 inhibited the NF κ B pathway in PC3 prostate cancer cells as evident by the reduction of NF κ B-regulated pro-inflammatory factors present in PC3 conditioned media. The majority of the downregulated factors are involved in various aspects of prostate cancer cell growth and metastasis, this explains -at least in part- the inhibitory effects of SU1349 on PC3 proliferation and motility described in chapter 3. For example, MCP-1 (monocyte chemotactic protein-1, aka. CCL2), which was the most downregulated cytokine by 60%, was previously found to be an autocrine and paracrine factor for prostate cancer cell growth and invasion *in vitro*, also it was associated with prostate cancer bone metastasis in patients (Lu et al., 2006b, Lu et al., 2007, Lu et al., 2009). Similarly, IL-1 β (the second most down-regulated factor) which was found to be important in prostate cancer invasiveness and angiogenesis *in vivo* (Voronov et al., 2003). EMMPRIN (extracellular matrix metalloproteinase inducer), was the only factor that was upregulated (by 20%) by SU1349 treatment. Although, overexpression of EMMPRIN has been correlated with prostate cancer progression (Hao et al., 2010a), overexpression of a less common alternative splice form of EMMPRIN was associated with inhibition of hepatocellular carcinoma proliferation and invasion (Liao et al., 2011). Interestingly, upregulation of EMMPRIN was also found to activate Wnt/ β -catenin signalling (Sidhu et al., 2010).

In this chapter I show that PC3 conditioned media activated NF κ B signalling in osteoclast precursors' and in chapter 4 I show that IKK α activity and expression had a positive role on osteoclast formation in co-cultures of PC3 cells with bone marrow cells. In agreement with these results, my microarray data show that most of SU1349

Chapter 6

Effects of IKK α on the NF κ B pathway

downregulated factors in PC3 conditioned media are involved in the positive regulation of osteoclast differentiation and function. For example, MCP-1 was found to increase the recruitment and differentiation of pre-osteoclasts (Li et al., 2007a). Furthermore, Lu *et al.*, show that knockdown of MCP-1 in PC3 cells reduced PC3 conditioned media induced osteoclast formation *in vitro* as well inhibiting PC3 tumour growth in bone after inter-tibial injection in mice (Lu et al., 2009).

In chapter 5, I described how IKK α knockdown in PC3 promoted osteoblastic differentiation and bone nodule formation *in vitro*, on the other hand, it inhibited adipocyte differentiation *in vitro*. In agreement with these results, a majority of the SU1349 downregulated factors were found to be involved in the negative regulation of osteoblast differentiation or activity, these include: IL-1 β , IL-1 α , OPN (Osteopontin), RBP4 (Retinol binding protein 4) and LCN2 (Lipocalin-2) (Taichman and Hauschka, 1992, Tanabe et al., 2004, Huang et al., 2004, Ghanem et al., 2017, Rucci et al., 2015). This may explain – at least in part- the stimulatory effects of IKK α knockdown in PC3 on osteoblast differentiation and bone nodule formation described in chapter 5. However, most of the SU1349 downregulated pro-inflammatory factors - with the exception of LCN2 and uPAR (urokinase plasminogen activator receptor)- were found to be involved in the negative regulation of adipocyte differentiation and function (Zhang et al., 2008, Kanno et al., 2010), which does not explain why knockdown of IKK α in PC3 inhibited adipocyte differentiation. In general, studies show that pro-inflammatory factors such as TNF α and IL-6, inhibit osteoblast differentiation by suppressing Wnt signalling and inhibit adipocyte differentiation by activating Wnt signalling (Heiland et al., 2010, Gustafson and Smith, 2006). In view of this, it is interesting to note that many of the SU1349 regulated factors described above have been shown to affect osteoblast or adipocyte differentiation by suppressing or enhancing Wnt signalling in these cells, these factors include: IL-24, IL-17a and IL-11 (Lee et al., 2012, Kragstrup et al., 2017, Wang et al., 2017, Matsumoto et al., 2012). Collectively, the microarray data indicate that SU1349 may also affect the levels of other non-inflammatory factors present in PC3 conditioned media that regulate osteoblast and adipocyte differentiation that are not captured by the microarray I used in my experiments. In future experiments, it will be interesting to do a more

Chapter 6

Effects of IKK α on the NF κ B pathway

comprehensive investigation of the effects of SU1349 on other factors present in PC3 conditioned media, particularly, its effects on agonists and antagonists of Wnt signalling.

Conclusion

In conclusion, I show evidence which verifies that selective IKK α inhibition, using SU1349, is effective in suppressing the NF κ B pathway in osteoclasts, osteoblasts and prostate cancer cells *in vitro*. Importantly, it suppressed NF κ B activation -both canonical and non-canonical- in osteoclasts and osteoblast precursors by prostate cancer derived factors *in vitro*, moreover, it suppressed the ability of prostate cancer cells to produce NF κ B regulated pro-inflammatory factors that regulate osteoclasts and osteoblasts. These results explain -to a large extent- the findings reported in previous chapters. Furthermore, I show evidence that SU1349 exerts differential effects on Wnt/ β -catenin signalling in osteoclast and osteoblast precursors' and this might further contribute to the differential effects of SU1349 on osteoclast and osteoblast differentiation observed in previous chapters. Collectively, the ability of verified IKK α inhibitor, SU1349, to suppress the NF κ B pathway in prostate cancer cells, osteoclasts and osteoblasts, and thus disrupt their behaviour and interactions *in vitro*, makes it a promising candidate for further study *in vivo*.

CHAPTER SEVEN

Effects of SU1349 on prostate cancer associated
osteolysis *in vivo*

7.1 Summary

In previous chapters, I show that the verified IKK α inhibitor, SU1349, reduced prostate cancer growth and motility, suppressed osteoclastogenesis and enhanced osteoblast differentiation and function, *in vitro*. Moreover, I showed that SU1349 disrupted prostate cancer cell regulation of osteoclasts and osteoblasts. In this chapter I test my hypothesis that the verified IKK α inhibitor, SU1349, reduces prostate tumour metastatic growth and bone osteolysis associated with prostate cancer metastasis *in vivo*. I show that SU1349 inhibition increased trabecular bone volume and this was associated with a reduction of osteoclast numbers and an increase in osteoblast numbers on the trabecular bone surface. Paradoxically, SU1349 had the opposite effect in the cortical bone compartment, where it reduced cortical bone volume and this was associated with reduced osteoblast numbers and increased osteoclast numbers on the endocortical bone surface. Moreover, SU1349 showed a trend of reducing metastatic growth in mice. Collectively, my results show a novel role for IKK α in the differential regulation of trabecular and cortical bone. Whilst the effects of pharmacological IKK α inhibition was positive in trabecular bone, the negative effects on cortical bone may limit its use as a bone preserving agent.

7.2 Introduction:

Prostate cancer progression to metastatic disease in patients and TRAMP mouse models of prostate cancer has been linked to the activation of the NF κ B that is evident by increased nuclear p65 and I κ B α phosphorylation in tissue sections (Shukla et al., 2004, Shukla et al., 2005). Genetic inactivation of NF κ B in PC3 cells was shown to delay the occurrence of lymph node metastasis after orthotopic injection in mice (Huang et al., 2001) and to inhibit PC3 growth in mouse bones after intratibial injection (Jin et al., 2013).

In prostate cancer, IKK α was shown to drive prostate cancer progression and metastasis and was shown to have a more important role in the development of prostate cancer than the related IKK β (Shukla et al., 2005, Nguyen et al., 2014b). TRAMP mice treated with apigenin, an IKK inhibitor with a greater specificity for IKK α over IKK β , and TRAMP mice with IKK α genetic inactivation both showed inhibited primary tumour growth (Shukla et al., 2004, Shukla et al., 2005, Luo et al., 2007). Furthermore, Luo *et al.*, showed that IKK α inactivation inhibited distant soft tissue metastasis, however, as TRAMP mice do not usually develop skeletal metastasis (Hensley and Kyprianou, 2012), the role of IKK α in regulating prostate cancer metastasis to bone remains unknown.

Inhibition of the NF κ B pathway has been shown to disrupt normal bone remodelling *in vivo*. Mice deficient in p105/p50 and p100/p52 members of the NF κ B pathway, were shown to have impaired osteoclast differentiation and increased bone volume (Iotsova et al., 1997). Similarly, RelB deletion in mice was shown to increase trabecular bone volume due to increased osteoblast bone formation and this was associated with increased osteoblast numbers on trabecular bone surface, however, osteoclast numbers remained unchanged (Yao et al., 2014). Constitutive genetic activation of IKK β was shown to result in severe bone loss in mice due to increased size and number of trabecular osteoclasts (Otero et al., 2012, Otero et al., 2010).

Whereas genetic inactivation of NF κ B in osteoblasts -by IKK γ deletion or expression of super I κ B α repressor- significantly increased bone trabecular volume in mice and protected against ovariectomy induced osteolysis (Chang et al., 2009). Interestingly,

Chapter 7

Effects of SU1349 on prostate cancer associated osteolysis *in vivo*

IKK α deletion in mice did not seem to affect bone volume, whereas IKK β deletion in mice resulted in increased bone volume which was associated with reduced osteoclast numbers (Chaisson et al., 2004).

Previous work by our group show that inhibition of IKK α/β using parthenolide protects against ovariectomy induced bone loss in mice and breast cancer induced osteolysis in rats by inhibiting osteoclast numbers and suppressing osteolytic bone resorption *in vivo* (Idris et al., 2009, Idris et al., 2010). More recently, work by Marino and colleagues from our group has demonstrated that pharmacological inhibition of the NF κ B pathway using parthenolide- a general inhibitor of IKK α/β - increased bone volume *in vivo* by inhibiting breast cancer induced osteolysis, this was associated with reduced osteoclasts numbers and increased osteoblasts numbers on the bone surface (Marino et al., 2018). However, the role of selective pharmacological inhibition of IKK α on cancer related bone remodelling remains is not well understood.

Chapter 7

Effects of SU1349 on prostate cancer associated osteolysis *in vivo*

7.3 Aims

In this chapter, I use a model of human PC3 cells intra-cardiacally injected into Immuno-deficient BALB/c mice, to investigate the effects of the verified IKK α inhibitor, SU1349, on prostate tumour metastatic growth in the skeleton and prostate cancer associated osteolysis *in vivo*. The effects of SU1349 on prostate tumour metastatic growth is analysed using live bioluminescence imaging, while the effects on bone osteolysis is measured using microCT and histomorphometry.

7.4 Results

7.4.1 Mice treated with the selective IKK α inhibitor SU1349 showed a trend of reduced metastatic prostate tumour growth

Genetic inactivation of IKK α kinase activity was previously shown to reduce prostate tumour growth and soft tissue metastasis in the TRAMP mouse model of prostate cancer (Luo et al., 2007). In previous chapters, I show that the verified IKK α inhibitor, SU1349, reduced prostate cancer growth and motility *in vitro*. Here, I investigated the effects of SU1349 on tumour growth in a model of prostate cancer metastasis. Immuno-deficient BALB/c mice (8 per group) were intra-cardiacally injected with luciferase expressing human PC3 cells and treated with SU1349 (20mg/kg/3-times-weekly) or vehicle control. Dosage and treatment regimen was based on previous data from Prof Simon MacKay (University of Strathclyde, UK; personnel communication). As shown in figure 7.1, my results showed a trend of reduced metastatic growth with SU1349 treatment, as assessed by IVIS-bioluminescence imaging, on day 17 (SU1349 treated group ($n=5$) vs. control group ($n=6$)), and on day 23 (SU1349 treated group $n=2$ vs. Control treated group $n=5$).

Chapter 7

Effects of SU1349 on prostate cancer associated osteolysis *in vivo*

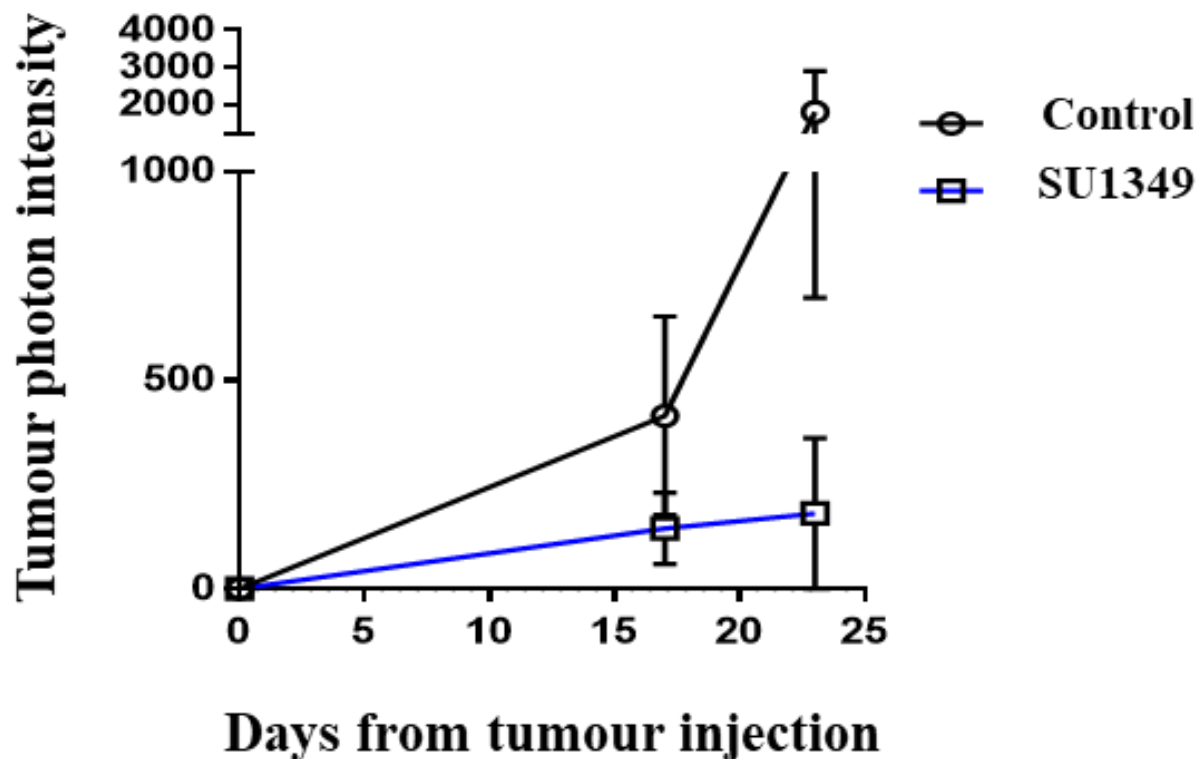


Figure 7.1: The IKK α inhibitor SU1349 showed a trend in reducing prostate tumour metastatic growth *in vivo*. Immuno-deficient BALB/c mice (8 mice per group) were intra-cardiacally injected with luciferase expressing human PC3 cells and treated with SU1349 (20mg/kg/3times-weekly) or vehicle control. The graph shows the effects of SU1349 or vehicle control treatment on prostate tumour metastatic growth as assessed by bioluminescence imaging of total tumour photon intensity measured on day 17 and 23 in BALB/c mice; Note: at day 23 there were 5 mice in the control group vs 2 mice in treated group. (This data was generated by our collaborators Marco Ponzetti and Prof Nadia Rucci in L'Aquila, Italy).

7.4.2 Mice treated with the selective IKK α inhibitor SU1349 exhibited increased trabecular bone volume

Recent work by Marino and colleagues from our group shows that pharmacological inhibition of the NF κ B pathway using parthenolide- a general inhibitor of IKK α/β - increased bone volume *in vivo* by inhibiting breast cancer induced osteolysis (Marino et al., 2018). However, the effects of selective IKK α inhibition on prostate cancer metastasis to bone and prostate cancer associated osteolysis remains unknown. In previous chapters I show that the verified IKK α inhibitor, SU1349, reduced PC3 cell growth and motility, suppressed PC3 ability to induce osteoclastogenesis as well as suppressing osteoclastogenesis directly *in vitro*. Here, I investigated the effects of the verified IKK α inhibitor, SU1349, on trabecular bone remodelling using microCT on the tibia of BALB/c mice intra-cardiacally injected with PC3 cells. I show that SU1349 treatment increased trabecular bone volume and protected trabecular bone from prostate cancer induced osteolysis. As shown in figure 7.2 (A-G): Trabecular bone volume (BV/TV) was increased by 175% ($p < 0.0001$); Trabecular thickness was increased by 32% ($p < 0.0001$); Trabecular separation was reduced by 88% ($p < 0.0001$); Trabecular number was increased by 200% ($p < 0.0001$); Trabecular porosity was reduced by 6% ($p < 0.0001$); Trabecular pattern factor (an indicator of trabecular connectivity) was increased by 1840% ($p < 0.0001$).

Chapter 7

Effects of SU1349 on prostate cancer associated osteolysis *in vivo*

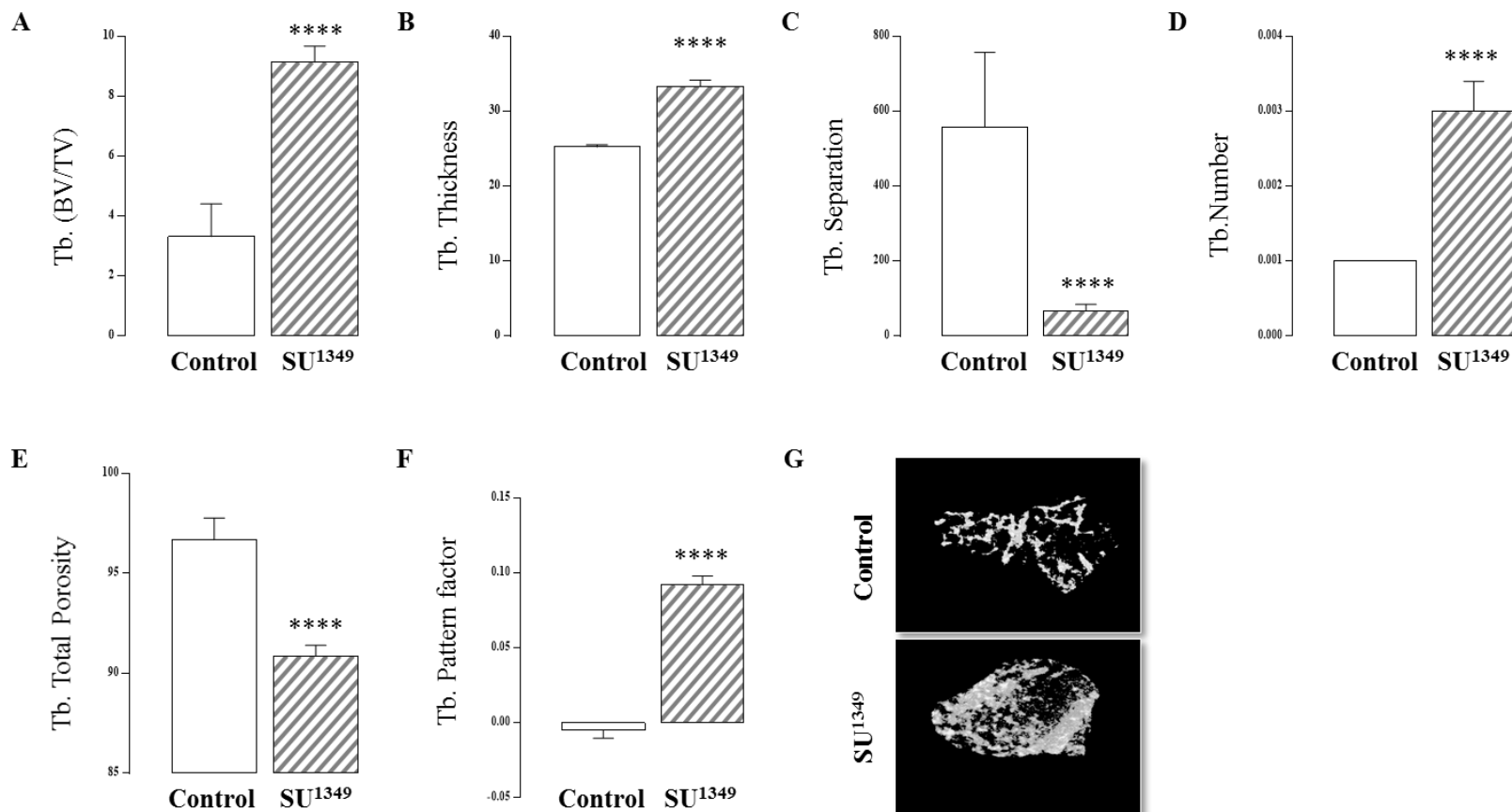


Figure 7.2: The IKK α inhibitor SU1349 increased trabecular bone volume in mice. Immuno-deficient BALB/c mice were intra-cardiacly injected with PC3 cells and treated with SU1349 (20mg/kg/3times-weekly) or vehicle control; at the end of the experiment, the mice tibia were subjected to microCT analysis. **A:** Trabecular bone volume fraction (BV/TV). **B:** Trabecular thickness. **C:** Trabecular separation. **D:** Trabecular number. **E:** Trabecular porosity. **F:** Trabecular pattern factor. **G:** Representative microCT images. Values in the graphs are mean \pm S.E.M. (control n=13; SU1349 n=16).

7.4.3 Mice treated with the selective IKK α inhibitor SU1349 exhibited reduced cortical bone volume

PC3 cells are known to mainly induce osteolytic lesions in mice (Fradet et al., 2013). In osteolytic disease, bone loss is typically exhibited in trabecular bone when compared to cortical bone, as it is more metabolically active and has a higher rate of bone turnover (Chen et al., 2010). I had already observed that SU1349 treatment in mice protected against prostate cancer induced osteolysis and increased trabecular bone volume. Here, I investigated the effects of SU1349 on cortical bone remodelling using microCT in the tibia of BALB/c mice intra-cardiacally injected with PC3 cells. As shown in figure 7.3 (A-C), cortical bone volume (BV/TV) was reduced by 36% ($p < 0.0001$) and cortical porosity was increased by 9% ($p < 0.0001$).

Chapter 7

Effects of SU1349 on prostate cancer associated osteolysis *in vivo*

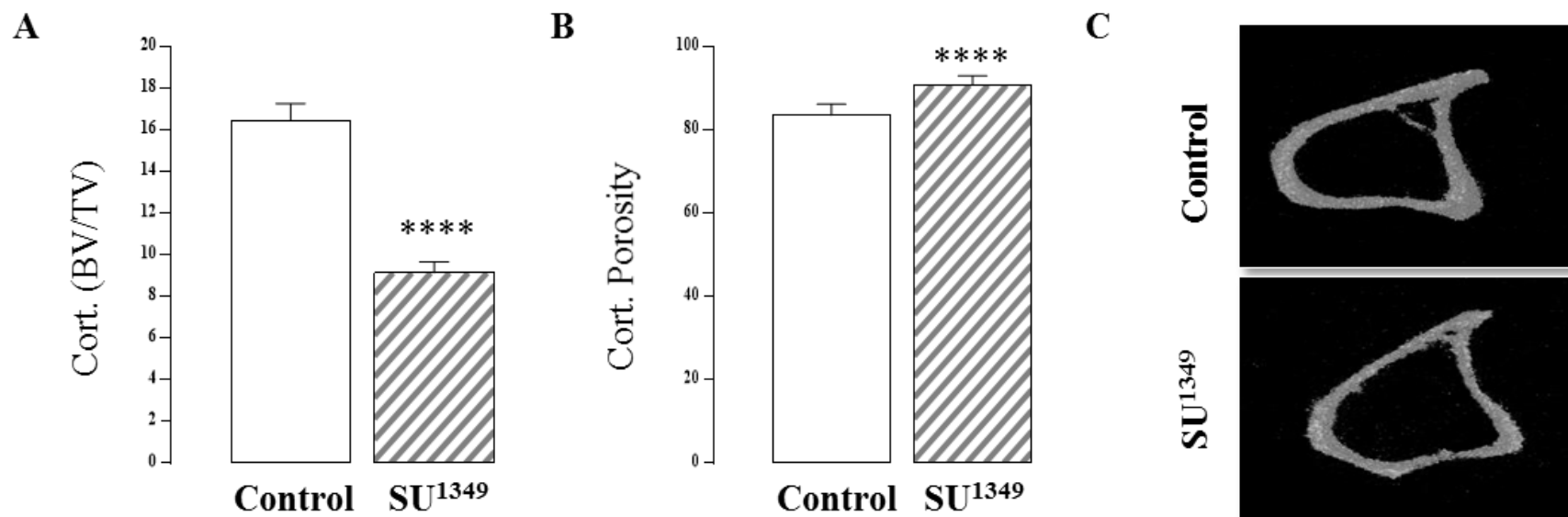


Figure 7.3: The IKK α inhibitor SU1349 reduced cortical bone volume in mice. Immuno-deficient BALB/c mice were intra-cardiacally injected with PC3 cells and treated with SU1349 (20mg/kg/3times-weekly) or vehicle control; at the end of the experiment, the mice tibia were subjected to microCT analysis. **A:** Cortical bone volume fraction (BV/TV). **B:** Cortical porosity. **C:** Representative microCT images. Values in the graphs are mean \pm S.E.M. (control n=13; SU1349 n=16).

7.4.4 The selective IKK α inhibitor SU1349 exerts differential effects on osteoclasts and osteoblasts numbers *in vivo*

In previous chapters I show that the verified IKK α inhibitor, SU1349, suppressed osteoclast differentiation and enhanced osteoblast differentiation *in vitro*. In this chapter I show, in mice intra-cardiacally injected with PC3 cells, SU1349 increased trabecular and reduced cortical bone volume. In order to examine this further, detailed histomorphometric analysis was carried out of mouse tibial bone sections- proximal to the metaphysis- to investigate the effects of SU1349 on osteoclast and osteoblast numbers in bone. As shown in figure 7.4 (A-D), per trabecular bone surface analysed, SU1349 increased osteoblast numbers by 177% ($p < 0.05$) as well as osteoblasts surface fraction was increased by 232% ($p = 0.0631$), whereas osteoclast numbers were decreased by 56% ($p < 0.01$) and osteoclast surface fraction was decreased by 48% ($p < 0.01$). On the other hand, analysis of endocortical bone surface, as shown in figure 7.4 (E-H), revealed that SU1349 decreased osteoblast number by 78% ($p < 0.05$) and osteoblast surface fraction by 77% ($p < 0.05$), whereas SU1349 increased osteoclast numbers by 448% ($p < 0.05$) and increased osteoclast surface fraction by 628% ($p < 0.05$).

Chapter 7

Effects of SU1349 on prostate cancer associated osteolysis *in vivo*

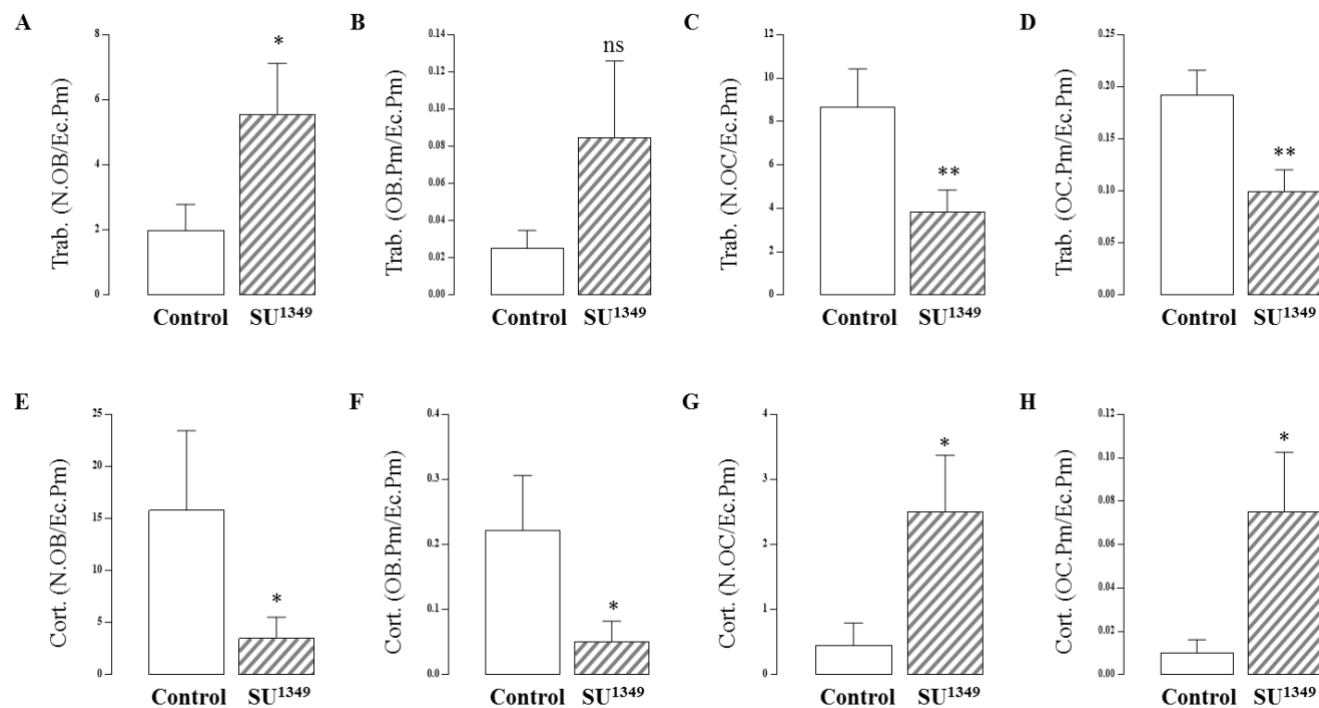


Figure 7.4: *In vivo* the IKK α inhibitor SU1349 reduced osteoclasts and increased osteoblast in trabecular bone, whereas in cortical bone SU1349 reduced osteoblasts and increased osteoclasts. Immuno-deficient BALB/c mice were intra-cardiacally injected with PC3 cells and treated with SU1349 (20mg/kg/3times-weekly) or vehicle control; at the end of the experiment sections of mouse tibial bone were TRAPc and haematoxylin stained before undergoing histomorphometric analysis using Osteomeasure. **A:** Trabecular osteoblast numbers/bone surface. **B:** Trabecular osteoblast surface/bone surface. **C:** Trabecular osteoclast numbers/bone surface. **D:** Trabecular osteoclast surface/bone surface. **E:** Cortical osteoblast numbers/endocortical bone surface. **F:** Cortical osteoblast surface/endocortical bone surface. **G:** Cortical osteoclast numbers/endocortical bone surface. **H:** Cortical osteoclast surface/endocortical bone surface. Values in the graphs are mean \pm s.d. representing at least $n=3$ in each experimental group.

Chapter 7

Effects of SU1349 on prostate cancer associated osteolysis *in vivo*

7.4.5 The selective IKK α inhibitor SU1349 had no significant effects on cachexia in mice

In this chapter I showed that the verified IKK α inhibitor, SU1349, showed a trend of reducing prostate tumour metastatic growth in mice, also it increased trabecular bone volume and reduced cortical bone volume in these mice. Here, I show the effects of SU1349 on cachexia in these mice as assessed by daily body weight monitoring. As shown in figure 7.5, cachexia analysis revealed no significant difference between SU1349 treated and untreated groups ($p=0.44$), however, unlike the control group all the mice in the SU1349 treated group had to be euthanized by day 35 before the planned end date for the experiment of day 40. Nonetheless, cachexia analysis clearly shows a rapid reduction in mice weights by 80% within three weeks of start of the experiment in both SU1349 treated and control groups.

Chapter 7

Effects of SU1349 on prostate cancer associated osteolysis *in vivo*

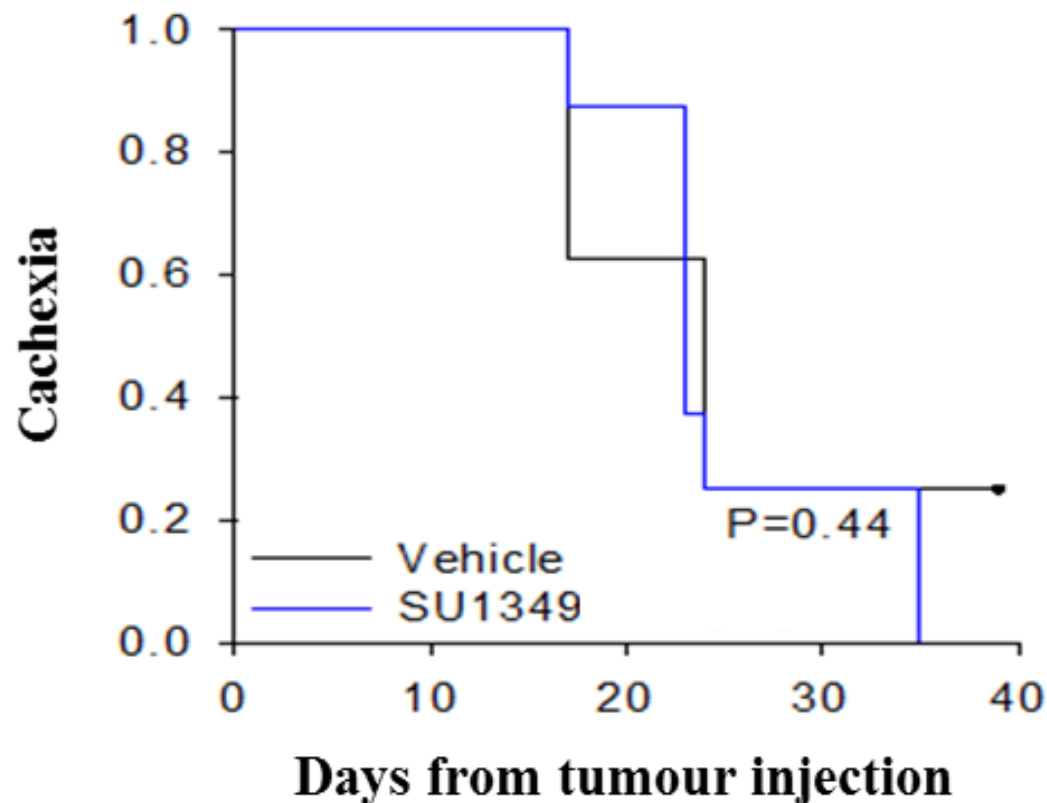


Figure 7.5: Cachexia in mice was not significantly affected by the IKK α inhibitor SU1349. Immuno-deficient BALB/c mice (8 mice per group) were intra-cardiacally injected with luciferase expressing human PC3 cells and treated with SU1349 (20mg/kg/3times-weekly) or vehicle control. The graph shows the effects of SU1349 or vehicle control treatment on cachexia in BALB/c mice as assessed by daily monitoring of body weight; cachexia is expressed as a ratio of mice weight measured during the experiment normalised against weight of mice at the start of the experiments. *p*-values for experimental endpoints are shown in the graphs. (This data was generated by our collaborators Marco Ponzetti and Prof Nadia Rucci in L'Aquila, Italy).

7.5 Discussion

In the key study by Luo *et al.*, genetic inactivation of IKK α kinase activity was demonstrated to inhibit prostate cancer metastasis in the TRAMP mouse model of prostate cancer (Luo *et al.*, 2007). However, since TRAMP mice do not usually develop skeletal metastasis (Hensley and Kyprianou, 2012), the value of IKK α inhibition in reducing prostate cancer metastasis to bone and reducing osteolysis associated with prostate cancer has remained unknown. In this chapter, I show that in a mouse model of prostate cancer bone metastasis, treatment with the novel IKK α inhibitor SU1349, had a novel bi-directional effect in protecting against prostate cancer associated bone loss.

Effects of SU1349 on prostate cancer induced osteolysis

MicroCT analysis of mice revealed that SU1349 treatment increased overall trabecular bone volume as shown by the increased trabecular bone volume fraction, increased trabecular thickness and increased trabecular numbers. SU1349 also reduced trabecular separation and trabecular porosity thereby indicating a reduction of osteolysis that is likely induced by prostate cancer. Moreover, SU1349 treatment increased trabecular pattern factor, which is a calculated index that indicates the interconnectedness of trabecular bone and thus their mechanical strength. Previous work shows that genetic inactivation of IKK α in mouse hematopoietic cells impaired osteoclastogenesis *in vitro* and reduced the number of multinucleated osteoclasts in mouse bones (Chaisson *et al.*, 2004). Also apigenin, an inhibitor of IKK α , was shown to inhibit osteoclastogenesis *in vitro* and to protect against ovariectomy induced osteolysis of mouse trabecular bone (Goto *et al.*, 2015). These results are in agreements with my own findings in chapter 4 that SU1349 has anti-osteolytic effects *in vitro*. Therefore, collectively this indicates that the increase in trabecular bone volume is likely due to SU1349 protection from prostate cancer associated osteolysis.

Chapter 7

Effects of SU1349 on prostate cancer associated osteolysis *in vivo*

Subsequent, histomorphometric analysis of tibial bone sections supported an anti-osteolytic effect for SU1349 as shown by the reduced osteoclast numbers on trabecular bone surface, however, it also revealed an increase in osteoblast numbers. Increased osteoblast numbers indicate that SU1349 treatment increased bone volume not only by protecting bone from osteolysis but also by enhancing bone formation. This is supported by my previously reported results that SU1349 stimulated osteoblast differentiation *in vitro* (chapter 5) and promoted pro-osteoblastic signalling (chapter 6) as shown by the reduced NF κ B signalling and increased Wnt signalling in osteoblasts.

Paradoxically, microCT analysis of cortical bone revealed that SU1349 treatment reduced cortical bone volume as shown by the reduction in bone volume fraction and the increased porosity. Subsequent histomorphometric analysis of the endocortical bone surface supported microCT data, revealing that SU1349 reduced osteoblasts numbers and this was associated with increased osteoclasts numbers. This indicates that the reduction of cortical bone volume is due to reduced bone formation as a result of reduced osteoblasts numbers, whereas the increase in cortical bone porosity is due to the associated increase in cortical osteoclasts numbers. It is important to note that osteoclasts were less commonly observed than osteoblasts on the endocortical bone surface. This suggests that the reduction in cortical bone volume is mainly a result of reduced osteoblast numbers and therefore reduced bone formation and not due to increased osteoclast activity. It is unlikely that the reduction in cortical osteoblast numbers is due to the reduction of osteoblast numbers seen with higher concentrations of SU1349 *in vitro* (chapter 5), on the contrary, I would expect any reductions in osteoblast numbers to be more pronounced in the trabecular compartment as it is more metabolically dynamic than cortical bone (Chen et al., 2010). Additionally, the increase in cortical osteoclasts was not associated with increased osteoclast size.

Altogether, histomorphometry data presented in this chapter revealed a positive correlation between bone cell numbers (both osteoclasts and osteoblasts) and the fraction of bone surface occupied by bone cells. This indicates that observed differences between SU1349 treated and control groups are due to changes in cell numbers and not due to differences in cell size. However, histomorphometry analysis

Chapter 7

Effects of SU1349 on prostate cancer associated osteolysis *in vivo*

of bone sections was particularly limited by poor TRAPc staining of osteoclasts. This is a result of the bones being left in formalin for a period of time that exceeded the recommended limit of up to 3-6 months. The formaldehyde present in formalin when left for extended periods of time can oxidize to form formic acid which can erode the integrity of bone tissue and this in turn will severely compromise staining methods that rely on the preservation of native protein integrity such as antibody based staining methods or staining methods that rely on enzyme activity such as TRAPc staining (Thavarajah et al., 2012). Nonetheless, the combination of TRAPc and haematoxylin staining and cell morphology did allow for the identification of osteoclasts.

A number of previous studies provide evidence for the differential regulation of osteoblasts in trabecular and cortical bone by various mechanisms that notably involve the NF κ B pathway. For example, RelB knockout mice exhibit increased trabecular bone volume due to increased bone formation and osteoblast differentiation, however, cortical bone volume was unaffected (Yao et al., 2014); RelB function is known to be tightly regulated by IKK α activation. In another study, a peptide inhibitor of RANK-RANKL signalling in mice was shown to increase cortical bone formation but not trabecular bone and this was associated with increased osteoblast differentiation and stimulation of Smad/BMP-2 signalling (Furuya et al., 2013); IKK α is also known to control Smad transcriptional activity (Brandl et al., 2010). The above studies clearly indicate that NF κ B pathway can differentially regulate cortical and trabecular bone. Interestingly, differential regulation of trabecular and cortical bone can also occur through dysregulation of Wnt signalling. For example, a study reported that GSK3 β inhibition increased trabecular but not cortical bone in mice with chronic kidney disease and these mice display increased bone fragility (Tatsumoto et al., 2016); In chapter 6, I show that GSK3 β - a negative regulator of Wnt signalling – was inhibited by SU1349 treatment in osteoblast precursors.

Intriguingly, in the literature, a number of other studies in mice report bone phenotypes that are more similar to the phenotype I observe that, either directly or indirectly, involve both Wnt and NF κ B signalling. For example, a study showed that mice deficient in sFRP4, which is a soluble Wnt antagonist, displayed increased trabecular bone volume and reduced cortical bone volume, and this was associated with

Chapter 7

Effects of SU1349 on prostate cancer associated osteolysis *in vivo*

differential regulation of Wnt and BMP signalling in the trabecular and cortical bone compartments (Kiper et al., 2016, Brommage et al., 2009). In a later study, microarray data revealed that NF κ B activation upregulates sFRP4 gene expression (Song et al., 2017). Another study reports that mice deficient in Wnt16 exhibited reduced cortical bone volume with increased cortical porosity whereas trabecular bone remained unaffected (Zheng et al., 2012, Moverare-Skrtic et al., 2015). Wnt16 is highly expressed in cortical but not trabecular bone (Moverare-Skrtic et al., 2014). Also, Wnt16 was shown to be mainly derived from osteoblast lineage cells and it acts to inhibit osteoclastogenesis by directly activating Wnt signalling in osteoclast precursors and by increasing OPG productions by osteoblasts (Moverare-Skrtic et al., 2014). However, Wnt16 did not seem to affect osteoblast differentiation, therefore, the possibility of SU1349 reducing Wnt16 levels might explain the increased cortical porosity and the increase in cortical osteoclasts seen with SU1349 treatment in my experiments but does not explain the decrease in cortical osteoblast numbers. Interestingly, prostate cancer derived Wnt16 was shown to be upregulated by NF κ B and promote prostate tumour survival and progression in mice in a paracrine manner by activating canonical Wnt signalling (Sun et al., 2012). Finally, ER α deficient male mice were shown to exhibit lower cortical bone volume, whereas their trabecular bone was unaffected (Almeida et al., 2013). IKK α is known to enhance the activity of ER α by its direct association and phosphorylation (Park et al., 2005). Additionally, genetic inactivation of ER α in osteoblast precursors, was shown suppress Wnt signalling and thereby inhibit their proliferation and differentiation *in vitro*, also it inhibited cortical bone formation at the periosteal surface in mice (Martin-Millan et al., 2010, Almeida et al., 2013). Due to poor staining and contrast in my bone sections it was not possible for me to analyse bone histomorphometry at the periosteal surface. Altogether, it is interesting to note that sFRP4, Wnt16 and ER α all seem to act on Wnt signalling at some level. Previously, I show that SU1349 affected the levels of prostate cancer derived factors that act as agonist and antagonists of Wnt signalling, and that SU1349 has differential effects on Wnt signalling that is cell type specific. In view of this, future experiments should investigate whether SU1349 alter the levels of protein such sFRP4, Wnt16 and ER α that could explain its effects on the cortical bone compartment.

Effects of SU1349 on prostate tumour metastatic growth

In this chapter, I also looked at the effects SU1349 on prostate tumour metastatic growth in a mouse model of prostate cancer bone metastasis. In both SU1349 treated and untreated mice groups prostate cancer metastasis appeared in various parts of the body including the head, torso and long bones of mice. However, SU1349 treatment appeared to show a non-significant trend in reducing prostate cancer metastatic growth. This is in broad agreement with previous studies. Luo *et al.*, report that genetic inactivation of IKK α kinase activity inhibited primary tumour growth and distant soft tissue metastasis (Luo et al., 2007). Similarly, apigenin, a plant derived IKK α inhibitor, significantly reduced primary tumour growth and abolished metastasis (Shukla et al., 2015). This also in agreement with previous *in vitro* data, which shows that SU1349 inhibited prostate cancer cell growth and motility (chapter 3) and suppressed prostate cancer production of pro-inflammatory factors important for prostate tumour growth and metastasis (chapter 6). Moreover, results presented in this chapter reveals that SU1349 treatment in mice did not significantly affect cachexia in mice. Cachexia progressed rapidly, and to a similar extent, in both SU1349 treated and control group primarily due to prostate tumour growth. Moreover, mice in both groups exhibited significant diarrhoea (personnel communication; Marco Ponzetti, L'Aquila, Italy). In our experiments mannitol was used as a vehicle to dissolve SU1349 and in control treatments. Mannitol is a water soluble sugar alcohol that is considered generally safe and is used in pharmacological and food preparations (Jaipal et al., 2015), however, several studies report that mannitol can induce diarrhoea and body weight loss in rats and mice (Til et al., 1996, Olsson and Hahn, 1996). Therefore, the reduced survival in both group might be partially explained by the adverse effects of mannitol. Nonetheless, there was evidence for SU1349 having more adverse effects on mice survival (personnel communication; Marco Ponzetti, L'Aquila, Italy). All mice in the SU1349 treated group were euthanized before the planned end date of the experiment unlike in the control group. IKK α has long been understood not to play an essential role in the activation of the canonical NF κ B pathway in comparison to the related IKK β (Hacker and Karin, 2006, Lee and Hung, 2008), however, this has been challenged by recent studies (Adli et al., 2010, Khandelwal et al., 2017). Despite the

Chapter 7

Effects of SU1349 on prostate cancer associated osteolysis *in vivo*

fact that the K_i values for SU1349 show it to be considerably more selective for IKK α over IKK β , nonetheless, I clearly showed (in chapter 6) that SU1349 is effective in significantly suppressing canonical NF κ B activation. Previous studies argue that due to the importance of the canonical NF κ B pathway in critical cellular process such as immunity, drugs that affect canonical NF κ B pathway can produce deleterious systemic effects *in vivo* (Verstrepen and Beyaert, 2014, Baud and Karin, 2009). Furthermore, because we were limited to the use of immunocompromised mice to model prostate cancer bone metastasis *in vivo*, this might have further amplified the deleterious effects of SU1349 on the immune system and thus on host survival.

Conclusion

In conclusion, although SU1349 seemed to show a trend of reducing prostate cancer metastasis in mice, however, this effect was not significant. In bone, SU1349 did protect trabecular bone from prostate cancer induced osteolysis, however, it was at the expense of increased cortical bone loss which may limit its utility as a bone preserving agent. Future work should investigate different dosing regimens for SU1349 in immune-competent mouse models. This could elucidate whether the adverse effects of SU1349 are due to its actions on immunity or due to some other mechanism. In prostate cancer research there is a shortage of cell and animal models that closely recapitulate prostate cancer progression in humans, specifically, there is a lack of spontaneous prostate cancer mouse models that develop bone metastasis, also there is a lack of well characterised syngeneic mouse prostate cancer cell lines that are suitable for orthotopic injection in immune-competent mouse models that subsequently develop bone metastasis (Cunningham and You, 2015, Ittmann et al., 2013). The RM-1 mouse cell line has been described to have a high rate of bone metastasis when injected intracardially into C57BL/6 mice (Power et al., 2009). More recently, researchers have developed a TRAMP-derived orthotopic prostate syngeneic (TOPS) model, although it was not reported to metastasize to bone, it is a model that seems to closely mirror prostate cancer disease progression in humans to date (Lardizabal et al., 2018). Lardizabal *et al.*, also derived luciferase expressing prostate cancer cells, TRAMP-C2, that are suitable for syngeneic injection into immune-competent C57/BL6 mice (therefore suitable for direct injection into bone) (Lardizabal et al., 2018).

Chapter 7

Effects of SU1349 on prostate cancer associated osteolysis *in vivo*

Furthermore, future experiments should also investigate the use of SU1349 in combination with other chemotherapeutic agents *in vivo*. Docetaxel is commonly used in the treatment of prostate cancer patients with advanced metastatic disease (Puentes et al., 2017); in preliminary *in vitro* experiments, I found that use of SU1349 in combination with chemotherapeutic agents including docetaxel had significant synergistic effects on reducing prostate cancer cell viability (see figure S7.2). Moreover, data from these experiments predict significant dose reduction values for SU1349 and docetaxel respectively when used in combination which indicate that lower doses of these drugs can be administered *in vivo* and thereby potentially minimizing their respective toxic effects. On the contrary, it is also possible that SU1349 and docetaxel might have an additive toxic effect *in vivo*. Regardless, based on my preliminary data, future experiments should investigate the utility of combinational treatments of SU1349 with conventional chemotherapy *in vivo*.

CHAPTER EIGHT

General Discussion

Prostate cancer is the second leading cause of cancer in men worldwide and it is amongst the leading causes of cancer related deaths (Haas et al., 2008, Center et al., 2012). A hallmark of advanced prostate cancer in patients is bone metastasis which significantly reduces survival rate and it is a major cause of morbidity (Jemal et al. 2008). Prostate cancer cells that metastasise to bone disrupt bone homeostasis and can lead to both aberrant increases in osteolytic bone resorption and osteoblastic bone formation (Logothetis and Lin, 2005). The development of bone metastasis leads to a variety of complications in patients that reduces their quality of life, this includes: bone pain, fractures, reduced mobility, anaemia and susceptibility to infections (Logothetis and Lin, 2005, Coleman, 2001). Drugs that influence bone remodelling have been the standard in the treatment of prostate cancer patients with bone metastases; however, these treatments are palliative and only address some of the complications associated with bone metastasis –primarily addressing increased bone resorption- but are unsuccessful in preventing disease progression and significantly improving survival (Clement-Demange and Clezardin, 2015, Todenhofer et al., 2015).

The nuclear factor kappa B (NF κ B) pathway is known to play an important role in regulating bone homeostasis and cancer progression (Novack, 2011, Xia et al., 2014). Aberrant activation of the NF κ B pathway is recognised to be important in promoting the ‘the vicious cycle’, that involves cancer cells, osteoclasts and osteoblasts, which drives bone metastasis (Roca and McCauley, 2015). The related I κ B kinases alpha (IKK α) and beta (IKK β) play key roles in the regulation of canonical and non-canonical NF κ B activation and signalling. IKK β and IKK α work cooperatively in the activation of the canonical NF κ B pathway, however, early studies have shown IKK β to be more crucial for the activation of this pathway than IKK α (Yamamoto et al., 2000). Whereas the non-canonical NF κ B pathway is dependent on IKK α (Clement et al., 2008). In prostate cancer, IKK α has been shown to be more important in the development of prostate cancer than IKK β (Shukla et al., 2005, Nguyen et al., 2014b).

Increased activation of IKK α was correlated with prostate cancer progression in humans and genetic inactivation of IKK α kinase activity was demonstrated to inhibit prostate cancer progression and metastasis in mouse models of prostate cancer (Luo et al., 2007). However, the mouse model used by Luo *et al.*, do not typically develop

bone metastasis and therefore the specific role of IKK α in prostate cancer bone metastasis has since remained unexplored. This would suggest that pharmacological inhibition of IKK α kinase activity represents an attractive therapeutic option for the treatment of prostate cancer progression and metastasis. Currently there is a lack of commercially available drugs that selectively inhibit the kinase activity of IKK α but not the related IKK β . In this thesis I investigate for the first the time effects of selective pharmacological inhibition of IKK α kinase activity, using the verified IKK α inhibitor SU1349, on the behaviour and interaction of prostate cancer cells and bone cells *in vitro*, and its efficacy in suppressing prostate cancer bone metastasis and prostate cancer associated bone disease *in vivo*.

Effects of IKK α inhibition on osteoclastogenesis

Activation of the NF κ B pathway is essential for osteoclast differentiation and survival (Soysa and Alles, 2009). In this thesis, I show that IKK α inhibition suppressed osteoclast formation *in vitro* and reduced osteoclasts numbers and osteolysis *in vivo*. Chaisson *et al.*, were first to demonstrate that knockout of IKK α in mouse hematopoietic precursors impairs osteoclast differentiation *in vitro* (Chaisson *et al.*, 2004). Similarly, previous work done by our group showed the non-selective IKK α/β inhibitor, parthenolide, inhibits osteoclastogenesis *in vitro* and *in vivo* (Idris *et al.*, 2010, Marino *et al.*, 2018). I show that the IKK α inhibitor SU1349, suppressed RANKL induced osteoclastogenesis in a dose dependent manner (chapter 4) and this was due to inhibition of RANKL-induced NF κ B activation in osteoclast precursors (chapter 6). Moreover, I show that cancer-specific IKK α activity regulates the ability of prostate cancer cells to influence osteoclastogenesis *in vitro*. In PC3-mouse bone marrow cell co-cultures, IKK α overexpression in PC3 significantly enhanced osteoclastogenesis whereas IKK α knockdown in PC3 or PC3 cells in the presence of SU1349 significantly suppressed osteoclastogenesis. Previously, constitutive activation of the NF κ B pathway in prostate cancer cells was shown to promote osteoclastogenesis in mouse bone marrow cultures (Jin *et al.*, 2013). In chapter 6, I show PC3 cell derived factors activated both canonical both canonical and non-canonical NF κ B signalling in osteoclast precursors. PC3 conditioned media has been reported to upregulate the expression of NF κ B regulated genes in osteoclasts (Akech *et al.*, 2010). Next, I show

that SU1349 was effective in suppressing prostate cancer induced NF κ B activation of both canonical and non-canonical signalling in osteoclast precursors. Although the suppression of canonical NF κ B signalling by SU1349 seems to go against the prevailing understanding from early studies that IKK α is not important for canonical NF κ B signalling, it is in agreement with more recent studies that show IKK α is important for canonical NF κ B activation and that this may be cell-type specific (Adli et al., 2010, Khandelwal et al., 2017). Furthermore, I show that SU1349 also suppressed Wnt signalling in osteoclast precursors. NF κ B signalling is known to influence the Wnt/ β -catenin pathway and activation of Wnt signalling inhibits osteoclast differentiation (Albers et al., 2013). Therefore, the effects of SU1349 on osteoclast differentiation can be explained, primarily, by the evident inhibition of NF κ B signalling, but may also be partly due to SU1349 inhibition of Wnt signalling. In chapter 7, I show SU1349 treatment in mice, increased trabecular bone volume and showed a reduction in indices of trabecular osteolysis, suggesting an inhibition of prostate cancer induced osteolysis. This effect of SU1349 on trabecular bone is supported by subsequent histomorphometry analysis which show that SU1349 treatment was associated with reduced osteoclast numbers on the trabecular bone surface. Previous work done in our group showed that parthenolide, an inhibitor of IKK α/β , suppressed breast cancer induced osteolysis and as a result increased trabecular bone volume (Marino et al., 2018). Although the role of IKK α in bone metastasis has not yet been explored, there is evidence that IKK α inhibition may have a role in osteolysis, for example, IKK α knockout reduced the number of multinucleated osteoclasts in mouse bones (Chaisson et al., 2004). Also apigenin, an inhibitor of IKK α , was shown to protect against ovariectomy induced osteolysis of mouse trabecular bone (Goto et al., 2015). Furthermore, the microarray data presented in chapter 6, shows that SU1349 downregulated the production of soluble pro-inflammatory factors by PC3 cells that promote osteoclast differentiation and function. For example, the downregulated factor MCP-1 was shown to promote prostate cancer induced osteoclast formation (Lu et al., 2009). SU1349 also down regulated PC3 production of other factors that are known to promote osteoclast differentiation or osteolytic bone resorption directly these notably include: ENA-78, IL-1 α and IL-8

(Sundaram et al., 2013, Tani-Ishii et al., 1999, Bendre et al., 2003). The downregulation of these pro-inflammatory factors might explain how IKK α inhibition suppressed PC3 induced osteoclast formation *in vitro* (chapter 4) and suppressed PC3 induced trabecular osteolysis *in vivo* (chapter 4).

Effects of IKK α inhibition on osteoblasts

Activation of the NF κ B pathway in osteoblasts is known to negatively regulate osteoblast differentiation and function (Chang et al., 2009, Alles et al., 2010). In this thesis, I show that that IKK α inhibition enhanced osteoblast differentiation *in vitro* and *in vivo*. In chapter 5, I show that the selective IKK α inhibitor, SU1349, significantly enhanced osteoblast differentiation and bone nodule formation function *in vitro*. This is in agreement with previous work by our group and others that show pharmacological inhibition of IKK α/β promotes osteoblast differentiation and bone nodule formation *in vitro* (Marino et al., 2018, Zhang et al., 2017b). Moreover, I show for the first time that conditioned media from PC3 cells with IKK α knockdown enhanced the differentiation and bone nodule formation of osteogenic cultures. This suggests that IKK α knockdown in PC3 either suppresses the production of factors that inhibit osteoblastic differentiation and function or it stimulate the production of factors that promote osteoblastic differentiation and function. In support of this, the microarray data presented in chapter 6, revealed that SU1349 downregulated the production of soluble factors by PC3 cells that are known to negatively regulate osteoblast differentiation and function, these include: IL-1 β , IL-1 α , Osteopontin, Lipocalin-2, TSP1 and GDF15 (Taichman and Hauschka, 1992, Tanabe et al., 2004, Huang et al., 2004, Rucci et al., 2015, Furlan et al., 2007, Westhrin et al., 2015). In contrast, I show that both SU1349 and conditioned media from PC3 cells with IKK α knockdown suppressed adipocyte differentiation *in vitro*. This is in broad agreement with the understanding that osteoblast and adipocytes share the same lineage and their differentiation from osteoprogenitor cells in the bone marrow microenvironment is generally mutually exclusive (Muruganandan and Sinal, 2014). Also, my findings are in agreement with a previous study which reports that IKK β inhibition suppressed adipocyte differentiation (Helsley et al., 2016). Taken altogether, this would suggest that IKK α inhibition in osteoprogenitor cells and prostate cancer specific effects of

IKK α inhibition on osteoprogenitors, act by the same mechanism to commit the differentiation programme of early MSC precursors found within bone microenvironment towards an osteoblast lineage at the expense of adipocytes. Future experiments should investigate the effect of IKK α inhibition on osteoprogenitor cell differentiation *in vitro* and *in vivo*.

In chapter 6, I demonstrate that PC3 conditioned media activated both canonical and non-canonical NF κ B signalling in osteoblast precursors. In the literature there is somewhat indirect evidence for this, where PC3 conditioned media is reported to upregulate the expression of NF κ B regulated genes in osteoblast precursors (Schulze et al., 2012), however, to my knowledge there has not been detailed examination of prostate cancer effects on NF κ B signalling in osteoblasts. Here, I show that SU1349 was effective in suppressing prostate cancer induced NF κ B activation of both canonical and non-canonical signalling in osteoblasts. Significantly, I show that SU1349 also led to an activation of Wnt signalling in osteoblasts. Activation of Wnt signalling is essential for osteoblast lineage commitment, differentiation and function (Gaur et al., 2005). My findings are in agreement, with previous work that shows that NF κ B inhibition enhances osteoblastic differentiation and function through enhanced Wnt signalling (Chang et al., 2013, Marino et al., 2018). Therefore, the enhancement of osteoblast differentiation and bone nodule formation by SU1349 presented in chapter 5, can be explained both by its inhibition of NF κ B pathway and stimulation of Wnt signalling. In agreement with this, I show that increase in trabecular bone volume in mice treated with SU1349 was associated with increased osteoblast numbers on the trabecular bone surface.

Paradoxical effects of IKK α inhibition on cortical bone

In contrast to the effects of SU1349 in trabecular bone, SU1349, unexpectedly appeared to exacerbate cortical bone loss. In chapter 7, microCT analysis revealed that SU1349 reduced cortical bone volume and increased cortical bone porosity. This was supported by histomorphometry which revealed reduced osteoblast numbers and increased osteoclast numbers on the endocortical bone surface. This indicates that effects of SU1349 on cortical bone is not simply due to reduced bone formation as a

result of reduced osteoblast numbers, but it may also be due to increased osteolysis. The differential effects of SU1349 on trabecular and cortical bone as well as osteoclasts and osteoblasts within these two compartments, is not unique. A number of studies show evidence for the differential regulation of cortical and trabecular bone and more specifically that osteoblasts in these two compartments are differentially regulated. There have been a number of studies that report that disruption of the NF κ B pathway can have differential effects on trabecular and cortical bone (Yao et al., 2014, Furuya et al., 2013, Brandl et al., 2010). However, these studies do not report a phenotype that closely matches what I observe with SU1349. Other reports involving the differential regulation of Wnt signalling by factors such as sFRP4, Wnt16 and ER α which incidentally are also regulated by the NF κ B pathway report a phenotype that is very similar to what I observe in trabecular and cortical bone (Kiper et al., 2016, Brommage et al., 2009, Zheng et al., 2012, Moverare-Skrtic et al., 2015, Almeida et al., 2013). Future studies should investigate if a mechanistic link exists between IKK α inhibition by SU1349 and the regulation of factors such as sFRP4, Wnt16 and ER α in bone cells that could explain the differential effects of SU1349 on trabecular and cortical bone. Overall SU1349 indicates a novel role for IKK α in the differential regulation of trabecular and cortical bone, however, its negative effects on cortical bone may limit its use as bone preserving agent.

Effects of IKK α inhibition on prostate cancer cell behaviour

Aberrant activation of IKK α has been found to drive prostate cancer progression and metastasis in mouse models of prostate cancer (Luo et al., 2007). However, Luo *et al.* did not examine the role of IKK α in bone metastasis associated with prostate cancer. In this thesis, I provide evidence that the novel IKK α inhibitor, SU1349, suppressed prostate cancer cell growth and motility *in vitro* and showed a trend of reducing prostate tumour metastatic growth *in vivo*. In chapter 3, I show that SU1349 potently inhibited the growth of various prostate cancer cell lines of various metastatic abilities. Previously, apigenin which is a plant derived inhibitor of IKK α/β , was reported to reduce the proliferation of prostate cancer cells and enhance their apoptosis (Shukla and Gupta, 2004, Shukla et al., 2015). In order to further validate the effects of SU1349 on prostate cancer cells I successfully generated stable overexpression and

knockdowns of IKK α in the highly aggressive human prostate cancer cell line PC3. I show that just as SU1349 reduced PC3 viability, knockdown of IKK α in PC3 reduced its viability whereas IKK α overexpression enhanced PC3 viability. This is in agreement with previous studies that showed that knockdown of IKK α in PC3 induced cell cycle arrest and reduced their proliferation (Shukla et al., 2015). Next, I tested the effects of SU1349 on PC3 motility and invasion *in vitro*. I show that PC3 directed migration, random migration and invasion were suppressed by SU1349 and IKK α knockdowns whereas it was enhanced by IKK α overexpression. This agrees with previous reports that IKK α inhibition in PC3 by siRNA or apigenin suppressed PC3 directed migration and invasion *in vitro* (Shukla and Gupta, 2004, Shukla et al., 2015, Mahato et al., 2011). In chapter 7, I show that SU1349 treatment in mice showed a non-significant trend of reducing prostate cancer metastatic growth without significantly affecting cachexia. This is supported by microarray data presented in chapter 6, which shows that SU1349 suppressed prostate cancer production of soluble pro-inflammatory factors that are important in regulating prostate cancer cell growth, survival, metastasis and invasion. For example, MCP-1 which was significantly downregulated by SU1349 in PC3 conditioned media, was found to be an autocrine and paracrine factor for prostate cancer cell growth and invasion *in vitro* (Lu et al., 2006b, Lu et al., 2007). In a later study Lu *et al.*, found MCP-1 to be significantly elevated in the serum of patients with prostate cancer bone metastasis as opposed to patients with primary prostate cancer (Lu et al., 2009).

Finally, there was some evidence that SU1349 also had adverse effects in mice, for example, more mice were euthanized in the SU1349 treated group compared to control group. Luo *et al.*, genetically inactivated IKK α kinase activity in TRAMP mouse models of prostate cancer that have a fully functioning immune system, and they showed IKK α inactivation not only significantly reduced primary tumour growth and metastasis, but it also considerably enhanced their survival compared to controls with catalytically active IKK α (Luo et al., 2007). This suggests that any adverse effects associated with SU1349 treatment is unlikely to be as a result of SU1349 selective inhibition of IKK α kinase activity alone, rather it might be due to a combination of the following reasons: toxicity of SU1349 due to some yet unknown off targets effects,

the effects of SU1349 on suppressing host immunity in combination with using an immune-compromised mouse model, finally, the use of mannitol as a vehicle which seemed to induce diarrhoea in mice.

Many of the drugs developed to inhibit the NF κ B pathway were shown to have adverse effects *in vivo* due to their effects on host immunity which is primarily regulated by the canonical NF κ B pathway (Baud and Karin, 2009, Verstrepen and Beyaert, 2014). Although the K_i values for SU1349 show its selectivity for IKK α over IKK β , I clearly show in chapter 6, that SU1349 significantly suppressed canonical NF κ B activation. Perhaps some of the adverse effects of SU1349 may be due to its effects in inhibiting canonical NF κ B signalling in host cells. Therefore, future studies should investigate the toxicity of SU1349 in immune-competent mice so as to understand if the observed adverse effects of SU1349 are due to negative effects on host immunity. Although there has been a lack of well characterised murine prostate cancer cell lines that are suitable for syngeneic use in immune-competent mice and are bone metastatic, the mouse RM-1 cell line has been described to be highly bone metastatic when injected intra-cardially into C57/BL6 mice (Power et al., 2009) and thus it may represent a suitable model to investigate the effects of SU1349 on bone metastasis and host immunity.

So far, the evidence for the efficacy of using the inhibitor of IKK α inhibitor, SU1349, in inhibiting prostate cancer metastasis and particularly bone metastasis appears mixed. On the one hand SU1349 appeared to show a trend of reducing metastatic growth, however, this did not reach significance possibly due to the reduced survival of mice in the SU1349 treated group. As mentioned previously the apparent adverse effects of SU1349 may have been confounded by our use of immune-compromised mice and this will need to be fully explored in future experiments in immune-competent mice. On the other hand, SU1349 did appear to mitigate prostate cancer induced osteolytic damage in the trabecular bone compartment whilst increasing bone loss in the cortical bone compartment. The negative effects of SU1349 on cortical bone may limit its use as bone preserving agent *in vivo*. Nevertheless, preliminary *in vitro* data I acquired also show that the use of SU1349 in combination with a conventional chemotherapeutic agent such as docetaxel (docetaxel is commonly used in the

treatment of advanced prostate cancer) had significant synergistic effects and predict significant dose reduction indices for each drug respectively. This indicates that *in vivo*, the dosage for each drug could be reduced in combinational treatments to achieve similar results to when individual drug treatments are used at higher doses and thereby this may limit some of the toxic effects of using higher doses of SU1349 or docetaxel alone. Future experiments should explore the use of SU1349 in combination with docetaxel on prostate cancer bone metastasis in mouse models.

Conclusion

In conclusion, I in this thesis characterised the role of IKK α kinase activity using a novel and highly selective small molecular inhibitor of IKK α kinase activity, SU1349, in prostate cancer cells and bone cell *in vitro* and in a model of prostate cancer bone metastasis *in vivo*. I show that SU1349 inhibited prostate cancer cell growth and metastatic behaviour, suppressed its ability to promote osteoclast formation and enhanced its ability to promote osteoblast differentiation *in vitro*. I show that SU1349 inhibition of the NF κ B pathway suppresses osteoclast differentiation and promotes osteoblast differentiation *in vitro*, and that these effects were associated with differential effects on Wnt/ β -catenin signalling. *In vivo* SU1349 protected against prostate cancer induced osteolysis in trabecular bone yet it increased cortical bone loss, this points to a novel role for IKK α in the differential regulation of trabecular and cortical bone; however, the negative effects of SU1349 may limit its use as a bone preserving agent. Finally, SU1349 had adverse effects on mice survival that may have been exacerbated by our use of immune-compromised mice, this makes any conclusions about the effects of SU1349 on metastasis and particularly bone metastasis inconclusive. Future studies should utilise immune-competent mice to investigate the effects of SU1349 alone and in combination with conventional therapeutic agents to elucidate any toxic effects of using SU1349 alone and better understand the efficacy of using SU1349 alone or in combinational treatments on prostate cancer bone metastasis.

APPENDIX

Appendix 1: Supplementary figures

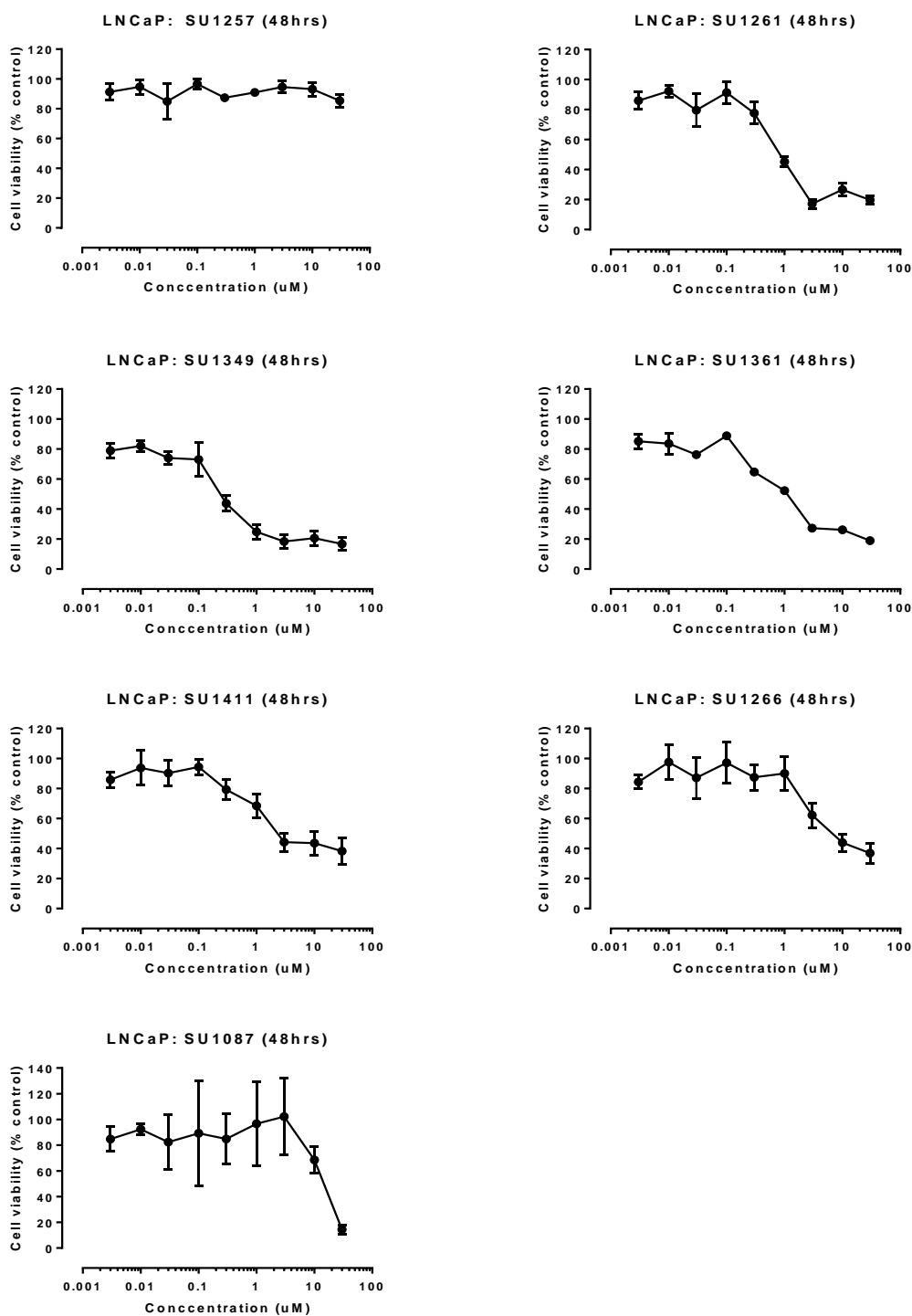


Figure S3.1.1: LNCaP cell viability for IKK α inhibitors used in IC₅₀ calculations (table 3.1). Shows Alamar blue cell viability results for LNCaP cells after treatment with IKK α inhibitors after 48hrs in complete media, as a percentage of the vehicle control (0.3% DMSO). Values in the graphs are mean \pm s.d. and are obtained from 3 independent experiments.

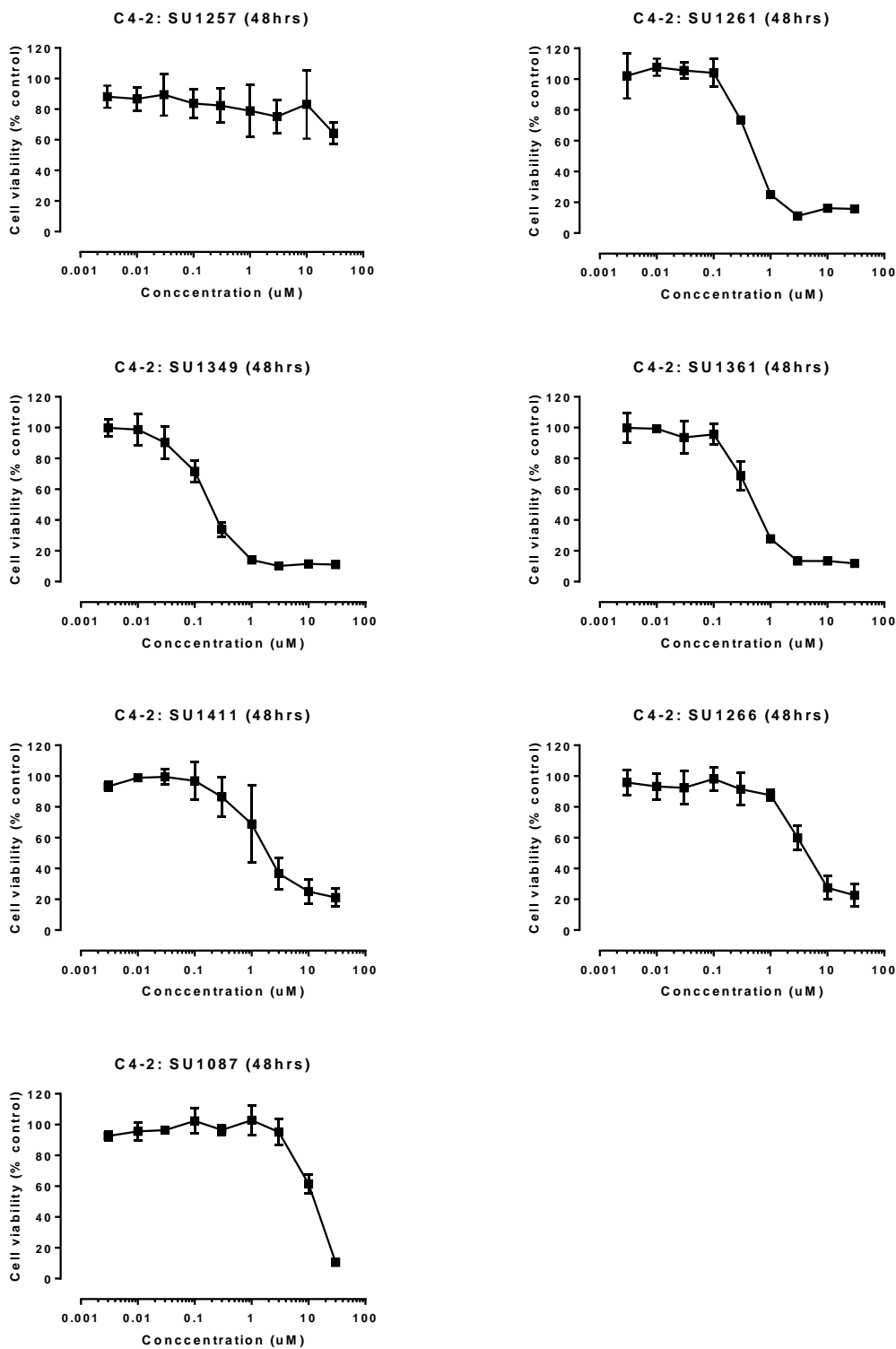


Figure S3.1.2: C4-2 cell viability for IKK α inhibitors used in IC50 calculations (table 3.1). Shows Alamar blue cell viability results for C4-2 cells after treatment with IKK α inhibitors after 48hrs in complete media, as a percentage of the vehicle control (0.3% DMSO). Values in the graphs are mean \pm s.d. and are obtained from 3 independent experiments.

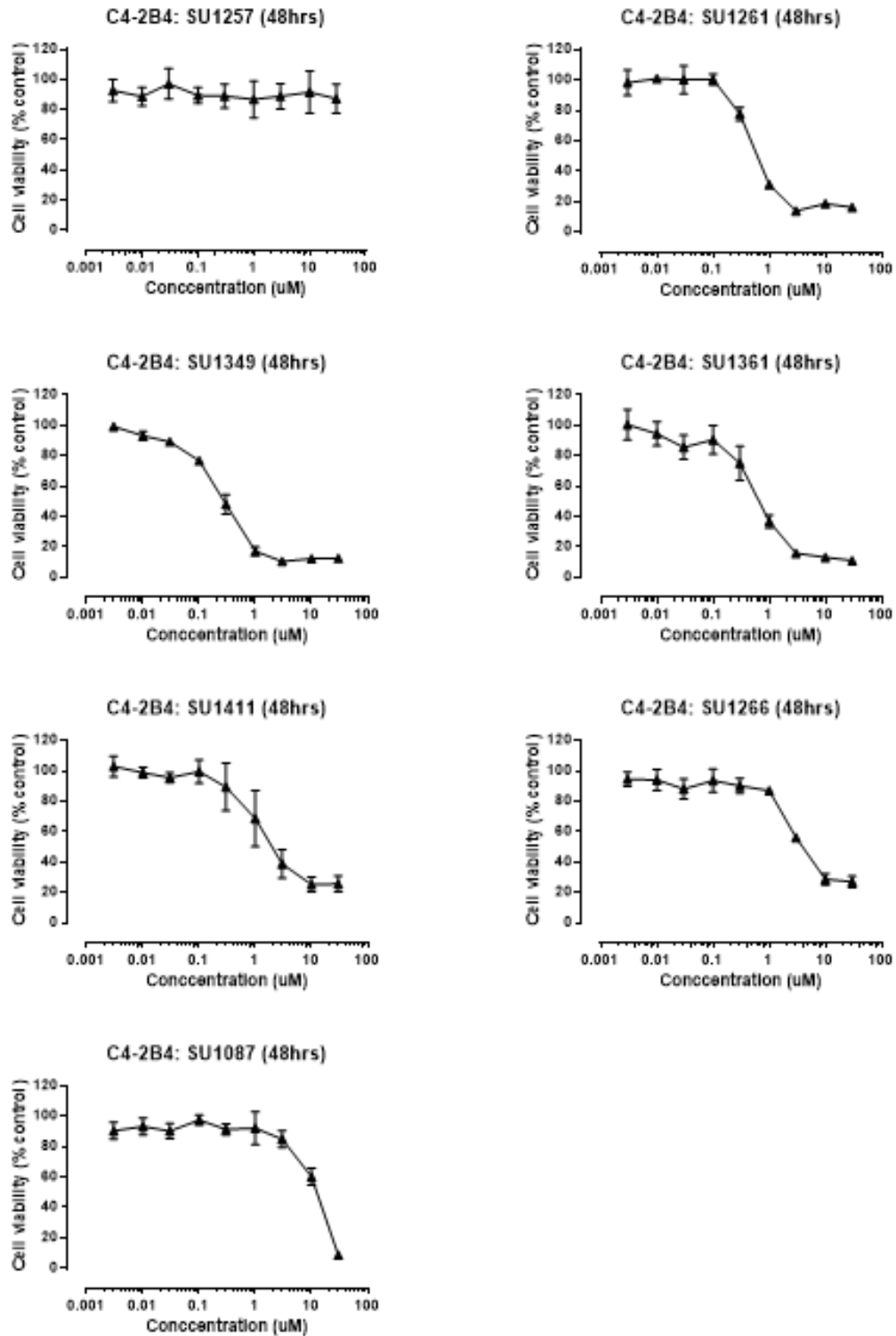


Figure S3.1.3: C4-2B4 cell viability for IKK α inhibitors used in IC₅₀ calculations (table 3.1). Shows Alamar blue cell viability results for C4-2B4 cells after treatment with IKK α inhibitors after 48hrs in complete media, as a percentage of the vehicle control (0.3% DMSO). Values in the graphs are mean \pm s.d. and are obtained from 3 independent experiments.

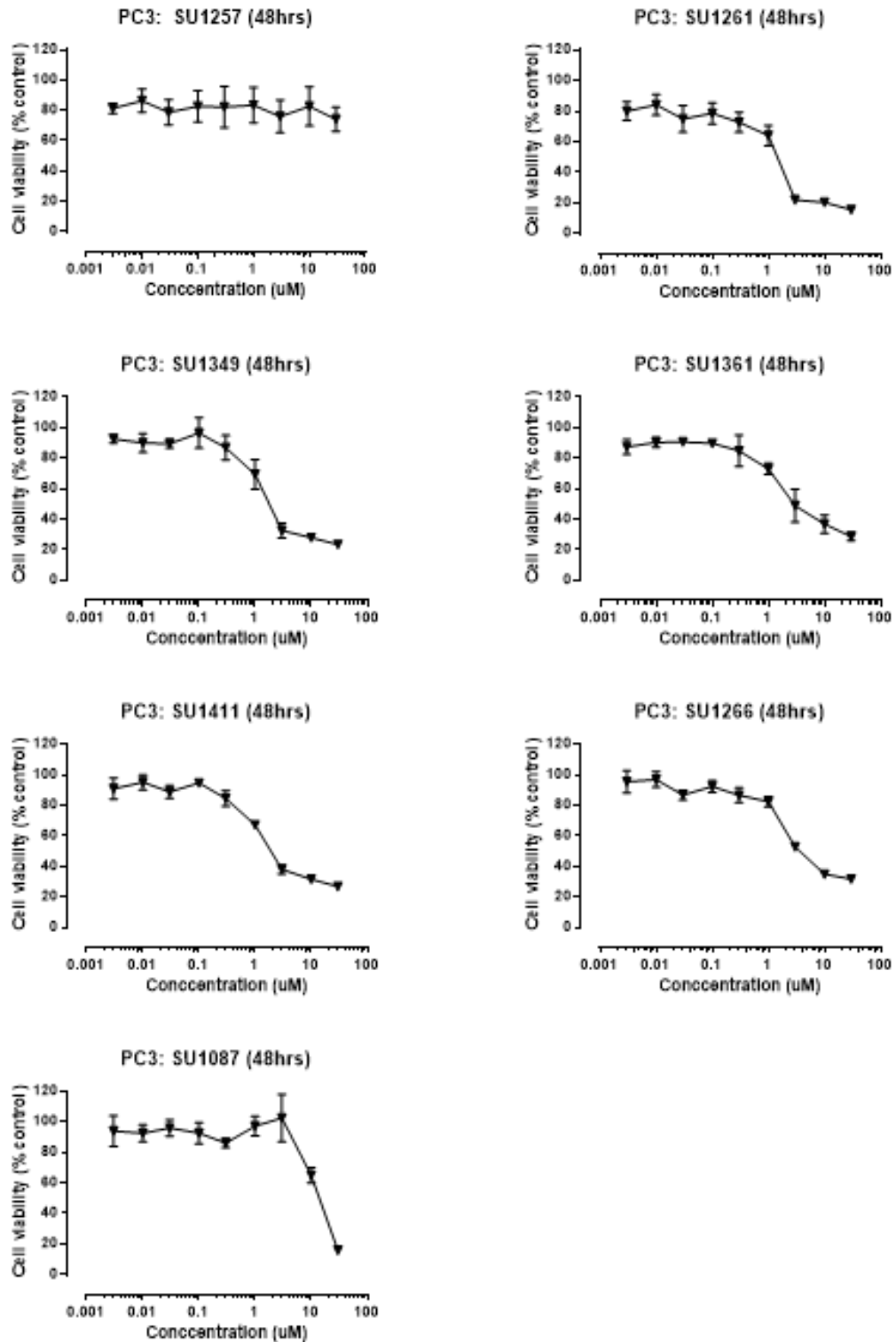


Figure S3.1.4: PC3 cell viability for IKK α inhibitors used in IC50 calculations (table 3.1). Shows Alamar blue cell viability results for PC3 cells after treatment with IKK α inhibitors after 48hrs in complete media, as a percentage of the vehicle control (0.3% DMSO). Values in the graphs are mean \pm s.d. and are obtained from 3 independent experiments.

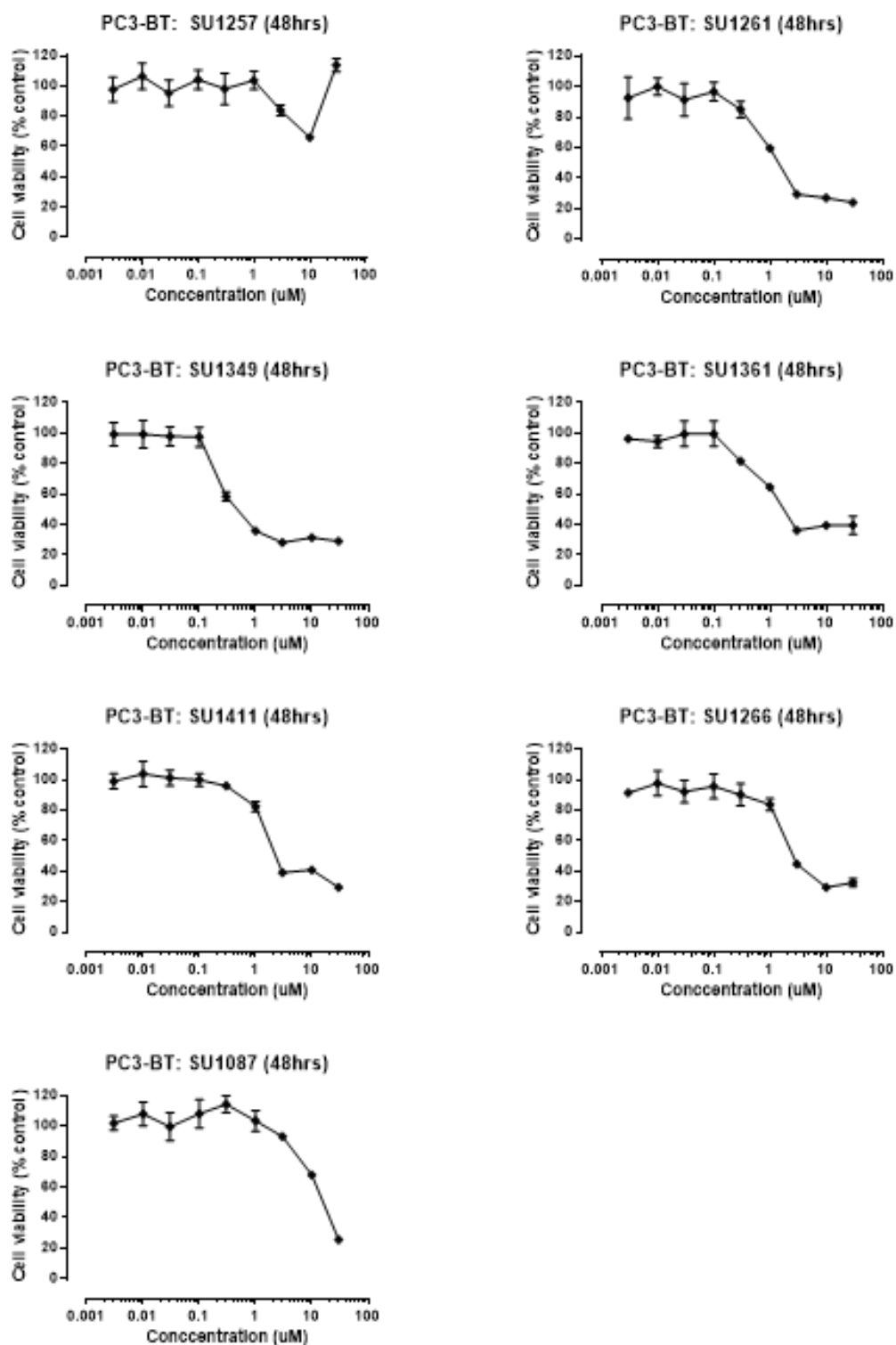


Figure S3.1.5: PC3-BT cell viability for IKK α inhibitors used in IC₅₀ calculations (table 3.1). Shows Alamar blue cell viability results for PC3-BT cells after treatment with IKK α inhibitors after 48hrs in complete media, as a percentage of the vehicle control (0.3% DMSO). Values in the graphs are mean \pm s.d. and are obtained from 3 independent experiments.

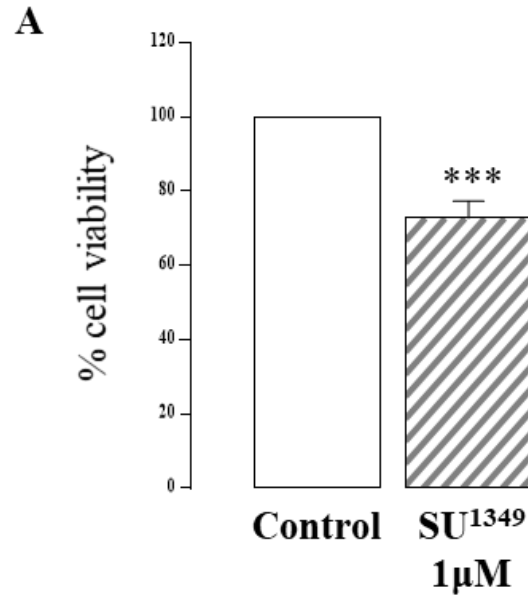


Figure S3.2: SU1349 suppressed the directed migration of PC3 cells pre-treated with mitomycin-C (10µg/L) *in vitro*. The PC3 cells pre-treated with 10µg/L mitomycin-C before additional treatment with 1µM SU1349 and compared to vehicle treated (0.1% DMSO) control. The graph shows the 2D migration of PC3 cells after 12 hours was suppressed to an almost identical extent to previous experiments in the absence of mitomycin-C treatment: by 27% ($p < 0.001$) compared to 26% ($p < 0.01$) previously. No significant effects were seen on the viability of PC3 cells at the end of the migration experiment as assessed using the Alamar blue assay. Values in the graphs are mean \pm s.d. and are obtained from 3 independent experiments (***) = $P \leq 0.001$).

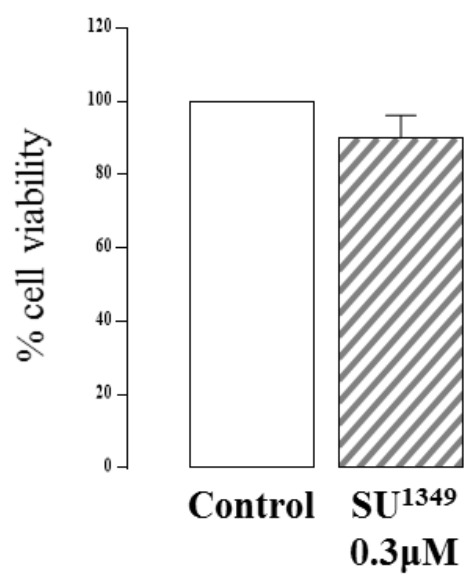


Figure S3.3: Concentration of SU1349 selected for invasion assay had no significant effects on PC3 viability *in vitro*. The graph shows the viability of PC3 cells seeded at 3000 cell per well of a 96 well plate and treated with 0.3µM SU1349 in serum free media for 72hrs.

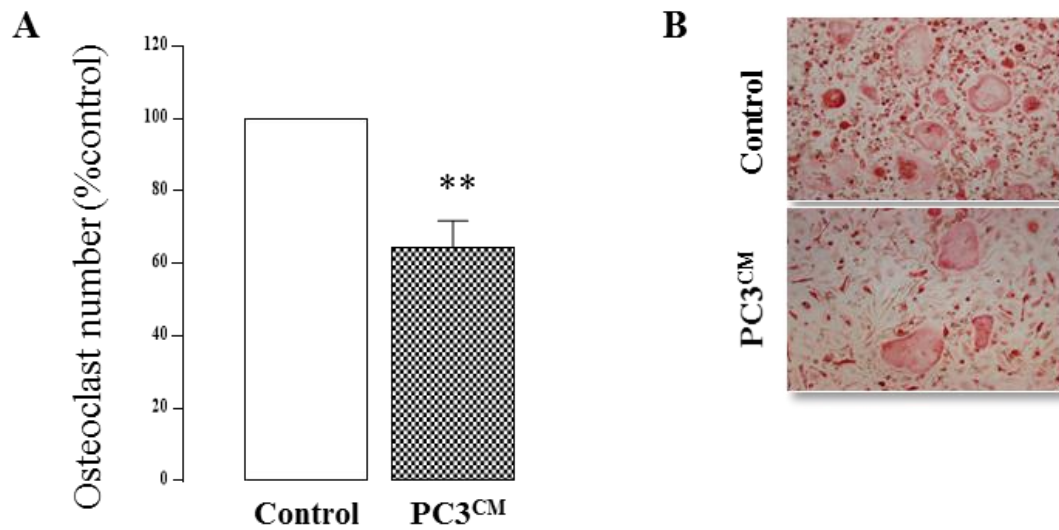


Figure S4.1: PC3 conditioned suppressed osteoclast formation *in vitro*. **A:** Shows the number of M-CSF (10 ng/ml) and RANKL (100 ng/ml) generated osteoclasts in mouse bone marrow cultures treated with 10% (v/v) PC3 conditioned media (PC3^{CM}) or standard control media every 48hrs. Cultures were maintained for up to 7 days. Osteoclasts number was assessed by counting multinucleated TRAcP positive cells. Values in the graphs are mean \pm s.d. and are obtained from 3 independent experiments (** = $P \leq 0.01$). **B:** representative microscopy images of TRAcP stained osteoclast cultures.

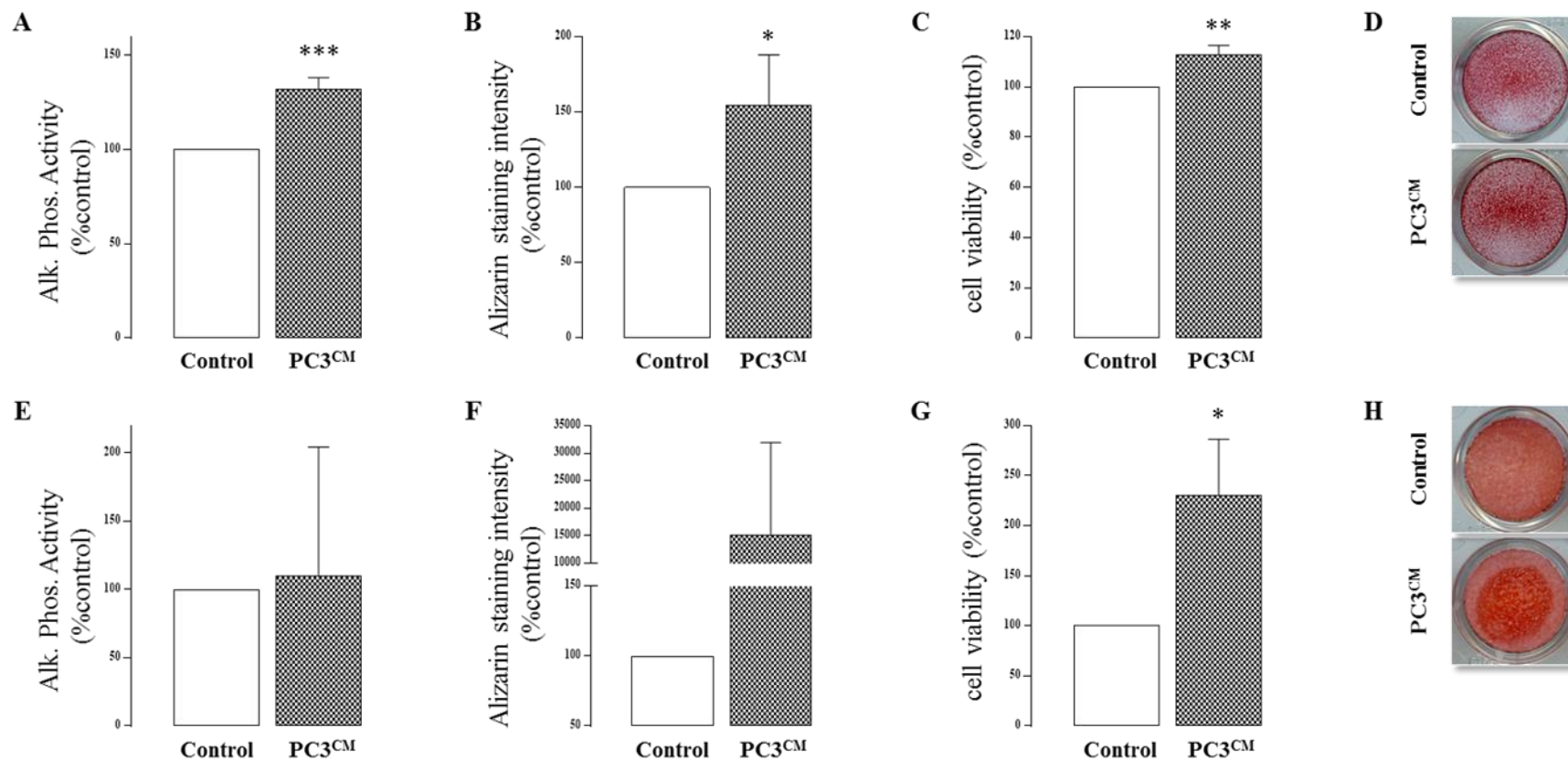


Figure S5.1: PC3 conditioned media stimulated osteoblastic differentiation, bone nodule formation activity and viability *in vitro*. Saos2 and MC3T3 cells were treated with PC3 conditioned media (20% v/v) for up to 3 weeks. At the end of the experiments culture well were assessed for: osteoblastic differentiation by measuring alkaline phosphatase activity; osteoblastic bone nodule formation by quantifying Alizarin red staining intensity; and cell culture viability using the Alamar Blue assay. **A-D**: Shows results for experiments in Saos2 after 10 days. **E-H**: Shows results for experiments in MC3T3 after 21 days. Values in the graphs are mean (expressed as % of vehicle control) \pm s.d. and are obtained from 3 independent experiments.

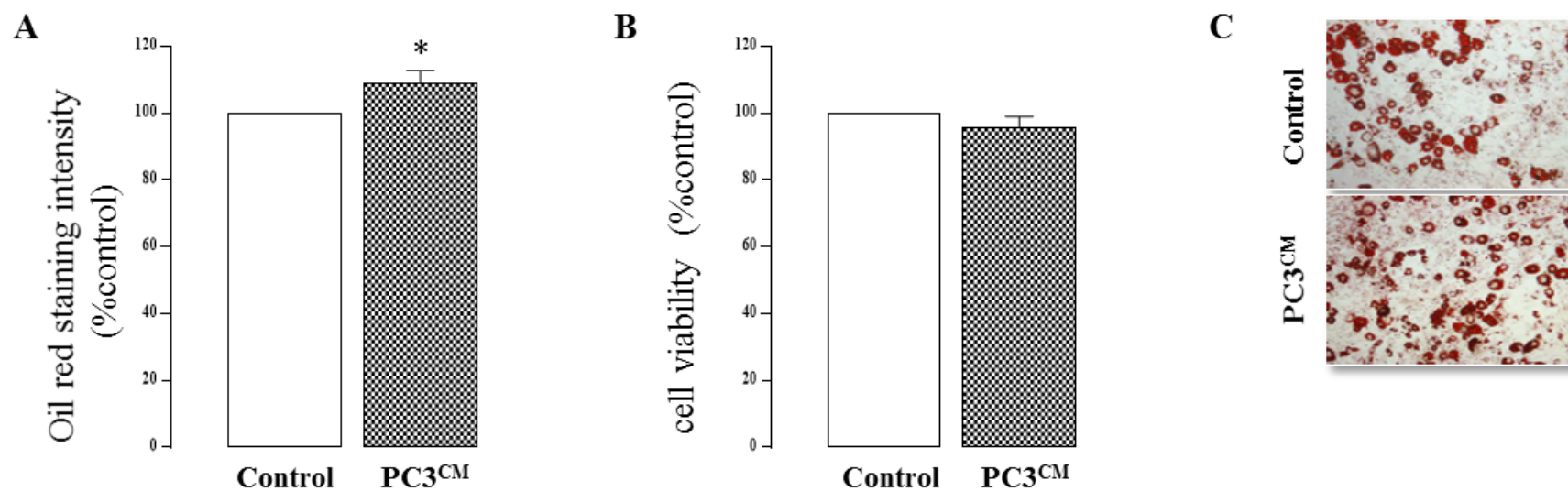


Figure S5.2: PC3 conditioned media stimulated 3T3L1 adipocyte differentiation *in vitro*. 3T3L1 cells were differentiated as described in section 2.4.5 in the presence and absence of PC3 conditioned media (20% v/v) for 15 days. At the end of the experiments the differentiation of 3T3L1 cultures was assessed by quantifying eluted oil red staining measured by spectrophotometry and the viability was measured using the Alamar Blue assay. **A-C:** Shows the differentiation and viability of 3T3L1 cells after treatment with 1 μ M SU1349 or vehicle control; representative images are shown (5x magnification). Values in the graphs are mean (expressed as % of control) \pm s.d. and are obtained from 3 independent experiments.

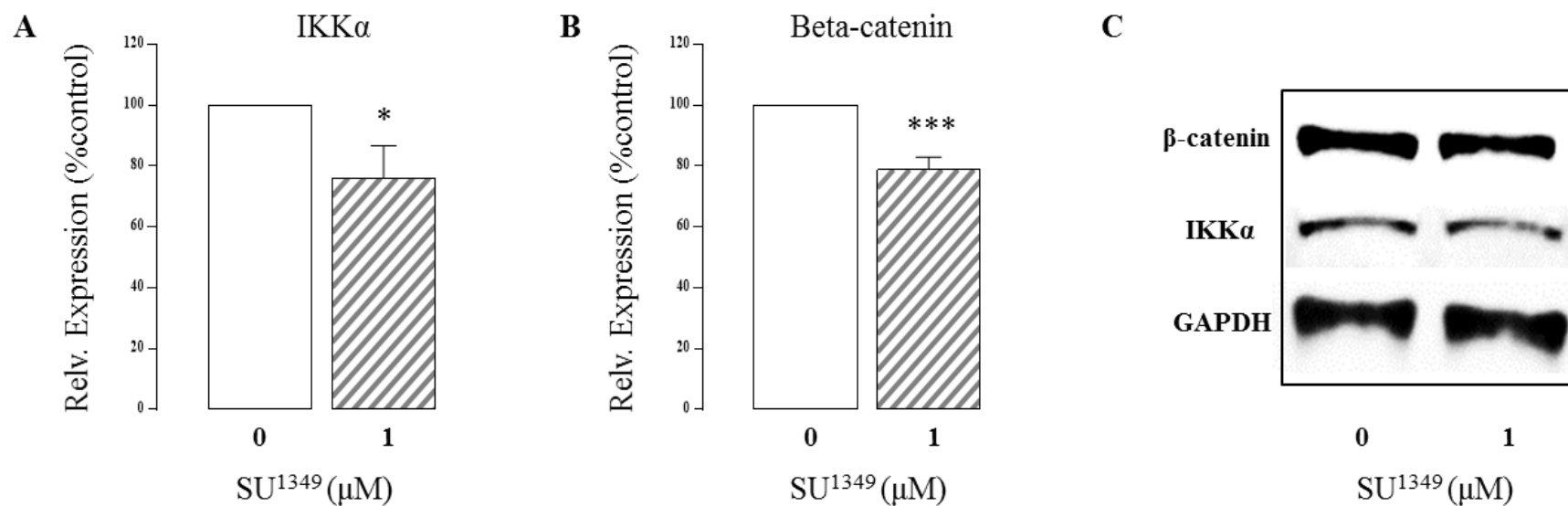


Figure S6.1: Pharmacological IKK α inhibition reduced total IKK α and β -catenin in PC3 cells. PC3 cells were treated with 1 μ M SU1349 or vehicle control in serum free media for 24rs. Total cellular lysates (50 μ g/lane) were subjected to western blot analysis normalised against GAPDH loading control; **A**: western blot analysis of total IKK α in response to SU1349. **B**: western blot analysis of total β -catenin in response to SU1349. **C**: representative blot images is shown. Values in the graphs are mean (expressed as % of control) \pm s.d. and are obtained from 3 independent experiments.

Table S6.2 Raw data for human XL cytokine microarray used in section 6.4.6. PC3 cells were treated with 1 μ M SU1349 or vehicle control (0.1% DMSO) for 24hrs (in serum free media) before probing PC3 conditioned media using Proteome ProfilerTM Human XL Cytokine Array Kit (R&D systems) followed by chemiluminescence detection and analysis.

Probed factor (spotted antibody duplicates)	Control(DMSO) (mean pixel density)	SU1349 (1 μ M) (mean pixel density)	Significance (t-test: 2 tail, type 2) *significant results highlighted in yellow
Reference Spots	1,147,856.00	1,105,520.00	0.0491
	1,154,744.00	1,121,496.00	
Adiponectin	36,928.00	34,508.00	0.6221
	30,184.00	26,608.00	
aggrecan	34,764.00	26,620.00	0.6060
	43,596.00	41,336.00	
Angiogenin	619,304.00	570,124.00	*0.0017
	615,568.00	569,004.00	
Angiopoietin-1	22,628.00	27,716.00	0.9489
	27,128.00	21,484.00	
Angiopoietin-2	34,916.00	36,652.00	0.5401
	40,368.00	34,276.00	
BAFF	29,244.00	26,752.00	0.5889
	36,856.00	33,048.00	
BDNF	43,540.00	40,068.00	0.0920
	42,592.00	37,408.00	
C5/C5a	33,184.00	29,552.00	*0.0362
	34,572.00	28,164.00	
CD14	38,708.00	29,032.00	0.0640
	34,616.00	26,844.00	
CD30	47,648.00	53,992.00	0.1289
	48,664.00	61,616.00	
Reference Spots	937,244.00	1,040,116.00	0.0507
	976,728.00	1,042,792.00	
CD40 ligand	32,784.00	36,260.00	0.6027
	38,984.00	30,200.00	
Chitinase 3-like 1	27,140.00	23,680.00	0.4720
	32,784.00	29,264.00	
Adipsin	108,824.00	89,860.00	*0.0183
	114,856.00	89,820.00	
C-Reactive Protein	35,892.00	29,984.00	0.2059
	31,964.00	22,892.00	
Cripto-1	24,576.00	22,352.00	0.1533
	27,700.00	22,816.00	
Cystatin C	58,816.00	50,504.00	0.3185
	70,092.00	59,448.00	
Dkk-1	381,600.00	377,360.00	0.7670

APPENDICIES

	377,180.00	384,172.00	
DPPIV	101,640.00	98,760.00	0.8613
	104,052.00	105,512.00	
EGF	59,176.00	46,124.00	0.3080
	47,180.00	43,620.00	
Emmprin	204,972.00	238,264.00	*0.0017
	205,116.00	241,132.00	
ENA-78	24,252.00	19,340.00	*0.0178
	24,396.00	20,520.00	
Endoglin	36,224.00	25,972.00	0.1619
	31,064.00	28,668.00	
Fas Ligand	30,528.00	26,216.00	0.6487
	27,112.00	29,064.00	
FGF basic	37,452.00	33,672.00	0.0812
	36,216.00	31,356.00	
FGF-7	24,440.00	21,524.00	0.1121
	28,220.00	20,224.00	
FGF-19	62,652.00	63,392.00	0.6346
	65,824.00	68,352.00	
Flt-3 Ligand	33,248.00	32,124.00	0.1490
	33,232.00	30,396.00	
G-CSF	32,716.00	30,968.00	0.8407
	43,000.00	41,404.00	
GDF-15	671,184.00	590,864.00	*0.0038
	676,072.00	599,296.00	
GM-CSF	42,976.00	45,536.00	0.7960
	46,204.00	42,296.00	
GRO α	23,728.00	22,652.00	0.9842
	27,256.00	28,484.00	
Growth Hormone	27,204.00	23,280.00	0.0674
	30,168.00	23,260.00	
HGF	27,784.00	22,216.00	0.0575
	25,692.00	22,700.00	
ICAM-1	39,656.00	39,196.00	0.2793
	43,376.00	32,248.00	
IFN- γ	35,192.00	31,188.00	0.0612
	34,448.00	28,796.00	
IGFBP-2	28,140.00	26,908.00	0.8251
	24,588.00	24,780.00	
IGFBP-3	28,620.00	23,924.00	0.2780
	30,188.00	28,184.00	
IL-1 α	35,992.00	26,616.00	*0.0524
	38,408.00	30,076.00	

APPENDICIES

IL-1β	32,536.00	25,304.00	*0.0391
	36,340.00	24,504.00	
IL-1ra	39,096.00	26,348.00	0.3894
	35,896.00	36,764.00	
IL-2	33,060.00	26,488.00	*0.0256
	35,640.00	26,380.00	
IL-3	30,916.00	21,760.00	0.0676
	26,860.00	20,324.00	
IL-4	24,624.00	22,784.00	0.5944
	24,420.00	24,916.00	
IL-5	21,420.00	22,556.00	0.6599
	22,760.00	20,268.00	
IL-6	33,252.00	25,152.00	0.0635
	32,800.00	28,424.00	
IL-8	67,812.00	53,200.00	*0.0284
	73,156.00	49,268.00	
IL-10	36,508.00	27,292.00	0.1501
	30,660.00	26,376.00	
IL-11	35,704.00	29,376.00	*0.0377
	37,740.00	31,008.00	
IL-12 p70	32,936.00	26,840.00	0.0820
	30,008.00	26,424.00	
IL-13	27,624.00	23,596.00	0.2577
	24,252.00	22,880.00	
IL-15	31,576.00	23,648.00	0.0796
	28,104.00	20,556.00	
IL-16	29,948.00	24,620.00	0.1071
	28,312.00	26,548.00	
IL-17A	57,552.00	43,772.00	*0.0465
	62,648.00	47,688.00	
IL-18 Bpa	29,676.00	24,992.00	0.0865
	34,296.00	22,968.00	
IL-19	19,652.00	19,904.00	0.5742
	25,900.00	21,376.00	
IL-22	34,136.00	31,972.00	0.3340
	32,100.00	31,664.00	
IL-23	32,296.00	27,696.00	0.1238
	31,184.00	22,752.00	
IL-24	35,988.00	26,960.00	*0.0423
	38,008.00	29,972.00	
IL-27	33,344.00	34,076.00	0.3573
	37,392.00	27,660.00	
IL-31	29,632.00	21,252.00	0.3206

APPENDICIES

	28,176.00	27,788.00	
IL-32	36,036.00	32,864.00	0.2779
	33,020.00	29,296.00	
IL-33	31,320.00	27,832.00	*0.0432
	30,908.00	26,096.00	
IL-34	30,060.00	23,076.00	0.0735
	27,264.00	23,996.00	
IP-10	32,168.00	24,164.00	0.0609
	29,876.00	26,152.00	
I-TAC	32,492.00	22,828.00	0.3277
	34,420.00	32,020.00	
Kallikrein 3	37,048.00	36,032.00	0.3123
	36,424.00	32,080.00	
Leptin	21,592.00	18,520.00	0.5399
	24,996.00	23,592.00	
LIF	24,428.00	22,480.00	0.9019
	22,456.00	24,832.00	
Lipocalin-2	52,716.00	41,508.00	*0.0071
	52,436.00	43,220.00	
MCP-1	29,236.00	20,704.00	*0.0038
	28,940.00	21,636.00	
MCP-3	28,736.00	33,880.00	0.8442
	26,176.00	23,432.00	
M-CSF	28,740.00	28,940.00	0.3411
	31,444.00	27,372.00	
MIF	232,832.00	224,624.00	0.2486
	225,604.00	217,764.00	
MIG	32,988.00	32,052.00	0.2618
	38,984.00	30,216.00	
MIP-1 α /MIP-1 β	25,928.00	23,692.00	0.0612
	27,500.00	22,832.00	
MIP-3 α	30,420.00	26,472.00	0.4394
	26,628.00	26,920.00	
MIP-3β	31,712.00	25,548.00	*0.0293
	29,984.00	25,980.00	
MMP-9	27,236.00	24,324.00	0.1513
	31,728.00	24,444.00	
Myeloperoxidase	19,528.00	18,128.00	0.7202
	23,664.00	22,564.00	
Osteopontin	37,196.00	28,464.00	*0.0269
	34,704.00	27,528.00	
PDGF-AA	29,532.00	19,864.00	0.2086
	26,908.00	25,384.00	

APPENDICIES

PDGF-AB/BB	19,184.00	19,796.00	0.9877
	23,940.00	23,432.00	
Pentraxin 3	37,364.00	36,372.00	0.2349
	42,516.00	33,924.00	
PF4	28,116.00	24,604.00	0.0588
	30,180.00	25,212.00	
RAGE	30,900.00	25,372.00	0.0576
	29,460.00	26,828.00	
RANTES	22,548.00	24,224.00	0.9801
	25,952.00	24,372.00	
RBP-4	162,392.00	113,296.00	*0.0039
	158,412.00	108,560.00	
Relaxin-2	33,392.00	24,744.00	0.1179
	30,768.00	28,112.00	
Resistin	40,224.00	35,024.00	0.4305
	36,088.00	36,856.00	
SDF-1 α	39,832.00	31,956.00	0.1552
	44,932.00	36,920.00	
Serpin E1	51,128.00	49,288.00	0.2145
	55,900.00	49,172.00	
SHBG	32,012.00	30,696.00	0.2738
	31,048.00	27,788.00	
ST2	25,812.00	25,584.00	0.6558
	23,780.00	25,092.00	
TARC	27,948.00	21,488.00	0.4382
	22,484.00	23,388.00	
TFF3	46,184.00	38,816.00	0.1728
	44,096.00	42,552.00	
TfR	28,540.00	24,128.00	0.2199
	31,992.00	27,676.00	
TGF-α	32,664.00	28,036.00	*0.0117
	32,212.00	27,068.00	
TSP-1	48,396.00	42,660.00	*0.0051
	47,996.00	43,296.00	
TNF- α	28,612.00	26,184.00	0.1024
	28,404.00	23,724.00	
uPAR	43,100.00	34,496.00	*0.0471
	40,036.00	34,900.00	
VEGF	34,988.00	26,872.00	0.1901
	34,528.00	32,200.00	
Reference Spots	1,034,860.00	1,081,072.00	0.9552
	1,048,356.00	1,006,924.00	
Vitamin D BP	33,628.00	36,068.00	0.9323

APPENDICIES

	31,028.00	27,752.00	
negative reference spot	20,972.00	17,440.00	0.4781
	16,872.00	16,816.00	

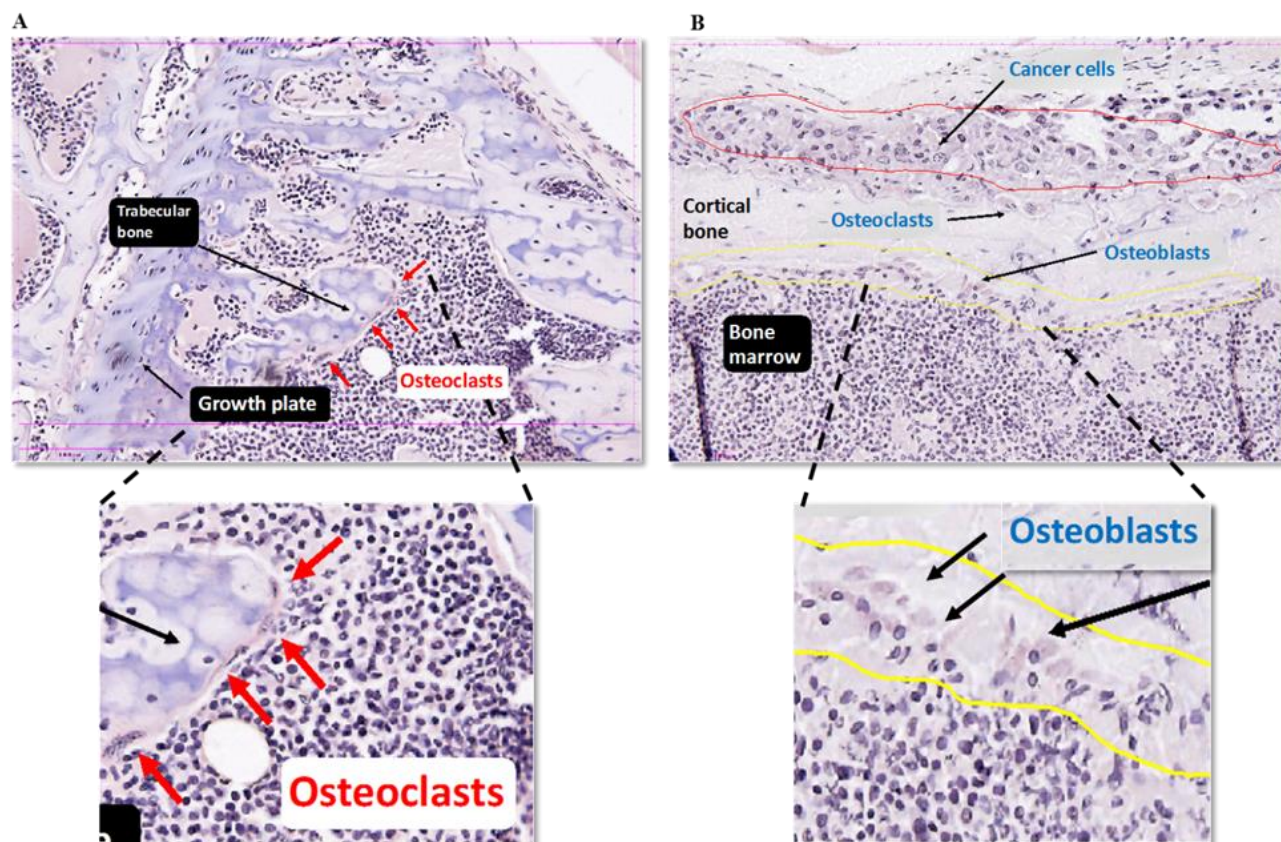


Figure S7.1 Example of stained bone sections analysed for histomorphometry. Immuno-deficient BALB/c mice were intra-cardiacally injected with PC3 cells and treated with SU1349 (20mg/kg/3times-weekly) or vehicle control; at the end of the experiment sections of mouse tibial bone were TRAPc and haematoxylin stained before undergoing histomorphometric analysis using Osteomeasure. **A:** Shows a photomicrograph of trabecular bone section near the growth plate; red arrows highlight osteoclasts. **B:** Shows a photomicrograph of cortical bone section; highlighted in yellow border is an area of the endocortical bone surface with mature osteoblasts; highlighted in red border is an area of prostate tumour growth outside of the periosteal surface of cortical bone; also shown are some osteoclasts on the periosteal surface of cortical bone.

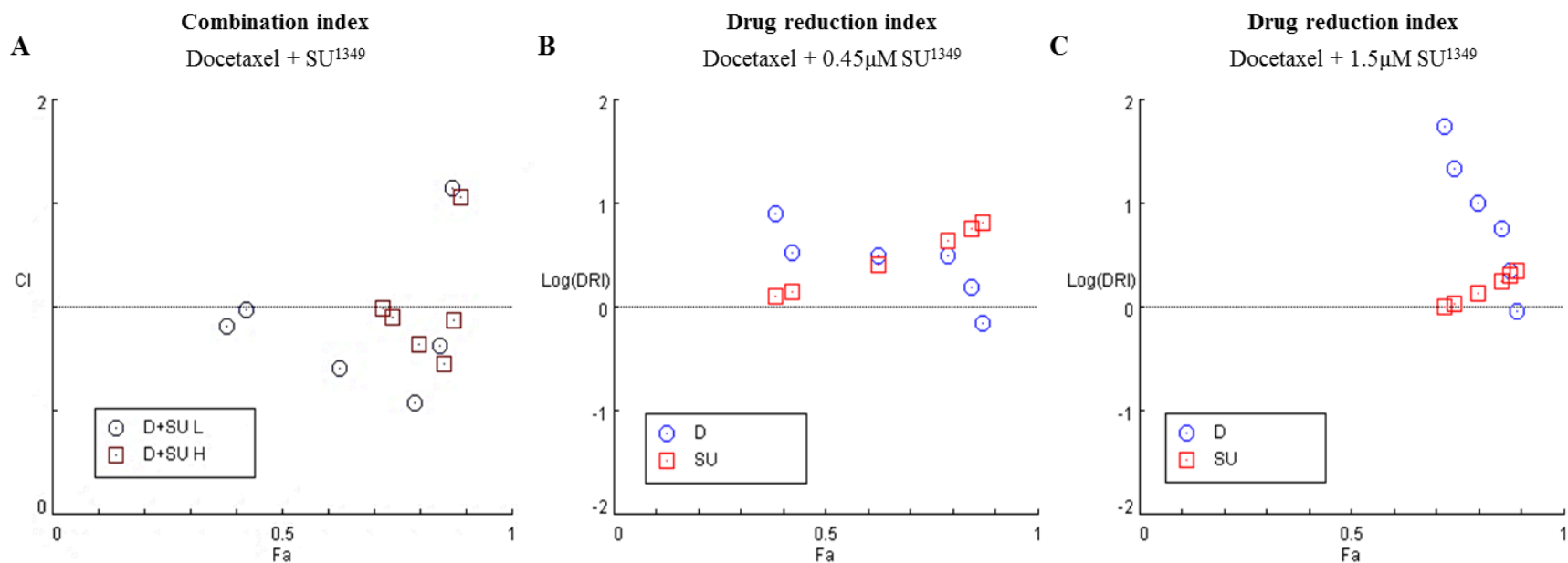


Figure S7.2 Combined IKK α inhibition and Docetaxel treatments showed synergistic effects on PC3 survival and favourable dose reduction potential for each drug. PC3 cells were pre-treated with Docetaxel (0.1, 0.3, 1, 3, 10, 30 μ M) for 24hrs before treatment with SU1349 for an additional 48hrs. **A:** Shows the combination index (CI) and Fraction affected (Fa) for Docetaxel concentrations in combination with 0.45 μ M SU1349 (D+SU L) or with 1.5 μ M SU1349 (D+SU H). The lower the CI value below the horizontal line (i.e. CI < 1) the more synergistic the effect is at that combination; CI values on the line (CI ~1) represent additive effects; CI values above the horizontal line (CI > 1) represents antagonistic combinations. Synergistic effects at higher Fa are more clinically relevant than synergism at lower Fa (e.g. Fa < 0.3 vs Fa > 0.9). **B** and **C:** Shows the dose reduction index (DRI), calculated for Docetaxel (D) and SU1349 (SU) at each experimental (Fa) combination point based on the computed dose for each drug to achieve the same Fa if used alone (i.e. not in combination), for Docetaxel + 0.45 μ M SU1349 and Docetaxel + 1.5 μ M SU1349 experiments respectively. The DRI represents degree fold in dose reduction; the higher the DRI values above the horizontal line (i.e. > 0) the more favourable the dose reduction. For example, at 0.1 μ M Docetaxel and 0.45 μ M SU1349, the Fa was 0.38, and the calculated DRIs for Docetaxel (blue circle) and SU1349 (red square) at that combination are both above the horizontal line. Fa values were calculated (using the combosyn software) based on Alamar blue results obtained from 3 independent experiments.

Appendix 2: Solutions and Recipes

Appendix 2.1 Solutions for TRAcP staining of cell cultures
<p><i>Naphthol-AS-BI-phosphate</i></p> <p>10 mg/ml Naphthol-AS-BI-phosphate in Dimethylformamide</p> <p><i>Veronal buffer</i></p> <p>1.17 g sodium acetate anhydrous and 2.94g sodium barbiturate both dissolved in 100 ml of dH₂O</p> <p><i>Acetate buffer</i></p> <p>0.82 g sodium acetate anhydrous dissolved in 100 ml of dH₂O and pH adjusted to 5.2 with 0.6 ml glacial acetic acid made up to 100 ml with dH₂O</p> <p><i>Pararosanilin</i></p> <p>1 g Pararosanilin dissolved in 20 ml of dH₂O and 5 ml of 5M HCl added to it. The solution was heated carefully whilst stirring and filtered after cooling.</p> <p><i>TRAcP Staining Solution</i></p> <p>The TRAcP staining solution was freshly prepared by mixing solution A and B as outlined below.</p> <p><i>Solution A</i></p> <p>150 ml of Naphthol-AS-BI-phosphate 750 ml of Veronal buffer 900 ml Acetate buffer 900 ml Acetate buffer with 100 mM Sodium Tartate</p> <p><i>Solution B</i></p> <p>120 ml of Pararosanilin 120 ml of Sodium Nitrate (4% w/v)</p>

Appendix 2.2 Solutions for ALP assay***Diethanolamine (DEA)/MgCl₂ buffer***

1 M DEA and 1 M MgCl₂ made up in 100 ml dH₂O and pH adjusted to 9.8.
Left at room
temperature for 24 hours

ALP Lysis buffer

0.05% Triton X-100 added to DEA/MgCl₂ buffer

p-Nitrophenol standard solution

p-Nitrophenol standards (1.25 – 30 nM) prepared in lysis buffer

Substrate solution

20 mM p-nitrophenol-phosphate made up in DEA/MgCl₂ buffer and pH
adjusted to 9.8

Appendix 2.3 Solution for cell Lysis***RIPA Lysis buffer***

1% Triton 100X, 0.5% (w/v) Sodium Deoxycholate, 0.1% (w/v) Sodium Dodecyl
Sulphate (SDS), 50 mM Tris-HCl (pH 7.4) and 150 mM Sodium Chloride were
dissolved in dH₂O

Cytoplasmic fraction Lysis buffer

10 mM Tris [pH 7.5], 0.05% NP-40, 3 mM MgCl₂, 100 mM NaCl, 1 mM EGTA
were dissolved in dH₂O

Appendix 2.4 Solutions for PAGE and western blot***Electrophoresis running buffer***

100 ml of TGS buffer (10X) in 1000 ml of dH₂O

Samples loading protein buffer (5X stock)

5.2 ml of 1M Tris-HCl pH adjusted to 6.8, 1 g of DL-Dithiothreitol (DTT), 3 g SDS, 6.5 ml glycerol and 130 μ l of 10% (w/v) Bromophenol Blue. Stored at -20°C.

Transfer buffer

3.63 g of Tris, 14.4g of Glycine, 200 ml of Methanol and 3.75 ml of 10% (w/v) SDS made up to 1000 ml with dH₂O. Stored at room temperature.

TBS

1 M of Tris and 1 M Tris-HCl. pH adjusted to 7.9 prior to addition of 3 M Sodium Chloride. Stored at room temperature.

TBST

0.1% (v/v) Tween-20 in TBS. Stored at room temperature.

Stripping buffer

1 mM DTT, 2% (w/v) SDS and 62.5 mM Tris-HCl (pH 6.7). Stored at room temperature.

Appendix 2.5 Solutions for TRAcP staining of slides (per 10 slides)***Parasosaniline***

1 g parasosaniline in 20 ml dH₂O plus 5ml HCL -> mix on hot plate (without boiling) for 30-45 minutes and allow to simmer for 5min

Acetate buffer

Per 10 slides 5.44 g sodium acetate trihydrate in 200ml dH₂O. adjust pH to 5.2 with 50-60ml 1.2% acetic acid. (freshly prepared)

Acetate-tartrate buffer

Per 10 slides add 4.6 g sodium tartrate to 200ml acetate buffer and warm to 37°C for 2-4 hours. (freshly prepared)

Naphthol-AS-BI-phosphate

40 mg/ml Naphthol-AS-BI-phosphate in Dimethylformamide

4% sodium nitrite

160 mg sodium nitrite in 4ml dH₂O.

TRAcP Staining Solution

The TRAcP staining solution was freshly prepared by mixing solution A and B as outlined below.

Solution A

1 ml of Naphthol-AS-BI-phosphate + 50 ml Acetate-tartrate buffer. Incubate sections for 30 minutes at 37°C.

Solution B

3 ml of Parasosanilin + 3 ml of Sodium Nitrate (4% w/v). leave for 5 minutes.

Just before use add 5ml of mixed solution in 50ml of acetate-tartrate buffer in prewarmed bottle and mix well. Incubate sections in solution B for 15-20 minutes 37°C.

Appendix 2.6 Solution for Immunohistochemistry

Citrate buffer

4.41g di hydrate tri-sodium citrate in 1.5 litres dH₂O, adjust pH to 6 and add
0.75ml TWEEN 20

Appendix 2.7 *In vivo* drug suspension

Drug suspension for IP injection

Dissolve 60mg of the SU1349 in 4.0 ml of DMSO.

Add 2mL Tween 20 and mix.

Add 14mL of 5% w/v mannitol in distilled water.

Inject 150µl via IP injection for a 20mg/kg dose

Appendix 3: Materials, Reagents, Apparatus and Software

3.1 Materials and Reagents used in this study:

Materials and reagents	Supplier
1.5ml Eppendorf tubes with cap	Starlab, Milton Keynes, UK
12% Criterion™ TGX™ Precast Midi Protein Gel, 12+2 well	Bio-Rad Laboratories, Hertfordshire, UK
3T3-L1	ATCC, Manassas, VA-USA
5-fluorouracil	Sigma Aldrich, Dorset, UK
Acetic Acid Glacial	Sigma Aldrich, Dorset, UK
AlamarBlue™ reagent	Invitrogen, Paisley, UK
Alizarin Red S	Sigma Aldrich, Dorset, UK
Ampicillin	Fisher Scientific, Leicestershire, UK
BD microlance needles (19, 21 and 25G)	Fisher Scientific, Leicestershire, UK
Bicinchoninic acid (BCA) solution	Sigma Aldrich, Dorset, UK
Bovine Insulin	Sigma Aldrich, Dorset, UK
Bovine serum albumin	Sigma Aldrich, Dorset, UK
Bromophenol Blue	BDH Laboratory Supplies, Poole, Dorset, UK
C4-2	ATCC, Manassas, VA-USA
C4-2B4	ATCC, Manassas, VA-USA
Centrifuge tubes 15ml	Scientific laboratory supplies (SLS), Nottingham UK
Centrifuge tubes 50ml	Fisher Scientific, Leicestershire, UK
Cetyl pyridinium chloride monohydrate	Sigma Aldrich, Dorset, UK
Clarity Western ECL Substrate	Bio-Rad Laboratories, Hertfordshire, UK
Collagenase (type 1A)	Sigma Aldrich, Dorset, UK
Copper (II)-sulfate	Sigma Aldrich, Dorset, UK
Corning™ Transwell™ Multiple Well Plate with Permeable Polycarbonate Membrane Inserts	Corning, Flintshire, UK
Cover slips	Fisher Scientific, Leicestershire, UK
Cyclophosphamide	Sigma Aldrich, Dorset, UK
DAKO	Agilent Technologies, Wokingham, UK
Dexamethasone	Sigma Aldrich, Dorset, UK
Diethanolamin	Sigma Aldrich, Dorset, UK
DL-Dithiothreitol (DTT)	Sigma Aldrich, Dorset, UK
DMSO	Sigma Aldrich, Dorset, UK
Docetaxel	Sigma Aldrich, Dorset, UK
Doxorubicin	Sigma Aldrich, Dorset, UK
DPX mounting medium	Sigma Aldrich, Dorset, UK
EDTA	Sigma Aldrich, Dorset, UK

APPENDICIES

Electrophoresis power supply	Bio-Rad Laboratories, Hertfordshire, UK
Ethanol Absolute	Sigma Aldrich, Dorset, UK
Fetal calf serum (FCS)	Fisher Scientific, Leicestershire, UK
Filter Tips any size	Starlab, Milton Keynes, UK
Forceps watchmaker's	Fisher Scientific, Leicestershire, UK
Glycine	Acros organics, Geel, Belgium
Hanks buffer (HBSS)	Sigma Aldrich, Dorset, UK
Human recombinant RANKL	Gift from Dr. Patrick Mollat (Proskelia SASU)
Isobutylmethylxanthine	Sigma Aldrich, Dorset, UK
Isopropanol	Fisher Scientific, Leicestershire, UK
Jackson ImmunoResearch Anti-rabbit secondary ab	Stratech Scientific Unit, Newmarket Suffolk, UK
Kaleidoscope Pre-stained standards	Bio-Rad Laboratories, Hertfordshire, UK
LNCaP	ATCC, Manassas, VA-USA
Luria-Bertani (broth & agar)	Sigma Aldrich, Dorset, UK
Magic Marker	Invitrogen, Paisley, UK
Magnesium chloride	Sigma Aldrich, Dorset, UK
MC3T3-E1	ATCC, Manassas, VA-USA
M-CSF mouse recombinant	R & D Systems, Abingdon, UK
Methanol	VWR International LTD, Leicestershire, UK
Microtubes (0.5, 1.5, 2ml)	Sarstedt Ltd, Leicester, UK
Minimum Essential Medium (α MEM)	Fisher Scientific, Leicestershire, UK
Minimum Essential Medium (DMEM)	Fisher Scientific, Leicestershire, UK
N,N-Dimethylformamide	Sigma Aldrich, Dorset, UK
Napthol-AS-BI-phosphate	Sigma Aldrich, Dorset, UK
Neubauer Haemocytometer	Hawksley, Lancing, UK
Oil Red O	Sigma Aldrich, Dorset, UK
Paclitaxel	Sigma Aldrich, Dorset, UK
Paraformaldehyde	Taab Lab, Berkshire, UK
Pararosanilin	Sigma Aldrich, Dorset, UK
PC3	ATCC, Manassas, VA-USA
PC3-BT	Dr. Colby Eaton (Sheffield, UK)
PC3-NW1 (luciferase labelled)	Dr. Colby Eaton (Sheffield, UK)
Penicillin/Streptomycin	Fisher Scientific, Leicestershire, UK
Pierce™ Bovine Serum Albumin Standard Pre-Diluted Set	Fisher Scientific, Leicestershire, UK
Phosphatase inhibitor cocktail	Sigma Aldrich, Dorset, UK
Phosphate buffered saline	Fisher Scientific, Leicestershire, UK

APPENDICIES

Pipette tips (all sizes)	Starlab, Milton Keynes, UK
Puromycin	Fisher Scientific, Leicestershire, UK
Protease inhibitor cocktail	Sigma Aldrich, Dorset, UK
Proteome Profiler™ Human XL Cytokine Array Kit	R&D Systems, Abingdon, UK
Prostate cancer tissue microarray (PR242b)	Biomax, MD, USA
4-Nitrophenyl phosphate disodium salt hexahydrate powder	Scientific laboratory supplies (SLS), Nottingham UK
Recombinant Human Semaphorin 3A Fc Chimera Protein, CF Saos-2	R & D Systems, Abingdon, UK
Scalpel, disposable	ATCC, Manassas, VA-USA
Scissors (fine points and spring bow handles)	VWR International LTD, Leicestershire, UK
Silver nitrate	S Murray & Co Ltd, Surrey, UK
Sodium acetate trihydrate	Sigma Aldrich, Dorset, UK
Sodium barbiturate	VWR International LTD, Leicestershire, UK
Sodium chloride	Sigma Aldrich, Dorset, UK
Sodium dodecyl sulphate (SDS)	Bio-Rad Laboratories, Hertfordshire, UK
Sodium hydroxide	VWR International LTD, Leicestershire, UK
Sodium phosphate	Sigma Aldrich, Dorset, UK
Sodium tartrate dibasic dihydrate	Sigma Aldrich, Dorset, UK
Starguard® laboratory gloves	Starlab, Milton Keynes, UK
Sterile filter (0.2 and 0.45µm)	Pall lifesciences, Portsmouth, UK
Stripettes (5, 10, 25 and 50ml)	Fisher Scientific, Leicestershire, UK
Superfrost Plus™ Adhesion Microscope Slides	Fisher Scientific, Leicestershire, UK
Syringes (all sizes)	Fisher Scientific, Leicestershire, UK
Tissue culture 25, 75, 175cm ² flasks	Fisher Scientific, Leicestershire, UK
Tissue culture microplates (6, 12, 24, 48 and 96-well plates)	Corning, Flintshire, UK
Transblot Turbo midi Size PVDF membrane	Bio-Rad Laboratories, Hertfordshire, UK
Transblot Turbo midi Size Transfer stacks	Bio-Rad Laboratories, Hertfordshire, UK
Tris	Bio-Rad Laboratories, Hertfordshire, UK
Tris-EDTA buffer	Sigma Aldrich, Dorset, UK
Tris-Glycine buffer 10x	Bio-Rad Laboratories, Hertfordshire, UK
Triton X-100™	Sigma Aldrich, Dorset, UK
Trizma® hydrochloride	Sigma Aldrich, Dorset, UK
Trizma® base	Sigma Aldrich, Dorset, UK
Trypsin/EDTA	Sigma Aldrich, Dorset, UK
Tween-20	Acros organics, Geel, Belgium
Ultraclear Xylene	Taab Lab, Berkshire, UK

APPENDICIES

L-Ascorbic acid	Sigma Aldrich, Dorset, UK
Western blot tips	Starlab, Milton Keynes, UK
XT-MOPS	Bio-Rad Laboratories, Hertfordshire, UK
Xylene	Sigma Aldrich, Dorset, UK
β -glycerophosphate disodium	Sigma Aldrich, Dorset, UK

3.2 Antibodies in this thesis:

Antibody	Supplier
Rabbit anti-p65	Cell Signalling technologies, USA
Rabbit anti-Actin	Sigma-Aldrich, UK
Rabbit anti- β -catenin	Cell Signalling technologies, USA
Rabbit anti-GAPDH	Sigma-Aldrich, UK
Rabbit anti-phospho-GSK3 β	Cell Signalling technologies, USA
Rabbit anti-Lamin A/C	Cell Signalling technologies, USA
Rabbit anti-I κ B α	Cell Signalling technologies, USA
Rabbit anti-phospho-I κ B α	Cell Signalling technologies, USA
Rabbit anti-IKK α	Cell Signalling technologies, USA
Rabbit anti-IKK α (mAb)	Novus Biologicals, UK

3.3 Apparatus used in this thesis:

Apparatus	Supplier
AA Hofer® protein transfer apparatus	Fisher Scientific, Leicestershire, UK
Bench-top Eppendorf centrifuge	Fisher Scientific, Leicestershire, UK
Grant OLS 200 water bath	Thistle Scientific, Glasgow, UK
Horizontal electrophoresis tanks	Fisher Scientific, Leicestershire, UK
Hotplate/stirrer	Thistle Scientific, Glasgow, UK
Ika Vortex	Thistle Scientific, Glasgow, UK
Leica AF6000	Leica Microsystems, Milton Keynes, UK
Nichiryo America Inc. Pipettes (2, 10, 100, 200 and 1000µl)	Thistle Scientific, Glasgow, UK
Origo PSU-400/200 power supply for electrophoresis	Anachem, Bedfordshire, UK
PowerPac basic™	Bio-Rad Laboratories, Hertfordshire, UK
QImaging Retiga 4000R CCD camera	Media Cybernetics UK, Berkshire, UK
SkyScan 1172 X-ray Microtomography system	SKYSCAN, Kontich, Belgium
SkyScan 1176 in-vivo micro-CT	SKYSCAN, Kontich, Belgium
SpectraMax® M5 microplate reader	Fisher Scientific, Leicestershire, UK
Syngene GeneGenius Gel Bio-Imaging system	Fisher Scientific, Leicestershire, UK
SynSyngene GeneGnome Bio-Imaging system for chemiluminescence	Fisher Scientific, Leicestershire, UK
Vertical Criterion™ gel tanks	Bio-Rad Laboratories, Hertfordshire, UK

3.4 Software used in this thesis:

Software	Supplier
CompuSyn	ComboSyn, NJ, USA
GraphPad Prism (version 7)	GraphPad Software Inc., CA-US
ImageJ	U. S. National Institutes of Health Bethesda, MA-US
Image Lab	Biorad, Watford, UK
Osteomeasure	Osteometrics, DA, USA
Skyscan 1172 MicroCT software	SKYSCAN, Kontich, Belgium
Skyscan CTAn analysis software	SKYSCAN, Kontich, Belgium
Skyscan CTVol software	SKYSCAN, Kontich, Belgium
Skyscan NRecon reconstruction system	SKYSCAN, Kontich, Belgium
SpectraMax® M5 plate reader software	Fisher Scientific, Leicestershire, UK
Syngene GeneSnap software	Fisher Scientific, Leicestershire, UK
Syngene GeneTool software	Fisher Scientific, Leicestershire, UK
TScratch	ETH Zürich, Switzerland

REFERENCES

REFERENCES

- Abu-Amer, Y., Erdmann, J., Alexopoulou, L., Kollias, G., Ross, F. P. and Teitelbaum, S. L. (2000) 'Tumor necrosis factor receptors types 1 and 2 differentially regulate osteoclastogenesis', *J Biol Chem*, 275(35), pp. 27307-10.
- Adli, M., Merkhofer, E., Cogswell, P. and Baldwin, A. S. (2010) 'IKKalpha and IKKbeta each function to regulate NF-kappaB activation in the TNF-induced/canonical pathway', *PLoS One*, 5(2), pp. e9428.
- Ahmed, M. and Gaffen, S. L. (2013) 'IL-17 inhibits adipogenesis in part via C/EBPalpha, PPARgamma and Kruppel-like factors', *Cytokine*, 61(3), pp. 898-905.
- Akech, J., Wixted, J. J., Bedard, K., van der Deen, M., Hussain, S., Guise, T. A., van Wijnen, A. J., Stein, J. L., Languino, L. R., Altieri, D. C., Pratap, J., Keller, E., Stein, G. S. and Lian, J. B. (2010) 'Runx2 association with progression of prostate cancer in patients: mechanisms mediating bone osteolysis and osteoblastic metastatic lesions', *Oncogene*, 29(6), pp. 811-21.
- Alameda, J. P., Moreno-Maldonado, R., Fernandez-Acenero, M. J., Navarro, M., Page, A., Jorcano, J. L., Bravo, A., Ramirez, A. and Casanova, M. L. (2011) 'Increased IKKalpha expression in the basal layer of the epidermis of transgenic mice enhances the malignant potential of skin tumors', *PLoS One*, 6(7), pp. e21984.
- Albers, J., Keller, J., Baranowsky, A., Beil, F. T., Catala-Lehnen, P., Schulze, J., Amling, M. and Schinke, T. (2013) 'Canonical Wnt signaling inhibits osteoclastogenesis independent of osteoprotegerin', *J Cell Biol*, 200(4), pp. 537-49.
- Alles, N., Soysa, N. S., Hayashi, J., Khan, M., Shimoda, A., Shimokawa, H., Ritzeler, O., Akiyoshi, K., Aoki, K. and Ohya, K. (2010) 'Suppression of NF-kappaB increases bone formation and ameliorates osteopenia in ovariectomized mice', *Endocrinology*, 151(10), pp. 4626-34.
- Almeida, M., Iyer, S., Martin-Millan, M., Bartell, S. M., Han, L., Ambrogini, E., Onal, M., Xiong, J., Weinstein, R. S., Jilka, R. L., O'Brien, C. A. and Manolagas, S. C. (2013) 'Estrogen receptor-alpha signaling in osteoblast progenitors stimulates cortical bone accrual', *J Clin Invest*, 123(1), pp. 394-404.
- Alsulaiman, M., Bais, M. V. and Trackman, P. C. (2016) 'Lysyl oxidase propeptide stimulates osteoblast and osteoclast differentiation and enhances PC3 and DU145 prostate cancer cell effects on bone in vivo', *J Cell Commun Signal*, 10(1), pp. 17-31.
- Amend, S. R., Uluckan, O., Hurchla, M., Leib, D., Novack, D. V., Silva, M., Frazier, W. and Weilbaecher, K. N. (2015) 'Thrombospondin-1 Regulates Bone Homeostasis Through Effects on Bone Matrix Integrity and Nitric Oxide Signaling in Osteoclasts', *Journal of Bone and Mineral Research*, 30(1), pp. 106-115.
- Ammirante, M., Kuraishy, A. I., Shalapour, S., Strasner, A., Ramirez-Sanchez, C., Zhang, W., Shabaik, A. and Karin, M. (2013) 'An IKKalpha-E2F1-BMI1 cascade activated by infiltrating B cells controls prostate regeneration and tumor recurrence', *Genes Dev*, 27(13), pp. 1435-40.
- Ammirante, M., Luo, J. L., Grivennikov, S., Nedospasov, S. and Karin, M. (2010) 'B-cell-derived lymphotoxin promotes castration-resistant prostate cancer', *Nature*, 464(7286), pp. 302-5.
- Anastas, J. N. and Moon, R. T. (2013) 'WNT signalling pathways as therapeutic targets in cancer', *Nat Rev Cancer*, 13(1), pp. 11-26.
- Andela, V. B., Gordon, A. H., Zotalis, G., Rosier, R. N., Goater, J. J., Lewis, G. D., Schwarz, E. M., Puzas, J. E. and O'Keefe, R. J. (2003) 'NFkappaB: a pivotal transcription factor in prostate cancer metastasis to bone', *Clin Orthop Relat Res*, (415 Suppl), pp. S75-85.

REFERENCES

- Anthony, N. G., Baiget, J., Berretta, G., Boyd, M., Breen, D., Edwards, J., Gamble, C., Gray, A. I., Harvey, A. L., Hatzieremia, S., Ho, K. H., Huggan, J. K., Lang, S., Llona-Minguez, S., Luo, J. L., McIntosh, K., Paul, A., Plevin, R. J., Robertson, M. N., Scott, R., Suckling, C. J., Sutcliffe, O. B., Young, L. C. and Mackay, S. P. (2017) 'Inhibitory Kappa B Kinase alpha (IKKalpha) Inhibitors That Recapitulate Their Selectivity in Cells against Isoform-Related Biomarkers', *J Med Chem*, 60(16), pp. 7043-7066.
- Ara, T. and Declerck, Y. A. (2010) 'Interleukin-6 in bone metastasis and cancer progression', *Eur J Cancer*, 46(7), pp. 1223-31.
- Armstrong, A. P., Miller, R. E., Jones, J. C., Zhang, J., Keller, E. T. and Dougall, W. C. (2008) 'RANKL acts directly on RANK-expressing prostate tumor cells and mediates migration and expression of tumor metastasis genes', *Prostate*, 68(1), pp. 92-104.
- Asamitsu, K., Yamaguchi, T., Nakata, K., Hibi, Y., Victoriano, A. F., Imai, K., Onozaki, K., Kitade, Y. and Okamoto, T. (2008) 'Inhibition of human immunodeficiency virus type 1 replication by blocking IkappaB kinase with noraristeromycin', *J Biochem*, 144(5), pp. 581-9.
- Attard, G., Parker, C., Eeles, R. A., Schroder, F., Tomlins, S. A., Tannock, I., Drake, C. G. and de Bono, J. S. (2015) 'Prostate cancer', *Lancet*.
- Bar-Shavit, Z. (2007) 'The osteoclast: a multinucleated, hematopoietic-origin, bone-resorbing osteoimmune cell', *J Cell Biochem*, 102(5), pp. 1130-9.
- Baritaki, S., Chapman, A., Yeung, K., Spandidos, D. A., Palladino, M. and Bonavida, B. (2009) 'Inhibition of epithelial to mesenchymal transition in metastatic prostate cancer cells by the novel proteasome inhibitor, NPI-0052: pivotal roles of Snail repression and RKIP induction', *Oncogene*, 28(40), pp. 3573-85.
- Barrack, E. R. (1997) 'TGF beta in prostate cancer: a growth inhibitor that can enhance tumorigenicity', *Prostate*, 31(1), pp. 61-70.
- Basseres, D. S. and Baldwin, A. S. (2006) 'Nuclear factor-kappaB and inhibitor of kappaB kinase pathways in oncogenic initiation and progression', *Oncogene*, 25(51), pp. 6817-30.
- Baud, V. and Karin, M. (2009) 'Is NF-kappaB a good target for cancer therapy? Hopes and pitfalls', *Nat Rev Drug Discov*, 8(1), pp. 33-40.
- Begley, L. A., Kasina, S., Mehra, R., Adsule, S., Admon, A. J., Lonigro, R. J., Chinnaiyan, A. M. and Macoska, J. A. (2008) 'CXCL5 promotes prostate cancer progression', *Neoplasia*, 10(3), pp. 244-54.
- Belldegrun, A., Tso, C. L., Zisman, A., Naitoh, J., Said, J., Pantuck, A. J., Hinkel, A., deKernion, J. and Figlin, R. (2001) 'Interleukin 2 gene therapy for prostate cancer: phase I clinical trial and basic biology', *Hum Gene Ther*, 12(8), pp. 883-92.
- Bendre, M. S., Montague, D. C., Peery, T., Akel, N. S., Gaddy, D. and Suva, L. J. (2003) 'Interleukin-8 stimulation of osteoclastogenesis and bone resorption is a mechanism for the increased osteolysis of metastatic bone disease', *Bone*, 33(1), pp. 28-37.
- Berish, R. B., Ali, A. N., Telmer, P. G., Ronald, J. A. and Leong, H. S. (2018) 'Translational models of prostate cancer bone metastasis', *Nat Rev Urol*, 15(7), pp. 403-421.
- Bing, C. (2015) 'Is interleukin-1beta a culprit in macrophage-adipocyte crosstalk in obesity?', *Adipocyte*, 4(2), pp. 149-52.
- Borghese, C., Cattaruzza, L., Pivetta, E., Normanno, N., De Luca, A., Mazzucato, M., Celegato, M., Colombatti, A. and Aldinucci, D. (2013) 'Gefitinib inhibits the cross-talk between mesenchymal stem cells and prostate cancer cells leading to tumor cell proliferation and inhibition of docetaxel activity', *J Cell Biochem*, 114(5), pp. 1135-44.

REFERENCES

- Boyce, B. F., Yao, Z. and Xing, L. (2010) 'Functions of nuclear factor kappaB in bone', *Ann N Y Acad Sci*, 1192, pp. 367-75.
- Brandl, M., Seidler, B., Haller, F., Adamski, J., Schmid, R. M., Saur, D. and Schneider, G. (2010) 'IKK(alpha) controls canonical TGF(ss)-SMAD signaling to regulate genes expressing SNAIL and SLUG during EMT in panc1 cells', *J Cell Sci*, 123(Pt 24), pp. 4231-9.
- Brommage, R., Liu, J. and Lee, E. C. (2009) *Elevated Trabecular Bone Mass with Reduced Cortical Bone Thickness in sFRP4 Knockout Mice*.
- Bubendorf, L., Schopfer, A., Wagner, U., Sauter, G., Moch, H., Willi, N., Gasser, T. C. and Mihatsch, M. J. (2000) 'Metastatic patterns of prostate cancer: an autopsy study of 1,589 patients', *Hum Pathol*, 31(5), pp. 578-83.
- Bussard, K. M., Venzon, D. J. and Mastro, A. M. (2010) 'Osteoblasts Are a Major Source of inflammatory Cytokines in the Tumor Microenvironment of Bone Metastatic Breast Cancer', *Journal of Cellular Biochemistry*, 111(5), pp. 1138-1148.
- Butterwith, S. C., Peddie, C. D. and Goddard, C. (1992) 'Effects of transforming growth factor-alpha on chicken adipocyte precursor cells in vitro', *J Endocrinol*, 134(2), pp. 163-8.
- Canalis, E. (2009) 'Growth factor control of bone mass', *J Cell Biochem*, 108(4), pp. 769-77.
- Carayol, N. and Wang, C. Y. (2006) 'IKKalpha stabilizes cytosolic beta-catenin by inhibiting both canonical and non-canonical degradation pathways', *Cell Signal*, 18(11), pp. 1941-6.
- Center, M. M., Jemal, A., Lortet-Tieulent, J., Ward, E., Ferlay, J., Brawley, O. and Bray, F. (2012) 'International variation in prostate cancer incidence and mortality rates', *Eur Urol*, 61(6), pp. 1079-92.
- Chaffer, C. L. and Weinberg, R. A. (2011) 'A perspective on cancer cell metastasis', *Science*, 331(6024), pp. 1559-64.
- Chaisson, M. L., Branstetter, D. G., Derry, J. M., Armstrong, A. P., Tometsko, M. E., Takeda, K., Akira, S. and Dougall, W. C. (2004) 'Osteoclast differentiation is impaired in the absence of inhibitor of kappa B kinase alpha', *J Biol Chem*, 279(52), pp. 54841-8.
- Chang, J., Liu, F., Lee, M., Wu, B., Ting, K., Zara, J. N., Soo, C., Al Hezaimi, K., Zou, W., Chen, X., Mooney, D. J. and Wang, C. Y. (2013) 'NF-kappaB inhibits osteogenic differentiation of mesenchymal stem cells by promoting beta-catenin degradation', *Proc Natl Acad Sci U S A*, 110(23), pp. 9469-74.
- Chang, J., Wang, Z., Tang, E., Fan, Z., McCauley, L., Franceschi, R., Guan, K., Krebsbach, P. H. and Wang, C. Y. (2009) 'Inhibition of osteoblastic bone formation by nuclear factor-kappaB', *Nat Med*, 15(6), pp. 682-9.
- Chang, Y. L., Stanford, C. M. and Keller, J. C. (2000) 'Calcium and phosphate supplementation promotes bone cell mineralization: implications for hydroxyapatite (HA)-enhanced bone formation', *J Biomed Mater Res*, 52(2), pp. 270-8.
- Chang, Y. S., Chen, W. Y., Yin, J. J., Tillman, H., Huang, J. and Liu, Y. N. (2015) 'EGF receptor promotes prostate cancer bone metastasis by downregulating miR-1 and activating TWIST1', *Cancer Res*.
- Chavey, C. and Fajas, L. (2009) 'CXCL5 drives obesity to diabetes, and further', *Aging (Albany NY)*, 1(7), pp. 674-7.
- Chen, Y. C., Sosnoski, D. M. and Mastro, A. M. (2010) 'Breast cancer metastasis to the bone: mechanisms of bone loss', *Breast Cancer Res*, 12(6), pp. 215.
- Chendil, D., Das, A., Dey, S., Mohiuddin, M. and Ahmed, M. M. (2002) 'Par-4, a pro-apoptotic gene, inhibits radiation-induced NF kappa B activity and Bcl-2 expression leading to induction of radiosensitivity in human prostate cancer cells PC-3', *Cancer Biol Ther*, 1(2), pp. 152-60.

REFERENCES

- Cildir, G., Low, K. C. and Tergaonkar, V. (2016) 'Noncanonical NF-kappaB Signaling in Health and Disease', *Trends Mol Med*, 22(5), pp. 414-429.
- Clement-Demange, L. and Clezardin, P. (2015) 'Emerging therapies in bone metastasis', *Curr Opin Pharmacol*, 22, pp. 79-86.
- Clement, J. F., Meloche, S. and Servant, M. J. (2008) 'The IKK-related kinases: from innate immunity to oncogenesis', *Cell Res*, 18(9), pp. 889-99.
- Codony-Servat, J., Marin-Aguilera, M., Visa, L., Garcia-Albeniz, X., Pineda, E., Fernandez, P. L., Filella, X., Gascon, P. and Mellado, B. (2013) 'Nuclear factor-kappa B and interleukin-6 related docetaxel resistance in castration-resistant prostate cancer', *Prostate*, 73(5), pp. 512-21.
- Coelho, M. J., Cabral, A. T. and Fernandes, M. H. (2000) 'Human bone cell cultures in biocompatibility testing. Part I: osteoblastic differentiation of serially passaged human bone marrow cells cultured in alpha-MEM and in DMEM', *Biomaterials*, 21(11), pp. 1087-94.
- Coleman, R. E. (2001) 'Metastatic bone disease: clinical features, pathophysiology and treatment strategies', *Cancer Treat Rev*, 27(3), pp. 165-76.
- Croes, M., Oner, F. C., van Neerven, D., Sabir, E., Kruyt, M. C., Blokhuis, T. J., Dhert, W. J. A. and Alblas, J. (2016) 'Proinflammatory T cells and IL-17 stimulate osteoblast differentiation', *Bone*, 84, pp. 262-270.
- Cunningham, D. and You, Z. (2015) 'In vitro and in vivo model systems used in prostate cancer research', *J Biol Methods*, 2(1).
- Cybulski, C., Huzarski, T., Gorski, B., Masojc, B., Mierzejewski, M., Debniak, T., Gliniewicz, B., Matyasik, J., Zlowocka, E., Kurzawski, G., Sikorski, A., Posmyk, M., Szwiec, M., Czajka, R., Narod, S. A. and Lubinski, J. (2004) 'A novel founder CHEK2 mutation is associated with increased prostate cancer risk', *Cancer Res*, 64(8), pp. 2677-9.
- De Marzo, A. M., Platz, E. A., Sutcliffe, S., Xu, J., Gronberg, H., Drake, C. G., Nakai, Y., Isaacs, W. B. and Nelson, W. G. (2007) 'Inflammation in prostate carcinogenesis', *Nat Rev Cancer*, 7(4), pp. 256-69.
- Ding, J., Ghali, O., Lencel, P., Broux, O., Chauveau, C., Devedjian, J. C., Hardouin, P. and Magne, D. (2009a) 'TNF-alpha and IL-1beta inhibit RUNX2 and collagen expression but increase alkaline phosphatase activity and mineralization in human mesenchymal stem cells', *Life Sci*, 84(15-16), pp. 499-504.
- Ding, Q., Mracek, T., Gonzalez-Muniesa, P., Kos, K., Wilding, J., Trayhurn, P. and Bing, C. (2009b) 'Identification of Macrophage Inhibitory Cytokine-1 in Adipose Tissue and Its Secretion as an Adipokine by Human Adipocytes', *Endocrinology*, 150(4), pp. 1688-1696.
- Doppler, H., Liou, G. Y. and Storz, P. (2013) 'Downregulation of TRAF2 mediates NIK-induced pancreatic cancer cell proliferation and tumorigenicity', *PLoS One*, 8(1), pp. e53676.
- Dougall, W. C. and Chaisson, M. (2006) 'The RANK/RANKL/OPG triad in cancer-induced bone diseases', *Cancer Metastasis Rev*, 25(4), pp. 541-9.
- DuBose, K. B., Zayzafoon, M. and Murphy-Ullrich, J. E. (2012) 'Thrombospondin-1 inhibits osteogenic differentiation of human mesenchymal stem cells through latent TGF-beta activation', *Biochemical and Biophysical Research Communications*, 422(3), pp. 488-493.
- Eeles, R., Goh, C., Castro, E., Bancroft, E., Guy, M., Al Olama, A. A., Easton, D. and Kote-Jarai, Z. (2014) 'The genetic epidemiology of prostate cancer and its clinical implications', *Nat Rev Urol*, 11(1), pp. 18-31.

REFERENCES

- Eliseev, R. A., Schwarz, E. M., Zuscik, M. J., O'Keefe, R. J., Drissi, H. and Rosier, R. N. (2006) 'Smad7 mediates inhibition of Saos2 osteosarcoma cell differentiation by NFkappaB', *Exp Cell Res*, 312(1), pp. 40-50.
- Erkko, H., Xia, B., Nikkila, J., Schleutker, J., Syrjakoski, K., Mannermaa, A., Kallioniemi, A., Pylkas, K., Karppinen, S. M., Rapakko, K., Miron, A., Sheng, Q., Li, G., Mattila, H., Bell, D. W., Haber, D. A., Grip, M., Reiman, M., Jukkola-Vuorinen, A., Mustonen, A., Kere, J., Aaltonen, L. A., Kosma, V. M., Kataja, V., Soini, Y., Drapkin, R. I., Livingston, D. M. and Winqvist, R. (2007) 'A recurrent mutation in PALB2 in Finnish cancer families', *Nature*, 446(7133), pp. 316-9.
- Ewing, C. M., Ray, A. M., Lange, E. M., Zuhlke, K. A., Robbins, C. M., Tembe, W. D., Wiley, K. E., Isaacs, S. D., Johng, D., Wang, Y., Bizon, C., Yan, G., Gielzak, M., Partin, A. W., Shanmugam, V., Izatt, T., Sinari, S., Craig, D. W., Zheng, S. L., Walsh, P. C., Montie, J. E., Xu, J., Carpten, J. D., Isaacs, W. B. and Cooney, K. A. (2012) 'Germline mutations in HOXB13 and prostate-cancer risk', *N Engl J Med*, 366(2), pp. 141-9.
- Favus, J. (2006) *Primer on the metabolic bone diseases and disorders of mineral metabolism*. 6th edn. Washington, DC: American Society for Bone and Mineral Research.
- Fernandez-Majada, V., Aguilera, C., Villanueva, A., Vilardell, F., Robert-Moreno, A., Aytes, A., Real, F. X., Capella, G., Mayo, M. W., Espinosa, L. and Bigas, A. (2007) 'Nuclear IKK activity leads to dysregulated notch-dependent gene expression in colorectal cancer', *Proc Natl Acad Sci U S A*, 104(1), pp. 276-81.
- Firlej, V., Mathieu, J. R. R., Gilbert, C., Lemonnier, L., Nakhle, J., Gallou-Kabani, C., Guarmit, B., Morin, A., Prevarskaya, N., Delongchamps, N. B. and Cabon, F. (2011) 'Thrombospondin-1 Triggers Cell Migration and Development of Advanced Prostate Tumors', *Cancer Research*, 71(24), pp. 7649-7658.
- Fradet, A., Sorel, H., Depalle, B., Serre, C. M., Farlay, D., Turtoi, A., Bellahcene, A., Follet, H., Castronovo, V., Clezardin, P. and Bonnelye, E. (2013) 'A new murine model of osteoblastic/osteolytic lesions from human androgen-resistant prostate cancer', *PLoS One*, 8(9), pp. e75092.
- Furlan, F., Galbiati, C., Jorgensen, N. R., Jensen, J. E., Mrak, E., Rubinacci, A., Talotta, F., Verde, P. and Blasi, F. (2007) 'Urokinase plasminogen activator receptor affects bone homeostasis by regulating osteoblast and osteoclast function', *J Bone Miner Res*, 22(9), pp. 1387-96.
- Furuya, K., Ozaki, T., Hanamoto, T., Hosoda, M., Hayashi, S., Barker, P. A., Takano, K., Matsumoto, M. and Nakagawara, A. (2007) 'Stabilization of p73 by nuclear IkkappaB kinase-alpha mediates cisplatin-induced apoptosis', *J Biol Chem*, 282(25), pp. 18365-78.
- Furuya, Y., Inagaki, A., Khan, M., Mori, K., Penninger, J. M., Nakamura, M., Udagawa, N., Aoki, K., Ohya, K., Uchida, K. and Yasuda, H. (2013) 'Stimulation of bone formation in cortical bone of mice treated with a receptor activator of nuclear factor-kappaB ligand (RANKL)-binding peptide that possesses osteoclastogenesis inhibitory activity', *J Biol Chem*, 288(8), pp. 5562-71.
- Furuya, Y., Nishio, R., Junicho, A., Nagakawa, O. and Fuse, H. (2005) 'Serum interleukin-11 in patients with benign prostatic hyperplasia and prostate cancer', *Int Urol Nephrol*, 37(1), pp. 69-71.
- Gallucci, M., Merola, R., Leonardo, C., De Carli, P., Farsetti, A., Sentinelli, S., Sperduti, I., Mottolese, M., Carlini, P., Vico, E., Simone, G. and Cianciulli, A. (2009) 'Genetic profile identification in clinically localized prostate carcinoma', *Urol Oncol*, 27(5), pp. 502-8.

REFERENCES

- Ganguly, S. S., Li, X. and Miranti, C. K. (2014) 'The host microenvironment influences prostate cancer invasion, systemic spread, bone colonization, and osteoblastic metastasis', *Front Oncol*, 4, pp. 364.
- Gasparian, A. V., Yao, Y. J., Kowalczyk, D., Lyakh, L. A., Karseladze, A., Slaga, T. J. and Budunova, I. V. (2002) 'The role of IKK in constitutive activation of NF-kappaB transcription factor in prostate carcinoma cells', *J Cell Sci*, 115(Pt 1), pp. 141-51.
- Gaur, T., Lengner, C. J., Hovhannisyanyan, H., Bhat, R. A., Bodine, P. V., Komm, B. S., Javed, A., van Wijnen, A. J., Stein, J. L., Stein, G. S. and Lian, J. B. (2005) 'Canonical WNT signaling promotes osteogenesis by directly stimulating Runx2 gene expression', *J Biol Chem*, 280(39), pp. 33132-40.
- Ghanem, A., Lu, Y. H., Cai, T. Y. and Mu, X. Z. (2017) 'Overexpression of RBP4 promotes proliferation, differentiation and mineralization of MC3T3-E1 (vol 10, pg 298, 2017)', *International Journal of Clinical and Experimental Pathology*, 10(7), pp. 8092-8092.
- Gil, J., Kerai, P., Lleonart, M., Bernard, D., Cigudosa, J. C., Peters, G., Carnero, A. and Beach, D. (2005) 'Immortalization of primary human prostate epithelial cells by c-Myc', *Cancer Res*, 65(6), pp. 2179-85.
- Gilbert, L. C., Rubin, J. and Nanes, M. S. (2005) 'The p55 TNF receptor mediates TNF inhibition of osteoblast differentiation independently of apoptosis', *Am J Physiol Endocrinol Metab*, 288(5), pp. E1011-8.
- Gilmore, T. D. (2006) 'Introduction to NF-kappaB: players, pathways, perspectives', *Oncogene*, 25(51), pp. 6680-4.
- Gloire, G., Horion, J., El Mjiyad, N., Bex, F., Chariot, A., Dejardin, E. and Piette, J. (2007) 'Promoter-dependent effect of IKKalpha on NF-kappaB/p65 DNA binding', *J Biol Chem*, 282(29), pp. 21308-18.
- Goto, T., Hagiwara, K., Shirai, N., Yoshida, K. and Hagiwara, H. (2015) 'Apigenin inhibits osteoblastogenesis and osteoclastogenesis and prevents bone loss in ovariectomized mice', *Cytotechnology*, 67(2), pp. 357-65.
- Graham, T. R., Agrawal, K. C. and Abdel-Mageed, A. B. (2010) 'Independent and cooperative roles of tumor necrosis factor-alpha, nuclear factor-kappaB, and bone morphogenetic protein-2 in regulation of metastasis and osteomimicry of prostate cancer cells and differentiation and mineralization of MC3T3-E1 osteoblast-like cells', *Cancer Sci*, 101(1), pp. 103-11.
- Gupta, A., Cao, W. and Chellaiah, M. A. (2012) 'Integrin alphavbeta3 and CD44 pathways in metastatic prostate cancer cells support osteoclastogenesis via a Runx2/Smad 5/receptor activator of NF-kappaB ligand signaling axis', *Mol Cancer*, 11, pp. 66.
- Gustafson, B. and Smith, U. (2006) 'Cytokines promote Wnt signaling and inflammation and impair the normal differentiation and lipid accumulation in 3T3-L1 preadipocytes', *J Biol Chem*, 281(14), pp. 9507-16.
- Haas, G. P., Delongchamps, N., Brawley, O. W., Wang, C. Y. and de la Roza, G. (2008) 'The worldwide epidemiology of prostate cancer: perspectives from autopsy studies', *Can J Urol*, 15(1), pp. 3866-71.
- Hacker, H. and Karin, M. (2006) 'Regulation and function of IKK and IKK-related kinases', *Sci STKE*, 2006(357), pp. re13.
- Hadjidakis, D. J. and Androulakis, II (2006) 'Bone remodeling', *Ann N Y Acad Sci*, 1092, pp. 385-96.
- Hall, C. L., Bafico, A., Dai, J., Aaronson, S. A. and Keller, E. T. (2005) 'Prostate cancer cells promote osteoblastic bone metastases through Wnts', *Cancer Res*, 65(17), pp. 7554-60.

REFERENCES

- Han, J. M., Wu, D., Denroche, H. C., Yao, Y., Verchere, C. B. and Levings, M. K. (2015) 'IL-33 Reverses an Obesity-Induced Deficit in Visceral Adipose Tissue ST2(+) T Regulatory Cells and Ameliorates Adipose Tissue Inflammation and Insulin Resistance', *Journal of Immunology*, 194(10), pp. 4777-4783.
- Hao, J., Chen, H., Madigan, M. C., Cozzi, P. J., Beretov, J., Xiao, W., Delprado, W. J., Russell, P. J. and Li, Y. (2010a) 'Co-expression of CD147 (EMMPRIN), CD44v3-10, MDR1 and monocarboxylate transporters is associated with prostate cancer drug resistance and progression', *Br J Cancer*, 103(7), pp. 1008-18.
- Hao, J. L., Cozzi, P. J., Khatri, A., Power, C. A. and Li, Y. (2010b) 'CD147/EMMPRIN and CD44 are Potential Therapeutic Targets for Metastatic Prostate Cancer', *Current Cancer Drug Targets*, 10(3), pp. 287-306.
- Hayden, M. S. and Ghosh, S. (2004) 'Signaling to NF-kappaB', *Genes Dev*, 18(18), pp. 2195-224.
- Hebbring, S. J., Fredriksson, H., White, K. A., Maier, C., Ewing, C., McDonnell, S. K., Jacobsen, S. J., Cerhan, J., Schaid, D. J., Ikonen, T., Autio, V., Tammela, T. L., Herkommer, K., Paiss, T., Vogel, W., Gielzak, M., Sauvageot, J., Schleutker, J., Cooney, K. A., Isaacs, W. and Thibodeau, S. N. (2006) 'Role of the Nijmegen breakage syndrome 1 gene in familial and sporadic prostate cancer', *Cancer Epidemiol Biomarkers Prev*, 15(5), pp. 935-8.
- Heiland, G. R., Zwerina, K., Baum, W., Kireva, T., Distler, J. H., Grisanti, M., Asuncion, F., Li, X., Ominsky, M., Richards, W., Schett, G. and Zwerina, J. (2010) 'Neutralisation of Dkk-1 protects from systemic bone loss during inflammation and reduces sclerostin expression', *Ann Rheum Dis*, 69(12), pp. 2152-9.
- Helsley, R. N., Sui, Y., Park, S. H., Liu, Z., Lee, R. G., Zhu, B., Kern, P. A. and Zhou, C. (2016) 'Targeting IkappaB kinase beta in Adipocyte Lineage Cells for Treatment of Obesity and Metabolic Dysfunctions', *Stem Cells*, 34(7), pp. 1883-95.
- Hensley, P. J. and Kyprianou, N. (2012) 'Modeling prostate cancer in mice: limitations and opportunities', *J Androl*, 33(2), pp. 133-44.
- Hill, P. A. (1998) 'Bone remodelling', *Br J Orthod*, 25(2), pp. 101-7.
- Hirata, Y., Maeda, S., Ohmae, T., Shibata, W., Yanai, A., Ogura, K., Yoshida, H., Kawabe, T. and Omata, M. (2006) 'Helicobacter pylori induces IkappaB kinase alpha nuclear translocation and chemokine production in gastric epithelial cells', *Infect Immun*, 74(3), pp. 1452-61.
- Hogstrom, M., Nordstrom, A. and Nordstrom, P. (2008) 'Retinol, retinol-binding protein 4, abdominal fat mass, peak bone mineral density, and markers of bone metabolism in men: the Northern Osteoporosis and Obesity (NO2) Study', *Eur J Endocrinol*, 158(5), pp. 765-70.
- Holen, I., Croucher, P. I., Hamdy, F. C. and Eaton, C. L. (2002) 'Osteoprotegerin (OPG) is a survival factor for human prostate cancer cells', *Cancer Res*, 62(6), pp. 1619-23.
- Hsu, Y. L., Hou, M. F., Kuo, P. L., Huang, Y. F. and Tsai, E. M. (2013) 'Breast tumor-associated osteoblast-derived CXCL5 increases cancer progression by ERK/MSK1/Elk-1/snail signaling pathway', *Oncogene*, 32(37), pp. 4436-47.
- Hu, Y., Baud, V., Delhase, M., Zhang, P., Deerinck, T., Ellisman, M., Johnson, R. and Karin, M. (1999) 'Abnormal morphogenesis but intact IKK activation in mice lacking the IKKalpha subunit of IkappaB kinase', *Science*, 284(5412), pp. 316-20.
- Hu, Y., Baud, V., Oga, T., Kim, K. I., Yoshida, K. and Karin, M. (2001) 'IKKalpha controls formation of the epidermis independently of NF-kappaB', *Nature*, 410(6829), pp. 710-4.

REFERENCES

- Huang, S., Pettaway, C. A., Uehara, H., Bucana, C. D. and Fidler, I. J. (2001) 'Blockade of NF-kappaB activity in human prostate cancer cells is associated with suppression of angiogenesis, invasion, and metastasis', *Oncogene*, 20(31), pp. 4188-97.
- Huang, W., Carlsen, B., Rudkin, G., Berry, M., Ishida, K., Yamaguchi, D. T. and Miller, T. A. (2004) 'Osteopontin is a negative regulator of proliferation and differentiation in MC3T3-E1 pre-osteoblastic cells', *Bone*, 34(5), pp. 799-808.
- Huang, W. C., Chen, W. S., Chen, Y. J., Wang, L. Y., Hsu, S. C., Chen, C. C. and Hung, M. C. (2012) 'Hepatitis B virus X protein induces IKKalpha nuclear translocation via Akt-dependent phosphorylation to promote the motility of hepatocarcinoma cells', *J Cell Physiol*, 227(4), pp. 1446-54.
- Huang, W. C. and Hung, M. C. (2013) 'Beyond NF-kappaB activation: nuclear functions of IkappaB kinase alpha', *J Biomed Sci*, 20, pp. 3.
- Huang, W. C., Ju, T. K., Hung, M. C. and Chen, C. C. (2007) 'Phosphorylation of CBP by IKKalpha promotes cell growth by switching the binding preference of CBP from p53 to NF-kappaB', *Mol Cell*, 26(1), pp. 75-87.
- Huh, J. Y., Park, Y. J., Ham, M. and Kim, J. B. (2014) 'Crosstalk between Adipocytes and Immune Cells in Adipose Tissue Inflammation and Metabolic Dysregulation in Obesity', *Molecules and Cells*, 37(5), pp. 365-371.
- Husaini, Y., Lockwood, G. P., Nguyen, T. V., Tsai, V. W. W., Mohammad, M. G., Russell, P. J., Brown, D. A. and Breit, S. N. (2015) 'Macrophage Inhibitory Cytokine-1 (MIC-1/GDF15) Gene Deletion Promotes Cancer Growth in TRAMP Prostate Cancer Prone Mice', *Plos One*, 10(2).
- Ibrahim, T., Flamini, E., Mercatali, L., Sacanna, E., Serra, P. and Amadori, D. (2010) 'Pathogenesis of osteoblastic bone metastases from prostate cancer', *Cancer*, 116(6), pp. 1406-18.
- Ide, H., Hatake, K., Terado, Y., Tsukino, H., Okegawa, T., Nutahara, K., Higashihara, E. and Horie, S. (2008) 'Serum level of macrophage colony-stimulating factor is increased in prostate cancer patients with bone metastasis', *Hum Cell*, 21(1), pp. 1-6.
- Ide, H., Yoshida, T., Matsumoto, N., Aoki, K., Osada, Y., Sugimura, T. and Terada, M. (1997) 'Growth regulation of human prostate cancer cells by bone morphogenetic protein-2', *Cancer Res*, 57(22), pp. 5022-7.
- Idris, A. I. (2012) 'Analysis of signalling pathways by western blotting and immunoprecipitation', *Methods Mol Biol*, 816, pp. 223-32.
- Idris, A. I., Krishnan, M., Simic, P., Landao-Bassonga, E., Mollat, P., Vukicevic, S. and Ralston, S. H. (2010) 'Small molecule inhibitors of IkappaB kinase signaling inhibit osteoclast formation in vitro and prevent ovariectomy-induced bone loss in vivo', *FASEB J*, 24(11), pp. 4545-55.
- Idris, A. I., Libouban, H., Nyangoga, H., Landao-Bassonga, E., Chappard, D. and Ralston, S. H. (2009) 'Pharmacologic inhibitors of IkappaB kinase suppress growth and migration of mammary carcinosarcoma cells in vitro and prevent osteolytic bone metastasis in vivo', *Mol Cancer Ther*, 8(8), pp. 2339-47.
- Ignatius, A., Schoengraf, P., Kreja, L., Liedert, A., Recknagel, S., Kandert, S., Brenner, R. E., Schneider, M., Lambris, J. D. and Huber-Lang, M. (2011) 'Complement C3a and C5a modulate osteoclast formation and inflammatory response of osteoblasts in synergism with IL-1beta', *J Cell Biochem*, 112(9), pp. 2594-605.
- Iotsova, V., Caamano, J., Loy, J., Yang, Y., Lewin, A. and Bravo, R. (1997) 'Osteopetrosis in mice lacking NF-kappaB1 and NF-kappaB2', *Nat Med*, 3(11), pp. 1285-9.

REFERENCES

- Ismail, H., Lessard, L., Mes-Masson, A. M. and Saad, F. (2004) 'Expression of NF-kappa B in prostate cancer lymph node metastases', *Prostate*, 58(3), pp. 308-313.
- Ittmann, M., Huang, J., Radaelli, E., Martin, P., Signoretti, S., Sullivan, R., Simons, B. W., Ward, J. M., Robinson, B. D., Chu, G. C., Loda, M., Thomas, G., Borowsky, A. and Cardiff, R. D. (2013) 'Animal models of human prostate cancer: the consensus report of the New York meeting of the Mouse Models of Human Cancers Consortium Prostate Pathology Committee', *Cancer Res*, 73(9), pp. 2718-36.
- Jaipal, A., Pandey, M. M., Charde, S. Y., Raut, P. P., Prasanth, K. V. and Prasad, R. G. (2015) 'Effect of HPMC and mannitol on drug release and bioadhesion behavior of buccal discs of bupirone hydrochloride: In-vitro and in-vivo pharmacokinetic studies', *Saudi Pharm J*, 23(3), pp. 315-26.
- Janssens, K., ten Dijke, P., Ralston, S. H., Bergmann, C. and Van Hul, W. (2003) 'Transforming growth factor-beta 1 mutations in Camurati-Engelmann disease lead to increased signaling by altering either activation or secretion of the mutant protein', *J Biol Chem*, 278(9), pp. 7718-24.
- Jemal, A., Siegel, R., Ward, E., Hao, Y., Xu, J., Murray, T. and Thun, M. J. (2008) 'Cancer statistics, 2008', *CA Cancer J Clin*, 58(2), pp. 71-96.
- Jenkins, R. B., Qian, J., Lieber, M. M. and Bostwick, D. G. (1997) 'Detection of c-myc oncogene amplification and chromosomal anomalies in metastatic prostatic carcinoma by fluorescence in situ hybridization', *Cancer Res*, 57(3), pp. 524-31.
- Jiang, R., Xia, Y., Li, J., Deng, L., Zhao, L., Shi, J., Wang, X. and Sun, B. (2010) 'High expression levels of IKKalpha and IKKbeta are necessary for the malignant properties of liver cancer', *Int J Cancer*, 126(5), pp. 1263-74.
- Jiang, X., Takahashi, N., Ando, K., Otsuka, T., Tetsuka, T. and Okamoto, T. (2003) 'NF-kappa B p65 transactivation domain is involved in the NF-kappa B-inducing kinase pathway', *Biochem Biophys Res Commun*, 301(2), pp. 583-90.
- Jilka, R. L. (1998) 'Cytokines, bone remodeling, and estrogen deficiency: a 1998 update', *Bone*, 23(2), pp. 75-81.
- Jin, R., Sterling, J. A., Edwards, J. R., DeGraff, D. J., Lee, C., Park, S. I. and Matusik, R. J. (2013) 'Activation of NF-kappa B signaling promotes growth of prostate cancer cells in bone', *PLoS One*, 8(4), pp. e60983.
- Jones, D. H., Kong, Y. Y. and Penninger, J. M. (2002) 'Role of RANKL and RANK in bone loss and arthritis', *Ann Rheum Dis*, 61 Suppl 2, pp. ii32-9.
- Jones, D. H., Nakashima, T., Sanchez, O. H., Koziarzki, I., Komarova, S. V., Sarosi, I., Morony, S., Rubin, E., Sarao, R., Hojilla, C. V., Komnenovic, V., Kong, Y. Y., Schreiber, M., Dixon, S. J., Sims, S. M., Khokha, R., Wada, T. and Penninger, J. M. (2006) 'Regulation of cancer cell migration and bone metastasis by RANKL', *Nature*, 440(7084), pp. 692-6.
- Kabir, S. M., Lee, E. S. and Son, D. S. (2014) 'Chemokine network during adipogenesis in 3T3-L1 cells: Differential response between growth and proinflammatory factor in preadipocytes vs. adipocytes', *Adipocyte*, 3(2), pp. 97-106.
- Kanda, H., Tateya, S., Tamori, Y., Kotani, K., Hiasa, K., Kitazawa, R., Kitazawa, S., Miyachi, H., Maeda, S., Egashira, K. and Kasuga, M. (2006) 'MCP-1 contributes to macrophage infiltration into adipose tissue, insulin resistance, and hepatic steatosis in obesity', *J Clin Invest*, 116(6), pp. 1494-505.
- Kanno, Y., Matsuno, H., Kawashita, E., Okada, K., Suga, H., Ueshima, S. and Matsuo, O. (2010) 'Urokinase-type plasminogen activator receptor is associated with the development of adipose tissue', *Thrombosis and Haemostasis*, 104(6), pp. 1124-1132.

REFERENCES

- Karin, M. and Ben-Neriah, Y. (2000) 'Phosphorylation meets ubiquitination: the control of NF- κ B activity', *Annu Rev Immunol*, 18, pp. 621-63.
- Karsenty, G. and Wagner, E. F. (2002) 'Reaching a genetic and molecular understanding of skeletal development', *Dev Cell*, 2(4), pp. 389-406.
- Katagiri, T. and Takahashi, N. (2002) 'Regulatory mechanisms of osteoblast and osteoclast differentiation', *Oral Dis*, 8(3), pp. 147-59.
- Kavitha, C. V., Deep, G., Gangar, S. C., Jain, A. K., Agarwal, C. and Agarwal, R. (2014) 'Silibinin inhibits prostate cancer cells- and RANKL-induced osteoclastogenesis by targeting NFATc1, NF- κ B, and AP-1 activation in RAW264.7 cells', *Mol Carcinog*, 53(3), pp. 169-80.
- Keller, D. C., Du, X. X., Srour, E. F., Hoffman, R. and Williams, D. A. (1993) 'Interleukin-11 Inhibits Adipogenesis and Stimulates Myelopoiesis in Human Long-Term Marrow Cultures', *Blood*, 82(5), pp. 1428-1435.
- Keller, E. T. and Brown, J. (2004) 'Prostate cancer bone metastases promote both osteolytic and osteoblastic activity', *J Cell Biochem*, 91(4), pp. 718-29.
- Khandelwal, K. D., Ockeloen, C. W., Venselaar, H., Boulanger, C., Brichard, B., Sokal, E., Pfundt, R., Rinne, T., van Beusekom, E., Bloemen, M., Vriend, G., Revencu, N., Carels, C. E. L., van Bokhoven, H. and Zhou, H. (2017) 'Identification of a de novo variant in CHUK in a patient with an EEC/AEC syndrome-like phenotype and hypogammaglobulinemia', *Am J Med Genet A*.
- Kim, H. J., Yoon, H. J., Yoon, K. A., Gwon, M. R., Jin Seong, S., Suk, K., Kim, S. Y. and Yoon, Y. R. (2015) 'Lipocalin-2 inhibits osteoclast formation by suppressing the proliferation and differentiation of osteoclast lineage cells', *Exp Cell Res*, 334(2), pp. 301-9.
- Kim, S. W., Kim, J. S., Papadopoulos, J., Choi, H. J., He, J., Maya, M., Langley, R. R., Fan, D., Fidler, I. J. and Kim, S. J. (2011) 'Consistent interactions between tumor cell IL-6 and macrophage TNF- α enhance the growth of human prostate cancer cells in the bone of nude mouse', *Int Immunopharmacol*, 11(7), pp. 862-72.
- Kingsley, L. A., Fournier, P. G., Chirgwin, J. M. and Guise, T. A. (2007) 'Molecular biology of bone metastasis', *Mol Cancer Ther*, 6(10), pp. 2609-17.
- Kiper, P. O. S., Saito, H., Gori, F., Unger, S., Hesse, E., Yamana, K., Kiviranta, R., Solban, N., Liu, J., Brommage, R., Boduroglu, K., Bonafe, L., Campos-Xavier, B., Dikoglu, E., Eastell, R., Gossiel, F., Harshman, K., Nishimura, G., Girisha, K. M., Stevenson, B. J., Takita, H., Rivolta, C., Superti-Furga, A. and Baron, R. (2016) 'Cortical-Bone Fragility - Insights from sFRP4 Deficiency in Pyle's Disease', *New England Journal of Medicine*, 374(26), pp. 2553-2562.
- Kitajima, I., Soejima, Y., Takasaki, I., Beppu, H., Tokioka, T. and Maruyama, I. (1996) 'Ceramide-induced nuclear translocation of NF- κ B is a potential mediator of the apoptotic response to TNF- α in murine clonal osteoblasts', *Bone*, 19(3), pp. 263-70.
- Kitami, S., Tanaka, H., Kawato, T., Tanabe, N., Katono-Tani, T., Zhang, F., Suzuki, N., Yonehara, Y. and Maeno, M. (2010) 'IL-17A suppresses the expression of bone resorption-related proteinases and osteoclast differentiation via IL-17RA or IL-17RC receptors in RAW264.7 cells', *Biochimie*, 92(4), pp. 398-404.
- Kobashi, C., Asamizu, S., Ishiki, M., Iwata, M., Usui, I., Yamazaki, K., Tobe, K., Kobayashi, M. and Urakaze, M. (2009) 'Inhibitory effect of IL-8 on insulin action in human adipocytes via MAP kinase pathway', *Journal of Inflammation-London*, 6.
- Kote-Jarai, Z., Jugurnauth, S., Mulholland, S., Leongamornlert, D. A., Guy, M., Edwards, S., Tymrakiewicz, M., O'Brien, L., Hall, A., Wilkinson, R., Al Olama, A. A., Morrison, J.,

REFERENCES

- Muir, K., Neal, D., Donovan, J., Hamdy, F., Easton, D. F., Eeles, R., Collaborators, U. and British Association of Urological Surgeons' Section of, O. (2009) 'A recurrent truncating germline mutation in the BRIP1/FANCI gene and susceptibility to prostate cancer', *Br J Cancer*, 100(2), pp. 426-30.
- Kote-Jarai, Z., Leongamornlert, D., Saunders, E., Tymrakiewicz, M., Castro, E., Mahmud, N., Guy, M., Edwards, S., O'Brien, L., Sawyer, E., Hall, A., Wilkinson, R., Dadaev, T., Goh, C., Easton, D., Collaborators, U., Goldgar, D. and Eeles, R. (2011) 'BRCA2 is a moderate penetrance gene contributing to young-onset prostate cancer: implications for genetic testing in prostate cancer patients', *Br J Cancer*, 105(8), pp. 1230-4.
- Kragstrup, T. W., Andersen, M. N., Schiottz-Christensen, B., Jurik, A. G., Hvid, M. and Deleuran, B. (2017) 'Increased interleukin (IL)-20 and IL-24 target osteoblasts and synovial monocytes in spondyloarthritis', *Clin Exp Immunol*, 189(3), pp. 342-351.
- Kragstrup, T. W., Greisen, S. R., Nielsen, M. A., Rhodes, C., Stengaard-Pedersen, K., Hetland, M. L., Horslev-Petersen, K., Junker, P., Ostergaard, M., Hvid, M., Vorup-Jensen, T., Robinson, W. H., Sokolove, J. and Deleuran, B. (2016) 'The interleukin-20 receptor axis in early rheumatoid arthritis: novel links between disease-associated autoantibodies and radiographic progression', *Arthritis Res Ther*, 18, pp. 61.
- Krane, S. M. and Inada, M. (2008) 'Matrix metalloproteinases and bone', *Bone*, 43(1), pp. 7-18.
- Krishnan, V., Bryant, H. U. and Macdougald, O. A. (2006) 'Regulation of bone mass by Wnt signaling', *J Clin Invest*, 116(5), pp. 1202-9.
- Kudo, O., Sabokbar, A., Pocock, A., Itonaga, I., Fujikawa, Y. and Athanasou, N. A. (2003) 'Interleukin-6 and interleukin-11 support human osteoclast formation by a RANKL-independent mechanism', *Bone*, 32(1), pp. 1-7.
- Kukreja, P., Abdel-Mageed, A. B., Mondal, D., Liu, K. and Agrawal, K. C. (2005) 'Up-regulation of CXCR4 expression in PC-3 cells by stromal-derived factor-1alpha (CXCL12) increases endothelial adhesion and transendothelial migration: role of MEK/ERK signaling pathway-dependent NF-kappaB activation', *Cancer Res*, 65(21), pp. 9891-8.
- Lahtela, J., Nousiainen, H. O., Stefanovic, V., Tallila, J., Viskari, H., Karikoski, R., Gentile, M., Saloranta, C., Varilo, T., Salonen, R. and Kestila, M. (2010) 'Mutant CHUK and severe fetal encasement malformation', *N Engl J Med*, 363(17), pp. 1631-7.
- Lamberti, C., Lin, K. M., Yamamoto, Y., Verma, U., Verma, I. M., Byers, S. and Gaynor, R. B. (2001) 'Regulation of beta-catenin function by the IkappaB kinases', *J Biol Chem*, 276(45), pp. 42276-86.
- Langenbach, F. and Handschel, J. (2013) 'Effects of dexamethasone, ascorbic acid and beta-glycerophosphate on the osteogenic differentiation of stem cells in vitro', *Stem Cell Res Ther*, 4(5), pp. 117.
- Lardizabal, J., Ding, J., Delwar, Z., Rennie, P. S. and Jia, W. (2018) 'A TRAMP-derived orthotopic prostate syngeneic (TOPS) cancer model for investigating anti-tumor treatments', *Prostate*, 78(6), pp. 457-468.
- Laurent, V., Guerard, A., Mazerolles, C., Le Gonidec, S., Toulet, A., Nieto, L., Zaidi, F., Majed, B., Garandeau, D., Socrier, Y., Golzio, M., Cadoudal, T., Chaoui, K., Dray, C., Monsarrat, B., Schiltz, O., Wang, Y. Y., Couderc, B., Valet, P., Malavaud, B. and Muller, C. (2016) 'Periprostatic adipocytes act as a driving force for prostate cancer progression in obesity', *Nat Commun*, 7, pp. 10230.

REFERENCES

- Lawrence, T., Bebien, M., Liu, G. Y., Nizet, V. and Karin, M. (2005) 'IKK α limits macrophage NF- κ B activation and contributes to the resolution of inflammation', *Nature*, 434(7037), pp. 1138-43.
- Le Henaff, C., Mansouri, R., Modrowski, D., Zarka, M., Geoffroy, V., Marty, C., Tarantino, N., Laplantine, E. and Marie, P. J. (2015) 'Increased NF- κ B Activity and Decreased Wnt/ β -Catenin Signaling Mediate Reduced Osteoblast Differentiation and Function in DeltaF508 Cystic Fibrosis Transmembrane Conductance Regulator (CFTR) Mice', *J Biol Chem*, 290(29), pp. 18009-17.
- Lecka-Czernik, B., Gubrij, I., Moerman, E. J., Kajkenova, O., Lipschitz, D. A., Manolagas, S. C. and Jilka, R. L. (1999) 'Inhibition of Osf2/Cbfa1 expression and terminal osteoblast differentiation by PPAR γ 2', *J Cell Biochem*, 74(3), pp. 357-71.
- Lee, B., Kim, T. H., Jun, J. B., Yoo, D. H., Woo, J. H., Choi, S. J., Lee, Y. H., Song, G. G., Sohn, J., Park-Min, K. H., Ivashkiv, L. B. and Ji, J. D. (2010) 'Direct inhibition of human RANK+ osteoclast precursors identifies a homeostatic function of IL-1 β ', *J Immunol*, 185(10), pp. 5926-34.
- Lee, D. F. and Hung, M. C. (2008) 'Advances in targeting IKK and IKK-related kinases for cancer therapy', *Clin Cancer Res*, 14(18), pp. 5656-62.
- Lee, J., Park, C., Kim, H. J., Lee, Y. D., Lee, Z. H., Song, Y. W. and Kim, H. H. (2017) 'Stimulation of osteoclast migration and bone resorption by C-C chemokine ligands 19 and 21', *Experimental and Molecular Medicine*, 49.
- Lee, K. M., Kang, H. A., Park, M., Lee, H. Y., Choi, H. R., Yun, C. H., Oh, J. W. and Kang, H. S. (2012) 'Interleukin-24 attenuates β -glycerophosphate-induced calcification of vascular smooth muscle cells by inhibiting apoptosis, the expression of calcification and osteoblastic markers, and the Wnt/ β -catenin pathway', *Biochem Biophys Res Commun*, 428(1), pp. 50-5.
- Leibbrandt, A. and Penninger, J. M. (2008) 'RANK/RANKL: regulators of immune responses and bone physiology', *Ann N Y Acad Sci*, 1143, pp. 123-50.
- Leitch, V. D., Dwivedi, P. P., Anderson, P. J. and Powell, B. C. (2013) 'Retinol-binding protein 4 downregulation during osteogenesis and its localization to non-endocytic vesicles in human cranial suture mesenchymal cells suggest a novel tissue function', *Histochem Cell Biol*, 139(1), pp. 75-87.
- Leongamornlert, D., Mahmud, N., Tymrakiewicz, M., Saunders, E., Dadaev, T., Castro, E., Goh, C., Govindasami, K., Guy, M., O'Brien, L., Sawyer, E., Hall, A., Wilkinson, R., Easton, D., Collaborators, U., Goldgar, D., Eeles, R. and Kote-Jarai, Z. (2012) 'Germline BRCA1 mutations increase prostate cancer risk', *Br J Cancer*, 106(10), pp. 1697-701.
- Leopizzi, M., Cocchiola, R., Milanetti, E., Raimondo, D., Politi, L., Giordano, C., Scandurra, R. and Scotto d'Abusco, A. (2017) 'IKK α inhibition by a glucosamine derivative enhances Maspin expression in osteosarcoma cell line', *Chem Biol Interact*, 262, pp. 19-28.
- Lerner, U. H. (2006) 'Bone remodeling in post-menopausal osteoporosis', *J Dent Res*, 85(7), pp. 584-95.
- Lessard, L., Karakievicz, P. I., Bellon-Gagnon, P., Alam-Fahmy, M., Ismail, H. A., Mes-Masson, A. M. and Saad, F. (2006) 'Nuclear localization of nuclear factor- κ B p65 in primary prostate tumors is highly predictive of pelvic lymph node metastases', *Clinical Cancer Research*, 12(19), pp. 5741-5745.
- Li, Q., Lu, Q., Hwang, J. Y., Buscher, D., Lee, K. F., Izpisua-Belmonte, J. C. and Verma, I. M. (1999a) 'IKK1-deficient mice exhibit abnormal development of skin and skeleton', *Genes Dev*, 13(10), pp. 1322-8.

REFERENCES

- Li, Q., Van Antwerp, D., Mercurio, F., Lee, K. F. and Verma, I. M. (1999b) 'Severe liver degeneration in mice lacking the IkappaB kinase 2 gene', *Science*, 284(5412), pp. 321-5.
- Li, S., Ibaragi, S. and Hu, G. F. (2011) 'Angiogenin as a molecular target for the treatment of prostate cancer', *Curr Cancer Ther Rev*, 7(2), pp. 83-90.
- Li, X., Qin, L., Bergenstock, M., Bevelock, L. M., Novack, D. V. and Partridge, N. C. (2007a) 'Parathyroid hormone stimulates osteoblastic expression of MCP-1 to recruit and increase the fusion of pre/osteoclasts', *J Biol Chem*, 282(45), pp. 33098-106.
- Li, Y., Li, A., Strait, K., Zhang, H., Nanes, M. S. and Weitzmann, M. N. (2007b) 'Endogenous TNFalpha lowers maximum peak bone mass and inhibits osteoblastic Smad activation through NF-kappaB', *J Bone Miner Res*, 22(5), pp. 646-55.
- Li, Z. W., Chu, W., Hu, Y., Delhase, M., Deerinck, T., Ellisman, M., Johnson, R. and Karin, M. (1999c) 'The IKKbeta subunit of IkappaB kinase (IKK) is essential for nuclear factor kappaB activation and prevention of apoptosis', *J Exp Med*, 189(11), pp. 1839-45.
- Liao, C. G., Kong, L. M., Song, F., Xing, J. L., Wang, L. X., Sun, Z. J., Tang, H., Yao, H., Zhang, Y., Wang, L., Wang, Y., Yang, X. M., Li, Y. and Chen, Z. N. (2011) 'Characterization of basigin isoforms and the inhibitory function of basigin-3 in human hepatocellular carcinoma proliferation and invasion', *Mol Cell Biol*, 31(13), pp. 2591-604.
- Liao, J., Li, X., Koh, A. J., Berry, J. E., Thudi, N., Rosol, T. J., Pienta, K. J. and McCauley, L. K. (2008) 'Tumor expressed PTHrP facilitates prostate cancer-induced osteoblastic lesions', *Int J Cancer*, 123(10), pp. 2267-78.
- Liou, G. Y., Doppler, H., Necela, B., Krishna, M., Crawford, H. C., Raimondo, M. and Storz, P. (2013) 'Macrophage-secreted cytokines drive pancreatic acinar-to-ductal metaplasia through NF-kappaB and MMPs', *J Cell Biol*, 202(3), pp. 563-77.
- Liu, M., Lee, D. F., Chen, C. T., Yen, C. J., Li, L. Y., Lee, H. J., Chang, C. J., Chang, W. C., Hsu, J. M., Kuo, H. P., Xia, W., Wei, Y., Chiu, P. C., Chou, C. K., Du, Y., Dhar, D., Karin, M., Chen, C. H. and Hung, M. C. (2012) 'IKKalpha activation of NOTCH links tumorigenesis via FOXA2 suppression', *Mol Cell*, 45(2), pp. 171-84.
- Liu, X. H., Wiley, H. S. and Meikle, A. W. (1993) 'Androgens regulate proliferation of human prostate cancer cells in culture by increasing transforming growth factor-alpha (TGF-alpha) and epidermal growth factor (EGF)/TGF-alpha receptor', *J Clin Endocrinol Metab*, 77(6), pp. 1472-8.
- Llona-Minguez, S., Baiget, J. and Mackay, S. P. (2013) 'Small-molecule inhibitors of IkappaB kinase (IKK) and IKK-related kinases', *Pharm Pat Anal*, 2(4), pp. 481-98.
- Logothetis, C. J. and Lin, S. H. (2005) 'Osteoblasts in prostate cancer metastasis to bone', *Nat Rev Cancer*, 5(1), pp. 21-8.
- Lu, Q., Lv, G., Kim, A., Ha, J. M. and Kim, S. (2013) 'Expression and clinical significance of extracellular matrix metalloproteinase inducer, EMMPRIN/CD147, in human osteosarcoma', *Oncology Letters*, 5(1), pp. 201-207.
- Lu, X., Gilbert, L., He, X., Rubin, J. and Nanes, M. S. (2006a) 'Transcriptional regulation of the osterix (Ox, Sp7) promoter by tumor necrosis factor identifies disparate effects of mitogen-activated protein kinase and NF kappa B pathways', *J Biol Chem*, 281(10), pp. 6297-306.
- Lu, Y., Cai, Z., Galson, D. L., Xiao, G. Z., Liu, Y. L., George, D. E., Melhem, M. F., Yao, Z. and Zhang, J. (2006b) 'Monocyte chemotactic protein-1 (MCP-1) acts as a paracrine and autocrine factor for prostate cancer growth and invasion', *Prostate*, 66(12), pp. 1311-1318.

REFERENCES

- Lu, Y., Chen, Q., Corey, E., Xie, W., Fan, J., Mizokami, A. and Zhang, J. (2009) 'Activation of MCP-1/CCR2 axis promotes prostate cancer growth in bone', *Clin Exp Metastasis*, 26(2), pp. 161-9.
- Lu, Y., Xiao, G., Galson, D. L., Nishio, Y., Mizokami, A., Keller, E. T., Yao, Z. and Zhang, J. (2007) 'PTHrP-induced MCP-1 production by human bone marrow endothelial cells and osteoblasts promotes osteoclast differentiation and prostate cancer cell proliferation and invasion in vitro', *Int J Cancer*, 121(4), pp. 724-33.
- Lubin, F. D. and Sweatt, J. D. (2007) 'The I κ B kinase regulates chromatin structure during reconsolidation of conditioned fear memories', *Neuron*, 55(6), pp. 942-57.
- Luo, J. L., Tan, W., Ricono, J. M., Korchynski, O., Zhang, M., Gonias, S. L., Cheresch, D. A. and Karin, M. (2007) 'Nuclear cytokine-activated IKK α controls prostate cancer metastasis by repressing Maspin', *Nature*, 446(7136), pp. 690-4.
- Ma, B. and Hottiger, M. O. (2016) 'Crosstalk between wnt/beta-Catenin and NF-kappa B Signaling Pathway during Inflammation', *Frontiers in Immunology*, 7.
- Maeda, S., Hayashi, M., Komiya, S., Imamura, T. and Miyazono, K. (2004) 'Endogenous TGF-beta signaling suppresses maturation of osteoblastic mesenchymal cells', *EMBO J*, 23(3), pp. 552-63.
- Mahato, R., Qin, B. and Cheng, K. (2011) 'Blocking IKK α expression inhibits prostate cancer invasiveness', *Pharm Res*, 28(6), pp. 1357-69.
- Manna, S., Singha, B., Phyo, S. A., Gatla, H. R., Chang, T. P., Sanacora, S., Ramaswami, S. and Vancurova, I. (2013) 'Proteasome inhibition by bortezomib increases IL-8 expression in androgen-independent prostate cancer cells: the role of IKK α ', *J Immunol*, 191(5), pp. 2837-46.
- Margheri, F., D'Alessio, S., Serrati, S., Pucci, M., Annunziato, F., Cosmi, L., Liotta, F., Angeli, R., Angelucci, A., Gravina, G. L., Rucci, N., Bologna, M., Teti, A., Monia, B., Fibbi, G. and Del Rosso, M. (2005) 'Effects of blocking urokinase receptor signaling by antisense oligonucleotides in a mouse model of experimental prostate cancer bone metastases', *Gene Ther*, 12(8), pp. 702-14.
- Marinari, B., Moretti, F., Botti, E., Giustizieri, M. L., Descargues, P., Giunta, A., Stolfi, C., Ballaro, C., Papoutsaki, M., Alema, S., Monteleone, G., Chimenti, S., Karin, M. and Costanzo, A. (2008) 'The tumor suppressor activity of IKK α in stratified epithelia is exerted in part via the TGF-beta antiproliferative pathway', *Proc Natl Acad Sci U S A*, 105(44), pp. 17091-6.
- Marino, S., Bishop, R. T., Logan, J. G., Mollat, P. and Idris, A. I. (2017) 'Pharmacological evidence for the bone-autonomous contribution of the NF κ B/beta-catenin axis to breast cancer related osteolysis', *Cancer Lett*, 410, pp. 180-190.
- Marino, S., Bishop, R. T., Mollat, P. and Idris, A. I. (2018) 'Pharmacological Inhibition of the Skeletal IKK β Reduces Breast Cancer-Induced Osteolysis', *Calcif Tissue Int*.
- Marino, S., Logan, J. G., Mellis, D. and Capulli, M. (2014) 'Generation and culture of osteoclasts', *Bonekey Rep*, 3, pp. 570.
- Martin-Millan, M., Almeida, M., Ambrogini, E., Han, L., Zhao, H., Weinstein, R. S., Jilka, R. L., O'Brien, C. A. and Manolagas, S. C. (2010) 'The estrogen receptor-alpha in osteoclasts mediates the protective effects of estrogens on cancellous but not cortical bone', *Mol Endocrinol*, 24(2), pp. 323-34.
- Marugame, T. and Katanoda, K. (2006) 'International comparisons of cumulative risk of breast and prostate cancer, from cancer incidence in five continents Vol. VIII', *Jpn J Clin Oncol*, 36(6), pp. 399-400.

REFERENCES

- Mathes, E., O'Dea, E. L., Hoffmann, A. and Ghosh, G. (2008) 'NF-kappaB dictates the degradation pathway of I kappa B alpha', *EMBO J*, 27(9), pp. 1357-67.
- Matsumoto, T., Kuriwaka-Kido, R., Kondo, T., Endo, I. and Kido, S. (2012) 'Regulation of osteoblast differentiation by interleukin-11 via AP-1 and Smad signaling', *Endocrine Journal*, 59(2), pp. 91-101.
- McCall, P., Bennett, L., Ahmad, I., Mackenzie, L. M., Forbes, I. W., Leung, H. Y., Sansom, O. J., Orange, C., Seywright, M., Underwood, M. A. and Edwards, J. (2012) 'NFkappaB signalling is upregulated in a subset of castrate-resistant prostate cancer patients and correlates with disease progression', *Br J Cancer*, 107(9), pp. 1554-63.
- Min, J., Zaslavsky, A., Fedele, G., McLaughlin, S. K., Reczek, E. E., De Raedt, T., Guney, I., Strohlic, D. E., Macconail, L. E., Beroukhim, R., Bronson, R. T., Ryeom, S., Hahn, W. C., Loda, M. and Cichowski, K. (2010) 'An oncogene-tumor suppressor cascade drives metastatic prostate cancer by coordinately activating Ras and nuclear factor-kappaB', *Nat Med*, 16(3), pp. 286-94.
- Morita, Y., Matsuyama, H., Serizawa, A., Takeya, T. and Kawakami, H. (2008) 'Identification of angiogenin as the osteoclastic bone resorption-inhibitory factor in bovine milk', *Bone*, 42(2), pp. 380-387.
- Morris, E. V. and Edwards, C. M. (2016) 'The role of bone marrow adipocytes in bone metastasis', *J Bone Oncol*, 5(3), pp. 121-123.
- Mosquera, J. M., Perner, S., Genega, E. M., Sanda, M., Hofer, M. D., Mertz, K. D., Paris, P. L., Simko, J., Bismar, T. A., Ayala, G., Shah, R. B., Loda, M. and Rubin, M. A. (2008) 'Characterization of TMPRSS2-ERG fusion high-grade prostatic intraepithelial neoplasia and potential clinical implications', *Clin Cancer Res*, 14(11), pp. 3380-5.
- Moverare-Skrtic, S., Henning, P., Liu, X., Nagano, K., Saito, H., Borjesson, A. E., Sjogren, K., Windahl, S. H., Farman, H., Kindlund, B., Engdahl, C., Koskela, A., Zhang, F. P., Eriksson, E. E., Zaman, F., Hammarstedt, A., Isaksson, H., Bally, M., Kassem, A., Lindholm, C., Sandberg, O., Aspenberg, P., Savendahl, L., Feng, J. Q., Tuckermann, J., Tuukkanen, J., Poutanen, M., Baron, R., Lerner, U. H., Gori, F. and Ohlsson, C. (2014) 'Osteoblast-derived WNT16 represses osteoclastogenesis and prevents cortical bone fragility fractures', *Nat Med*, 20(11), pp. 1279-88.
- Moverare-Skrtic, S., Wu, J. Y., Henning, P., Gustafsson, K. L., Sjogren, K., Windahl, S. H., Koskela, A., Tuukkanen, J., Borjesson, A. E., Lagerquist, M. K., Lerner, U. H., Zhang, F. P., Gustafsson, J. A., Poutanen, M. and Ohlsson, C. (2015) 'The bone-sparing effects of estrogen and WNT16 are independent of each other', *Proceedings of the National Academy of Sciences of the United States of America*, 112(48), pp. 14972-14977.
- Mundy, G. R., Rodan, S. B., Majeska, R. J., DeMartino, S., Trimmier, C., Martin, T. J. and Rodan, G. A. (1982) 'Unidirectional migration of osteosarcoma cells with osteoblast characteristics in response to products of bone resorption', *Calcif Tissue Int*, 34(6), pp. 542-6.
- Muruganandan, S. and Sinal, C. J. (2014) 'The impact of bone marrow adipocytes on osteoblast and osteoclast differentiation', *IUBMB Life*.
- Nanes, M. S. (2003) 'Tumor necrosis factor-alpha: molecular and cellular mechanisms in skeletal pathology', *Gene*, 321, pp. 1-15.
- Neveu, B., Moreel, X., Deschenes-Rompere, M. P., Bergeron, A., LaRue, H., Ayari, C., Fradet, Y. and Fradet, V. (2014) 'IL-8 secretion in primary cultures of prostate cells is associated with prostate cancer aggressiveness', *Res Rep Urol*, 6, pp. 27-34.
- Nguyen, D. P., Li, J. and Tewari, A. K. (2014a) 'Inflammation and prostate cancer: the role of interleukin 6 (IL-6)', *BJU Int*, 113(6), pp. 986-92.

REFERENCES

- Nguyen, D. P., Li, J., Yadav, S. S. and Tewari, A. K. (2014b) 'Recent insights into NF-kappaB signalling pathways and the link between inflammation and prostate cancer', *BJU Int*, 114(2), pp. 168-76.
- Nitta, H., Wada, Y., Kawano, Y., Murakami, Y., Irie, A., Taniguchi, K., Kikuchi, K., Yamada, G., Suzuki, K., Honda, J., Wilson-Morifuji, M., Araki, N., Eto, M., Baba, H. and Imamura, T. (2013) 'Enhancement of Human Cancer Cell Motility and Invasiveness by Anaphylatoxin C5a via Aberrantly Expressed C5a Receptor (CD88)', *Clinical Cancer Research*, 19(8), pp. 2004-2013.
- Norseen, J., Hosooka, T., Hammarstedt, A., Yore, M. M., Kant, S., Aryal, P., Maruyama, H., Kraus, B. J., Usheva, A., Davis, R. J., Smith, U. and Kahn, B. B. (2012) 'RBP4 Inhibits Insulin Signaling in Adipocytes by Inducing Pro-Inflammatory Cytokines in Macrophages through a JNK- and TLR4-Dependent and Retinol-Independent Mechanism', *Diabetes*, 61, pp. A85-A85.
- Nottingham, L. K., Yan, C. H., Yang, X., Si, H., Coupar, J., Bian, Y., Cheng, T. F., Allen, C., Arun, P., Gius, D., Dang, L., Van Waes, C. and Chen, Z. (2014) 'Aberrant IKKalpha and IKKbeta cooperatively activate NF-kappaB and induce EGFR/AP1 signaling to promote survival and migration of head and neck cancer', *Oncogene*, 33(9), pp. 1135-47.
- Novack, D. V. (2011) 'Role of NF-kappaB in the skeleton', *Cell Res*, 21(1), pp. 169-82.
- Oeckinghaus, A., Hayden, M. S. and Ghosh, S. (2011) 'Crosstalk in NF-kappaB signaling pathways', *Nat Immunol*, 12(8), pp. 695-708.
- Okamoto, M., Udagawa, N., Uehara, S., Maeda, K., Yamashita, T., Nakamichi, Y., Kato, H., Saito, N., Minami, Y., Takahashi, N. and Kobayashi, Y. (2014) 'Noncanonical Wnt5a enhances Wnt/beta-catenin signaling during osteoblastogenesis', *Sci Rep*, 4, pp. 4493.
- Olivotto, E., Otero, M., Marcu, K. B. and Goldring, M. B. (2015) 'Pathophysiology of osteoarthritis: canonical NF-kappaB/IKKbeta-dependent and kinase-independent effects of IKKalpha in cartilage degradation and chondrocyte differentiation', *RMD Open*, 1(Suppl 1), pp. e000061.
- Olsson, J. and Hahn, R. G. (1996) 'Survival after high-dose intravenous infusion of irrigating fluids in the mouse', *Urology*, 47(5), pp. 689-92.
- Onuma, M., Bub, J. D., Rummel, T. L. and Iwamoto, Y. (2003) 'Prostate cancer cell-adipocyte interaction: leptin mediates androgen-independent prostate cancer cell proliferation through c-Jun NH2-terminal kinase', *J Biol Chem*, 278(43), pp. 42660-7.
- Otero, J. E., Chen, T., Zhang, K. and Abu-Amer, Y. (2012) 'Constitutively active canonical NF-kappaB pathway induces severe bone loss in mice', *PLoS One*, 7(6), pp. e38694.
- Otero, J. E., Dai, S., Alhawagri, M. A., Darwech, I. and Abu-Amer, Y. (2010) 'IKKbeta activation is sufficient for RANK-independent osteoclast differentiation and osteolysis', *J Bone Miner Res*, 25(6), pp. 1282-94.
- Ozes, O. N., Mayo, L. D., Gustin, J. A., Pfeffer, S. R., Pfeffer, L. M. and Donner, D. B. (1999) 'NF-kappaB activation by tumour necrosis factor requires the Akt serine-threonine kinase', *Nature*, 401(6748), pp. 82-5.
- Panagakos, F. S. (1994) 'Transforming growth factor--alpha stimulates chemotaxis of osteoblasts and osteoblast-like cells in vitro', *Biochem Mol Biol Int*, 33(4), pp. 643-50.
- Park, K. J., Krishnan, V., O'Malley, B. W., Yamamoto, Y. and Gaynor, R. B. (2005) 'Formation of an IKKalpha-dependent transcription complex is required for estrogen receptor-mediated gene activation', *Mol Cell*, 18(1), pp. 71-82.

REFERENCES

- Pasparakis, M. (2009) 'Regulation of tissue homeostasis by NF-kappaB signalling: implications for inflammatory diseases', *Nat Rev Immunol*, 9(11), pp. 778-88.
- Peng, C., Zhou, K. L., An, S. S. and Yang, J. (2015) 'The effect of CCL19/CCR7 on the proliferation and migration of cell in prostate cancer', *Tumor Biology*, 36(1), pp. 329-335.
- Perkins, N. D. (2006) 'Post-translational modifications regulating the activity and function of the nuclear factor kappa B pathway', *Oncogene*, 25(51), pp. 6717-30.
- Perkins, N. D. and Gilmore, T. D. (2006) 'Good cop, bad cop: the different faces of NF-kappaB', *Cell Death Differ*, 13(5), pp. 759-72.
- Phielers, J., Chung, K. J., Chatzigeorgiou, A., Klotzsche-von Ameln, A., Garcia-Martin, R., Sprott, D., Moisidou, M., Tzanavari, T., Ludwig, B., Baraban, E., Ehrhart-Bornstein, M., Bornstein, S. R., Mziaut, H., Solimena, M., Karalis, K. P., Economopoulou, M., Lambris, J. D. and Chavakis, T. (2013) 'The Complement Anaphylatoxin C5a Receptor Contributes to Obese Adipose Tissue Inflammation and Insulin Resistance', *Journal of Immunology*, 191(8), pp. 4367-4374.
- Polley, S., Passos, D. O., Huang, D. B., Mulero, M. C., Mazumder, A., Biswas, T., Verma, I. M., Lyumkis, D. and Ghosh, G. (2016) 'Structural Basis for the Activation of IKK1/alpha', *Cell Rep*, 17(8), pp. 1907-1914.
- Power, C. A., Pwint, H., Chan, J., Cho, J., Yu, Y., Walsh, W. and Russell, P. J. (2009) 'A novel model of bone-metastatic prostate cancer in immunocompetent mice', *Prostate*, 69(15), pp. 1613-23.
- Proff, P. and Romer, P. (2009) 'The molecular mechanism behind bone remodelling: a review', *Clin Oral Investig*, 13(4), pp. 355-62.
- Pu, H., Collazo, J., Jones, E., Gayheart, D., Sakamoto, S., Vogt, A., Mitchell, B. and Kyprianou, N. (2009) 'Dysfunctional transforming growth factor-beta receptor II accelerates prostate tumorigenesis in the TRAMP mouse model', *Cancer Res*, 69(18), pp. 7366-74.
- Puente, J., Grande, E., Medina, A., Maroto, P., Lainez, N. and Arranz, J. A. (2017) 'Docetaxel in prostate cancer: a familiar face as the new standard in a hormone-sensitive setting', *Therapeutic Advances in Medical Oncology*, 9(5), pp. 307-318.
- Qin, Y., He, L. D., Sheng, Z. J., Yong, M. M., Sheng, Y. S., Dong, X. W., Wen, T. W. and Ming, Z. Y. (2014) 'Increased CCL19 and CCL21 levels promote fibroblast ossification in ankylosing spondylitis hip ligament tissue', *Bmc Musculoskeletal Disorders*, 15.
- Qu, Y., Zhang, Q. Y., Ma, S. Q., Liu, S., Chen, Z. Q., Mo, Z. F. and You, Z. B. (2016) 'Interleukin-17A Differentially Induces Inflammatory and Metabolic Gene Expression in the Adipose Tissues of Lean and Obese Mice', *International Journal of Molecular Sciences*, 17(4).
- Quinn, J. M., Itoh, K., Udagawa, N., Hausler, K., Yasuda, H., Shima, N., Mizuno, A., Higashio, K., Takahashi, N., Suda, T., Martin, T. J. and Gillespie, M. T. (2001) 'Transforming growth factor beta affects osteoclast differentiation via direct and indirect actions', *J Bone Miner Res*, 16(10), pp. 1787-94.
- Ribeiro, R., Monteiro, C., Silvestre, R., Castela, A., Coutinho, H., Fraga, A., Principe, P., Lobato, C., Costa, C., Cordeiro-da-Silva, A., Lopes, J. M., Lopes, C. and Medeiros, R. (2012) 'Human periprostatic white adipose tissue is rich in stromal progenitor cells and a potential source of prostate tumor stroma', *Experimental Biology and Medicine*, 237(10), pp. 1155-1162.
- Richardson, P. G., Mitsiades, C., Hideshima, T. and Anderson, K. C. (2005) 'Proteasome inhibition in the treatment of cancer', *Cell Cycle*, 4(2), pp. 290-6.

REFERENCES

- Ricote, M., Garcia-Tunon, I., Bethencourt, F. R., Fraile, B., Paniagua, R. and Royuela, M. (2004) 'Interleukin-1 (IL-1alpha and IL-1beta) and its receptors (IL-1RI, IL-1RII, and IL-1Ra) in prostate carcinoma', *Cancer*, 100(7), pp. 1388-96.
- Ries, W. L., Seeds, M. C. and Key, L. L. (1989) 'Interleukin-2 stimulates osteoclastic activity: increased acid production and radioactive calcium release', *J Periodontal Res*, 24(4), pp. 242-6.
- Ritchie, C. K., Andrews, L. R., Thomas, K. G., Tindall, D. J. and Fitzpatrick, L. A. (1997) 'The effects of growth factors associated with osteoblasts on prostate carcinoma proliferation and chemotaxis: implications for the development of metastatic disease', *Endocrinology*, 138(3), pp. 1145-50.
- Roca, H., Jones, J. D., Purica, M. C., Weidner, S., Koh, A. J., Kuo, R., Wilkinson, J. E., Wang, Y., Daignault-Newton, S., Pienta, K. J., Morgan, T. M., Keller, E. T., Nor, J. E., Shea, L. D. and McCauley, L. K. (2018) 'Apoptosis-induced CXCL5 accelerates inflammation and growth of prostate tumor metastases in bone', *J Clin Invest*, 128(1), pp. 248-266.
- Roca, H. and McCauley, L. K. (2015) 'Inflammation and skeletal metastasis', *Bonekey Rep*, 4, pp. 706.
- Roodman, G. D. (2004) 'Mechanisms of bone metastasis', *N Engl J Med*, 350(16), pp. 1655-64.
- Rucci, N., Capulli, M., Piperni, S. G., Cappariello, A., Lau, P., Frings-Meuthen, P., Heer, M. and Teti, A. (2015) 'Lipocalin 2: a new mechanoresponding gene regulating bone homeostasis', *J Bone Miner Res*, 30(2), pp. 357-68.
- Rucci, N., Millimaggi, D., Mari, M., Del Fattore, A., Bologna, M., Teti, A., Angelucci, A. and Dolo, V. (2010) 'Receptor Activator of NF-kappa B Ligand Enhances Breast Cancer-Induced Osteolytic Lesions through Upregulation of Extracellular Matrix Metalloproteinase Inducer/CD147', *Cancer Research*, 70(15), pp. 6150-6160.
- Ruijtenberg, S. and van den Heuvel, S. (2016) 'Coordinating cell proliferation and differentiation: Antagonism between cell cycle regulators and cell type-specific gene expression', *Cell Cycle*, 15(2), pp. 196-212.
- Russo, A., Bronte, G., Rizzo, S., Fanale, D., Di Gaudio, F., Gebbia, N. and Bazan, V. (2010) 'Anti-endothelin drugs in solid tumors', *Expert Opin Emerg Drugs*, 15(1), pp. 27-40.
- Ryan, C. J., Haqq, C. M., Simko, J., Nonaka, D. F., Chan, J. M., Weinberg, V., Small, E. J. and Goldfine, I. D. (2007) 'Expression of insulin-like growth factor-1 receptor in local and metastatic prostate cancer', *Urol Oncol*, 25(2), pp. 134-40.
- Sabbota, A. L., Kim, H. R., Zhe, X., Fridman, R., Bonfil, R. D. and Cher, M. L. (2010) 'Shedding of RANKL by tumor-associated MT1-MMP activates Src-dependent prostate cancer cell migration', *Cancer Res*, 70(13), pp. 5558-66.
- Saleh, H., Eeles, D., Hodge, J. M., Nicholson, G. C., Gu, R., Pompolo, S., Gillespie, M. T. and Quinn, J. M. W. (2011) 'Interleukin-33, a Target of Parathyroid Hormone and Oncostatin M, Increases Osteoblastic Matrix Mineral Deposition and Inhibits Osteoclast Formation in Vitro', *Endocrinology*, 152(5), pp. 1911-1922.
- Sanchez-Fernandez, M. A., Gallois, A., Riedl, T., Jurdic, P. and Hoflack, B. (2008) 'Osteoclasts control osteoblast chemotaxis via PDGF-BB/PDGF receptor beta signaling', *PLoS One*, 3(10), pp. e3537.
- Saranchova, I., Han, J., Huang, H., Fenninger, F., Choi, K. B., Munro, L., Pfeifer, C., Welch, I., Wyatt, A. W., Fazli, L., Gleave, M. E. and Jefferies, W. A. (2016) 'Discovery of a Metastatic Immune Escape Mechanism Initiated by the Loss of Expression of the Tumour Biomarker Interleukin-33', *Scientific Reports*, 6.

REFERENCES

- Sathianathan, N. J., Konety, B. R., Crook, J., Saad, F. and Lawrentschuk, N. (2018) 'Landmarks in prostate cancer', *Nat Rev Urol*.
- Sauane, M., Su, Z. Z., Gupta, P., Lebedeva, I. V., Dent, P., Sarkar, D. and Fisher, P. B. (2008) 'Autocrine regulation of mda-7/IL-24 mediates cancer-specific apoptosis', *Proc Natl Acad Sci U S A*, 105(28), pp. 9763-8.
- Schipani, E., Maes, C., Carmeliet, G. and Semenza, G. L. (2009) 'Regulation of osteogenesis-angiogenesis coupling by HIFs and VEGF', *J Bone Miner Res*, 24(8), pp. 1347-53.
- Schneider, M. R., Sibilio, M. and Erben, R. G. (2009) 'The EGFR network in bone biology and pathology', *Trends Endocrinol Metab*, 20(10), pp. 517-24.
- Schramek, D., Sigl, V. and Penninger, J. M. (2011) 'RANKL and RANK in sex hormone-induced breast cancer and breast cancer metastasis', *Trends Endocrinol Metab*, 22(5), pp. 188-94.
- Schrecengost, R. and Knudsen, K. E. (2013) 'Molecular pathogenesis and progression of prostate cancer', *Semin Oncol*, 40(3), pp. 244-58.
- Schulze, J., Weber, K., Baranowsky, A., Streichert, T., Lange, T., Spiro, A. S., Albers, J., Seitz, S., Zustin, J., Amling, M., Fehse, B. and Schinke, T. (2012) 'p65-Dependent production of interleukin-1beta by osteolytic prostate cancer cells causes an induction of chemokine expression in osteoblasts', *Cancer Lett*, 317(1), pp. 106-13.
- Scott, L. J., Clarke, N. W., George, N. J., Shanks, J. H., Testa, N. G. and Lang, S. H. (2001) 'Interactions of human prostatic epithelial cells with bone marrow endothelium: binding and invasion', *Br J Cancer*, 84(10), pp. 1417-23.
- Setlur, S. R., Royce, T. E., Sboner, A., Mosquera, J. M., Demichelis, F., Hofer, M. D., Mertz, K. D., Gerstein, M. and Rubin, M. A. (2007) 'Integrative Microarray analysis of pathways dysregulated in metastatic prostate cancer', *Cancer Research*, 67(21), pp. 10296-10303.
- Shah, K. M., Stern, M. M., Stern, A. R., Pathak, J. L., Bravenboer, N. and Bakker, A. D. (2016) 'Osteocyte isolation and culture methods', *Bonekey Rep*, 5, pp. 838.
- Sharma, A., Yeow, W. S., Ertel, A., Coleman, I., Clegg, N., Thangavel, C., Morrissey, C., Zhang, X., Comstock, C. E., Witkiewicz, A. K., Gomella, L., Knudsen, E. S., Nelson, P. S. and Knudsen, K. E. (2010) 'The retinoblastoma tumor suppressor controls androgen signaling and human prostate cancer progression', *J Clin Invest*, 120(12), pp. 4478-92.
- Shiah, H. S., Gao, W., Baker, D. C. and Cheng, Y. C. (2006) 'Inhibition of cell growth and nuclear factor-kappaB activity in pancreatic cancer cell lines by a tylophorine analogue, DCB-3503', *Mol Cancer Ther*, 5(10), pp. 2484-93.
- Shih, V. F. S., Tsui, R., Caldwell, A. and Hoffmann, A. (2011) 'A single NF kappa B system for both canonical and non-canonical signaling', *Cell Research*, 21(1), pp. 86-102.
- Shukla, S. and Gupta, S. (2004) 'Suppression of constitutive and tumor necrosis factor alpha-induced nuclear factor (NF)-kappaB activation and induction of apoptosis by apigenin in human prostate carcinoma PC-3 cells: correlation with down-regulation of NF-kappaB-responsive genes', *Clin Cancer Res*, 10(9), pp. 3169-78.
- Shukla, S., MacLennan, G. T., Flask, C. A., Fu, P., Mishra, A., Resnick, M. I. and Gupta, S. (2007) 'Blockade of beta-catenin signaling by plant flavonoid apigenin suppresses prostate carcinogenesis in TRAMP mice', *Cancer Res*, 67(14), pp. 6925-35.
- Shukla, S., MacLennan, G. T., Fu, P., Patel, J., Marengo, S. R., Resnick, M. I. and Gupta, S. (2004) 'Nuclear factor-kappaB/p65 (Rel A) is constitutively activated in human prostate adenocarcinoma and correlates with disease progression', *Neoplasia*, 6(4), pp. 390-400.

REFERENCES

- Shukla, S., MacLennan, G. T., Marengo, S. R., Resnick, M. I. and Gupta, S. (2005) 'Constitutive activation of P 13 K-Akt and NF-kappaB during prostate cancer progression in autochthonous transgenic mouse model', *Prostate*, 64(3), pp. 224-39.
- Shukla, S., Shankar, E., Fu, P., MacLennan, G. T. and Gupta, S. (2015) 'Suppression of NF-kappaB and NF-kappaB-Regulated Gene Expression by Apigenin through IkappaBalpha and IKK Pathway in TRAMP Mice', *PLoS One*, 10(9), pp. e0138710.
- Sidhu, S. S., Nawroth, R., Retz, M., Lemjabbar-Alaoui, H., Dasari, V. and Basbaum, C. (2010) 'EMMPRIN regulates the canonical Wnt/beta-catenin signaling pathway, a potential role in accelerating lung tumorigenesis', *Oncogene*, 29(29), pp. 4145-56.
- Sil, A. K., Maeda, S., Sano, Y., Roop, D. R. and Karin, M. (2004) 'IkappaB kinase-alpha acts in the epidermis to control skeletal and craniofacial morphogenesis', *Nature*, 428(6983), pp. 660-4.
- Simmons, J., Elshafae, S., Keller, E., McCauley, L. and Rosol, T. (2014) 'Review of Animal Models of Prostate Cancer Bone Metastasis', *Veterinary Sciences*, 1(1), pp. 16.
- Singh, R. K. and Lokeshwar, B. L. (2011) 'The IL-8-regulated chemokine receptor CXCR7 stimulates EGFR signaling to promote prostate cancer growth', *Cancer Res*, 71(9), pp. 3268-77.
- Song, L., Martinez, L., Zigmond, Z. M., Hernandez, D. R., Lassance-Soares, R. M., Selman, G. and Vazquez-Padron, R. I. (2017) 'c-Kit modifies the inflammatory status of smooth muscle cells', *PeerJ*, 5, pp. e3418.
- Soysa, N. S. and Alles, N. (2009) 'NF-kappaB functions in osteoclasts', *Biochem Biophys Res Commun*, 378(1), pp. 1-5.
- Soysa, N. S., Alles, N., Weih, D., Lovas, A., Mian, A. H., Shimokawa, H., Yasuda, H., Weih, F., Jimi, E., Ohya, K. and Aoki, K. (2010) 'The pivotal role of the alternative NF-kappaB pathway in maintenance of basal bone homeostasis and osteoclastogenesis', *J Bone Miner Res*, 25(4), pp. 809-18.
- Stark, T., Livas, L. and Kyprianou, N. (2015) 'Inflammation in prostate cancer progression and therapeutic targeting', *Transl Androl Urol*, 4(4), pp. 455-63.
- Starkey, J. M., Haidacher, S. J., LeJeune, W. S., Zhang, X., Tieu, B. C., Choudhary, S., Brasier, A. R., Denner, L. A. and Tilton, R. G. (2006) 'Diabetes-induced activation of canonical and noncanonical nuclear factor-kappaB pathways in renal cortex', *Diabetes*, 55(5), pp. 1252-9.
- Storz, P. (2013) 'Targeting the alternative NF-kappaB pathway in pancreatic cancer: a new direction for therapy?', *Expert Rev Anticancer Ther*, 13(5), pp. 501-4.
- Strong, A. L., Pei, D. T., Hurst, C. G., Gimble, J. M., Burow, M. E. and Bunnell, B. A. (2017) 'Obesity Enhances the Conversion of Adipose-Derived Stromal/Stem Cells into Carcinoma-Associated Fibroblast Leading to Cancer Cell Proliferation and Progression to an Invasive Phenotype', *Stem Cells Int*, 2017, pp. 9216502.
- Sun, S. C. (2017) 'The non-canonical NF-kappa B pathway in immunity and inflammation', *Nature Reviews Immunology*, 17(9), pp. 545-558.
- Sun, Y., Campisi, J., Higano, C., Beer, T. M., Porter, P., Coleman, I., True, L. and Nelson, P. S. (2012) 'Treatment-induced damage to the tumor microenvironment promotes prostate cancer therapy resistance through WNT16B', *Nature Medicine*, 18(9), pp. 1359-+.
- Sundaram, K., Rao, D. S., Ries, W. L. and Reddy, S. V. (2013) 'CXCL5 stimulation of RANK ligand expression in Paget's disease of bone', *Lab Invest*, 93(4), pp. 472-9.

REFERENCES

- Taichman, R. S., Cooper, C., Keller, E. T., Pienta, K. J., Taichman, N. S. and McCauley, L. K. (2002) 'Use of the stromal cell-derived factor-1/CXCR4 pathway in prostate cancer metastasis to bone', *Cancer Res*, 62(6), pp. 1832-7.
- Taichman, R. S. and Hauschka, P. V. (1992) 'Effects of interleukin-1 beta and tumor necrosis factor-alpha on osteoblastic expression of osteocalcin and mineralized extracellular matrix in vitro', *Inflammation*, 16(6), pp. 587-601.
- Tak, P. P. and Firestein, G. S. (2001) 'NF-kappaB: a key role in inflammatory diseases', *J Clin Invest*, 107(1), pp. 7-11.
- Takahashi, N., MacDonald, B. R., Hon, J., Winkler, M. E., Derynck, R., Mundy, G. R. and Roodman, G. D. (1986) 'Recombinant human transforming growth factor-alpha stimulates the formation of osteoclast-like cells in long-term human marrow cultures', *J Clin Invest*, 78(4), pp. 894-8.
- Takayanagi, H. (2005) 'Mechanistic insight into osteoclast differentiation in osteoimmunology', *J Mol Med (Berl)*, 83(3), pp. 170-9.
- Takeda, K., Takeuchi, O., Tsujimura, T., Itami, S., Adachi, O., Kawai, T., Sanjo, H., Yoshikawa, K., Terada, N. and Akira, S. (1999) 'Limb and skin abnormalities in mice lacking IKKalpha', *Science*, 284(5412), pp. 313-6.
- Tanabe, N., Ito-Kato, E., Suzuki, N., Nakayama, A., Ogiso, B., Maeno, M. and Ito, K. (2004) 'IL-1alpha affects mineralized nodule formation by rat osteoblasts', *Life Sci*, 75(19), pp. 2317-27.
- Tanaka, M., Fuentes, M. E., Yamaguchi, K., Durnin, M. H., Dalrymple, S. A., Hardy, K. L. and Goeddel, D. V. (1999) 'Embryonic lethality, liver degeneration, and impaired NF-kappa B activation in IKK-beta-deficient mice', *Immunity*, 10(4), pp. 421-9.
- Tang, S. Y. and Alliston, T. (2013) 'Regulation of postnatal bone homeostasis by TGFbeta', *Bonekey Rep*, 2, pp. 255.
- Tani-Ishii, N., Tsunoda, A., Teranaka, T. and Umemoto, T. (1999) 'Autocrine regulation of osteoclast formation and bone resorption by IL-1 alpha and TNF alpha', *J Dent Res*, 78(10), pp. 1617-23.
- Tarapore, R. S., Lim, J., Tian, C., Pacios, S., Xiao, W., Reid, D., Guan, H., Mattos, M., Yu, B., Wang, C. Y. and Graves, D. T. (2016) 'NF-kappaB Has a Direct Role in Inhibiting Bmp- and Wnt-Induced Matrix Protein Expression', *J Bone Miner Res*, 31(1), pp. 52-64.
- Tardelli, M., Zeyda, K., Moreno-Viedma, V., Wanko, B., Grun, N. G., Staffler, G., Zeyda, M. and Stulnig, T. M. (2016) 'Osteopontin is a key player for local adipose tissue macrophage proliferation in obesity', *Mol Metab*, 5(11), pp. 1131-1137.
- Tatsumoto, N., Arioka, M., Yamada, S., Takahashi-Yanaga, F., Tokumoto, M., Tsuruya, K., Kitazono, T. and Sasaguri, T. (2016) 'Inhibition of GSK-3 beta increases trabecular bone volume but not cortical bone volume in adenine-induced uremic mice with severe hyperparathyroidism', *Physiological Reports*, 4(21).
- Teitelbaum, S. L. (2000) 'Bone resorption by osteoclasts', *Science*, 289(5484), pp. 1504-8.
- Thavarajah, R., Mudimbaimannar, V. K., Elizabeth, J., Rao, U. K. and Ranganathan, K. (2012) 'Chemical and physical basics of routine formaldehyde fixation', *J Oral Maxillofac Pathol*, 16(3), pp. 400-5.
- Thobe, M. N., Clark, R. J., Bainer, R. O., Prasad, S. M. and Rinker-Schaeffer, C. W. (2011) 'From prostate to bone: key players in prostate cancer bone metastasis', *Cancers (Basel)*, 3(1), pp. 478-93.
- Thomas, B. G. and Hamdy, F. C. (2000) 'Bone morphogenetic protein-6: potential mediator of osteoblastic metastases in prostate cancer', *Prostate Cancer Prostatic Dis*, 3(4), pp. 283-285.

REFERENCES

- Thoms, J. W., Dal Pra, A., Anborgh, P. H., Christensen, E., Fleshner, N., Menard, C., Chadwick, K., Milosevic, M., Catton, C., Pintilie, M., Chambers, A. F. and Bristow, R. G. (2012) 'Plasma osteopontin as a biomarker of prostate cancer aggression: relationship to risk category and treatment response', *Br J Cancer*, 107(5), pp. 840-6.
- Til, H. P., Kuper, C. F., Falke, H. E. and Bar, A. (1996) 'Subchronic oral toxicity studies with erythritol in mice and rats', *Regul Toxicol Pharmacol*, 24(2 Pt 2), pp. S221-31.
- Todenhofer, T., Stenzl, A., Hofbauer, L. C. and Rachner, T. D. (2015) 'Targeting bone metabolism in patients with advanced prostate cancer: current options and controversies', *Int J Endocrinol*, 2015, pp. 838202.
- Tourniaire, F., Romier-Crouzet, B., Lee, J. H., Marcotorchino, J., Gouranton, E., Salles, J., Malezet, C., Astier, J., Darmon, P., Blouin, E., Walrand, S., Ye, J. P. and Landrier, J. F. (2013) 'Chemokine Expression in Inflamed Adipose Tissue Is Mainly Mediated by NF-kappa B', *Plos One*, 8(6).
- Trebec-Reynolds, D. P., Voronov, I., Heersche, J. N. and Manolson, M. F. (2010) 'IL-1alpha and IL-1beta have different effects on formation and activity of large osteoclasts', *J Cell Biochem*, 109(5), pp. 975-82.
- Troen, B. R. (2003) 'Molecular mechanisms underlying osteoclast formation and activation', *Exp Gerontol*, 38(6), pp. 605-14.
- Tse, B. W., Scott, K. F. and Russell, P. J. (2012) 'Paradoxical roles of tumour necrosis factor-alpha in prostate cancer biology', *Prostate Cancer*, 2012, pp. 128965.
- Tu, Z., Prajapati, S., Park, K. J., Kelly, N. J., Yamamoto, Y. and Gaynor, R. B. (2006) 'IKK alpha regulates estrogen-induced cell cycle progression by modulating E2F1 expression', *J Biol Chem*, 281(10), pp. 6699-706.
- Tung, M. C., Hsieh, S. C., Yang, S. F., Cheng, C. W., Tsai, R. T., Wang, S. C., Huang, M. H. and Hsieh, Y. H. (2013) 'Knockdown of lipocalin-2 suppresses the growth and invasion of prostate cancer cells', *Prostate*, 73(12), pp. 1281-90.
- Uehara, H., Takahashi, T. and Izumi, K. (2013) 'Induction of retinol-binding protein 4 and placenta-specific 8 expression in human prostate cancer cells remaining in bone following osteolytic tumor growth inhibition by osteoprotegerin', *Int J Oncol*, 43(2), pp. 365-74.
- Um, J. Y., Rim, H. K., Kim, S. J., Kim, H. L. and Hong, S. H. (2011) 'Functional polymorphism of IL-1 alpha and its potential role in obesity in humans and mice', *PLoS One*, 6(12), pp. e29524.
- Ustach, C. V., Huang, W., Conley-LaComb, M. K., Lin, C. Y., Che, M., Abrams, J. and Kim, H. R. (2010) 'A novel signaling axis of matriptase/PDGF-D/ss-PDGFR in human prostate cancer', *Cancer Res*, 70(23), pp. 9631-40.
- Vaananen, H. K. and Laitala-Leinonen, T. (2008) 'Osteoclast lineage and function', *Arch Biochem Biophys*, 473(2), pp. 132-8.
- Vaira, S., Johnson, T., Hirbe, A. C., Alhawagri, M., Anwisyte, I., Sammut, B., O'Neal, J., Zou, W., Weilbaecher, K. N., Faccio, R. and Novack, D. V. (2008) 'RelB is the NF-kappaB subunit downstream of NIK responsible for osteoclast differentiation', *Proc Natl Acad Sci U S A*, 105(10), pp. 3897-902.
- Valta, M. P., Tuomela, J., Bjartell, A., Valve, E., Vaananen, H. K. and Harkonen, P. (2008) 'FGF-8 is involved in bone metastasis of prostate cancer', *Int J Cancer*, 123(1), pp. 22-31.
- van't Hof, R. J., Tuinenburg-Bol Raap, A. C. and Nijweide, P. J. (1995) 'Induction of osteoclast characteristics in cultured avian blood monocytes; modulation by osteoblasts and 1,25-(OH)₂ vitamin D₃', *Int J Exp Pathol*, 76(3), pp. 205-14.

REFERENCES

- van der Pluijm, G. (2011) 'Epithelial plasticity, cancer stem cells and bone metastasis formation', *Bone*, 48(1), pp. 37-43.
- Varma, V., Yao-Borengasser, A., Bodles, A. M., Rasouli, N., Phanavanh, B., Nolen, G. T., Kern, E. M., Nagarajan, R., Spencer, H. J., Lee, M. J., Fried, S. K., McGehee, R. E., Peterson, C. A. and Kern, P. A. (2008) 'Thrombospondin-1 is an adipokine associated with obesity, adipose inflammation, and insulin resistance', *Diabetes*, 57(2), pp. 432-439.
- Verstrepen, L. and Beyaert, R. (2014) 'Receptor proximal kinases in NF-kappaB signaling as potential therapeutic targets in cancer and inflammation', *Biochem Pharmacol*, 92(4), pp. 519-29.
- Vielma, S. A., Klein, R. L., Levingston, C. A. and Young, M. R. (2013) 'Adipocytes as immune regulatory cells', *Int Immunopharmacol*, 16(2), pp. 224-31.
- Viennois, E., Chen, F. and Merlin, D. (2013) 'NF-kappaB pathway in colitis-associated cancers', *Transl Gastrointest Cancer*, 2(1), pp. 21-29.
- Voronov, E., Shouval, D. S., Krelin, Y., Cagnano, E., Benharroch, D., Iwakura, Y., Dinarello, C. A. and Apte, R. N. (2003) 'IL-1 is required for tumor invasiveness and angiogenesis', *Proc Natl Acad Sci U S A*, 100(5), pp. 2645-50.
- Wang, Z., Jia, Y., Du, F., Chen, M., Dong, X., Chen, Y. and Huang, W. (2017) 'IL-17A Inhibits Osteogenic Differentiation of Bone Mesenchymal Stem Cells via Wnt Signaling Pathway', *Med Sci Monit*, 23, pp. 4095-4101.
- Watson, P. A., Arora, V. K. and Sawyers, C. L. (2015) 'Emerging mechanisms of resistance to androgen receptor inhibitors in prostate cancer', *Nat Rev Cancer*, 15(12), pp. 701-11.
- Weir, E. C., Horowitz, M. C., Baron, R., Centrella, M., Kacinski, B. M. and Insogna, K. L. (1993) 'Macrophage colony-stimulating factor release and receptor expression in bone cells', *J Bone Miner Res*, 8(12), pp. 1507-18.
- Westhrin, M., Moen, S. H., Holien, T., Mylin, A. K., Heickendorff, L., Olsen, O. E., Sundan, A., Turesson, I., Gimsing, P., Waage, A. and Standal, T. (2015) 'Growth differentiation factor 15 (GDF15) promotes osteoclast differentiation and inhibits osteoblast differentiation and high serum GDF15 levels are associated with multiple myeloma bone disease', *Haematologica*, 100(12), pp. E511-E514.
- Xia, Y., Shen, S. and Verma, I. M. (2014) 'NF-kappaB, an active player in human cancers', *Cancer Immunol Res*, 2(9), pp. 823-30.
- Xiao, M., Inal, C. E., Parekh, V. I., Li, X. H. and Whitnall, M. H. (2009) 'Role of NF-kappaB in hematopoietic niche function of osteoblasts after radiation injury', *Exp Hematol*, 37(1), pp. 52-64.
- Yamaguchi, T., Miki, Y. and Yoshida, K. (2007) 'Protein kinase C delta activates I kappa B-kinase alpha to induce the p53 tumor suppressor in response to oxidative stress', *Cell Signal*, 19(10), pp. 2088-97.
- Yamamoto, Y., Verma, U. N., Prajapati, S., Kwak, Y. T. and Gaynor, R. B. (2003) 'Histone H3 phosphorylation by IKK-alpha is critical for cytokine-induced gene expression', *Nature*, 423(6940), pp. 655-9.
- Yamamoto, Y., Yin, M. J. and Gaynor, R. B. (2000) 'I kappa B kinase alpha (IKKalpha) regulation of IKKbeta kinase activity', *Mol Cell Biol*, 20(10), pp. 3655-66.
- Yamate, T., Mocharla, H., Taguchi, Y., Igietseme, J. U., Manolagas, S. C. and Abe, E. (1997) 'Osteopontin expression by osteoclast and osteoblast progenitors in the murine bone marrow: demonstration of its requirement for osteoclastogenesis and its increase after ovariectomy', *Endocrinology*, 138(7), pp. 3047-55.
- Yanagitai, M., Kitagawa, T., Okawa, K., Koyama, H. and Satoh, T. (2012) 'Phenylenediamine derivatives induce GDF-15/MIC-1 and inhibit adipocyte differentiation of mouse 3T3-

REFERENCES

- L1 Cells', *Biochemical and Biophysical Research Communications*, 417(1), pp. 294-298.
- Yang, L., You, S., Kumar, V., Zhang, C. and Cao, Y. (2012) 'In vitro the behaviors of metastasis with suppression of VEGF in human bone metastatic LNCaP-derivative C4-2B prostate cancer cell line', *J Exp Clin Cancer Res*, 31, pp. 40.
- Yang, Q., McHugh, K. P., Patntirapong, S., Gu, X., Wunderlich, L. and Hauschka, P. V. (2008) 'VEGF enhancement of osteoclast survival and bone resorption involves VEGF receptor-2 signaling and beta3-integrin', *Matrix Biol*, 27(7), pp. 589-99.
- Yao, Z., Li, Y., Yin, X., Dong, Y., Xing, L. and Boyce, B. F. (2014) 'NF-kappaB RelB negatively regulates osteoblast differentiation and bone formation', *J Bone Miner Res*, 29(4), pp. 866-77.
- Yilmaz, Z. B., Kofahl, B., Beaudette, P., Baum, K., Ipenberg, I., Weih, F., Wolf, J., Dittmar, G. and Scheidereit, C. (2014) 'Quantitative dissection and modeling of the NF-kappaB p100-p105 module reveals interdependent precursor proteolysis', *Cell Rep*, 9(5), pp. 1756-1769.
- Yin, J. J., Mohammad, K. S., Kakonen, S. M., Harris, S., Wu-Wong, J. R., Wessale, J. L., Padley, R. J., Garrett, I. R., Chirgwin, J. M. and Guise, T. A. (2003) 'A causal role for endothelin-1 in the pathogenesis of osteoblastic bone metastases', *Proc Natl Acad Sci U S A*, 100(19), pp. 10954-9.
- Yoshida, K., Ozaki, T., Furuya, K., Nakanishi, M., Kikuchi, H., Yamamoto, H., Ono, S., Koda, T., Omura, K. and Nakagawara, A. (2008) 'ATM-dependent nuclear accumulation of IKK-alpha plays an important role in the regulation of p73-mediated apoptosis in response to cisplatin', *Oncogene*, 27(8), pp. 1183-8.
- Zeigler-Johnson, C. M., Rennert, H., Mittal, R. D., Jalloh, M., Sachdeva, R., Malkowicz, S. B., Mandhani, A., Mittal, B., Gueye, S. M. and Rebbeck, T. R. (2008) 'Evaluation of prostate cancer characteristics in four populations worldwide', *Can J Urol*, 15(3), pp. 4056-64.
- Zeyda, M., Gollinger, K., Todoric, J., Kiefer, F. W., Keck, M., Aszmann, O., Prager, G., Zlabinger, G. J., Petzelbauer, P. and Stulnig, T. M. (2011) 'Osteopontin Is an Activator of Human Adipose Tissue Macrophages and Directly Affects Adipocyte Function', *Endocrinology*, 152(6), pp. 2219-2227.
- Zhang, H., Hilton, M. J., Anolik, J. H., Welle, S. L., Zhao, C., Yao, Z., Li, X., Wang, Z., Boyce, B. F. and Xing, L. (2014) 'NOTCH inhibits osteoblast formation in inflammatory arthritis via noncanonical NF-kappaB', *J Clin Invest*, 124(7), pp. 3200-14.
- Zhang, J., Wu, Y., Zhang, Y., Leroith, D., Bernlohr, D. A. and Chen, X. (2008) 'The role of lipocalin 2 in the regulation of inflammation in adipocytes and macrophages', *Mol Endocrinol*, 22(6), pp. 1416-26.
- Zhang, L., Altuwaijri, S., Deng, F., Chen, L., Lal, P., Bhanot, U. K., Korets, R., Wenske, S., Lilja, H. G., Chang, C., Scher, H. I. and Gerald, W. L. (2009) 'NF-kappaB regulates androgen receptor expression and prostate cancer growth', *Am J Pathol*, 175(2), pp. 489-99.
- Zhang, Q., Liu, S., Parajuli, K. R., Zhang, W., Zhang, K., Mo, Z., Liu, J., Chen, Z., Yang, S., Wang, A., Myers, L. and You, Z. (2017a) 'Interleukin-17 promotes prostate cancer via MMP7-induced epithelial-to-mesenchymal transition', *Oncogene*, 36(5), pp. 687-699.
- Zhang, X. F., Chen, Q. P., Liu, J. W., Fan, C., Wei, Q., Chen, Z. T. and Mao, X. L. (2017b) 'Parthenolide Promotes Differentiation of Osteoblasts Through the Wnt/beta-Catenin Signaling Pathway in Inflammatory Environments', *Journal of Interferon and Cytokine Research*, 37(9), pp. 406-414.

REFERENCES

- Zheng, H. F., Tobias, J. H., Duncan, E., Evans, D. M., Eriksson, J., Paternoster, L., Yerges-Armstrong, L. M., Lehtimäki, T., Bergstrom, U., Kahonen, M., Leo, P. J., Raitakari, O., Laaksonen, M., Nicholson, G. C., Viikari, J., Ladouceur, M., Lyytikäinen, L. P., Medina-Gomez, C., Rivadeneira, F., Prince, R. L., Sievanen, H., Leslie, W. D., Mellstrom, D., Eisman, J. A., Moverare-Skrtic, S., Goltzman, D., Hanley, D. A., Jones, G., St Pourcain, B., Xiao, Y., Timpson, N. J., Smith, G. D., Reid, I. R., Ring, S. M., Sambrook, P. N., Karlsson, M., Dennison, E. M., Kemp, J. P., Danoy, P., Sayers, A., Wilson, S. G., Nethander, M., McCloskey, E., Vandenput, L., Eastell, R., Liu, J., Spector, T., Mitchell, B. D., Streeten, E. A., Brommage, R., Pettersson-Kymmer, U., Brown, M. A., Ohlsson, C., Richards, J. B. and Lorentzon, M. (2012) 'WNT16 influences bone mineral density, cortical bone thickness, bone strength, and osteoporotic fracture risk', *PLoS Genet*, 8(7), pp. e1002745.